

2012

## Efficacy of Multifunctionalized Saccharide Constructs for the Attenuation of Amyloid-beta Toxicity

Dhruva Dilip Dhavale

*Louisiana State University and Agricultural and Mechanical College*

Follow this and additional works at: [https://repository.lsu.edu/gradschool\\_dissertations](https://repository.lsu.edu/gradschool_dissertations)



Part of the [Chemical Engineering Commons](#)

---

### Recommended Citation

Dhavale, Dhruva Dilip, "Efficacy of Multifunctionalized Saccharide Constructs for the Attenuation of Amyloid-beta Toxicity" (2012). *LSU Doctoral Dissertations*. 2446.

[https://repository.lsu.edu/gradschool\\_dissertations/2446](https://repository.lsu.edu/gradschool_dissertations/2446)

This Dissertation is brought to you for free and open access by the Graduate School at LSU Scholarly Repository. It has been accepted for inclusion in LSU Doctoral Dissertations by an authorized graduate school editor of LSU Scholarly Repository. For more information, please contact [gradetd@lsu.edu](mailto:gradetd@lsu.edu).

EFFICACY OF MULTIFUNCTIONALIZED SACCHARIDE CONSTRUCTS FOR THE  
ATTENUATION OF AMYLOID-BETA TOXICITY

A Dissertation

Submitted to the Graduate Faculty of the  
Louisiana State University and  
Agricultural and Mechanical College  
in partial fulfillment of the  
requirements for the degree of  
Doctor of Philosophy

in

The Department of Chemical Engineering

by

Dhruva Dhavale

B.S., University of Pune, 2006

M.S., Louisiana State University, 2009

May 2012

## **DEDICATION**

To my parents, for their unconditional love

To my brother, for the wonderful memories we share

To my fiancée, you are the best thing that ever happened to me

## ACKNOWLEDGEMENTS

The path towards completing this work was convoluted, and, so many people have contributed to get me where I am today. Please accept my appreciation for all those who have helped me along the way.

I want to express my immense sense of gratitude and appreciation for Dr. James Henry. He has been a true guide and a perfect example of how a mentor should be. It is due to your encouragement, support and belief in me that this work was possible. I have learned so much from him and I am proud to be his student. Again, thank you for everything.

Thank you, Dr. Michael Benton, for giving me the opportunity to complete this work. I am grateful that you accepted me in your group. Thank you for all the guidance, awesome suggestions and the help you have given me these last months.

I would also like to thank Dr. Todd Monroe, Dr. John Flake and Dr. K. Aryana for their efforts to review and evaluate my research.

Special thanks to Ms. Thaya from the School of Veterinary Medicine, LSU for being very helpful and accommodating for the use of their instruments. Also, thank you, Yujie Wang for help with SAS programming.

I would also like to acknowledge the funding agencies, Chemical engineering department at LSU and its staff, especially Darla Dao, for their assistance in completing this work.

On a personal note, a special thanks to Shivkumar, Shafi, Nitin, Ramesh, Murali, Akanksha, Neha, Datta and several other friends at LSU for making me feel at home.

Special thanks to all my family and friends back in India. Every time I visit, you all make it special for me. I miss you all very much.

Words fail to express the support, encouragement and love Supriya has given me. Your cheerful nature and beautiful smile are the highlights of my day. I truly enjoy our talks, our chemistry and our trips together. I cannot wait to spend my entire life with you!

I owe everything I am today to my parents, Dilip and Varsha Dhavale. Baba, you will always be my role model and the standard by which I measure myself. Aai, your love and caring nature has given me the strength to be what I am today. My brother Puru, my best friend, I miss the times of us growing up!

## TABLE OF CONTENTS

DEDICATION .....	ii
ACKNOWLEDGEMENTS .....	iii
LIST OF TABLES .....	viii
LIST OF FIGURES .....	ix
ABSTRACT .....	xiv
1. OVERVIEW .....	1
1.1. Introduction.....	1
1.2. Rationale for This Project .....	4
2. LITERATURE REVIEW .....	9
2.1. Hallmarks of Alzheimer’s Disease .....	12
2.1.1. Tau Protein .....	12
2.1.2. Amyloid-beta Peptide .....	13
2.2. Characteristics of A $\beta$ Peptide .....	15
2.3. Evidence of A $\beta$ Induced Neurotoxicity.....	18
2.4. The Amyloid Cascade Hypothesis .....	20
2.5. Mechanisms of A $\beta$ Neurotoxicity .....	22
2.6. Normal Roles of A $\beta$ and APP.....	23
2.7. Neurotoxicity of A $\beta$ : Who Is the Real Culprit?.....	24
2.8. Structure of Aggregated A $\beta$ Peptide .....	27
2.9. Interaction Between A $\beta$ -Cell Membranes.....	29
2.10. Role of Gangliosides in Alzheimer’s Disease Pathology .....	30
2.11. Current and Emerging Therapeutic Approaches in AD.....	36
2.11.1. Approved Drugs Against Alzheimer’s Disease .....	36
2.11.2. Immunotherapy for AD.....	39
2.11.3. Inhibition/Modulation of Secretases.....	40
2.11.4. A $\beta$ Aggregation Inhibitors .....	41
2.11.5. Strategies Involving Metal Interactions of A $\beta$ .....	43
2.11.6. Drugs Based On Epidemiology .....	43
2.11.7. Novel A $\beta$ Sequestering Agents: OUR FOCUS .....	44
2.12. Chitosan, Backbone Molecule .....	46
2.13. Biological Sugars Selected for Conjugation with Chitosan.....	49
2.14. Conjugation Chemistry Using EDC with Sulfo-NHS .....	52
2.15. Experimental Design .....	55
2.15.1. Brief Background.....	55
2.15.2. Review of A $\beta$ Studies from Published Literature.....	57
2.15.2. Summary .....	89
2.15.3. Design of Experiments: Guidelines.....	92

3.	SIALIC ACID CONJUGATED CHITOSAN FOR THE ATTENUATION OF AMYLOID-BETA TOXICITY: DEGREE OF LABELING STUDY.....	97
3.1.	Introduction.....	97
3.2.	Materials and Methods.....	99
3.2.1.	Materials.....	99
3.2.2.	Peptide Preparation.....	99
3.2.3.	Cell Culture.....	99
3.2.4.	Synthesis and Purification of Sialic Acid Labeled Chitosan.....	100
3.2.5.	Verification and Quantification of the Extent of Sialic Acid Conjugation.....	101
3.2.6.	MTT Toxicity Assay.....	103
3.2.7.	Statistical Analysis.....	103
3.3.	Results and Discussion.....	104
3.3.1.	Verification of Sialic Acid Conjugation to Chitosan.....	104
3.3.2.	Quantification of Sialic Acid Conjugation to Chitosan.....	106
3.3.3.	Intrinsic Toxicity of Sialic Acid-Chitosan Complexes and Unlabeled Chitosan.....	109
3.3.4.	A $\beta$ Toxicity Attenuation Studies of Sialic Acid-Chitosan Complexes and Unlabeled Chitosan.....	111
3.4.	Statistical Analysis of Intrinsic Toxicity and A $\beta$ Toxicity Attenuation Data.....	114
3.4.1.	Intrinsic Toxicity of Sialic Acid-Chitosan Complexes and Unlabeled Chitosan.....	117
3.4.2.	A $\beta$ Toxicity Attenuation Studies of Sialic Acid-Chitosan Complexes and Unlabeled Chitosan.....	127
3.4.3.	Our Hypothesis for the Observed Results.....	138
3.4.4.	Summary of the Statistical Analysis.....	140
4.	EVALUATION OF SIALIC ACID-ANALOGS FOR THE ATTENUATION OF AMYLOID-BETA TOXICITY.....	145
4.1.	Introduction.....	145
4.2.	Materials and Methods.....	146
4.2.1.	Materials.....	146
4.2.2.	Peptide Preparation.....	147
4.2.3.	Cell Culture.....	147
4.2.4.	Synthesis and Purification of Sugar-Chitosan Complexes.....	148
4.2.5.	Quantification of KDN Present in KDN-Chitosan Complex.....	149
4.2.6.	Quantification of GA Present in GA-Chitosan Complex.....	150
4.2.7.	MTT Toxicity Assay.....	151
4.2.8.	Verification of Sugar Conjugation to Chitosan.....	151
4.2.9.	Statistical Analysis.....	152
4.3.	Results and Discussion.....	152
4.3.1.	Verification of Sugar Conjugation to Chitosan.....	152
4.3.2.	Quantification of Sugar Conjugation to Chitosan.....	155
4.3.3.	Intrinsic Toxicity of Sugar Analogs and Sugar-Chitosan Complexes.....	158
4.3.4.	Efficacy of Sugar Analogs and Sugar-Chitosan Complexes to Attenuate A $\beta$ Toxicity.....	162
4.4.	Statistical Analysis of Intrinsic Toxicity and A $\beta$ Toxicity Attenuation Data.....	166

4.4.1.	Intrinsic Toxicity of Pure Sugar Analogs.....	169
4.4.2.	Intrinsic Toxicity of Sugar-Chitosan Complexes .....	176
4.4.3.	A $\beta$ Toxicity Attenuation Properties of Pure Sugar Analogs.....	182
4.4.4.	A $\beta$ Toxicity Attenuation Properties of the Sugar-Chitosan Complexes .....	187
4.4.5.	Summary of the Statistical Analysis.....	194
5.	CONCLUSIONS .....	201
5.1.	Introduction.....	201
5.2.	Sialic Acid Labeled Chitosan for the Attenuation of A $\beta$ Toxicity.....	202
5.3.	Evaluation of Sialic Acid Analogs for the Attenuation of A $\beta$ Toxicity .....	204
6.	FUTURE WORK .....	208
	REFERENCES .....	211
	APPENDIX: STATISTICAL OUTPUT DATA BY TUKEY'S TEST.....	235
	VITA.....	296

## LIST OF TABLES

Table 1: Common neurodegenerative diseases caused by deposition of misfolded or aggregated proteins .....	14
Table 2: Characteristics of drugs approved for AD [43, 140, 141]. .....	38
Table 3: SH-SY5Y viabilities after 24h incubation for different A $\beta$ concentrations and different A $\beta$ aggregation times, from ref. [196].....	64
Table 4: SH-SY5Y viabilities after different incubation times with A $\beta$ at different concentrations, from ref. [201] .....	65
Table 5: SH-SY5Y viabilities assessed after 24h of addition of 100 $\mu$ M A $\beta$ (40) aggregated according to different conditions, from ref. [199] .....	74
Table 6: PC-12 viabilities exposed to two batches to A $\beta$ (40) aggregated under similar conditions, from ref [198].....	78
Table 7: SH-SY5Y viability after 24h aggregation with different concentration of A $\beta$ and different viability assays, from ref. [183].....	82
Table 8: Percentage labeling of chitosan by sialic acid from EDC chemistry.....	107
Table 9: Percentage labeling of chitosan by different sugars .....	157

## LIST OF FIGURES

Figure 1: Theoretical hypothesis for the progression of Alzheimer's disease, showing the bottleneck region.....	5
Figure 2: Our hypothesis to prevent A $\beta$ toxicity .....	7
Figure 3: Metabolism of APP and the formation of A $\beta$ peptide.....	16
Figure 4 : Sequences of Alzheimer's A $\beta$ peptides .....	18
Figure 5: Mechanism of amyloid cascade hypothesis.....	21
Figure 6: Modes of A $\beta$ aggregation: Believed to be a nucleation dependent process .....	26
Figure 7: Chemical structures of major gangliosides present in neurons .....	32
Figure 8: Hypothetical mechanism of ganglioside-mediated A $\beta$ fibrillization. ....	36
Figure 9: Structure of Chitosan.....	47
Figure 10: Structure of different sugars conjugated to chitosan.....	51
Figure 11: Conjugation Mechanism using EDC chemistry with Sulfo-NHS .....	54
Figure 12: Results from typical PC-12 cell toxicity tests illustrated to denote lot-by-lot variability .....	58
Figure 13: Normalized viability of SH-SY5Y cells as a function of time of incubation of cells with 100 $\mu$ M A $\beta$ (40), viability from different assays .....	83
Figure 14: Normalized viability of SH-SY5Y cells as a function of A $\beta$ concentration assessed by different assays.....	84
Figure 15: Normalized viability of A $\beta$ (40) incubated for various periods of time as obtained from the PI (A) and annexin-PE/7AAD (B) assay .....	85
Figure 16: Direct toxicity of A $\beta$ (40) in high density rat hippocampal cultures. ....	88
Figure 17: FTIR results of sialic acid conjugated chitosan complex B (dashed line) and pure chitosan (solid line). ....	105
Figure 18: FTIR results of sialic acid conjugated chitosan complex F (dashed line) and pure chitosan (solid line) .....	105

Figure 19: FTIR results of sialic acid conjugated chitosan complex G (dashed line) and pure chitosan (solid line) .....	106
Figure 20: Results of Warren assay on pure sialic acid – standard curve.....	108
Figure 21: Saturation curve for EDC labeling of chitosan.....	109
Figure 22: Intrinsic toxicity of sialic acid chitosan complexes (A to G) and naïve chitosan exposed to SH-SY5Y .....	110
Figure 23: Attenuation of 50µM Aβ toxicity by sialic acid chitosan complexes (A to G) and Naïve chitosan.....	113
Figure 24: Grouping example- Statistical analysis and graph for KDN complex intrinsic toxicity data.....	116
Figure 25: Unlabeled chitosan=0%: Intrinsic toxicity studies .....	119
Figure 26: Sialic acid-chitosan complex A =7.8% labeling: Intrinsic toxicity studies .....	120
Figure 27: Sialic acid-chitosan complex B =14.1% labeling: Intrinsic toxicity studies .....	120
Figure 28: Sialic acid-chitosan complex C =17.6% labeling: Intrinsic toxicity studies .....	121
Figure 29: Sialic acid-chitosan complex D = 24.1% labeling: Intrinsic toxicity studies.....	122
Figure 30: Sialic acid-chitosan complex E = 37.3% labeling: Intrinsic toxicity studies .....	122
Figure 31: Sialic acid-chitosan complex F = 40.7% labeling: Intrinsic toxicity studies.....	123
Figure 32: Sialic acid-chitosan complex G=48% labeling: Intrinsic toxicity studies .....	124
Figure 33: All sialic acid-chitosan complexes: Intrinsic toxicity compared at 1µM, 3µM, 5µM.....	125
Figure 34: All sialic acid-chitosan complexes: Intrinsic toxicity compared at 10µM, 20µM, 30µM .....	126
Figure 35: Unlabeled chitosan = 0% labeling: Aβ toxicity attenuation studies .....	128
Figure 36: Sialic acid-chitosan complex A = 7.8% labeling: Aβ toxicity attenuation studies ....	130
Figure 37: Sialic acid-chitosan complex B = 14.1% labeling: Aβ toxicity attenuation studies ..	130
Figure 38: Sialic acid-chitosan complex C = 17.6% labeling: Aβ toxicity attenuation studies ..	131

Figure 39: Sialic acid-chitosan complex D = 24.1% labeling: A $\beta$ toxicity attenuation studies ..	132
Figure 40: Sialic acid-chitosan complex E = 37.3% labeling: A $\beta$ toxicity attenuation studies...	132
Figure 41: Sialic acid-chitosan complex F = 40.7% labeling: A $\beta$ toxicity attenuation studies...	133
Figure 42: Sialic acid-chitosan complex G = 48% labeling: A $\beta$ toxicity attenuation studies .....	134
Figure 43: All sialic acid-chitosan complexes at 1 $\mu$ M, 3 $\mu$ M, 5 $\mu$ M: A $\beta$ toxicity attenuation studies .....	135
Figure 44: All sialic acid-chitosan complexes at 10 $\mu$ M, 20 $\mu$ M, 30 $\mu$ M: A $\beta$ toxicity attenuation studies .....	137
Figure 45: FTIR spectra for unlabeled chitosan (solid blue line) and KDN-chitosan complex (dashed red line).....	153
Figure 46: FTIR spectra for unlabeled chitosan (solid blue line) and GA-chitosan complex (dashed red line).....	154
Figure 47: FTIR spectra for unlabeled chitosan (solid blue line) and Pyran-chitosan complex (dashed red line).....	154
Figure 48: FTIR spectra for unlabeled chitosan (solid blue line) and CHC-chitosan complex (dashed red line).....	155
Figure 49: Results for the quantification of Keto-deoxynonulosonic acid (KDN)-chitosan complex .....	156
Figure 50: Results for quantification of Galacturonic acid (GA)-chitosan complex .....	157
Figure 51: Toxicity of sugar-analogs exposed to SH-SY5Y .....	159
Figure 52: Toxicity of sugar-chitosan complexes exposed to SH-SY5Y .....	160
Figure 53: Comparison of the intrinsic toxicity before and after complexation of sugars .....	161
Figure 54: Attenuation of 50 $\mu$ M A $\beta$ toxicity by sugar analogs .....	163
Figure 55: Attenuation of 50 $\mu$ M A $\beta$ toxicity by sugar-chitosan complexes.....	164
Figure 56: Grouping example: Statistical analysis and graph for KDN-complex intrinsic toxicity data.....	168
Figure 57: KDN analog- Intrinsic toxicity studies .....	171

Figure 58: GA analog- Intrinsic toxicity studies .....	172
Figure 59: Pyran analog- Intrinsic toxicity studies.....	172
Figure 60: CHC analog- Intrinsic toxicity studies.....	173
Figure 61: All sugar analogs at 3 $\mu$ M, 5 $\mu$ M, 10 $\mu$ M- Intrinsic toxicity studies .....	174
Figure 62: All sugar analogs at 20 $\mu$ M, 30 $\mu$ M, 40 $\mu$ M, 48 $\mu$ M- Intrinsic toxicity studies.....	175
Figure 63: KDN-chitosan complex- Intrinsic toxicity studies .....	177
Figure 64: GA-chitosan complex- Intrinsic toxicity studies.....	178
Figure 65: Pyran-chitosan complex- Intrinsic toxicity studies .....	179
Figure 66: CHC-chitosan complex- Intrinsic toxicity studies .....	180
Figure 67: All sugar-chitosan complexes at 3 $\mu$ M, 5 $\mu$ M, 10 $\mu$ M- Intrinsic toxicity studies.....	181
Figure 68: All sugar-chitosan complexes at 20 $\mu$ M, 30 $\mu$ M, 40 $\mu$ M, 48 $\mu$ M- Intrinsic toxicity studies .....	182
Figure 69: KDN analog: A $\beta$ toxicity attenuation studies.....	183
Figure 70: GA analog: A $\beta$ toxicity attenuation studies.....	184
Figure 71: Pyran analog: A $\beta$ toxicity attenuation studies .....	185
Figure 72: CHC analog: A $\beta$ toxicity attenuation studies .....	185
Figure 73: All sugar analogs at 3 $\mu$ M, 5 $\mu$ M, 10 $\mu$ M: A $\beta$ toxicity attenuation studies .....	186
Figure 74: All sugar analogs at 20 $\mu$ M, 30 $\mu$ M, 40 $\mu$ M, 48 $\mu$ M: A $\beta$ toxicity attenuation studies ...	187
Figure 75: KDN-chitosan complex: A $\beta$ toxicity attenuation studies .....	188
Figure 76: GA-chitosan complex: A $\beta$ toxicity attenuation studies .....	189
Figure 77: Pyran-chitosan complex: A $\beta$ toxicity attenuation studies.....	190
Figure 78: CHC-chitosan complex: A $\beta$ toxicity attenuation studies.....	191
Figure 79: All sugar-chitosan complexes at 3 $\mu$ M, 5 $\mu$ M, 10 $\mu$ M: A $\beta$ toxicity attenuation study..	192

Figure 80: All sugar-chitosan complexes at 20 $\mu$ M, 30 $\mu$ M, 40 $\mu$ M, 48 $\mu$ M: A $\beta$  toxicity attenuation study.....193

## ABSTRACT

There is evidence that amyloid-beta ( $A\beta$ ) toxicity is mediated through interactions and binding with neuronal surface sialic acids in Alzheimer's disease (AD). The binding affinity is higher if the sialic acids are clustered and toxicity of  $A\beta$  was attenuated by removal of neuronal sialic acids. Thus, interfering with cell membrane- $A\beta$  binding using biomimetics that could reproduce the clustered sialic acid structure could present us with a potential target for therapeutic intervention in AD.

Based on this hypothesis, we developed several multifunctionalized sialic acid labeled chitosan compounds of different valency, or number of sialic acid per chitosan molecule, to attenuate  $A\beta$  toxicity. A cross-linker, 1-Ethyl-3-(3-dimethylaminopropyl) carbodiimide hydrochloride (EDC) was used, which provided control over the degree of labeling of chitosan. After characterization, the ability of the complexes to attenuate toxicity of  $A\beta(1-40)$  was investigated *in vitro*. We found that all linear polysialylated complexes showed significant ability to attenuate  $A\beta$  toxicity, with optimum balance between intrinsic toxicity and protection around 37% labeling of chitosan. Moreover, unlabeled chitosan also showed some level of protective properties to the labeled compounds.

Then, four biological sugars that are structural analogs of sialic acid (N-Acetylneuraminic acid) were used to decorate approximately 35% of the chitosan backbone using EDC chemistry. After characterization, the ability of these sugar complexes to attenuate toxicity of  $A\beta$  was investigated *in vitro*. We investigated whether sugars other than sialic acid provided better toxicity attenuation and attempted to understand the impact of sub-structures or unique -R groups of sialic acid and its analogs in  $A\beta$  toxicity attenuation. Our results show that oxygen substitution in the ring structure contributes to the intrinsic toxicity but also plays a role in  $A\beta$

toxicity attenuation. Similarly, the multi -OH tail present in sialic acid plays an important role in A $\beta$  toxicity attenuation.

This approach of designing effective biomimetics and of determining the structure-activity relationship has relevance with respect to the development of new intelligent class of therapeutic agents for AD. Although this work focuses on AD, this approach can be extended to other diseases involving misfolded proteins.

# 1. OVERVIEW

## 1.1. Introduction

At a medical conference in 1906, a German neurologist, Dr. Alois Alzheimer described the autopsy findings of a 51 year old patient who had died from what he described as a course of progressive dementia[1, 2]. Today, more than a century after it was first described, this condition, called “Alzheimer’s disease”, affects almost 37 million people worldwide with an estimated cost of healthcare exceeding a staggering \$600 billion, the bulk attributed to long-term care for patients unable to care for themselves[3, 4]. Statistics indicate that almost 10% of people above 65 years and 50% of people above 85 years will be affected by Alzheimer’s disease (AD). Additionally, AD has a very slow progression, so, with the rising life expectancy, the prevalence of AD continuously increases, leading to an untenable burden on the healthcare system in terms of both services and cost.

At the present time, there are no absolute causal pathways defined or techniques available for definitive diagnosis of AD, although several theories are hypothesized. Plus, there is no known cure for AD, with the medicines currently available being simply symptom relieving and do not stop or hinder the progression of the disease.

The only definite confirmation of AD comes from the autopsy of the affected brain. The affected brains show massive death of neurons and the loss of synaptic connections with the abnormal presence of neurofibrillary tangles and senile plaques [5-9]. The primary species identified in the senile plaques is a 39 to 43 amino acid long peptide, called amyloid-beta ( $A\beta$ ). Even though  $A\beta$  is necessary for the proper functioning of the human brain, its level drastically rises in an AD patient. The enzymes  $\gamma$ -secretase and  $\beta$ -secretase cleave the amyloid precursor protein (APP) generating  $A\beta$  [10, 11]. The unique feature of  $A\beta$  is that the peptide is

amphipathic, with a hydrophobic region (C-terminal) with residues 24 to 42 and a hydrophilic region (N-terminal) with residues 1 to 28[12]. This allows A $\beta$  to self-assemble and form aggregates with a host of different morphologies (dimers, trimers, dodecamers, filaments, protofibrils, amyloid-beta derived diffusible ligands (ADDLs), and fibrils). Numerous studies have confirmed that these A $\beta$  species play a critical role in the pathogenesis of AD [8, 9, 13-16]. Earlier studies indicated that the insoluble fibrils were the toxic species. However, recent data is contrasting and suggests that the soluble small A $\beta$  oligomers are the neurotoxic species, with the amyloid fibrils being the protective mechanism. However, the exact toxic species is not agreed upon, and currently, the aggregated A $\beta$  species such as oligomers, ADDL's and protofibrils are the most pursued targets for the diagnostic and therapeutic treatment of AD.

Researchers have postulated several mechanisms and hypotheses to explain the pathways by which A $\beta$  is toxic to the neurons. A $\beta$  is known to cause synaptic dysfunction, neuroinflammation, oxidative stress, decrease membrane fluidity, lipid peroxidation and microglial inflammation, which leads to cell death. Evidence has shown that A $\beta$  generates reactive oxygen species and nitric oxide that are extremely harmful to cells [17]. A $\beta$  has been known to disrupt Ca<sup>2+</sup> and K<sup>+</sup> homeostasis leading to the formation of ion channels in the cells [17, 18]. It has been shown that A $\beta$  binds to specific cell receptors that eventually prove detrimental to cells. Thus, evidence tells that the mechanism of A $\beta$  toxicity is a very complex phenomenon with many interrelated or simultaneous mechanisms taking place. Another mechanism by which A $\beta$  can exert toxicity is through interactions with the neuronal membrane. It is these interactions that will be the focus of this work.

For A $\beta$  to be toxic to cells, an interaction (either direct or indirect) between the toxic species and neuronal membrane must exist. Studies have linked cell membranes or their

components to A $\beta$  generation, self-assembly and in toxicity to neurons[4]. Thus, there is a variety of evidence that points to the harmful interactions between the cell membranes and A $\beta$ . Particularly, several glutamate receptors, as well as cellular prion protein (PrPc) have been identified to which A $\beta$  oligomers bind. These receptors reside or partition into cholesterol rich microdomains that are a part of cell membranes called lipid-rafts. There is evidence that shows that membrane environment modulates the actions of secretases, with the decrease in membrane fluidity triggering the amyloidogenic processing of APP. It is hypothesized that A $\beta$  interacts with the cell membranes through hydrogen bonding and electrostatic interactions in addition to specific receptor binding. The first physical evidence of this behavior result from the investigation by Yanagisawa et al., which showed a ganglioside bound A $\beta$ , specifically, GM1 ganglioside, in the brains of patients affected by AD [19-23]. This species was not detected in the brains of non-AD patients, pointing to the need of a more detailed investigation into ganglioside-A $\beta$  interactions. Gangliosides are very complex lipids demonstrating strong amphiphillic characteristics due to the presence of a double tailed hydrophobic moiety and a large saccharide hydrophilic head group. The saccharide head group is composed of a wide variety of sugars containing carboxylic groups, of which the sialic acid family of compounds are the most prominent and greatest in numbers compared to other sugars [24, 25]. Thus, gangliosides exhibit strong polar characteristics and are particularly abundant in neuronal cell membrane. Studies have shown that A $\beta$  specifically interacts with the surface sialic acids present on the various gangliosides. Moreover, it is postulated that the interaction and binding affinity is higher if the gangliosides on the cell surface are clustered together [8, 26-30]. It is believed that A $\beta$  interacts with the surface sialic acids leading to the formation of a ganglioside-A $\beta$  moiety (GA $\beta$ ) with an altered conformation that is highly prone to aggregation. This species (GA $\beta$ ) then acts as a seed

for further amyloid aggregation [23, 31, 32]. Another argument in the favor of the importance of sialic acids in AD pathology is that the removal of surface sialic acids have been found to attenuate A $\beta$  toxicity towards cells in culture[33].

Now that the etiology of AD has been explained, there are a number of diagnostic and therapeutic approaches that are being investigated. Some major approaches are briefly described below. One approach is to target the secretases with different modulators and inhibitors. However, this is extremely risky, dangerous, and unproven as A $\beta$  is required by the healthy brain and the exact roles of the different secretases have not been established. A number of A $\beta$  aggregate inhibitors are also under review. However, this approach is still suspect, as the exact toxic species in AD has not been established. Thus, it suffices to say that most of the current approaches in AD suffer from the fact that the majority of mechanisms, causes, chain of events and agents involved have not been completely identified or understood. This makes designing effective therapeutics for AD a very difficult task.

## **1.2. Rationale for This Project**

Looking at all the information provided, it is evident that membrane interactions with A $\beta$  are critical in Alzheimer's disease. Additionally, the fact remains that to be toxic to the cells, there has to be some sort of interaction between the neurons and the toxic species of A $\beta$ . Thus, a novel therapeutic approach is being considered to target the theoretical "bottleneck" in the progression of Alzheimer's disease, namely, the interaction of A $\beta$  with neurons. It is our opinion that this is the bottleneck region as there are several theorized environmental conditions that lead to the excessive formation of A $\beta$  species. Additionally, the exact form of A $\beta$  (oligomers, protofibrils, ADDLs or fibrils) that is toxic to the cells is not yet proven.

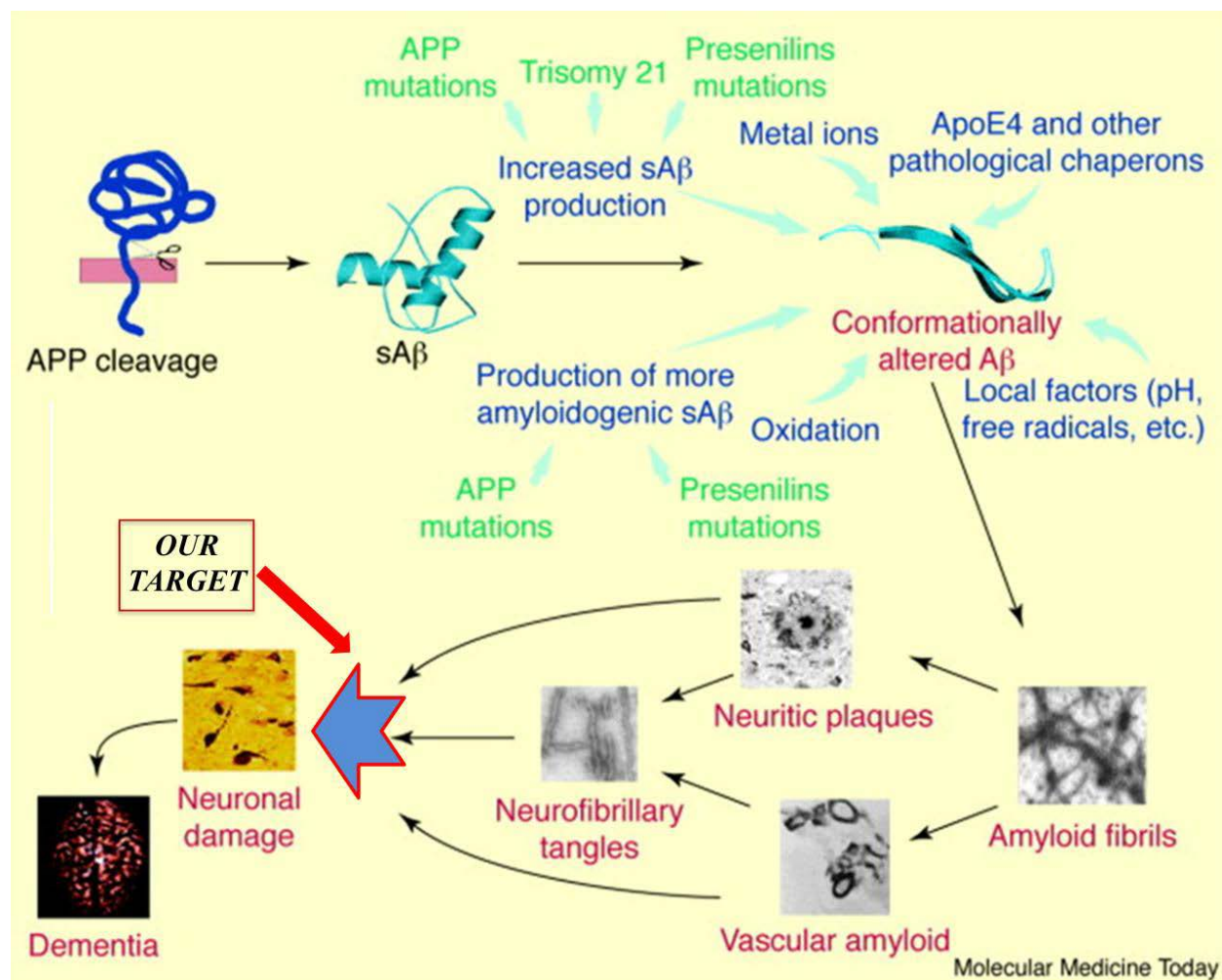


**Figure 1: Theoretical hypothesis for the progression of Alzheimer’s disease, showing the bottleneck region**

The hypothesis is that there are several conditions and factors in AD that are still unclear, unknown in the pathogenesis of AD. However, there must be some sort of A $\beta$ -cell interaction for the toxic species to be fatal to cells. Thus, this represents the target bottleneck region, which we plan to attack. If we prevent cellular interaction with A $\beta$ , we prevent toxicity associated with A $\beta$ . Figure modified from [34].

It is possible that multiple species are toxic with interchangeability between them. Other factors such as APP cleavage, APP mutations, ApoE4 and other chaperons are not well understood and their exact role in AD unproven. However, what is certain is that A $\beta$  interaction occurs through gangliosides or sialic acids and these gangliosides that are clustered.

Our first hypothesis is that aggregated A $\beta$  interacts with neuronal cells and this interaction is eventually fatal. If this is true, then it would be beneficial to develop cell membrane mimicking materials that have antibody-like affinity towards A $\beta$ . The design would be such that these biomimetic's would compete favorably with the cell surface for A $\beta$  binding, reducing the free A $\beta$  left to interact with the neurons, and thus protecting them from A $\beta$  neurotoxicity.

With this postulate as the basis, the first part of the dissertation focuses on the synthesis of membrane mimicking compounds that are multivalent in sialic acid residues. To be multivalent and clustered, we need a backbone molecule on which these sialic acids or sugars can be successfully attached. The approach of using biomimetic's against A $\beta$  has been used earlier with limited success [8, 26]. Thus, as an improvement over previous works and to mimic sialic acids present on gangliosides (especially GM1); sialic acid was conjugated to a chitosan backbone. Chitosan was chosen as a backbone due to its biocompatibility, flexibility and non-toxic nature. Chitosan is also a FDA approved polymer for implantation. This conjugation was achieved using 1-Ethyl-3-(3-dimethylaminopropyl) carbodiimide hydrochloride (EDC) chemistry which facilitated the conjugation of the amine groups of chitosan with the carboxylic acid groups present in sialic acid. Several sialic acid-chitosan complexes of different valency, number of sialic acids per chitosan molecule, were synthesized to attenuate the toxicity of A $\beta$  *in vitro*. Numerous studies have stressed the importance of sialic acid clustering on neuronal cell membranes to be critical in A $\beta$  binding. Thus, the use of a flexible backbone, such as chitosan, will allow for the necessary flexibility, allowing for the sialic acids to effectively cluster. This critical improvement will also allow us to predict the cluster size needed for the optimal protection from A $\beta$  toxicity. Additionally, sialic acid decorated chitosan will closely mimic neuronal cell adhesion molecules (NCAM), providing another mimetic target for A $\beta$ . The

hypothesis is presented in Figure 2. The development of such novel sialic acid conjugated chitosan complexes and their toxicity studies with and without A $\beta$  are described in Chapter 3.

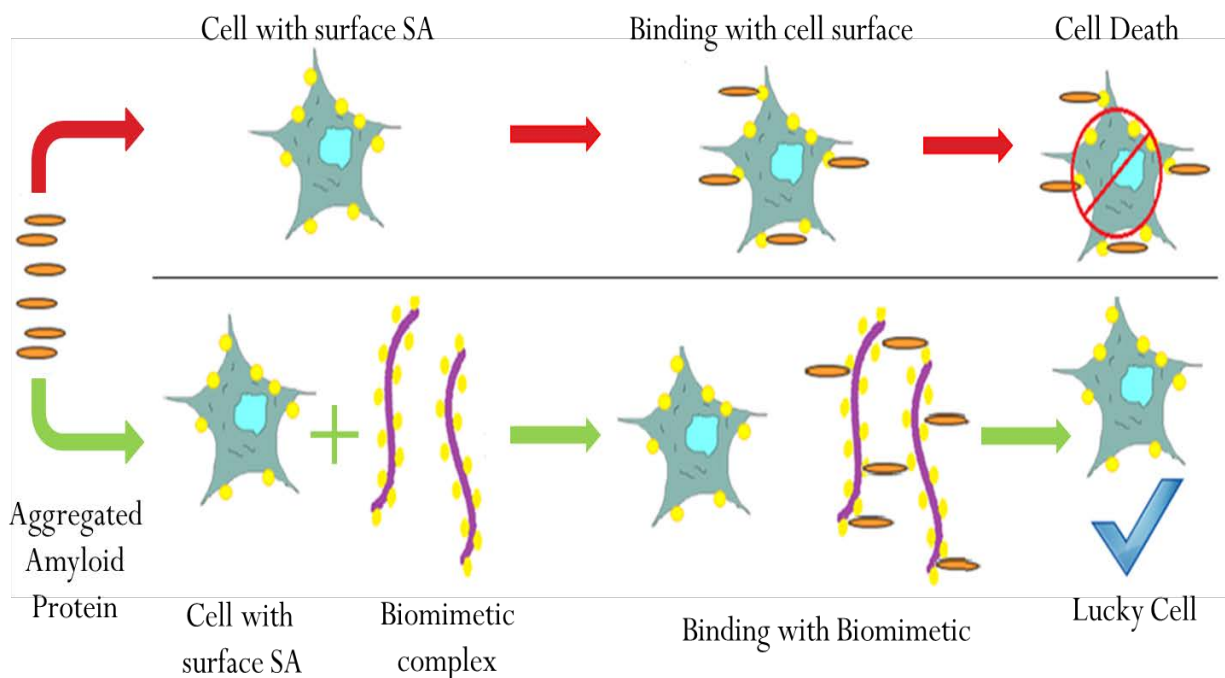


**Figure 2: Our hypothesis to prevent A $\beta$  toxicity**

Aggregated A $\beta$  peptide recognizes the sialic acids on cell membranes and binds to them causing cell death. Introduction of a biomimetic compound having higher affinity towards A $\beta$  interferes with the cellular-A $\beta$  binding thereby preventing toxicity. Introduction of a biomimetic allows us to target the bottleneck region in AD pathology.

The results from the work with sialic acid conjugated chitosan complexes indicated that we were successful in mimicking the neuronal cell membrane as all the compounds tested showed significant ability to attenuate the toxicity of A $\beta$ . The study also allowed us to predict the sialic acid clustering, or the degree of sialylation, necessary for optimum toxicity attenuation of A $\beta$ . Interestingly, unlabeled chitosan also showed toxicity attenuation properties which prompted us to investigate other biological sugars that might show similar or greater protective properties against A $\beta$ .

The second part of the project, described in Chapter 4, will serve multiple purposes. Chitosan is again selected as the backbone molecules because of excellent results shown in earlier results (see Chapter 3). By conjugating sugars to a chitosan backbone, we will be able to benefit from its protective effects, its flexibility, and biocompatibility. The criteria for selecting the biological sugars are based on the structure of sialic acid. Thus, in this work, in addition to sialic acid (N-acetylneuraminic acid); 2-Keto-3-deoxy-nononic acid (KDN), Galacturonic acid (GA), Tetrahydropyran-2-carboxylic acid (Pyran) and Cyclohexanecarboxylic acid (CHC) were conjugated to chitosan and characterized.

The work described from Chapter 4 will also help to identify which unique -R groups, or core structures of N-Acetylneuraminic acid, are involved in toxicity attenuation. This is critical as it will be possible to predict which subgroup of sialic acid on neuronal membranes is necessary for A $\beta$  binding. It also addresses the question whether sugars other than sialic acid can be effectively used to attenuate the toxicity of A $\beta$ . This will shed more light on the type of interactions that occur between A $\beta$  and cell membranes. It will allow for the development of specific polysaccharide therapeutic targets against the A $\beta$  peptide in AD. The major conclusions from all the studies are presented in Chapter 5. Lastly, Chapter 6 suggests possible future directions that could be investigated based on this work.

## 2. LITERATURE REVIEW

According to the latest statistics from Alzheimer's Association, AD is the 5<sup>th</sup> leading cause of death in Americans over the age of 65 years with an estimated 5.4 million people currently suffering from this fatal disease. Total payments in 2011 for health care, long-term care, and hospice services for people aged  $\geq 65$  years with AD and other dementias are expected to be \$183 billion (not including the contributions of unpaid caregivers). Projections estimate 11 to 16 million people will be affected in the US alone with AD by the mid-century 2050[35]. Thus, unless medical breakthroughs identify ways to treat or cure AD, the burden it will place on the healthcare system will be tremendous. Alzheimer's disease has a long and stressful clinical course in which the patients need special attention, ranging from home care to special nursing homes. Apart from its impact on the patients, this disease puts a significant physical, emotional and financial burden to the families and relatives of the patients as well. Due to advances in science and medicine, the general life expectancy is increasing; making AD a problem of epic proportions that needs to be addressed.

Despite over a century of research, AD still remains a complex disease which is not fully understood. There is no definitive cause and no known cure. The challenge now is to identify the cascade of events that lead to AD. The progression of the disease is slow and the average period of survival is eight years, with some patients surviving in excess of twenty years[36]. The course of the disease depends on the health issues and the age at which diagnosis was done for the individual. The progression of the disease can be subcategorized into three stages [37]: In the first stage, some change in personality with decline in short term memory and beginning of faulty judgment is observed. The patient becomes less productive and spontaneous in everyday activities. The next stage results in more memory loss, impairment of language, attention and

visual-spatial and executive functions. Ability of a patient to perform day-to-day activities (eating, washing, grooming) start declining and the patient becomes more dependent on others. Short term memory becomes drastically impaired and only long established memories persist. Sleeping disorders, aggression, verbal outbursts and other troublesome behavior sets in. In the third stage, only fragments of memory remain. All cognitive functions are lost and the patient becomes mute, incontinent and eventually unresponsive to communication. The patient is at the mercy of the caregivers at this stage. Loss of immunity is the typical outcome making patients susceptible to infections which leads to death [38].

Simply put, aging is the main risk factor of the disease [39]. Mutations in the amyloid precursor protein (APP) gene on chromosome 21, the presenilin 1 (PS1) gene on chromosome 14 and the presenilin 2 (PS2) gene on chromosome 1 have been implicated in AD [40, 41]. Presence of apolipoprotein E (ApoE) e4 allele was shown to increase the risk of getting AD in conjunction with lowering the age of onset of the disease [36, 42]. Other risk factors include decreased reserve capacity of brain [43], poor linguistic ability in early life [44], low mental and leisure activity, traumatic head injury, cardiovascular diseases like hyperlipidemia, hypertension, diabetes, obesity etc. See [41] for additional review.

The affected brain in AD shows the presence of massive neuronal death and the loss of synaptic connections [45]. The progression of AD starts in the hippocampus (an area of brain responsible for new memories) [36], then spreads to the association areas of the cerebral complex (responsible for language and reasoning) and finally to the neocortex (responsible for the sensory and motor area functionalities). This progression results in tissue loss throughout the brain thereby causing the brain to shrink in size and also the enlargement of the ventricles (fluid filled spaces within the brain). Proteinaceous deposits are observed in both the intracellular and

extracellular compartments of the brain. Researchers have shown that the intracellular deposits are composed of neurofibrillary tangles (NFT) which are primarily formed due to the hyperphosphorylation of the tau protein [5, 46]. NFTs are intra-neuronal bundles of paired helical filaments formed by the microtubules, but they are not specific to AD and are found in various other neurodegenerative conditions such as Frontotemporal dementia, Hallervorden-Spatz disease etc. [47]. Amyloid plaques are extracellular aggregates of the A $\beta$  peptide and many researchers have found a direct correlation between the presence of these plaques and the severity of AD [10, 48]. Earlier, the large insoluble plaques were thought as the toxic species, but recent evidence suggests that it is the small oligomers that may be the toxic species. The real insight into the disease was after 1984, when Glenner and Wong identified the amino acid sequence of A $\beta$  peptides [49].

In the treatment of AD, many researchers are targeting the production and the aggregation process of A $\beta$ . Since the identification of AD as a unique condition, a number of theories and hypotheses have been put forward. The two major hypotheses that have been postulated to explain the molecular mechanisms of AD are the cholinergic hypothesis and the amyloid cascade hypothesis [10, 48]. The amyloid cascade hypothesis is relevant to the work done in this thesis and is discussed in the later sections. Also, there is much evidence that points to the central role of A $\beta$  in AD that supports the amyloid cascade hypothesis. As of now, none of the hypotheses are perfect and can satisfactorily explain AD but, they provide a conceptual framework and a valuable roadmap for all researchers. With more and more advances in science, the missing links and pieces are being identified. This will be a valuable tool which will aid researchers in accurate diagnosis and in designing therapeutics for the treatment and cure of AD. Finally, progress in defeating this disease is hampered by the fact that AD is a very complex

disease whose exact mechanisms and pathways still remain a mystery. The following sections will be devoted to understanding some of the aspects of AD with an aim to design better therapeutic for its treatment.

## **2.1. Hallmarks of Alzheimer's Disease**

Researchers have identified the two main hallmarks of AD: the deposition of neurofibrillary tangles (NFT) composed of tau protein and the aggregation deposition of senile plaques comprised majorly of the amyloid- $\beta$  peptide.

### **2.1.1. Tau Protein**

Microtubules play an important role in maintaining the structural and physiological integrity of neurons. The biological activity of tau in promoting assembly and stability of the microtubules is regulated by its degree of phosphorylation [46]. Evidence has shown that abnormal hyperphosphorylation of tau protein disrupts the microtubule structure resulting in the aggregation of tau into bundles of paired helical filaments (PHF), twisted ribbons and/or straight filaments collectively called neurofibrillary tangles [46, 50]. Glycogen synthase kinase-3 (GSK-3) and cyclin dependent protein kinase-5 (cdk5) are the major protein kinases that have been implicated in the abnormal hyperphosphorylation of tau [7, 46, 50]. This abnormal deposition of tau is observed in several other human neurodegenerative disorders and not just in AD. The NFTs are known to be toxic to the neurons, which slowly and progressively lead to their death. Studies from different groups suggests that hyperphosphorylation of tau can be considered as one of the primary cause of AD, but not the fundamental one [7, 46, 51, 52]. Thus, inhibition of abnormal hyperphosphorylation of tau protein is a promising, but not ideal approach for the development of therapeutic drugs [53]. Drugs which inhibit GSK-3 and cdk5 have been

developed by the industry and many of them are at different phases of clinical trials. Other strategies include inhibiting the misfolding of tau and to directly stabilize the microtubules. As hyperphosphorylated tau is toxic by sequestering, normal mitogen activated proteins (MAPs), small molecules that can compete with this sequestering are being developed that can effectively attenuate toxicity of tau [7, 53]. For review see [46, 53-56].

### **2.1.2. Amyloid-beta Peptide**

A common pathogenic mechanism in many different neurodegenerative disorders including AD is the aggregation and deposition of misfolded proteins, mostly in the brain. As summarized in Table 1, nearly every major neurodegenerative disease is characterized by the insidious accumulation of insoluble filamentous aggregates of normally soluble proteins in the central nervous system (CNS). These diseases are usually grouped together as the filamentous aggregates show similar ultra-structural and tinctorial (staining or coloring) properties of amyloid (i.e. ~10nm wide fibrils with crossed  $\beta$ -sheet structures which stain with congo red, thioflavin-S or other related dyes). Hence, they are collectively known as brain amyloidosis. Glenner and Wong first identified the major protein component of vascular amyloid, an approximately 4kDa polypeptide now referred to as  $\beta$ -amyloid protein [12, 49]. This protein was also found to be a major component of amyloid plaques [57, 58] which led to the identification of its precursor, the amyloid precursor protein (APP). Soon after the discovery, the APP gene was cloned allowing the disease to be examined at molecular levels. Subsequently, mapping of mutations in APP gene, the association of AD with Down's syndrome (People with Down's syndrome have an extra copy of chromosome 21, which also contains APP), higher prevalence of AD with increased copy number of APP and the identification of mutations in presenilin 1 (PS1) all confirmed the central role of A $\beta$  peptide and APP in Alzheimer's disease [9, 13, 14].

**Table 1: Common neurodegenerative diseases caused by deposition of misfolded or aggregated proteins**

<b>Disease</b>	<b>Microscopic lesion</b>	<b>Location</b>	<b>Aggregated protein</b>
Alzheimer's Disease	Amyloid Plaque	Extracellular	Amyloid- $\beta$ (A $\beta$ )
	Neurofibrillary Tangle	Intracytoplasmic (neurons)	Tau
	Lewy bodies (seen in Lewy body variant)	Intracytoplasmic (neurons)	$\alpha$ -synuclein
Amyotrophic lateral sclerosis	Hyaline Inclusions	Intracytoplasmic (neurons)	Superoxide dismutase-1 (SOD-1)
Cortical basal degeneration/ progressive supranuclear palsy	Tau positive inclusions	Intracytoplasmic (neurons, oligodendroglia and astrocytes)	Tau
Dementia with Lewy bodies	Lewy bodies	Intracytoplasmic (neurons)	$\alpha$ -synuclein
Huntington Disease	Neuronal Inclusions	Intranuclear (neurons)	Huntington (With Polyglutamine repeat expansion)
Multiple system atrophy	Glial cytoplasmic inclusions	Intracytoplasmic (oligodendroglia)	$\alpha$ -synuclein
Parkinson's Disease	Lewy Bodies	Intracytoplasmic (neurons)	$\alpha$ -synuclein
Pick's Disease	Pick Bodies	Intracytoplasmic (neurons)	Tau
Prion Diseases	Prion Plaques	Extracellular	Protease-resistant prion protein (PrP), Creutzfeldt Jakob disease, Kuru
Amylin (IAPP)			Type 2 diabetes
Calcitonin			Finnish amyloidosis
Transthyretin			Peripheral amyloidosis

## 2.2. Characteristics of A $\beta$ Peptide

Amyloid- $\beta$ , a 39 to 43 amino acid long peptide, is cleaved from the C-terminal region of the membrane spanning glycoprotein, the amyloid precursor protein (APP). APP is found in tissues throughout the body but its primary function is still unknown[11, 36]. A large part of the APP lies in the ectodomain and contains the N-terminus, whereas its C-terminus is located in the cytoplasmic domain. APP has the characteristics of a cell surface receptor and is located on chromosome 21. The A $\beta$  sequence itself comprises part of the ectodomain of the APP and extends into, but not all the way through, the transmembrane domain[59]. A $\beta$  contains 28 amino acids from the extracellular part of APP and the remaining 11 – 15 residues are located in the transmembrane domain [60].

The formation of A $\beta$  peptide is shown in Figure 3. There are two pathways by which the APP can be metabolized in the cells and tissues: the non-amyloidogenic and amyloidogenic pathway [61]. In the non-amyloidogenic pathway, the APP is cleaved by  $\alpha$ -secretase between residues 687 and 688, which releases a soluble extracellular sequence ( $\alpha$ -sAPP) and a membrane attached C-terminal fragment (CTF $\alpha$ ). The CTF $\alpha$  is further cleaved at a variable position (between the C-terminus and residue 712) by  $\gamma$ -secretase in the transmembrane region which releases the harmless, 3kDa, p3 fragment and the APP Intracellular C-terminal domain (ACID) [11, 61]. This cleavage of  $\alpha$ -secretase takes place within the A $\beta$  fragment, thereby preventing the release of the full-length A $\beta$  polypeptide, hence referred to as the non-amyloidogenic pathway[10, 62].

In the amyloidogenic pathway, the A $\beta$  peptide is formed when the APP is cleaved by  $\beta$ -secretase in between residues 671 and 672 followed by cleavage in between the C-terminal and

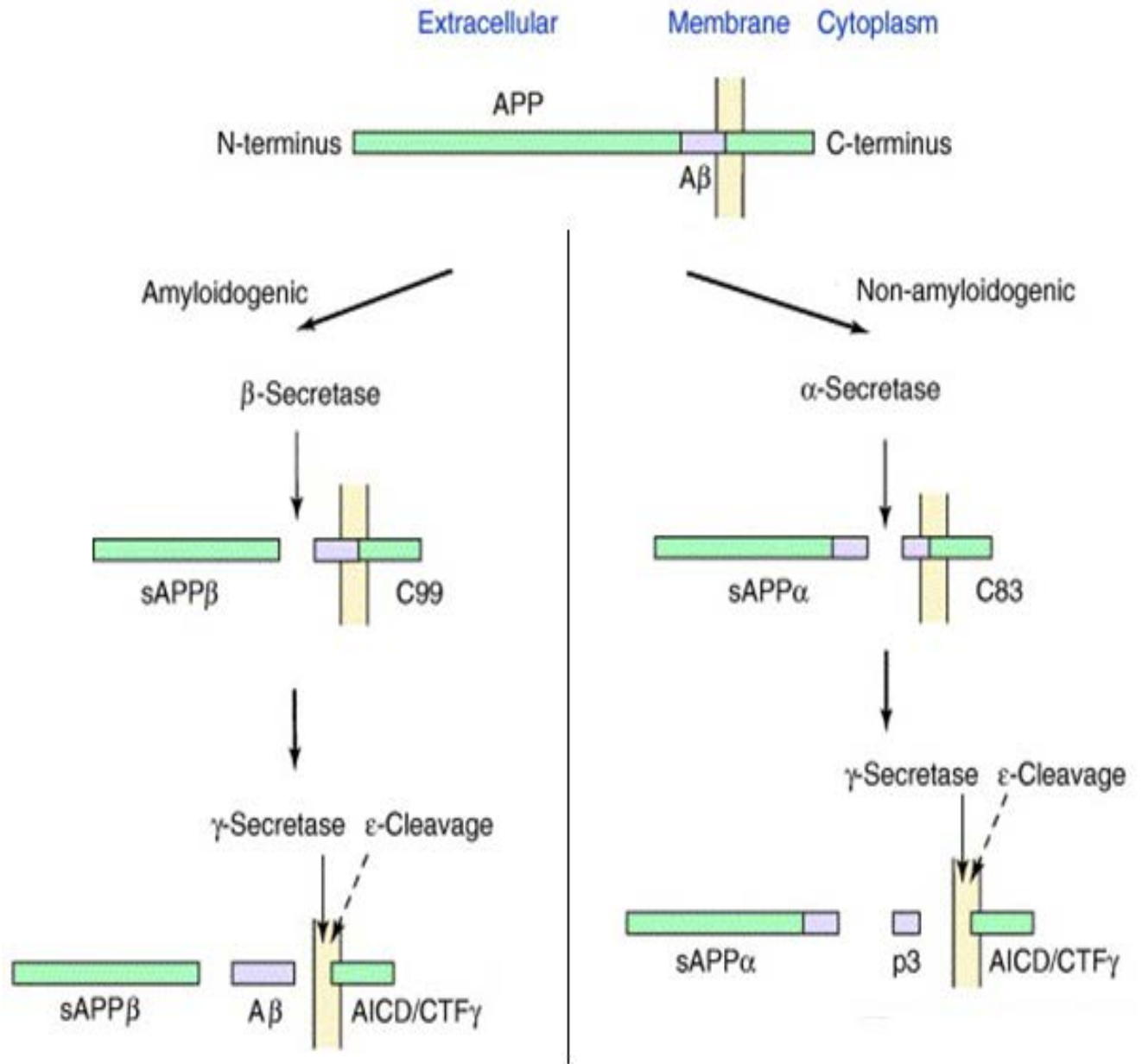


**Figure 3: Metabolism of APP and the formation of A $\beta$  peptide**

In the amyloidogenic pathway, the A $\beta$  peptide is formed when the APP is cleaved by  $\beta$ -secretase in between residues 671 and 672 followed by cleavage in between the C-terminal and residue 712 by  $\gamma$ -secretase Reprinted [63] with permission from Elsevier Ltd.

residue 712 by  $\gamma$ -secretase [10]. Along with the soluble extracellular  $\beta$ -sAPP fragment, several isoforms of A $\beta$  can be produced of which the 40 and 42 amino acid forms are the most common ones [11, 61]. A $\beta$  (1-40) is the predominant species produced, whereas A $\beta$  (1-42) accounts for only 10% of the total secreted A $\beta$ . However, A $\beta$  (1-42) is considerably more prone to aggregation and is regarded as more neurotoxic [57]. The levels of A $\beta$  (1-42) are believed to be elevated in AD. The A $\beta$  (1-40)/A $\beta$  (1-42) ratio can be influenced by several factors such as substrate concentration, PS1, PS2 mutations and effect the formation of senile plaques.

Three different proteases appear to be responsible for the  $\alpha$ -secretase activity: TACE (TNF- $\alpha$  converting enzyme), ADAM-9 and ADAM-10 (a disintegrin and metalloprotease domain protein). The protein responsible for  $\beta$ -cleavage has been identified as a novel transmembrane aspartyl protease BACE1 ( $\beta$ -site APP cleaving enzyme 1) and it is posited that levels of BACE1 increase in AD. As  $\beta$ -secretase is the A $\beta$  producing enzyme, it is the ideal therapeutic target, but complete abolishment of BACE1 has shown deleterious effects in knockout mice [64]. The enzyme  $\gamma$ -secretase is believed to be a complex of at least four proteins: Presenilin 1(PS1) or Presenilin 2 (PS2), Nicastrin, Pen-2 and Aph-1, but other protein components of this complex may also exist. Notch signaling is also affected by  $\gamma$ -secretase [61]. It is the  $\gamma$ -secretase dependent cleavage affected by missense mutations that is predominant cause of excess production of A $\beta$  (1-42). However, all these enzymes have not been completely identified. Much is unknown about the different substrates that they act on. Research has shown that  $\alpha$ -secretase and  $\beta$ -secretase compete for the APP substrate, as increase in one pathway has shown decrease in other pathway and vice-versa [64].

In the A $\beta$  sequence, the first 16 residues (N-terminal region) are found to be largely hydrophilic whereas the remaining residues (C-terminal region) form the hydrophobic domain.

Thus, amphipathic A $\beta$  has propensity towards self-aggregation and accumulation, which is hypothesized to initiate a cascade that triggers complex pathological reactions, eventually leading to AD. The A $\beta$  peptide forms various structures such as dimers, 5-mers, oligomers, protofibrils and fibrils through the aggregation process. It is the central region of A $\beta$ (12-23) that has been implicated as the self-recognition site for the formation of dimmers and higher oligomers [36].

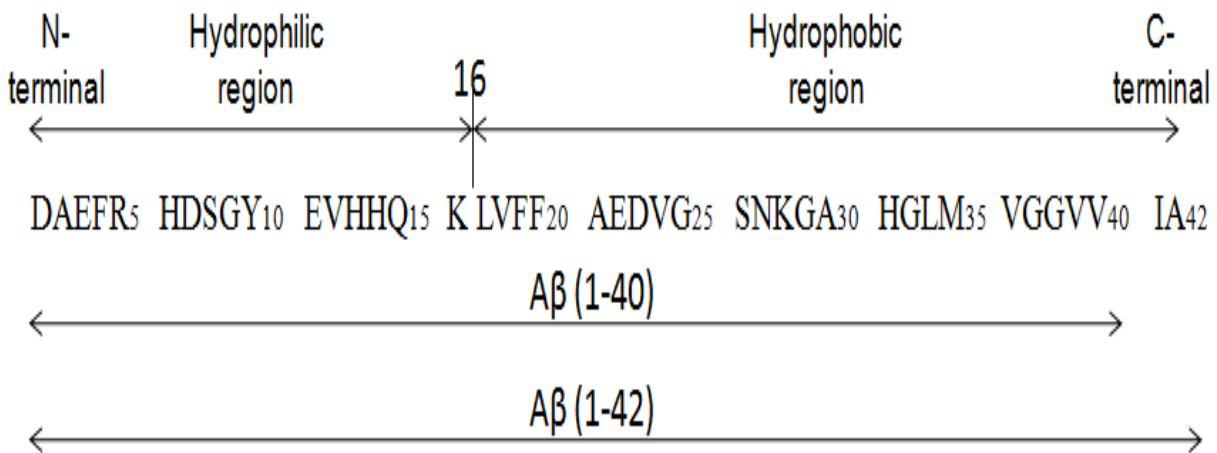


**Figure 4 : Sequences of Alzheimer’s A $\beta$  peptides**

References [12, 36, 49, 65, 66]

### 2.3. Evidence of A $\beta$ Induced Neurotoxicity

It was observed that AD patients showed evidence of extensive oxidative stress [36] caused by reactive oxygen species (ROS) present in the brains [67]. One of the sources of ROS is believed to be the A $\beta$  peptide, which works in conjunction with metal ions and oxygen. It was also noted that oxidative stress also led to the over-expression and misprocessing of the APP

gene, which further led to more production of A $\beta$ . This results in a dangerous cycle that eventually leads to neuronal death and brain degeneration [68].

In addition to oxidative stress, cell membrane permeability is severely compromised by A $\beta$  peptide when it forms calcium permeable ion channels in the plasma cell membrane [36]. These channels allow excess calcium influx and disrupt the normal calcium homeostasis. *In vitro* studies by Lin et.al showed that A $\beta$ (1-42) induced rapid neuritic degeneration at physiological concentrations [69]. Recent evidences have suggested that formation of ion-permeable pores maybe the condition before A $\beta$  is released in the extracellular space.

Researchers have also shown that A $\beta$  causes damage to the blood brain barrier (BBB) through the production of superoxide and the involvement of homocysteine [36]. There is evidence suggesting that A $\beta$  binds to an intracellular polypeptide called ERAB, producing a toxicity level that is directly related to the expression of ERAB [70]. A $\beta$  is involved in decreasing synaptic activity and causing progressive neuronal degradation. The fact that neuronal death is observed in the immediate vicinity of A $\beta$  deposits further implicates A $\beta$  in the pathogenesis of AD [71].

These factors have confirmed the central role of A $\beta$  and APP in the etiology of the Alzheimer's disease, resulting in much of the work in designing effective therapeutics for AD being focused on the A $\beta$  peptide. A number of different hypotheses have been proposed, out of which, the amyloid cascade hypothesis presented by Hardy and Higgins [14] has received the most attention [9]. It is reviewed in the next section.

## 2.4. The Amyloid Cascade Hypothesis

In 1992, Hardy and Higgins presented the “amyloid cascade hypothesis” which explained the pathogenesis of sporadic AD. The hypothesis proposes that the increased production or decreased clearance of A $\beta$  peptide is the fundamental cause of AD. They proposed that A $\beta$  causes the hyperphosphorylation of tau protein which starts the cascade of events leading to the formation of amyloid plaques and neurofibrillary tangles [14].

Since, the amyloid cascade hypothesis has undergone alterations as newer research findings are being presented. A decade after the hypothesis was originally presented, Hardy and Selkoe proposed an amended version which took into consideration mutations in the APP, PS1 or PS2 genes which increases A $\beta$  production. This results in the accumulation of A $\beta$  followed by the oligomerization and deposition of A $\beta$  as plaques. These A $\beta$  plaques cause increased synapse destruction, altered neuronal ionic homeostasis and oxidative injury, which leads to hyperphosphorylation of tau protein and causing the deposition of NFT's and neuronal destruction [14, 43, 72]. Support for this theory includes the fact that AD brains demonstrate extensive A $\beta$  deposition [8]; mutation in the genes implicated in familial forms are all related to APP processing, which increases A $\beta$  production [9, 11, 43, 73]; Down's syndrome patients (who have an extra APP gene) develop A $\beta$  plaques early in life [17, 43, 74] and several *in vitro* studies have also demonstrated the neurotoxic nature of soluble A $\beta$  oligomers in *in vitro* and *in vivo* studies [9, 75].

Still, the amyloid cascade hypothesis is not perfect and the exact mechanism of A $\beta$  toxicity remains elusive as the specific neurotoxic species of A $\beta$  and the nature of its effects on neuronal function have not been defined *in vivo*. Earlier, it was thought that A $\beta$  deposited as

plaques were neurotoxic. However, recent findings demonstrate that soluble pre-fibrillar oligomers of A $\beta$  are likely to be the toxic species that initiate neurodegeneration [17].

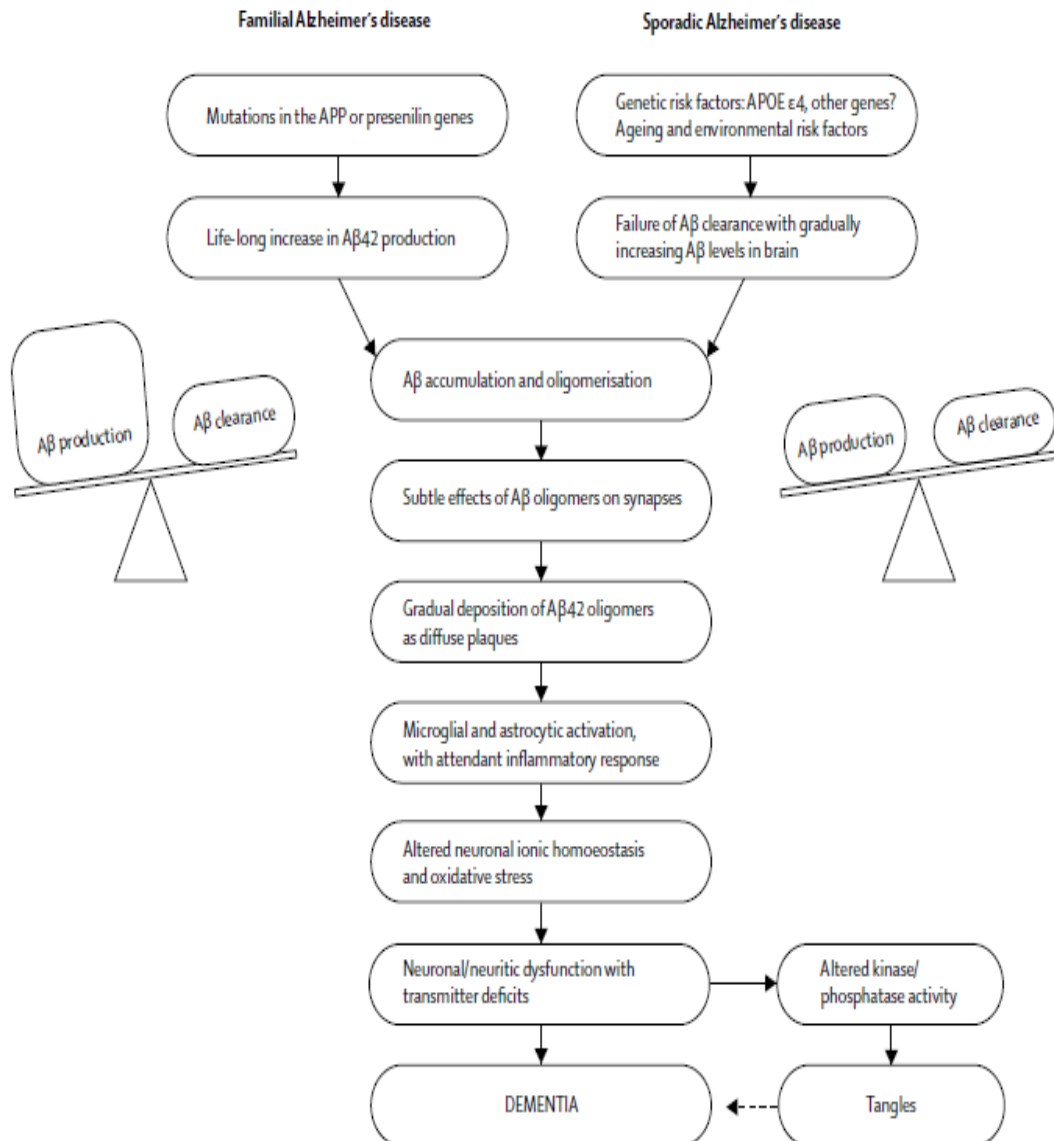


**Figure 5: Mechanism of amyloid cascade hypothesis.**

The central event in the disease pathogenesis is an imbalance between A $\beta$  production and clearance, with increased A $\beta$  production in familial AD and decreased A $\beta$  clearance in sporadic AD. This accumulation of A $\beta$  leads to microglial activation and inflammatory response. The loss of homeostasis and oxidative stress leads to synaptic dysfunction, altered kinase activity affecting tau production. The NFTs and plaques lead to neuronal death and dementia. [43] Reprinted with permission from Elsevier Ltd.

## 2.5. Mechanisms of A $\beta$ Neurotoxicity

A number of mechanisms have been suggested to explain the pathway by which A $\beta$  induces neurotoxicity. Some of them are explained in brief below:

Studies have shown that A $\beta$  binds to a metal substrate generating reactive oxygen species (ROS). A $\beta$  also causes loss of calcium homeostasis, generating reactive nitrogen species (RNS). One plausible explanation is that the A $\beta$  can enter the mitochondria, where it increases the production of ROS, significantly reducing the levels of antioxidants (e.g., vitamins E, C and glutathione) thereby altering the balance in the brain [36]. Depending on the substrate attacked, oxidative stress will manifest as protein, DNA, RNA oxidation or lipid peroxidation [67]. These species are extremely reactive, causing damage to DNA, RNA, lipids and proteins via oxidation. This creates an imbalance which leads to oxidative stress and induces inflammation in the neurons, resulting in death [10, 36, 76].

Another mechanism that has received considerable thought is that A $\beta$  causes synaptic dysfunction. Neurons are connected to each other through junctions called as synapses, and tiny electrical pulses are transmitted through these junctions as a means of communication between two neurons. It is believed that synaptic terminals are critically dependent on levels of cortical A $\beta$ . After the onset of AD, levels of A $\beta$  start rising which leads to synaptic dysfunction, thereby inducing neurotoxicity [17, 77].

Neuroinflammation and microglial activation is another possible mechanism of A $\beta$  induced neurotoxicity. A $\beta$  plaques have been found with clusters of microglia. Microglia are considered to be the brain resident macrophages responsible for the maintenance of homeostasis within the brain. They are activated when the brain detects signs of oxidative stress and neuronal

damage. It is believed that the microglia cells are activated to clear the A $\beta$  by phagocytosis. This process involves the release of ROS, pro-inflammatory cytokines, excitotoxins and proteases; all potentially neurotoxic substances [17].

Interaction with tau protein is considered as another mechanism through which A $\beta$  is thought to induce neurotoxicity. It is believed that A $\beta$ (1-42) and ApoE4 activates various kinases that results in the hyperphosphorylation of the tau protein, which in turn form NFTs.

A $\beta$  also adheres to endothelial cell walls forming damaged tissues or lesions. Over time, accumulation of A $\beta$  deposits can lead to a condition known as cerebral amyloid angiopathy (CAA), which leads to internal bleeding in the brain. A $\beta$  causes pore formation in the membranes that lead to loss of calcium homeostasis and an influx of Ca<sup>2+</sup> into the neurons. This is believed to start a cascade of events which ultimately leads to neuronal death [36, 69].

Other mechanisms proposed for A $\beta$  neurotoxicity include increased membrane fluidity [18], alteration of cytoskeleton and nucleus [78]; redox active iron [79], binding of A $\beta$  to ApoE and catalases. It is believed that several mechanisms might be active simultaneously and could be interrelated and dependent on each other. However, no consensus has been reached on a perfect mechanism for A $\beta$  neurotoxicity, which makes the design of therapeutics for AD a difficult task.

## **2.6. Normal Roles of A $\beta$ and APP**

The exact roles of APP and A $\beta$  in the normal functioning of cells are not fully understood. A $\beta$  is secreted by neuronal cells as a part of normal metabolism. Ill effects such as lower weight, reduced locomotor activity and impaired neuronal functions in brains are observed in experiments on APP knockout mice [80]. The APP intracellular domain (AICD) formed by

the  $\gamma$ -cleavage of APP, is believed to regulate phosphoinositide-mediated calcium signaling, which plays an important role in cell differentiation [81]. Studies have shown that A $\beta$ (1-40) is produced as a cellular antioxidant [82], A $\beta$ (1-40) modulates potassium channels in neurons with A $\beta$ (1-42) and it also counteracts the effects of secretase inhibitors [83].

## 2.7. Neurotoxicity of A $\beta$ : Who Is the Real Culprit?

A $\beta$  protein is derived from APP and is found to be present in the cerebrospinal fluid (CSF) and in brains of normal humans. Hence, the mere presence of A $\beta$  cannot be the cause of dementia. However, ordered self-association of A $\beta$  molecules seems to be the factor causing neuronal degradation [84]. Self-association and aggregation of A $\beta$  can lead to various forms of aggregates such as monomeric species, small dimers, trimers, oligomers, larger assemblies commonly referred to as A $\beta$ -derived diffusible ligands (ADDL), protofibrils, A $\beta$ \*56 and large insoluble fibrils. [85]

Initially, the large insoluble fibrils[86], which deposited as plaques were considered neurotoxic because these fibrils were detectable and characterization of the assemblies that formed *in vitro* were limited [84]. However, the fact that amyloid fibrils are the AD causing species is frequently challenged as a weak correlation is found between the amount of plaques deposited and the severity of dementia in patients.

Recent evidence has suggested that soluble oligomers are likely to be the real culprits [87]. Studies have shown that oligomeric A $\beta$ , in the absence of monomers and fibrils resulted in toxicity *in vivo* and oligomer-specific antibodies could block the toxicity in neurons. A strong correlation was found between the soluble A $\beta$  levels, loss of synapses and severity of dementia, further implicating soluble A $\beta$  as the toxic intermediate [84, 88]. The term, ‘soluble A $\beta$ ’

describes the form of A $\beta$  that can remain in solution even after high speed ultracentrifugation. Studies from synthetic A $\beta$  peptides, APP over-expressed cell culture systems, APP transgenic mice, human CSF and postmortem brain have indicated that soluble non-fibrillar A $\beta$  induces toxicity in cells [84]. Review on A $\beta$  oligomers [89-93].

Protofibrils (PFs)[94] are a group of structures ranging from spheres (about 5nm in diameter) to curvilinear structures about 200nm in length. PFs are physically similar to amyloid fibrils but they have the ability to form both true amyloid fibrils or dissociate into low molecular weight species of A $\beta$ . PFs and amyloid fibrils also have distinct biological activities [15, 16, 84]. Shortly after the discovery of protofibrils, Lambert et al. observed small (5-6nm) globular structures of synthetic A $\beta$ (1-42) with the C-terminal region of A $\beta$  forming a hydrophobic core, which they referred to as Amyloid- $\beta$  derived diffusible ligands (ADDLs) [95]. The ADDLs are the smallest assemblies of PFs, about 6nm and have been shown to cause neuronal death, block long-term potentiation (LTP), inhibit reduction of MTT in neural cells and avidly bind and decorate dendritic arbors of certain cultured neurons [84, 85]. A dodecamer, labeled A $\beta$ \*56 for its weight in kD, is proposed to induce memory loss independent of neuronal plaques before amyloid plaques started developing [85, 96]. However, no consensus has been reached on the exact toxic species and it is thought that toxicity can be induced by multiple assemblies rather than any particular form. However, the fact remains that the *in vivo* environment is quite different than the *in vitro* environment and the hydrophobic nature of the A $\beta$  peptide makes it ambiguous whether the pathway observed would also work *in vivo*.

Now that the different assemblies of A $\beta$  have been discussed, the pathway by which A $\beta$  aggregates needs to be addressed. It is proposed that A $\beta$  aggregation is a nucleation dependent polymerization process, which is significantly affected by the presence of small peptide

aggregates or ‘seeds’ [97] and by the rate of elongation of the seeds [15]. Walsh et al. [15] showed that A $\beta$  oligomers arise through a series of short lived intermediates that form PFs, which act as centers for the growth of mature insoluble fibers. Thus, the monomers can be in equilibrium with dimers to form fibril nuclei from which protofibrils emerge. The end to end or lateral association of PFs forms “self-templates”, onto which the monomers/dimers bind and polymerize. Most of the other models proposed are variation of what is depicted in figure 6.

Huang et al. [97] suggested two pathways for A $\beta$  aggregation. In one pathway, an ordered  $\beta$ -sheet conformation is observed, which leads to AD like symptoms and the formation of other, unstructured aggregates called diffuse amyloid or preamyloid. The preamyloid species exist in an amorphous form and are non-toxic to the neuronal cells. It is hypothesized that A $\beta$  takes the ordered  $\beta$ -sheet pathway only when levels of total A $\beta$  are above 10 $\mu$ M in the brain. This hypothesis explains why normal healthy brains do not develop AD like symptoms despite having A $\beta$  present in them.

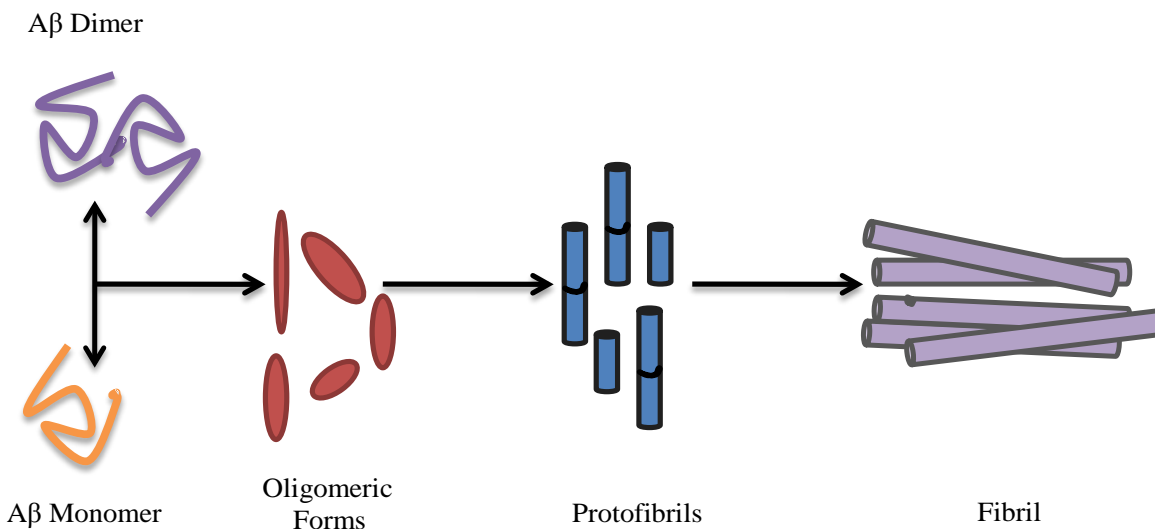


**Figure 6: Modes of A $\beta$  aggregation: Believed to be a nucleation dependent process**

## 2.8. Structure of Aggregated A $\beta$ Peptide

Elucidating the exact structure of aggregated A $\beta$  could prove extremely useful in designing effective inhibitors for prevention of AD. However, previous studies have established that A $\beta$  (1-40) and its different fragments A $\beta$  (16-22), A $\beta$  (11-25), A $\beta$  (10-35) adopt different conformations depending on the environmental conditions [66, 98]. Also, A $\beta$  (1-42) has a great propensity to aggregate because it has 2 extra residues, Ile at 41 and Ala at 42 at the C-terminus of the peptide[86]. At physiological conditions, the A $\beta$  peptide displays an unstructured random coil structure *in vitro*. The first 16 residues of A $\beta$  are largely hydrophilic and the remaining residues form a part of a largely hydrophobic domain. Residues 12-23 have been identified as the self-recognition sites for formation of dimers and higher oligomers. It is also posited that the hydrophobic stretch at residues 17-21 is critical in the formation of fibrillar structure [99]. The exact structure of monomeric A $\beta$  in solution is still uncertain as the physiological environment is difficult to achieve under laboratory conditions. Aqueous A $\beta$  (1-40) was analyzed using Circular Dichroism and the result showed a mixed coil,  $\beta$ -turn,  $\beta$ -sheet and  $\alpha$ -helical content for A $\beta$  structure. Also, other groups observed a high  $\beta$ -sheet content at the air-water interface [100], whereas in sodium dodecyl sulphate (SDS) micelles and later in 40% trifluoroethanol, monomeric A $\beta$  showed an extensive  $\alpha$ -helical content [101]. However, the exact structure remains debated and it is postulated that A $\beta$  adopts  $\alpha$ -helical conformation in organic solvents whereas in aqueous environments it is predominantly  $\beta$ -sheet [102].

Intermolecular  $\beta$ -sheet structure of the A $\beta$  peptide fibrils was confirmed by a variety of techniques such as electron microscopy, Fourier transform infrared spectroscopy (FTIR), and CD [102, 103]. The  $\beta$ -sheets are composed of cross- $\beta$ -strands which are perpendicular to the axis of the fibril and intermolecular hydrogen bonding occurring parallel to its axis. Tjernberg et al.

suggested that the smallest fibril forming sequence was A $\beta$  (14-23) and this was the core of the A $\beta$  fibril [104]. It is proposed that residues 16-23 have a high propensity to form a  $\beta$ -sheet structure and residues 11-24 are implicated in  $\alpha$ -helix to  $\beta$ -sheet conversion [102]. One study indicated the presence of anti-parallel  $\beta$ -sheets in the A $\beta$  fibrils and a turn at positions 25-28 due to the presence of the amide-I band of the infrared absorption spectra. On the other hand, structural studies on A $\beta$  (10-35) using solid-state NMR have established a parallel  $\beta$ -sheet structure. This has led to a conclusion that A $\beta$  fibrils can adopt both parallel and anti-parallel structure depending on the sequences and composition of the amino acid residues [103]. By the use of solid-state NMR, it was suggested that fibrils made from different lengths of A $\beta$  peptide were the same [105]. In another study, it was proposed that the first 10 residues of A $\beta$  (1-40) are structurally disordered. Petkova et al. presented a model in which residues 12-24 and 30-40 formed the  $\beta$ -sheet structure. The two  $\beta$ -sheets are in contact through side chain-side chain interactions with residues 25-29 forming the bend of the peptide [106]. In the case of A $\beta$ (1-40) fibrils, the side-chain interactions are intramolecular, whereas for A $\beta$ (1-42) fibrils, the upper layer sheet is displaced relative to the lower sheet so that the two  $\beta$  strands of A $\beta$  molecule ( $i$ ) form intermolecular side-chain interactions with the strands of molecules ( $i+1$ ) and ( $i-1$ ) respectively [98]. Many models have been proposed having different configurations, number of turns and patterns, with each satisfying different constraints. Recent evidence suggests that the molecular structure formed by the A $\beta$  fibrils *in vitro* depends on solvent composition, temperature, protein concentration, pH, ionic strength, and external mechanical forces such as agitation. Simple variation in these conditions can lead to the formation of fibrils with a completely different morphology [107]. Also, direct structural measurements of A $\beta$  fibrils are not possible due to the small quantities and the lack of isotopic labeling *in vivo*. It was also

demonstrated by Paravastu et al. that the molecular structure of A $\beta$  fibrils seeded from AD brain fibrils were markedly different than those seeded with synthetic A $\beta$  [108]. Thus, even though *in vitro* studies on A $\beta$  fibrils have provided a plethora of knowledge, the exact structure of A $\beta$  fibrils formed *in vivo* remains uncertain.

## **2.9. Interaction Between A $\beta$ -Cell Membranes**

There have been studies that document the role of lipid rafts in the cell membranes and peptides in the loss of neuronal function and potentially cell death in AD, Parkinson's disease [109, 110], Huntington's, Prion diseases and amyotrophic lateral sclerosis (ALS)[111]. Focusing on AD, it is well documented from pathological, genetic and cell culture studies that A $\beta$  40/42 is the neurotoxic species in AD. Several investigators have postulated that the interaction of A $\beta$  with cellular membranes may be the mechanism leading to cell death [28, 112-119]. Interactions of A $\beta$  peptide with artificial and biological membranes is reviewed in [120]. Membrane rafts are implicated in A $\beta$  production [121], aggregation and binding of peptide moieties. A $\beta$  is known to interact with cell membranes and also with membranes of other subcellular components such as Golgi bodies, lysosomes and endoplasmic reticulum [119]. A $\beta$  in the aggregated form binds to neuronal membranes via hydrogen bonding and electrostatic interactions. It has been posited that A $\beta$ (40/42) decreases the fluidity of the fatty acyl and head groups of the plasma, lysosomal and endosomal membranes whereas it increases the Golgi membrane fluidity [122]. Investigations by Yanagisawa et al. showed the presence of monosialoganglioside GM1-bound A $\beta$  (GM1-A $\beta$ ) in the brains of AD patients which is not detected in non-AD brains [21]. Terzi and co-workers showed that A $\beta$  had higher binding affinity to the negatively charged phospholipids than zwitterionic and cationic lipids [123, 124]. It has been shown that cholesterol, gangliosides and membrane composition affect A $\beta$  formation, A $\beta$  aggregation and A $\beta$  membrane association

[125]. It is postulated that hydrogen binding as well as hydrophobic interactions with sugar groups in the gangliosides are responsible to A $\beta$ -membrane interactions [126]. Some of the mechanisms that have been postulated to induce membrane-related toxicity are as follows: Strong physiological interactions of A $\beta$  with membranes can lead to detrimental change in the fluidity of the membranes; interaction of A $\beta$  with membranes leads to alterations in ion permeability, formation of ion channels, changes in intracellular Ca<sup>2+</sup> levels leading to disturbed homeostasis and membrane depolarization; interaction of A $\beta$  with membranes leads to disruption of neuronal homeostasis and loss of neuronal function [117, 119]. Thus, it is of utmost importance to understand the mechanisms and pathways through which A $\beta$ -membrane association induces toxicity. There can be several mechanisms working together that may be the cause of increased A $\beta$  or polymerized A $\beta$ . However, we know for sure that A $\beta$  interacts with the cell membrane where it binds to membrane lipids and this somehow leads to or contributes to toxicity. It is this theoretical bottleneck region that we are going to target in this thesis. For this, the role of gangliosides in AD must be reviewed. Some of the experimental strategies to investigate membrane or lipids interaction with amyloidogenic proteins or peptides has been reviewed by Raz Jelinek [127].

## **2.10.Role of Gangliosides in Alzheimer’s Disease Pathology**

Lipid components such as glycerophospholipids, sphingolipids and cholesterol are the major components of cell membranes. Gangliosides are a type of glycosphingolipids containing one or more sialic acid residues, with sialic acid being a generic term for *N*-acetyl- or *N*-glycoloyl-neuraminic acid [24, 128]. The hydrophilic characteristics of the big saccharidic headgroup and the hydrophobic characteristics of the double tailed sphingolipid, called ceramide, impart a strong amphiphilic nature to the gangliosides. The ceramide is composed by a long-

chain amino alcohol, 2-amino-1,3-dihydroxy-octadec-4-ene, connected to a fatty acid by an amide linkage [25]. The sugar structure, content, sequence, and bonding atoms in the oligosaccharide chain can vary along with the lipid moiety making gangliosides a very large family of compounds. Presence of sialic acid on the saccharidic headgroup differentiates gangliosides from neutral glycosphingolipids and sulfatides. The three main sialic acids known to be present in gangliosides are 5-*N*-acetyl-, 5-*N*-acetyl-9-*O*-acetyl and 5-*N*-glycolyl derivative. Due to their specific location, gangliosides are able to interact with a variety of biological entities such as glycoproteins, antibodies, peptides, hormones, growth factors etc. They are postulated to play an important role in cell differentiation, biosignaling, inducing neuritogenesis and play a protective role in the case of neuronal injury [129, 130]. GM1, GD1a, GD1b, and GT1b are the major gangliosides found in the human brain comprising almost 65% to 85% of the total content [111, 131]. The structures of the major gangliosides are given in Figure 7. It was observed that AD brains showed alterations in ganglioside levels and metabolism [129, 132] indicating that interactions between A $\beta$  and membranes play a vital role in the pathology of AD. A novel ganglioside bound A $\beta$  (GM1-A $\beta$ ) species was isolated from AD brains, which was postulated to function as a seed for amyloid fibril formation [19]. Terzi et al. first reported the conformational change in A $\beta$  from random coil to  $\beta$ -sheet after binding to negatively charged lipid vesicles [129, 133]. After that, many studies have reported the interaction between A $\beta$  and gangliosides, especially GM1, which results in an altered secondary structure of the A $\beta$  peptide [28, 112-114, 116, 129]. Some studies have revealed that the A $\beta$  attaches between the hydrophobic/hydrophilic interface of the ganglioside clusters, exhibiting an up- and down- topological mode in which the  $\alpha$ -helices and particular segments of A $\beta$  interact with the ganglioside clusters[31]. It is hypothesized that the hydrophobic side of the ganglioside cluster is responsible for the

conformational change in A $\beta$ , whereas the sugar chains or the hydrophilic side is involved in the determination of the binding affinity between the A $\beta$  and gangliosides [31].

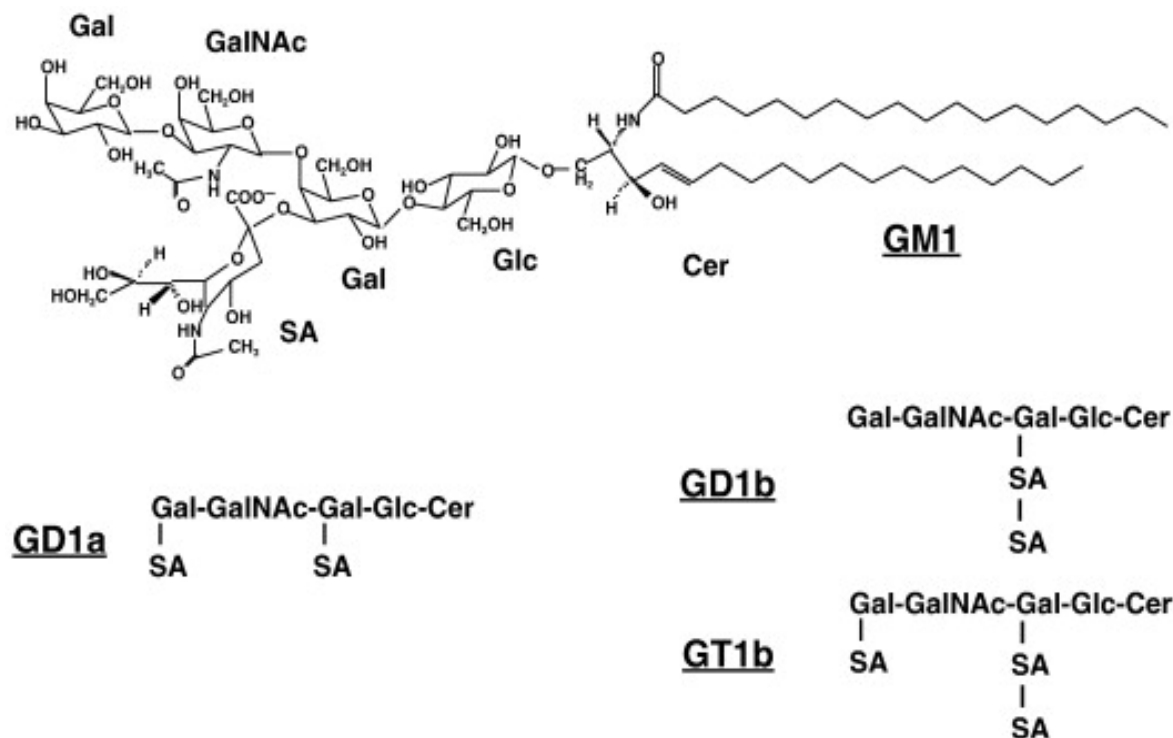


**Figure 7: Chemical structures of major gangliosides present in neurons**

Cer, ceramide; Glc, glucose; Gal, galactose; GalNAc, *N*-acetylgalactosamine; SA, sialic acid. [131] Reprinted with permission from Elsevier Ltd.

In an important observation, Choo-Smith et al. showed that A $\beta$  peptide interacts specifically with membrane gangliosides with affinities ranging from  $10^{-6}$  to  $10^{-7}$ M depending on the ganglioside sugar moiety. However, isolated oligosaccharide moiety on the ganglioside was not sufficient to induce the conformational change in A $\beta$  peptide which indicated the role of the lipid component in the binding. They posited that the gangliosides function as high affinity receptors towards A $\beta$  which leads to conformational changes from random coil to ordered  $\beta$ -sheet [134]. Another important observation came from the studies of McLaurin and Chakrabarty, who reported that A $\beta$  peptide disrupted acidic phospholipid membranes and the

gangliosides induce A $\beta$ 40/42 to adopt a novel  $\alpha/\beta$  conformation at neutral pH. They observed that the sialic acid moiety on the oligosaccharide chain was important for inducing this disruption of the membranes. They speculated that gangliosides could sequester A $\beta$  and thereby prevent ordered  $\beta$ -sheet formation; alternatively, gangliosides may be involved in normal A $\beta$  functioning and/or clearance [113]. McLaurin et al. suggested that the association with a carbohydrate backbone was necessary along with the sialic acid for binding to A $\beta$ . The study showed that the binding of A $\beta$  (1-40) to mixed gangliosides or GM1 induced  $\alpha$ -helical structure at pH 7.0 and  $\beta$ -sheet structure at pH 6.0. They posited that increasing the number of sialic acid residues on the carbohydrate backbone leads to increased net negative surface charge on the lipid vesicles which favors the formation of an ordered  $\beta$ -sheet structure and inhibits the  $\alpha$ -helical structure [112]. This observation was further supported by the work of Matsuzaki and Horikiri, who suggested that A $\beta$ (1-40) peptide binds more strongly to a ganglioside-rich domain in which the binding site was the sialic acid moiety, with the A $\beta$  peptide adopting an antiparallel  $\beta$ -sheet lying parallel to the lipid bilayer [116]. In another work by Ariga et al. it was found that GM1 ganglioside had affinities in the following order of binding strengths: A $\beta$  (1-42) > A $\beta$  (40-1) > A $\beta$  (1-40) > A $\beta$  (1-38). A $\beta$ -APP analogs had very low binding affinities for gangliosides. They also showed that A $\beta$  (1-40) binds to a number of gangliosides with the following order of binding strength: GQ1b $\alpha$  > GT1a $\alpha$  > GQ1b > GT1b > GD3 > GD1a = GD1b > LM1 > GM1 > GM2 = GM3 > GM4. Their results suggested that an  $\alpha$ 2,3NeuAc residue on the neutral oligosaccharide core of gangliosides was required for binding along with the  $\alpha$ 2,6NeuAc residue linked to the GalNAc in the  $\alpha$ -series [135]. In another related study, researchers showed that A $\beta$  has higher affinity towards clustered ganglioside GM1 and to gangliosides having higher number of sialic acid content, the formation of which is regulated by cholesterol content in the brain [27].

In a study by Wang et al., reduction of cellular cholesterol and removal of cell surface sialic acids protected cells from A $\beta$  toxicity, stressing the importance of surface sialic acids [125]. The clustering effect of gangliosides is supported by the theory of lipid rafts. Lipid rafts are membrane microdomains that are enriched in cholesterol, sphingomyelin and sphingolipids (especially GM1 ganglioside) [136]. These lipid rafts are more ordered and tightly packed than surrounding bilayers, have certain proteins, signaling molecules clustered in it and have the ability to float freely in the cell membrane. Williamson et al. demonstrated with NMR studies that interaction of <sup>15</sup>N-labeled A $\beta$ (1-40) and A $\beta$ (1-42) with GM1 micelles is localized to the N-terminal and His13 to Leu17 region of the peptide. They showed that the fibrillogenic seed nucleus involves an interaction of His13 with the sialic acid moiety of GM1 ganglioside. This indicated that A $\beta$  binds to the carboxylic acid group on sialic acid via a positively charged amino acid residue. However, they observed no binding to the isolated pentasaccharide headgroup, suggesting the need for a polyanionic membrane like surface [137]. Investigators found that the ability of fibrils binding to membranes was significantly affected when cells were treated with neuraminidase, which did not affect the membrane fluidity, but removed the negatively charged sialic acid residue in GM1 [23]. This suggests that A $\beta$  fibrils interact with the negative charges in the sialic acids and demonstrates the importance of electrostatic interactions between fibrils and cellular membranes.

A number of studies have observed the accumulation of specific ganglioside bound A $\beta$  complex in the AD brain [19-21, 129]. Other studies showed the interaction between gangliosides and A $\beta$  peptides in neuronal cells leading to the amyloid fibril formation. Glucosylcermid synthase inhibition, one of the rate limiting steps in ganglioside synthesis, results in decreased A $\beta$  production. AD brains have also shown elevated GM1 levels and increased

sialidase activity [62]. All of these results point to the pivotal role of gangliosides, especially GM1 in the pathogenesis of Alzheimer's disease. Researchers propose that the initial step in AD is ganglioside binding with the A $\beta$  peptide; the peptide then undergoes self-association on the membrane surface by undergoing a conformational change from random coil to ordered  $\beta$ -sheet. This surface associated, ordered  $\beta$  sheet peptide then acts as a specific template ("seed") which causes additional soluble A $\beta$  to form fibrils by  $\beta$ -sheet augmentation mechanism [129, 134]. [Please see [129] for excellent review]. In a related recent study of A $\beta$ (1-40) fibrillation in the presence of lipid bilayers composed of GM1, cholesterol and sphingomyelin at low protein densities (A $\beta$ :GM1 less than  $\sim$ 0.013 units concentration) the helical A $\beta$  species was observed. At mid-level protein densities (A $\beta$ :GM1 between  $\sim$ 0.013 and  $\sim$ 0.044), the helical species and aggregated  $\beta$ -sheet species were seen together. At higher densities (A $\beta$ :GM1 more than  $\sim$ 0.044), the  $\beta$ -sheet structure had converted to a second seed-prone  $\beta$ -structure [32]. Another study developed GM1-A $\beta$  specific monoclonal antibody that specifically recognized the unique changed conformation shown by the GM1-A $\beta$  in the AD affected brain, which in turn acts a seed for further aggregation [22]. In another recent study, the interaction of both model and living cell membranes with A $\beta$  (1-40) and A $\beta$  (1-42) was studied where they observed 10-fold more amyloidogenic activity from A $\beta$ (1-42) compared to A $\beta$ (1-40) [138].

It was also observed that A $\beta$ (1-40) fibrils grown on GM1 have different structural features and much higher toxicity due to their increased stability and ability to bind to neurons with respect to the same fibrils that are grown in the absence of GM1[23]. In a clinical study where 100mg of GM1 was administered for 18-32 days to patients with spinal cord injury, patient's showed enhanced recovery of neurologic function. However, same studies on a much larger group of 760 patients did not show any significant benefit. In another related study,

administering 200mg of GM1 per day for 18 weeks did not show any significant changes in the blood chemistry of patients [111]. This direct GM1 study further supports our approach given that GM1 administration is ineffective and we need a better biomimetic that can bind to A $\beta$ .

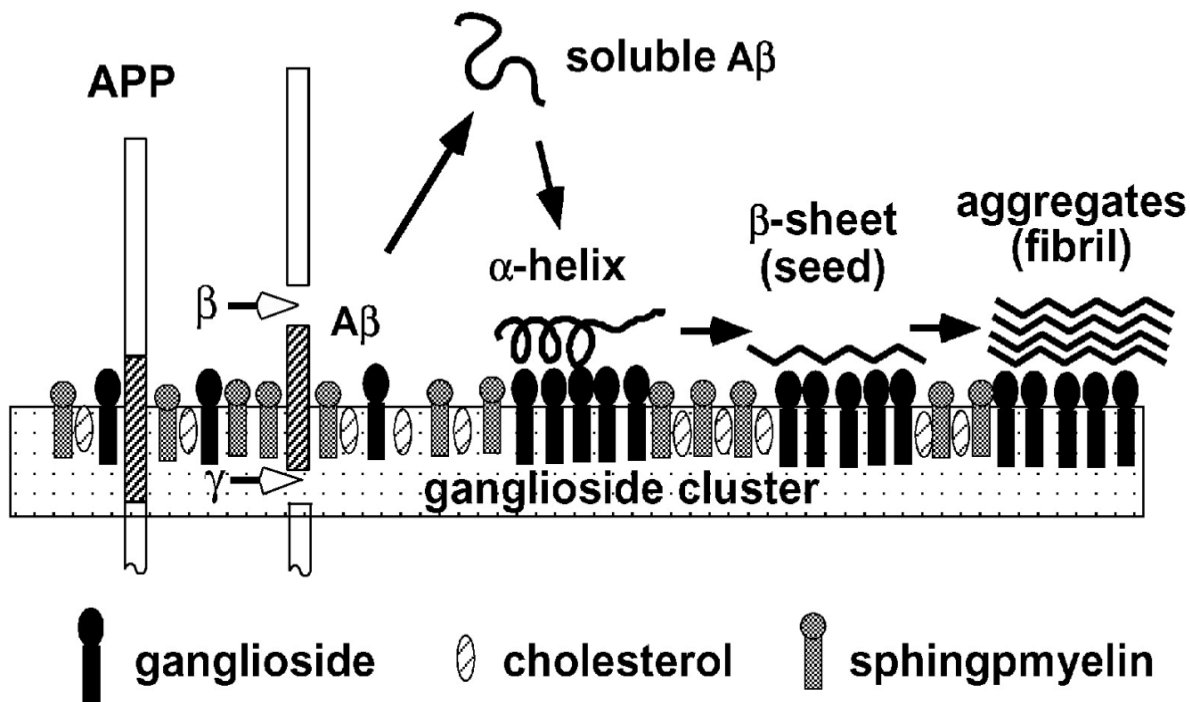


**Figure 8: Hypothetical mechanism of ganglioside-mediated A $\beta$  fibrillization.**

Enzymatic cleavage ( $\gamma$ - and  $\beta$ -secretase) of APP generates soluble A $\beta$  in the lipid rafts composed of cholesterol and sphingolipids. Cholesterol mediates the formation of ganglioside clusters (especially GM1), A $\beta$  binds to the clusters, forming a seed for further soluble amyloid deposition into ordered  $\beta$ -sheet form at higher peptide to ganglioside ratios [129]. Reprinted with permission from Elsevier Ltd.

## 2.11. Current and Emerging Therapeutic Approaches in AD

### 2.11.1. Approved Drugs Against Alzheimer's Disease

Currently available treatments for AD are merely symptom alleviating, providing temporary cognitive improvement and deferred decline. However, they show very little to no

evidence of slowing disease progression or curing AD [139]. Table 2 lists the drugs currently approved by the Food and Drug Administration (FDA).

Most of the drugs approved today are cholinesterase inhibitors. The enzyme cholinesterase is responsible for the degradation of acetylcholine, which is released into the synaptic cleft after the firing of the synapses from one neuron to another [139]. As neurons are under attack in AD, they produce less acetylcholine and hence, inhibition of its destruction causing enzyme makes more neurotransmitters available for communication between neurons. Galantamine, Donepezil and Rivastigmine are the 3 inhibitors of cholinesterase available in the market today and are approved for mild to moderate treatment of AD [11, 43, 48, 139]. Galantamine and Donepezil selectively inhibit acetylcholinesterase hydrolysis in the brain, while Rivastigmine in addition to cholinesterases also inhibits butyrylcholinesterase, which has a similar role to that of cholinesterase. Based on their mechanism of action it is evident that these medications only temporarily mitigate symptoms and are not expected to change the course of AD [43]. All drugs reported positive effects in several randomized, double-blind, placebo-controlled studies; however, a direct comparison of these three cholinesterase inhibitors has not been done. Another drug available is Memantine, an NMDA (*N*-methyl-*D*-aspartate) -receptor, which is approved for the treatment of moderate to severe AD. In AD, it is observed that NMDA glutamate receptors are overactivated which leads to disturbed calcium homeostasis causing neurodegeneration. Memantine is a non-competitive NMDA-receptor antagonist with moderate affinity that appears to be able to protect neurons while leaving physiological NMDA-receptor activation unaffected [139]. Several other potential NMDA receptors are in active phases of development. Some researchers postulate that the use of Memantine with cholinesterase inhibitors might be a viable approach in treating AD. In a randomized, double-blind, placebo-

controlled clinical trial of patients with moderate to severe AD, the combination therapy showed a statistically significant benefit over monotherapy of Donepezil, with regard to the measures of cognitive function, activities of daily living, and behavior [139]. However, this theory needs to be investigated further. Flurizan (Myriad Genetics, USA) is a  $\gamma$ -secretase inhibitor that showed promise but failed in Phase III trials [6]. Semagucestat (Eli Lilly & Company, USA) made patients worse with increased risk of skin cancer. Information on other drugs investigated is presented in [6].

**Table 2: Characteristics of drugs approved for AD [43, 140, 141].**

	Donepezil	Galantamine	Rivastigmine	Memantine
Manufacturer	Eisai Inc. / Pfizer, NY	Ortho-McNeil Neurologics Inc.	Novartis Pharmaceuticals Corporation	Forest Pharmaceuticals
Launched	1997	2001	2000	2003
Indication	Mild to Moderate AD	Mild to Moderate AD	Mild to Moderate AD	Moderate to Severe AD
Mode of Action	Selective Cholinesterase inhibition	Selective Cholinesterase inhibition	Selective Cholinesterase and Bututylcholinesterase inhibition	Non-Competitive NMDA-receptor antagonist
Half-Life	Long (70h)	Short (7-8h)	Very Short (1h)	Long (60-100h)
Major Side Effects	Nausea, vomiting, diarrhea, fatigue, insomnia, muscle cramps, anorexia	Nausea, vomiting, diarrhea, anorexia, weight loss	Nausea, vomiting, loss of appetite, indigestion, weakness, dizziness, diarrhea, stomach pain	Dizziness, constipation, confusion, headache

### 2.11.2. Immunotherapy for AD

Immunotherapy is an emerging and promising approach because it promotes the possibility of peripheral treatment of A $\beta$  that eliminates the need to design molecules that can cross the blood-brain barrier (BBB). The idea behind immunotherapy is that by decreasing the A $\beta$  levels in the blood, more A $\beta$  can be removed from the brain. The use of A $\beta$  immunotherapy was first reported by Schenk and co-workers from the study in APP transgenic mice, wherein active immunization with fibrillar A $\beta$  attenuated A $\beta$  deposition and improved behavior [139, 142]. Similar results were obtained by the use of passive immunization with antibodies against A $\beta$  [143]. This led to the clinical trials on mild AD patients with vaccine AN1792, composed of preaggregated A $\beta$ (1-42). However, in phase II, it was found that 6% of the vaccinated cases had developed aseptic meningoencephalitis and the trial was discontinued [144]. The researchers attributed this side-effect due to the T-cell response against the mid-terminal and C-terminal part of the peptide [43, 48].

Still, refined forms of active immunization are considered as a viable option and some clinical trials are in Phase I [145]. Researchers have also focused on the development of passive vaccinations for the treatment of AD. Several trials with passive immunization are underway with selective monoclonal antibodies which have been shown to decrease A $\beta$  plaque pathology and reduce behavioral impairments in transgenic mice [11]. Phase III trials are under way for an anti-A $\beta$  antibody named Bapineuzumab, which has shown affinity for both soluble and insoluble A $\beta$ . One phase II and two phase I trials are also underway for other antibodies [145]. Thus, active/passive immunization or vaccination can prove to be a viable option for the treatment of A $\beta$ . A very good strategy in immunotherapy is to develop an A $\beta$  sequestering molecule that does not elicit an immune response.

### 2.11.3. Inhibition/Modulation of Secretases

According to the amyloid cascade hypothesis, the production of A $\beta$  is the root-cause of AD. Assuming this to be true, the inhibition/modulation of secretases would be the cleanest approach and would remove monomeric A $\beta$ , therefore preventing the production of oligomers and fibrils. Thus, up-regulation of  $\alpha$ -secretase, down-regulation/inhibition of  $\beta$ -secretase, and inhibition/ modulation of  $\gamma$ -secretase are some of the potentially viable approaches that are being investigated currently.

$\gamma$ -Secretase inhibitors can reduce A $\beta$  synthesis, which can further inhibit the downstream cascade of events. DAPT, LY450139 dihydrate, MRK-560 and BMS-299897 are some of the  $\gamma$ -secretase inhibitors that have shown marked reduction in A $\beta$  levels in brains, CSF and plasma in transgenic mice [48, 139]. However, it was found that  $\gamma$ -secretase cleaves substrates other than APP such as Notch [11]. Thus, inhibition of  $\gamma$ -secretase can have adverse effects. Hence, modulating the activity of  $\gamma$ -secretase to produce less A $\beta$  is a more viable strategy. Recently, a  $\gamma$ -secretase inhibitor was developed that was able to inhibit A $\beta$  production without affecting Notch signaling [146]. Another  $\gamma$ -secretase modulator that has entered phase III study is R-flurbiprofen, which is believed to lower the production of the more toxic A $\beta$ (1-42) by shifting the cleavage of APP from producing A $\beta$ (1-42) to other shorter, less toxic peptide fragments [147]. Several other  $\gamma$ -secretase modulators are currently being developed or undergoing phase I trials [11]. Also,  $\beta$ -secretase appears to be the perfect therapeutic target as it represents the first step in A $\beta$  production. Studies on  $\beta$ -secretase (BACE1) knockout mice revealed very small quantities of A $\beta$  thereby establishing BACE1 as the primary  $\beta$ -secretase enzyme acting *in vivo* [139, 146]. However, the physiological roles of BACE1 and its homologue BACE2 are unknown even though they are expressed throughout the body. The complete inhibition of  $\beta$ -secretase has

displayed potentially deleterious effects in mice. It was observed that  $\beta$ -secretase can also act on other non-APP substrates [64, 148]. It has been difficult to develop potent brain penetrating BACE1 inhibitors as it was observed that most of BACE inhibitors showed nanomolar binding affinities in cell free assays but were unsuitable for *in vivo* experiments [48]. Recently, it was announced that a potent BACE1 inhibitor, named CTS-21166 [64] was safe and well-tolerated in Phase I study. In AD, it is believed that  $\beta$  and  $\alpha$ -secretase compete for the APP substrate and there exists a balance between the two activities. For review see [149].

Progress in developing efficient inhibitors and modulators of secretases has been impeded as most of these secretases have not been fully identified and understood. Their psychological roles are unknown. Not everything is known about the different substrates they attack and it is believed that most secretases attack more than one substrate. Thus, there is a need for developing selective and highly targeted drugs that can only inhibit or modulate the APP cleavage process. Also, the compounds developed should be capable of crossing the blood-brain barrier. Such constraints make the development of specific drugs a challenging task.

#### **2.11.4. A $\beta$ Aggregation Inhibitors**

Preventing the aggregation of A $\beta$ , thereby preventing the formation of presumed toxic oligomers and fibrils by specifically binding molecules is another promising approach for the treatment of AD. Alzhemed (3-amino-1-propanesulphonic acid), a small molecule developed by Neurochem Inc., has been shown to inhibit the interaction of A $\beta$  with glycosaminoglycans thereby inhibiting formation of A $\beta$  aggregates. Clioquinol (PBT-1) developed by Prana Biotechnology, has shown good results in reducing A $\beta$  deposition in APP transgenic mice by binding to zinc and copper, which are postulated to be involved in A $\beta$  aggregation process [146].

Also, another metal chelating agent, PBT-2 is in phase II trials [148]. Another approach is to design inhibitors based on histological dyes used to characterize amyloid *in vitro* and *in vivo*. A number of polyphenols such as Curcumin, Catechins, Gingo Biloba are also being investigated are potent inhibitors of A $\beta$  aggregation and to prevent neurotoxicity [150].

Compared to small molecules, several peptide based therapeutic strategies are under investigation, as they are thought to be more effective as they can interact with the extended regions of A $\beta$ . Tjernberg et al. reported that a pentapeptide KLVFF of A $\beta$ (16-20) binds to and disrupts fibrils formation [151]. Ghanta et al. reported a prototype inhibitor composed of residues 15-25 of the A $\beta$  peptide linked to an oligosine disrupting element [99]. The use of the recognition element helps in specificity whereas the disrupting element interferes with A $\beta$  aggregation pathway. Selective substitution of proline at key positions on a peptide homologous to the central 17-21 regions of A $\beta$  was shown to convert A $\beta$  fibrils to amorphous aggregates and inhibit toxicity *in vitro* and *in vivo* [152]. The use of *N*-methylated peptides is another promising approach which is known to lock the residues into a  $\beta$ -conformation. *N*-methylated peptides function by binding to the face of the aggregating peptide through the amide -NH groups at the outer edge of the  $\beta$ -sheet, effectively blocking intermolecular hydrogen bonding, thus preventing aggregation and toxicity [150]. For reviews see [12].

However, most of these strategies are under development and their beneficial effects on AD patients are still not clear. Another major problem is that the most toxic species of A $\beta$  has not been identified. Also, determining the correct chain of events in AD development is challenging and this is another major hurdle in the development of a specific A $\beta$  inhibiting molecule.

### **2.11.5. Strategies Involving Metal Interactions of A $\beta$**

Researchers are investigating the role of metals in AD pathology. Abnormally high levels of metals such as Cu (~400 $\mu$ M), Zn (~1mM) and Fe (~1mM) have been found in AD brains with significant ROS and evidence of oxidative stress. One approach is to selectively inhibit the metal binding sites in an A $\beta$  peptide to prevent A $\beta$  metal interaction. Another approach is to synthesize metal-protein attenuating compounds (MPACs) which target the metal bound A $\beta$  and restore the metals back to the synapses. MPAC Clioquinol (5-chloro-7-iodo-8-hydroxyquinoline) and MPAC PBT2 are in Phase II clinical trials. However, simply removing metals using chelators does not work as many metals play essential roles in neuronal function and chelators or metal complexes are very difficult to get across the BBB. For excellent review see [153].

### **2.11.6. Drugs Based On Epidemiology**

Epidemiological studies have observed the protective effect of different types of drugs and supplements on AD patients. One such class of drugs being investigated are anti-inflammatory drugs as inflammation type characteristics are observed in the immediate vicinity of plaques. Hence, it is believed that use of anti-inflammatory drugs may have preventative effects in the development of AD either by the inhibition of cyclo-oxygenase (COX-1 or COX-2) or by direct action on  $\gamma$ -secretase [43, 139]. However, clinical trials on drugs such as Prednisone, Hydroxychloroquine, Naproxen, Celecoxib and Rofecoxib were negative [148]. The use of cholesterol reducing drugs (statins) is suggested as a viable treatment option for AD as *in vivo* and *in vitro* studies showed altered levels of APP and A $\beta$  along with cholesterol levels [154]. However, clinical trials of these drugs have showed ambiguous results [139, 154]. One of the reasons may be that the exact role of cholesterol in AD is unknown. Dietary intake of anti-

oxidants such as Vitamin E has shown beneficial results as oxidative stress is lessened in an AD brain. However, most of these strategies target post-cell damage and are therefore not optimal disease modifying agents.

#### **2.11.7. Novel A $\beta$ Sequestering Agents: OUR FOCUS**

In the earlier sections, we have already reviewed the interaction between A $\beta$ , gangliosides and the neuronal membrane. We know that A $\beta$  interacts with cells via binding to surface glycolipids and glycoproteins, and that the affinity of this interaction increases when the gangliosides or sialic acid molecules on the cell surface are clustered [8, 26-28, 118, 134, 135, 137]. Based on these observations, the approach is to design membrane mimics that would reproduce the clustered sialic acid structure of the cell surface thus successfully competing with the cell surface for A $\beta$  binding. Then, A $\beta$  would have higher affinity towards the mimic, binding it instead of the cell membrane, and thus sequestering the A $\beta$ , thereby reducing its neurotoxicity [8, 26, 143]. Such a strategy has already been applied with good results to many biological systems such as the prevention of influenza viral adhesion and infection both *in vitro* and *in vivo* [155-159]. Patel et al. synthesized sialic acid conjugated dendrimers which were more effective than unconjugated dendrimers alone at reducing A $\beta$  toxicity. The reported binding affinities for A $\beta$  to gangliosides in various literatures are in the order of  $10^{-6}$ M [114, 134, 135] whereas the observed binding affinities for A $\beta$  to sialic acid conjugated dendrimers were on the order of  $10^{-7}$  to  $10^{-9}$  M. The improved affinity was attributed to the clustering of sialic acids on dendrimers, or the combined effect of electrostatic interactions of A $\beta$  with the dendrimer backbone and the interaction of A $\beta$  with the surface sialic acids on the dendrimer [8]. However, the dendrimer backbone itself was toxic to the cells, leading to lower viability. This observation was in agreement with that observed in literature for dendrimer toxicity [158, 160]. Also, it is possible

that due to the rigid structure of the dendrimer used, the star burst type, it could have partly reduced the binding of labeled sialic acid to specific A $\beta$  sites. In another related work by Patel et al., the difference in A $\beta$  attenuation using physiologically relevant attachment (via anomeric hydroxyl) versus non-physiologically attached (carboxyl attached) chemistry of dendrimers was investigated. They found that though physiologically attached dendrimers attenuated A $\beta$  toxicity at lower concentrations than non-physiologically attached dendrimers, there was no significant improvement in the binding affinities [161]. Furthermore, they postulated that, greater A $\beta$  toxicity attenuation could be achieved by the use of a less highly charged polymer backbone and longer spacer between the charged polymer and sialic acid [26]. In the work by Cowan et al., use of photocrosslinked sialic acid containing oligosaccharides 3'-sialyl-*N*-acetyllactosamine (3'SLN) and disialyllacto-*N*-tetraose (DSLNT), showed almost complete attenuation of toxicity but at very high polymer concentration. Their results suggested that the mechanism of toxicity attenuation of A $\beta$  might not be direct competition for A $\beta$  binding and that, better attenuation of toxicity could be achieved at lower concentrations by increasing the valency of sialic acids on the polymers [156]. All these observations support the fact that multivalency can increase the binding affinity of a ligand to receptors [162]. By the use of mathematical models, Cowan et al. showed that the closest qualitative explanation for the membrane mimic attenuating toxicity was that the sialic acid mimic bound to A $\beta$ , the A $\beta$ -mimic complex was still toxic to the cells, but with a reduced toxicity compared to A $\beta$  alone. It is predicted that at physiological ionic strengths, electrostatic effects are likely to play a role in sialic acid polymer toxicity attenuation of A $\beta$  only for very highly charged polymers [162].

All these observations certainly indicate that there are yet to be understood mechanisms that are possibly playing a role in attenuating A $\beta$  toxicity such as the possibility of different -R

group sugars that have better properties. Since, a number of studies have highlighted the role of multivalent sialic acids in attenuating toxicity, it will be crucial to investigate how multivalency affects A $\beta$  binding. In addition, the effect of different backbones on the A $\beta$  needs to be investigated as backbone toxicity can significantly affect viability. This leaves the field open for the design of better membrane mimicking compounds that can attenuate toxicity at even lower concentration with higher affinity.

Towards this goal, there is a need for a suitable backbone structure that is biocompatible, flexible, non-toxic and easy to label among other things. Chitosan is an aminopolysaccharide that seems ideal as a backbone for sialic acid labeling. We will aim to synthesize sugar labeled chitosan by the use of a suitable cross-linker and test the efficiency of this complex to attenuate A $\beta$  toxicity. Next section describes the properties of chitosan.

## **2.12. Chitosan, Backbone Molecule**

Throughout the project, chitosan was chosen as a backbone molecule for attaching different sugars. We expect excellent biological properties offered due to the use of chitosan, especially that it has been FDA approved for use in wound dressing [163]. Additionally, chitosan is one of the most extensively studied biopolymer or biomaterial. Chitosan, identified in 1884 [164], is a natural amino-polysaccharide comprising copolymers of D-glucosamine and N-acetyl-D-glucosamine linked together by  $\beta(1-4)$  glycosidic bonds [165]. The individual chains of chitosan assume a linear structure which undergoes one full twist every 10.1-10.5A<sup>0</sup> along the chain axis. Each monosaccharide unit is chiral, the rotations of polymer chains show evident left or right. Three crystal types of chitosan are identified,  $\alpha$ ,  $\beta$  and  $\gamma$ - type, out of which  $\alpha$ -type is the most common identified from X-ray models and NMR spectra [166]. It is derived by partial

deacetylation of chitin from crustacean shells. The content of glucosamine in chitosan is called the Degree of Deacetylation (DD), which affects its solubility [167]. In chitosan, the DD ranges from 40% to 98% and the molecular weight ranges between 300Da to over 1000kDa depending on the source and method of preparation [168, 169]. The distribution of the two monomer units that make up chitosan can be determined using various techniques such as IR, elemental analysis, enzymatic reaction, UV, <sup>1</sup>H liquid state NMR and solid-state <sup>13</sup>C-NMR [166]. Other important properties of chitosan include viscosity, molecular weight, DD, crystallinity index, number of monomeric units, water retention value, pKa and energy of hydration [170]. Generally, studies have shown greater solubility and faster degradation for chitosan with low molecular weights and low DD compared to high molecular weight chitosan[171]. The oral mean lethal dose of chitosan in mice was found to be in excess of 16g/day/kg, which is higher than sucrose [171, 172].

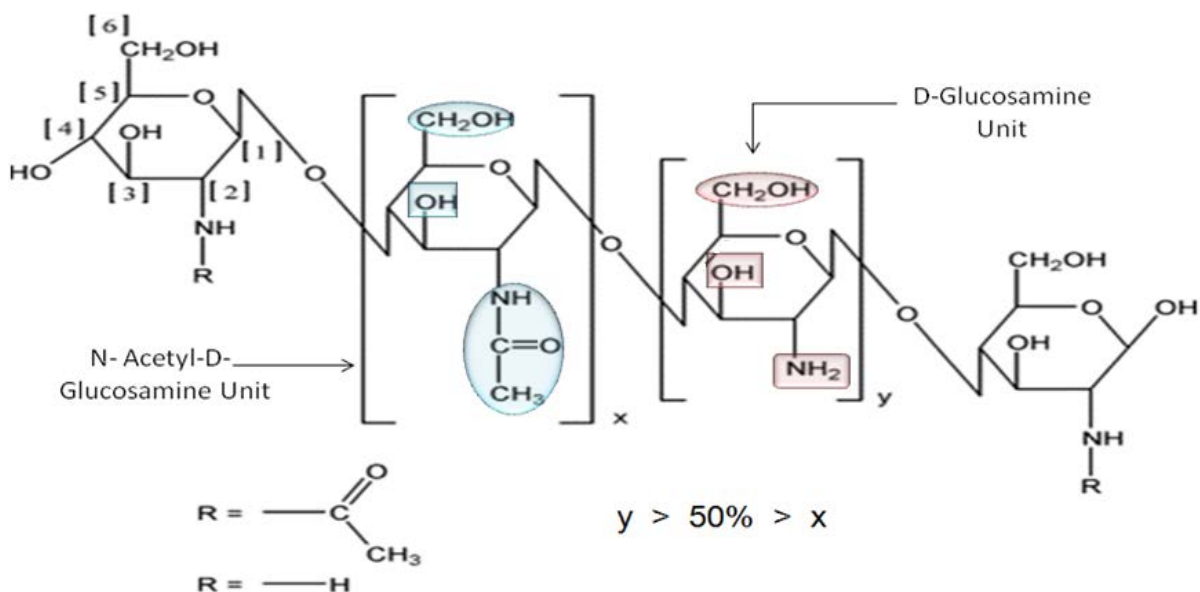


**Figure 9: Structure of Chitosan**

Also shown are the functional groups that can be modified for various applications. In our case, amine group at C2 position is used to couple sugars to chitosan

Chitosan is normally insoluble in aqueous solutions above pH 7 and in dilute acids (pH < 6), the amino groups on glucosamine become protonated (positively charged) (pKa value of 6.3) facilitating solubility of chitosan, making it a cationic polyelectrolyte. There is a strong possibility of the interaction of the positive charges of chitosan polymer with the negatively charged surface of the cell membrane, particularly the sialic acid moieties [167, 173]. Chitosan exhibits high charge density which makes it adhere to negatively charged surfaces [170]. When chitosan solution pH increases above 6.0, the chitosan's amines become deprotonated, chitosan loses its charge and becomes insoluble [163]. It has been reported that chitosan with higher DD shows low toxicity at low molecular weight [171]. This property of chitosan can be explored for drug adsorption enhancement. Generally, chitosan has three types of reactive functional groups, an amino group as well as both primary and secondary hydroxyl groups at the C2, C3 and C6 positions, respectively, which allow modification of chitosan for various applications [168]. This large quantity of amines at C2 position compared to other biopolymers makes chitosan the target of a host of chemical modifications and potential applications.

The amino functionality gives rise to chemical reactions such as acetylation, amide formation, quaternization, reactions with ketones and aldehydes, alkylation, grafting, chelation of metals, flocculation etc. Much work has been reported on chemical modifications of chitosan and the reactions have been reviewed extensively [165, 168, 169, 174, 175]. There have been extensive applications of chitosan in the field of controlled drug delivery. Chitosan nanoparticles offer better stability, low toxicity and simpler preparation methods with novel routes for delivery of drugs. For review on application of chitosan nanoparticles see [171, 176]. Thiol modification of chitosan has been extensively studied as non-invasive drug delivery applications [167]. The tissue engineering application of chitosan, applications in hydrogels, bone substitute has also

been studied extensively [177]. Commercial hemostatic dressing based on chitosan include HemCom and Chitoflex by HemCom, Chitoseal by Abbott, Clo-Sur by Scion, TraumaStat by Ore-Medix to name a few. Chitosan and its derivatives have been shown to have several interesting properties such as biocompatibility, biodegradability to harmless products, physiological inertness, remarkable affinity to proteins, nontoxicity, antibacterial, hemostatic behavior [166], wound healing, fungistatic, antitumoral, anti-acid, non-allergic, antiviral and anticholesteremic properties [165, 168, 169, 175]. Such unique properties of chitosan make it a very interesting topic of research with a host of applications [165-169, 174, 175]. Summary of applications of chitosan and drug are presented in [170]. Another excellent source on chitosan applications is the latest review (published in 2011) published by Dash et. al. that gives information about the toxicity, biological properties, biomedical applications (types and methods), drug delivery, wound healing, tissue engineering, gene therapy, green chemistry and pharmaceutical applications of chitosan [163].

### **2.13. Biological Sugars Selected for Conjugation with Chitosan**

A host of sugars, particularly, sialic acids, polysialic acids and oligosialic acid chains discovered so far are directly or indirectly connected to membrane chemistry. The action of sialic acids/poly/oligosialic compounds [178] results from the combination of:

Repulsive interactions: in-between sugars or between sugars and membrane proteins.

Attractive interactions: between poly/oligosialic chains and membrane protein, or lipids or soluble peptides/proteins/proteoglycans

Modulation of surface charge density: due to negative charge associated with sugar monomers

Modulation of pH at the membrane surface: the carboxylic groups on the sugar chains affect the pH at the microenvironment

**Sialic acid or N-Acetylneuraminic acid (SA):** In the sialic acid family of compounds, N-acetylneuraminic acid (SA), is one of the most frequently occurring member. It is an electronegatively charged monosaccharide, and is a major component of most proteins and lipids of cell membranes. SA is conveniently positioned on the outer end of these molecules, which implies a strong influence on cell biology. Its role in AD is well documented in the earlier pages of the report. Thus, SA, is studied first in this research and will enable us to use SA as a standard. Structure of SA is shown in figure 10.

**2-Keto-3-deoxy-nononic acid (KDN):** KDN is another electro-negatively charged member of the sialic acid family occurring most frequently in cell membranes after N-acetylneuraminic acid (SA). The only difference between SA and KDN is the substitution at the C-5 position. This critical difference will help us to isolate the effect of the –R group at C-5 position. The structure of KDN is shown in figure 10.

**Galacturonic acid (GA):** GA is a monobasic carboxylic acid derived from the oxidation of D-galactose. It is found in many natural polymers such as pectins and is a common component of cells walls. It has hydroxyl substitutions at C-5 and C-6 position instead of the –R groups found in sialic acids. The structure of GA is shown in figure 10.

**Tetrahydropyran-2-carboxylic acid (Pyran):** This compound was selected to test the ability of the ring structure in A $\beta$  attenuation properties. Pyran has no substitutions that are present in sialic acid family. It has a conveniently located carboxylic acid group at the C-2 location which can be

coupled with the amines in chitosan via EDC chemistry. Structure is shown in figure 10. However, to the best of knowledge, Pyran has not been studied in a neuronal cell system.

**Cyclohexanecarboxylic Acid (CHC):** CHC is a cyclohexane with a carboxylic acid group conveniently attached for coupling with amines of chitosan. This will help us to understand the difference due to the cyclic ring structure. Also, the difference in properties shown by CHC and Pyran ring will help to identify the role of –O substitution found in the Pyran structure. However, to the best of knowledge, CHC has not been studied in a neuronal cell system.

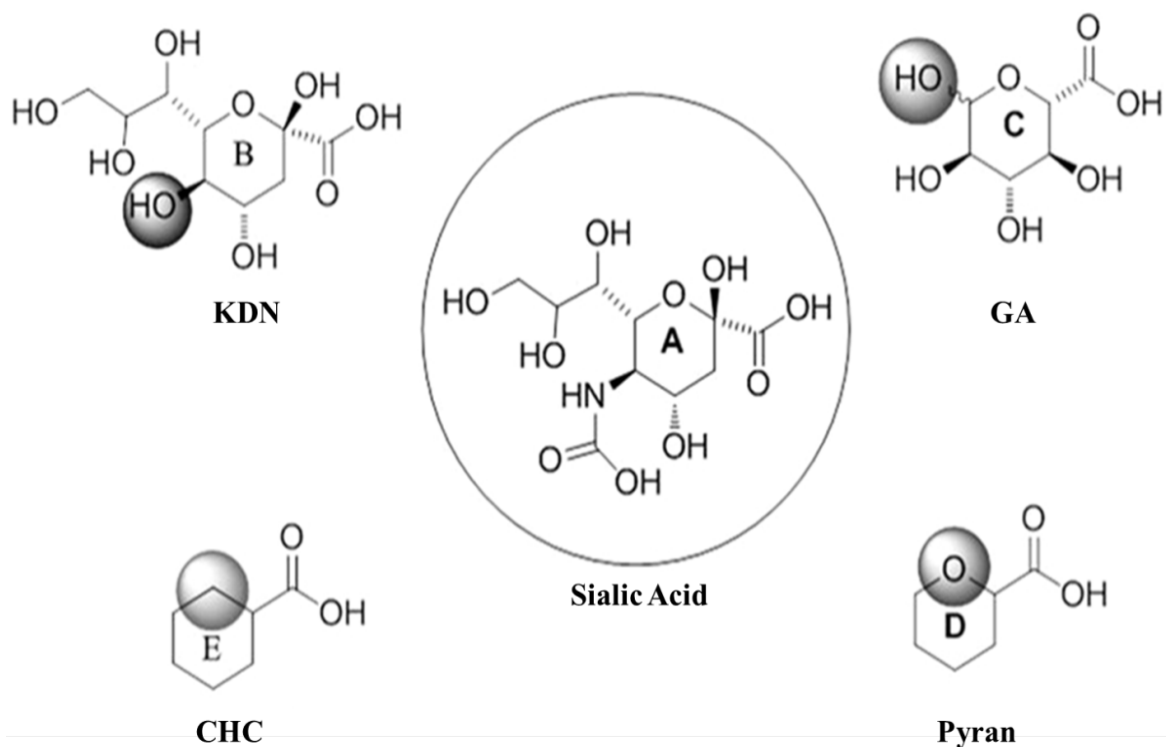


**Figure 10: Structure of different sugars conjugated to chitosan**

The structural differences from sialic acid are indicated by the shaded region. (A) Sialic acid (N-Acetylneuraminic acid), (B) Keto-deoxynonulosonic acid (KDN), (C) D(+)-Galacturonic acid (GA), (D) Tetrahydropyran-2-carboxylic acid (Pyran), and (E) Cyclohexanecarboxylic acid (CHC) structures are shown to elucidate these differences.

## 2.14. Conjugation Chemistry Using EDC with Sulfo-NHS

We envisioned the synthesis of cyclic sugar labeled chitosan biomaterials that can mimic the sialic acid structure present on the cell membrane. For this reason, a suitable conjugation chemistry should be investigated that can attach these sugars to chitosan with control over the degree of labeling. As it can be seen from figure 10, there is a carboxylic acid group at the C1 position on each of the sugars that are coupled with the amines on chitosan. A number of chemistry methods have been developed that can couple  $\text{-NH}_2$  group to a  $\text{-COOH}$  group resulting in amide linkage. The sugars that will be conjugated to chitosan are shown in figure 10 and the structure of chitosan is shown in figure 9.

Crosslinking reagents are commonly used to couple two molecules together. Homobifunctional crosslinkers (e.g. Imidoesters to couple amines) are used when the two crosslinking molecules have the same functional groups and heterobifunctional crosslinkers (eg. carbodiimides to form amide linkages) are used when the two targeted molecules have different functional groups. In using conjugation chemistry, the length of the spacer arm or bridge is an important consideration as it can affect the steric interactions and affinity between linked molecules [179].

EDC or 1-Ethyl-3-(3-dimethylaminopropyl) carbodiimide hydrochloride is a zero-length, water soluble crosslinker used commonly to couple carboxylic acids with primary amines. EDC first reacts with the carboxyl groups to form a highly reactive, *O*-acylisourea intermediate. This active species then reacts with an amino group to form an amide bond by release of an isourea derivative as by-product. However, the intermediate is unstable in aqueous solutions and therefore, a two-step conjugation procedure is preferred using *N*-hydroxysuccinimide (NHS) or

*N*-hydroxysulfosuccinimide (Sulfo-NHS) for stabilization. Sulfo-NHS esters are water soluble hydrophilic active groups that react rapidly with amino groups on target molecules. This two-step procedure of using EDC and Sulfo-NHS has advantages such as enhanced coupling efficiency, slow hydrolysis in water, extension of the half-life of activated carboxylate from seconds to hours and increased stability in coupling. Thus, in the first step, EDC reacts with the carboxyl group on first target compound forming the unstable *O*-acylisourea ester intermediate. Sulfo-NHS, added at the same time as EDC, reacts with the unstable intermediate to form semi-stable amine reactive NHS ester with improved stability. In the second step, the amino group containing molecules are added. In the presence of amino groups that can attack the carbonyl group of the ester, the *N*-hydroxysulfosuccinimide group rapidly leaves, creating a stable amide linkage with the amine molecule. Failure to react with an amine results in hydrolysis of the intermediate, regeneration of the carboxyl groups and release of *N*-substituted urea [179-181]. The mechanism of EDC chemistry is given in figure 11.

The EDC coupling reaction is dependent of temperature, pH and buffer composition [179]. Studies have found that reactions with EDC and Sulfo-NHS are most efficient at pH between 4.7 and 6. At low pH, MES buffer (2-[morpholino]ethanesulfonic acid) at 0.1M is recommended whereas for neutral pH reactions, phosphate buffers can be used. Amine or carboxylate containing buffers can interfere with the EDC chemical pathway and hence should be avoided. For the two step conjugation process, the first reaction is usually performed in MES buffer (or other non-amine, non-carboxylate buffer) at pH 5.0-6.0. After activation is complete, the pH is raised by using phosphate buffer (or other non-amine buffer) to 7.0-7.5 immediately before addition of amine containing compound (Ref: NHS, Sulfo-NHS product information sheet, Pierce Biotechnology, IL, USA) [180, 181]. Thus, EDC chemistry is extensively used to

couple two proteins, haptens to carrier proteins, surface molecule attachment and a host of other applications. Practically, any two molecules having a carboxyl group and amine group can be conjugated by this chemistry. The disadvantages of this chemistry include unwanted polymerization, precipitation of conjugating molecules, hydrolysis and unwanted side reactions in presence of certain compounds.

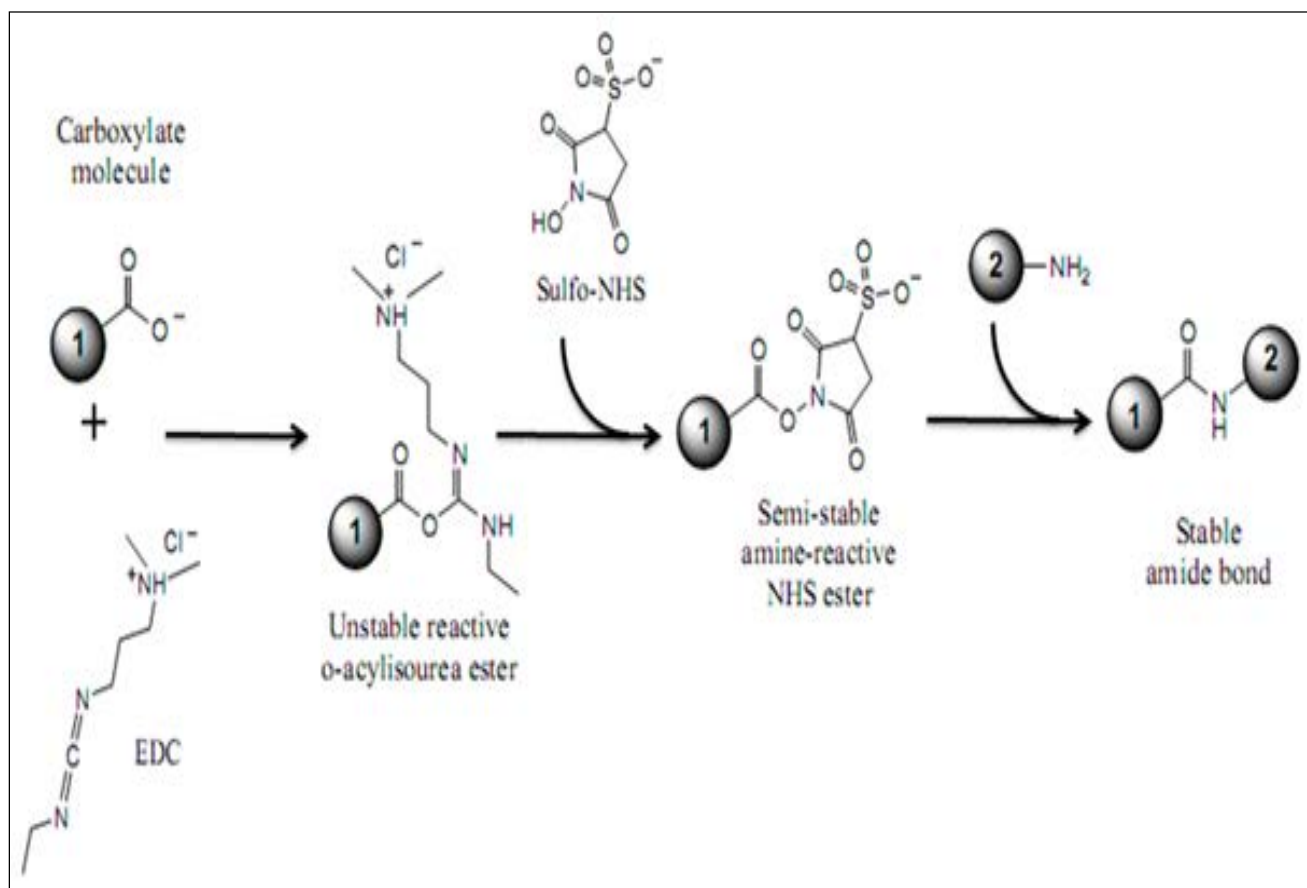


**Figure 11: Conjugation Mechanism using EDC chemistry with Sulfo-NHS**

This chemistry is used to couple carboxylate containing molecules (Sugars in this case) with amine containing molecules (Chitosan in this case) showing intermediate steps in the reaction [180] (<http://www.piercenet.com/products/browse.cfm?fldID=02040114>)

## 2.15. Experimental Design

The therapeutic development in Alzheimer's disease (AD) is hampered by the fact that the amyloid-beta ( $A\beta$ ) peptide is amphiphilic and highly prone to aggregation. Until now, the exact structure of aggregated  $A\beta$  has not been agreed upon (section 2.8 gives literature on the structures of  $A\beta$ , its aggregated states and the work done in those fields). For the  $A\beta$  experiments done *in vitro*, in this work, it is important that the protocols and design followed are consistent with that in the community. The following sections describe the work of other researchers with aggregated  $A\beta$  and its toxicity attenuation studies.

### 2.15.1. Brief Background

$A\beta$  peptide is highly prone to aggregation and exhibits dual nature in many studies.  $A\beta$  is an amphiphilic peptide whose aggregation is dependent on a host of factors such as length of the peptide, solvent hydrophobicity, peptide counter ions ( $CF_3COO^-$  vs.  $Cl^-$ ), pH, temperature, peptide concentration, type of solvent, salt concentration and pretreatment [182, 183]. There are a host of conformational forms that  $A\beta$  can take and all these forms have shown different behavior and toxicity profiles depending on several environmental factors. Additionally, depending on the commercial source, peptide batch, particular aggregation conditions, there are significant discrepancies observed across different studies [182]. Before making the aggregated  $A\beta$  peptide that is neurotoxic, the lyophilized powder of  $A\beta$  peptide is dissolved in a highly polar solvent such as dimethyl sulfoxide (DMSO), 1,1,1,3,3,3-Hexafluoro-2-propanol (HFIP) or trifluoroacetic acid (TFA), aqueous TFA, aqueous acetonitrile with TFA etc. so that no aggregated  $A\beta$  species preexist that can act as a seed for aggregation. For the  $A\beta(40)$  peptide, solvents such as DMSO and HFIP are more suitable [182]. This addition of a polar solvent

makes each A $\beta$  monomer into a single species which is then added to the cell culture medium for aggregation over different periods of time (depending on the type of study to be done). Amyloid-beta A $\beta$ (40), A $\beta$ (1-42) and A $\beta$ (25-35) are the most widely used A $\beta$  species that are investigated for their neurotoxic effects. In the human body, more than 90% of the A $\beta$  produced from the amyloid precursor protein is the A $\beta$ (40) compared to other species, namely A $\beta$ (42), which is more neurotoxic A $\beta$ (42). A $\beta$ (42) has two additional residues in the hydrophobic domain compared to A $\beta$ (40), thus, it is more prone to aggregation and has been proved to be more toxic to cells in culture[184-187]. A $\beta$ (25-35) is the small fragment isolated from APP, one of the active part of A $\beta$ (1-42) that has shown similar neurotoxic effects (compared to A $\beta$  fragments) to cells in cultures [188, 189]. Additionally, section 2.7 lists the type of aggregated species that are isolated and identified. Each of these species exhibits their own morphology, aggregation states and toxicity profiles. Till this date, the exact toxic species in AD has not been agreed upon.

Given below are the studies done with A $\beta$  peptides and its different protocols regarding aggregation or cell culture or viability assessment. Details include, type of peptide used, concentration of A $\beta$  used, time of aggregation, protocol of aggregation, cell culture system used, toxicity assay used to assess viability and the time of A $\beta$  incubated with cells is mentioned. Finally, the viabilities (Percentage of cell surviving) obtained from each experiment are mentioned. Only the A $\beta$  control viability is will be given. The A $\beta$  control represents the viability obtained after the addition of A $\beta$  peptide solution (in any aggregated form) to cells in the absence of any other test or experimental compound. Thus, viability of cells with just toxic aggregated A $\beta$  added represents the A $\beta$  control. All values are relative to the live control, which are 100% cells, with no A $\beta$  or any other test/experimental compound added to them.

### 2.15.2. Review of A $\beta$ Studies from Published Literature

The issue of variability and unpredictable nature of the *in vitro* toxicity of synthetic A $\beta$ (40) was investigated by using different batches of A $\beta$ (40) and a model system of PC-12 cells [190]. A $\beta$ (40) peptides obtained from different sources were aggregated under similar conditions and the viability assessed by the trypan-blue assay. To form aggregated solutions, A $\beta$ (40) powders were dissolved in either 10% DMSO or 100% DMSO and sonicated, then centrifuged at 14000rpm for 5min. Then, these stock solutions were diluted into the serum free media for cell culture studies. For comparing toxicity studies, A $\beta$ (40) solutions were added to PC-12 cells for 24h after which viability assessed with the trypan blue assay. Viable cells exclude trypan dye. All A $\beta$ (40) peptide protocols and cell studies were done in a consistent manner to minimize variations in the study. Control cells were cell treated with either 0.1 or 1% DMSO as that was the solvent in which A $\beta$  was initially dissolved. First, from 18 PC-12 cell toxicity experiments (with 18 different batches of A $\beta$ (40)), statistically significant cell death was observed in 67% of the experiments. On the other hand, no toxicity was seen in 37% of the tests, indicating that 6 out of 18 A $\beta$ (40) batches were non-toxic to cells. These results show lot-to-lot variability in toxicity from A $\beta$ (40) solutions even under consistent conditions. See (figure 12 C.) below for detailed explanation on the results seen from the publication. In the next experiment, 46 $\mu$ M A $\beta$ (40) from the same lot, (ZK568) was used in each experiment performed on separate days. In these two experiments, same numbers of cells were added to the plates. Two experiments, done on two separate dates, with the same batch (ZK568) of A $\beta$ (40) and with the same number of cells gave very high toxicity (~24% viability of cells were in A $\beta$  control) in one experiment whereas no toxicity ( ~91% viability in A $\beta$  control) in the other. The actual result, adapted from the publication is shown in figure 12(A). This indicates the within lot variability of A $\beta$ (40) peptides.

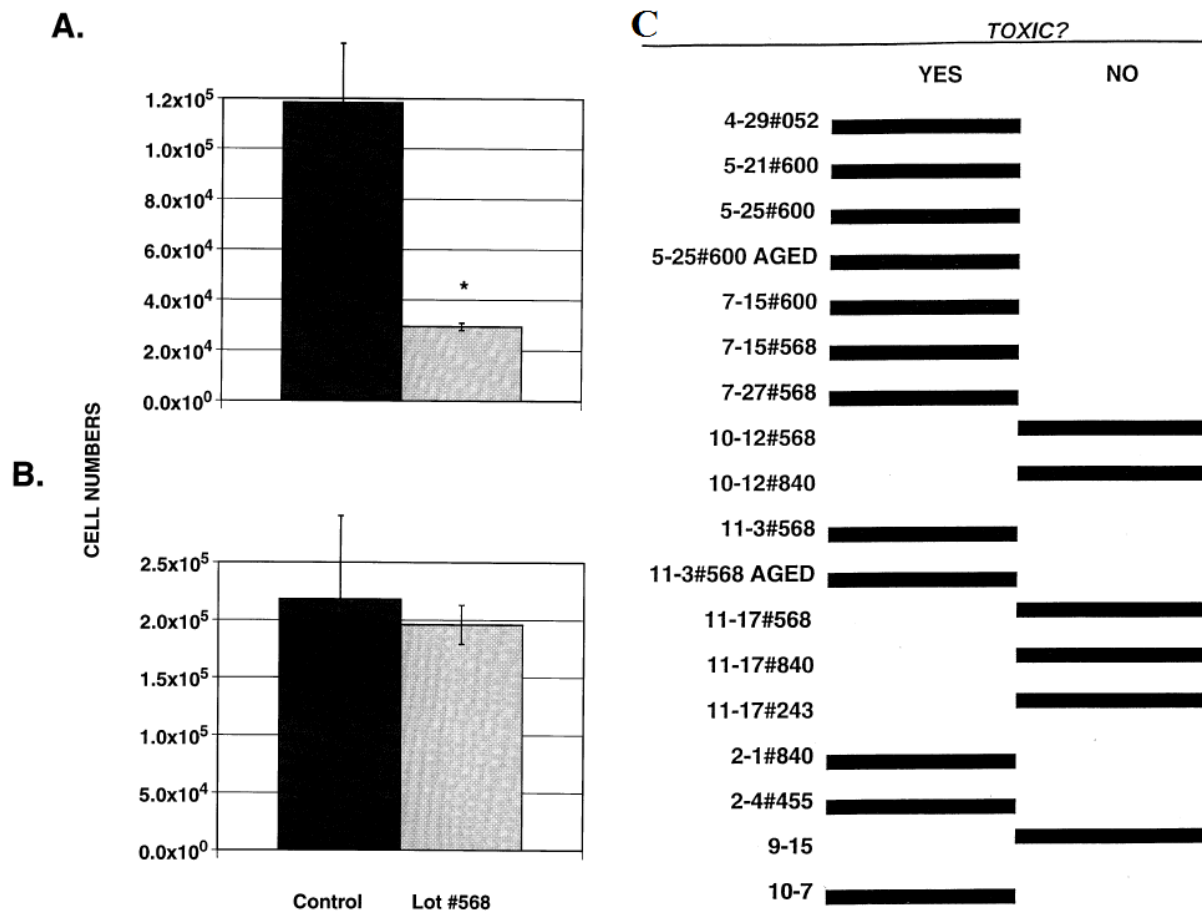


**Figure 12: Results from typical PC-12 cell toxicity tests illustrated to denote lot-by-lot variability**

Figure 12.A: Amyloid- $\beta(40)$  at  $46\mu\text{M}$  concentration of the same lot (#ZK568) of  $\text{A}\beta(40)$  was used in each experiment. Cell toxicity was defined relative to control cells that had received vehicle only (DMSO). All dishes started out with the same number of cells. Results of cell counting on the third day after addition of  $\text{A}\beta(40)$ . Comparison of these results illustrates the within-lot variability documented in Figure 12. C, experiments dated 7-15 are shown in (12.A) and the 10-12 results in (12.B). Figure (12.A) A typical result in which Lot#568  $\text{A}\beta(40)$  was toxic to PC-12 cells Figure (12.B) A typical result in which same lot# 568  $\text{A}\beta(40)$  was not toxic to PC-12 cells.

Figure 12.C: The numbers (#) refer to lot numbers of  $\text{A}\beta(40)$  (note that there are no lot numbers for the privately obtained material, dates 9-15 and 10-7). *Yes* refers to experiments in which the  $\text{A}\beta(40)$  was toxic and *NO* indicates experiments in which  $\text{A}\beta(40)$  was not toxic. In 67% of the cases,  $\text{A}\beta(40)$  was toxic to PC-12 cells and it was not toxic in 33% of the experiments. These results demonstrate the lot-to-lot variability and the within-lot variability in toxicity of  $\text{A}\beta(40)$  solutions. Figures adapted from publication [190], with permission from Elsevier Science Inc.)

In a study by Jarvis et al., a dose-dependent study to decide optimum A $\beta$  concentration was performed before other cytotoxicity experiments [191]. Briefly, neurons from the septal nucleus of the rat were treated with 0.1 $\mu$ M, 1 $\mu$ M and 10 $\mu$ M concentrations of aggregated A $\beta$  fragment (25-35). In the dose-dependent study, live control (no A $\beta$ ) was ~87% cell survival, the addition of 0.1 $\mu$ M A $\beta$ (25-35) gave ~79% viability, 1 $\mu$ M gave ~73% cell survival, and 10 $\mu$ M A $\beta$ (25-35) gave ~64% cell survival. The study determined 10 $\mu$ M A $\beta$ (25-25) to be the concentration for later studies. However, in the later experiments under similar conditions of aggregation and cell culture, the control value was around ~66% and the % cell survival with the same 10 $\mu$ M A $\beta$ (25-35) was ~21%. This indicates that even after a dose-dependent study with the same A $\beta$  fragment, same aggregation protocol, same cell culture system and same experimental conditions gives completely different viabilities and cell survival due to variability in the toxicity of aggregated A $\beta$ . This difference between the viability from dose-dependent study (~64%) and later experiments (~21%) indicates that dose-dependent studies are not a good predictor of A $\beta$  toxicity values for subsequent studies.

The protective effect of TEMPOL, a cyclic nitroxide to prevent A $\beta$ (42) induced oxidative injury in SH-SY5Y cells was investigated by Chonpathompikunlert & Nagasaki et al. [192]. Aggregated A $\beta$ (42) was prepared by dissolving the peptide in cell culture medium and incubating at 37<sup>0</sup>C for 72h prior to the addition to cells. In all experiments, the incubation time of A $\beta$ (42) with SH-SY5Y cells was 48h after which the viability was determined by the WST-8 assay. The WST-8 reduction by the cells gives a spectrophotometric reading that is proportional to the number of viable cells in the sample. In the dose-dependent study with aggregated A $\beta$ (42), compared to 100% live cells, 1.5 $\mu$ M A $\beta$ (42) gave ~72% viability, 10 $\mu$ M A $\beta$ (42) gave ~56% viability, 12.5 $\mu$ M A $\beta$ (42) gave ~40% viability, 15 $\mu$ M and 20 $\mu$ M A $\beta$ (42) gave ~26% viability of

SH-SY5Y cells after 48h of incubation with A $\beta$ (42) peptide. From this study, 20 $\mu$ M A $\beta$ (42) was chosen for the next experiments. When 20 $\mu$ M of aggregated A $\beta$ (42) prepared by same methods was used, the A $\beta$  control viability was observed to be ~40%. Thus, using the same concentration of A $\beta$ (42) and the same aggregation and cell culture protocols, different viabilities in SH-SY5Y cultures were observed. This indicates that the viabilities from a dose-dependent study are not an accurate predictor of the viabilities obtained in later studies.

The protective effect of TEMPOL, a cyclic nitroxide to prevent A $\beta$ (42) induced oxidative injury in SH-SY5Y cells was investigated by Chonpathompikunlert & Nagasaki et al. [192]. Aggregated A $\beta$ (42) was prepared by dissolving the peptide in cell culture medium and incubating at 37<sup>0</sup>C for 72h prior to the addition to cells. In all experiments, the incubation time of A $\beta$ (42) with SH-SY5Y cells was 48h after which the viability was determined by the WST-8 assay. The WST-8 reduction by the cells gives a spectrophotometric reading that is proportional to the number of viable cells in the sample. In the dose-dependent study with aggregated A $\beta$ (42), compared to 100% live cells, 1.5 $\mu$ M A $\beta$ (42) gave ~72% viability, 10 $\mu$ M A $\beta$ (42) gave ~56% viability, 12.5 $\mu$ M A $\beta$ (42) gave ~40% viability, 15 $\mu$ M and 20 $\mu$ M A $\beta$ (42) gave ~24% viability of SH-SY5Y cells after 48h of incubation with A $\beta$ (42) peptide. From this study, 20 $\mu$ M A $\beta$ (42) was chosen for the next experiments. When 20 $\mu$ M of aggregated A $\beta$ (42) prepared by same methods was used, the A $\beta$  control viability was observed to be ~40%. Thus, using the same concentration of A $\beta$ (42) and the same aggregation and cell culture protocols, different viabilities in SH-SY5Y cultures were observed. This indicates that the viabilities from a dose-dependent study (~24% at 20 $\mu$ M) are not an accurate predictor of the viabilities obtained in later studies (~40% at 20 $\mu$ M).

Lee et al., [193] investigated different hybrid molecules to reduce the effects of aggregated A $\beta$ (42) on the model human neuroblastoma cell line SH-SY5Y. The SH-SY5Y cells

were differentiated for 8 days prior to use in the experiments using trans-retinoic acid in 96-well plates. A $\beta$ (42) was dissolved in DMSO to make 500 $\mu$ M and 1mM stock solutions and then diluted to their final concentration in cell media. After addition of aggregated A $\beta$ (42) and other hybrid molecules, the cells were incubated for 24h and then viability assessed by the 3(4,5-dimethylthiazol-2-yl)2,5-diphenyl-2H-tetrazolium bromide (MTT) assay. This is the same assay used in our experiments. In this study, no dose-response studies with aggregated A $\beta$  are done before toxicity studies. Using a concentration of 5 $\mu$ M A $\beta$ (42), the results show a viability of ~77% when no other molecule is added to the wells except 5 $\mu$ M A $\beta$  (figure 1 in ref [193] ). In the same publication, the effect of 0.5 $\mu$ M A $\beta$ (42) was assessed on SH-SY5Y cells along with 4 different hybrid complexes. In these four separate experiments, differentiated SH-SY5Y showed viability ranging from ~56% to ~64% after treatment with 0.5 $\mu$ M A $\beta$ (42). It is interesting to note that in this study, treatment with 0.5 $\mu$ M A $\beta$ (42) showed ~56% to ~64% SH-SY5Y viability, whereas treatment with a higher 5 $\mu$ M concentration of toxic A $\beta$ (42) showed a contradictory ~77% viability even when the aggregation protocols were the same.

In a publication in PEDS [194], a new protocol for the solubilization of A $\beta$  peptide is presented along with the toxicity studies with neuroblastoma SH-SY5Y cells. The protocol to give seed free A $\beta$  for aggregation involves a series of solubilizations in organic solvents such as DMSO and hexafluoroisopropanol. 1 $\mu$ M to 50 $\mu$ M of A $\beta$ (40) and A $\beta$ (42) aggregated solutions were added to SH-SY5Y cells and the viability assessed after 48h using the Cell Titer-Blue (Promega) cell viability assay. The results show that no toxicity is seen at 1 $\mu$ M to 20 $\mu$ M of the aggregated A $\beta$ (40) species and A $\beta$ (40) displays toxicity towards SH-SY5Y after 30 $\mu$ M (~22% viability) concentration. Also, there is a huge drop in viability between 20 $\mu$ M (~90% viability) and 30 $\mu$ M (~22% viability). SH-SY5Y cells are completely killed above the concentration of

30 $\mu$ M till 50 $\mu$ M A $\beta$ (40) concentration. In the case of A $\beta$ (42) prepared by the proposed method, aggregated A $\beta$ (42) species show toxicity from 7.5 $\mu$ M to 10 $\mu$ M. At concentrations of 10 $\mu$ M and 30 $\mu$ M, the observed viability is ~12% with complete loss of viability at higher concentrations. This study shows that very high toxicities (0% viability at  $\geq$  30 $\mu$ M A $\beta$ ) can be achieved from lower concentrations to A $\beta$  peptides (higher limit is ~100 $\mu$ M). Also, the no toxicity observed from A $\beta$ (40) up to 20 $\mu$ M is in contrast to other studies that have used even less concentration of A $\beta$  (40) with significant toxicity seen in toxicity studies [195, 196].

Milton and group studied the effects of compounds, cannabinoids and noladin ether, on the toxicity of A $\beta$ (1-40) induced in human neuronal NT-2 and mouse myeloma SP2 cell cultures [195]. A $\beta$  aggregated solutions were prepared by dissolving in PBS and incubating for 24h to prepare cytotoxic species. In this study, no dose-dependent study on aggregated A $\beta$  peptides was done. Focusing only on the neuronal cell line NT-2, addition of 5 $\mu$ M aggregated A $\beta$ (40) to NT-2 cells gave ~42% viability (seen from figure 1 in publication) determined by the 3(4,5-dimethylthiazol-2yl)2,5-diphenyl-2H-tetrazolium bromide (MTT) assay. In a contradictory results, addition of 25 $\mu$ M aggregated A $\beta$ (40) by the same aggregation protocol to NT-2 cells gave ~48% viability (refer figure 2 in publication), which ideally should be lower than the viability obtained at 5 $\mu$ M A $\beta$ . In this study, two different A $\beta$  concentrations are used out of which the lower concentration of toxic A $\beta$  has higher toxicity compared to higher concentration of A $\beta$ , which indicates different toxicity profiles at different concentrations of the same peptide.

Studies have shown that A $\beta$  is a random coil monomer, well solvated in DMSO [197] or 1,1,1,3,3,3-hexafluoro-2-propanol (HFIP) [15], forms a “seedless” monomer, which renatures when diluted to buffers or cell media solutions. These studies show that using a strong polar

solvent such as DMSO will eliminate any preexisting aggregation that may lead to inconsistent results after aggregation.

Mie, Liu et al. studied the effects of cryptotanshinione on the inhibition of aggregated fibril A $\beta$ (42) toxicity was studied in an SH-SY5Y cell system [198]. A $\beta$  was solubilized in distilled water to a concentration of 200 $\mu$ M and stored at -20°C. The viability of SH-SY5Y was assessed by the MTT assay after 24h of addition of A $\beta$  peptides. In the dose dependent study, a gradient of 1 $\mu$ M to 10 $\mu$ M of A $\beta$ (42) was applied and viability assessed 24h later via MTT assay. The viability of SH-SY5Y ranged from 100% viability (0.0 $\mu$ M A $\beta$ ) to ~70% viability (10 $\mu$ M A $\beta$ ). Later, in the same study, the viability with 10 $\mu$ M A $\beta$  was ~66% after 24h. This study indicates that dose-dependent study viabilities do not match exactly with viabilities observed in later studies. Also, 10 $\mu$ M A $\beta$ (42) in another study gave ~12% viability in SH-SY5Y cell cultures [194]. This indicates that, at the same concentration of A $\beta$  and same cultures, different viabilities can be obtained based on individual protocols used.

The effect of peptide based aggregation inhibitors were investigated on fresh and aged A $\beta$  peptide solutions [196]. The effect of these inhibitors in a system of different concentrations of A $\beta$  and SH-SY5Y cells was investigated. Aggregated A $\beta$ (40) and A $\beta$ (42) were made by dissolving peptides in water and then in PBS to give 100 $\mu$ M of the peptides. SH-SY5Y viability was assessed after 24h of the addition of peptide inhibitors and aggregated A $\beta$  peptides 40 and 42 by using the 3(4,5-dimethylthiazol-2-yl)2,5-diphenyl-2H-tetrazolium bromide (MTT) assay. The different concentrations of fresh A $\beta$ (40), aged A $\beta$ (40) and aged A $\beta$ (42) studied were 3.125 $\mu$ M, 6.25 $\mu$ M, 12.5 $\mu$ M and 25 $\mu$ M. The SH-SY5Y viabilities assessed after 24h for A $\beta$  control is given below. The table indicates that when different types of procedures or conditions

of aging are used, the A $\beta$  species give completely different viabilities for SH-SY5Y cells. These viability values are different than those obtained by other researchers [190, 199, 200].

**Table 3: SH-SY5Y viabilities after 24h incubation for different A $\beta$  concentrations and different A $\beta$  aggregation times, from ref. [196]**

A $\beta$ Species	Concentration of A $\beta$ applied for 24h to SH-SY5Y	% of average control obtained from MTT assay: A $\beta$ control
Fresh A $\beta$ (40)	3.12 $\mu$ M	~90%
	6.25 $\mu$ M	~87%
	12.5 $\mu$ M	~70%
	25 $\mu$ M	~52%
Aged A $\beta$ (40)	3.12 $\mu$ M	~72%
	6.25 $\mu$ M	~60%
	12.5 $\mu$ M	~56%
	25 $\mu$ M	~42%
Aged A $\beta$ (42)	0.3125 $\mu$ M	~84%
	3.12 $\mu$ M	~60%
	6.25 $\mu$ M	~58%
	12.5 $\mu$ M	~52%
	25 $\mu$ M	~39%

In the study presented by Wang et al.[201], synthetic A $\beta$ (40) was aggregated by dissolving in a strong polar solvent TFA and rotated for 24h. Then, aggregated A $\beta$ (40) was diluted to its final concentration and added to SH-SY5Y cell culture. The viability was assessed using the MTT reduction assay. This procedure is consistent with that followed in our work in this dissertation. The toxicity of A $\beta$ (40) peptide was determined as a function of time (20h, 41h, 65h) at different concentration of A $\beta$  protein. As the aggregation protocol, cell culture systems are consistent (except time of incubation, in our work, 24h) with that of this work, the viabilities obtained for A $\beta$  control are given in the table below. The viabilities indicate that different

incubation times of the A $\beta$  peptide with SH-SY5Y cells give completely different viabilities. Thus, time of incubation of cells with A $\beta$  influences the toxicity profile observed. In our case, 24h is the incubation time with 50 $\mu$ M A $\beta$ .

**Table 4: SH-SY5Y viabilities after different incubation times with A $\beta$  at different concentrations, from ref. [201]**

For 20h incubation with A $\beta$		For 41h incubation with A $\beta$		For 65h incubation with A $\beta$	
Conc. of A $\beta$	Viability	Conc. of A $\beta$	Viability	Conc. of A $\beta$	Viability
10 $\mu$ M A $\beta$ (40)	~79%	10 $\mu$ M A $\beta$ (40)	~62%	10 $\mu$ M A $\beta$ (40)	~50%
20 $\mu$ M A $\beta$ (40)	~75%	20 $\mu$ M A $\beta$ (40)	~58%	20 $\mu$ M A $\beta$ (40)	~40%
30 $\mu$ M A $\beta$ (40)	~70%	30 $\mu$ M A $\beta$ (40)	~48%	30 $\mu$ M A $\beta$ (40)	~30%

In this study [202], aggregated A $\beta$ (42) concentrations at 25 $\mu$ M and 100 $\mu$ M were added to a system of SH-SY5Y cells to evaluate the ability of ectoine and hydroectoine to inhibit aggregate formation. The aggregates were prepared by dissolving in HCl and DMSO for 3 days. To observe the effect on SH-SY5Y viability, A $\beta$ (42) seed samples were made by incubating 25 $\mu$ M or 100 $\mu$ M solution at 37<sup>0</sup>C for 24h. The viability of SH-SY5Y was assessed after 48h incubation with the seed-aggregated A $\beta$ (42) peptide using the 3(4,5-dimethylthiazol-2yl)2,5-diphenyl-2H-tetrazolium bromide (MTT) assay. For the same concentration of A $\beta$ (42), the viabilities obtained at 25 $\mu$ M A $\beta$ (42) are different in the same experiment. In one case, the SH-SY5Y viability was ~75% and in the other ~65% (see figure 4A in the publication). Thus, at the same concentration and at the same experiment, different SH-SY5Y viabilities were observed, which is most likely due to the differences in toxicities of the aggregates formed. Addition of 100 $\mu$ M A $\beta$ (42) gave around ~53% viability. It can be seen that researchers use A $\beta$  concentrations as high as 100 $\mu$ M and the viabilities of A $\beta$  peptide, at the same concentration and the same conditions can be different.

Green et al. investigated the use of estradiol to attenuate the toxicity of A $\beta$ (25-35) in a human neuroblastoma cell line SK-N-SH using the MTT assay[203]. The lyophilized peptide A $\beta$ (25-35) was suspended in PBS and incubated for 1h prior to use by diluting to its final concentration in culture media. The SK-N-SH cells were exposed to varying concentration of A $\beta$  for 24h. Compared to 100% live control, 5 $\mu$ M A $\beta$ (25-35) gave ~95% viability, 10 $\mu$ M A $\beta$  gave ~85% viability and 20 $\mu$ M A $\beta$  gave ~66% viability. The paper reports that incubation times of A $\beta$  with cells up 96h did not further increase attenuation in MTT reduction (i.e. did not cause further toxicity in cells), however, other studies have shown that as the incubation time of cells with A $\beta$  increase, changes in toxicity are observed. See [199-201, 204] for conflicting reports. This indicates contradictory results with respect to toxicity observed in cells incubated for various time periods with A $\beta$  peptides.

A study with estrogen to protect human neuroblastoma SH-SY5Y cells from A $\beta$ (42) toxicity is presented below [205]. A 10 $\mu$ M concentration of A $\beta$ (42) was prepared by “aging” the dissolved peptide for 24h. Before selecting this concentration, no dose dependent study with A $\beta$  was done. In the first experiment, the viability of SH-SY5Y was assessed after incubating the cells with 10 $\mu$ M A $\beta$ (42) for 5h, 24h and 48h using the MTT assay. The viability of cells are as follows: 5h incubation with 10 $\mu$ M A $\beta$ (42): ~70% viability, 24h incubation with 10 $\mu$ M A $\beta$ (42): ~78% cell viability, 48h incubation with 10 $\mu$ M A $\beta$ (42): ~75% viability. Thus, in this case, the viability observed is less after 5h incubation with the toxic peptide but increases at 24h (and remains almost the same at 48h incubation) which is in contrast with other studies (see publication with [203]). In the next experiment with estrogen receptor agonists, 10 $\mu$ M A $\beta$ (42) control viability was ~60% after 24h of incubation with SH-SY5Y. Thus, SH-SY5Y viabilities have a wide difference (~78% and ~60% viability) for the experiments done at the same

concentration (10 $\mu$ M) of A $\beta$ (42) with the same incubation time (24h) at the same condition in the single publication. This indicates that even with the same likely batch of A $\beta$  peptide (although this cannot be proved looking at the data presented) and the same experimental conditions, it is possible to have different toxicities associated with the peptide.

Zhang et al. studied the protective effect of galantamine on A $\beta$ (40) induced toxicity in human neuroblastoma cells SH-SY5Y [206]. A 5 $\mu$ M A $\beta$ (40) solution was prepared by incubating the peptides in DI water for 24h at 37<sup>0</sup>C. No dose dependent study was done before choosing this concentration to work in the experiments. After incubating a solution of 5 $\mu$ M A $\beta$ (40) with SH-SY5Y cells for 24h, the viability observed was (~63.23%  $\pm$  1.2%). Again, other studies with A $\beta$ (40) concentration upto 20 $\mu$ M applied to SH-SY5Y showed ~100% viability [194].

This publication demonstrated the use of Hsp20, novel  $\alpha$ -crystallin heat shock protein, to attenuate the toxicity of A $\beta$ (40) in a system of SH-SY5Y cell line and PC12 cell line[207]. A $\beta$ (40) was dissolved in trifluoroacetic acid (TFA) and then diluted to its final concentration in cell culture media for testing with cells *in vitro*. The A $\beta$  peptides were rotated for 24h to ensure aggregation. A concentration of 100 $\mu$ M aggregated A $\beta$ (40) was tested on SH-SY5Y cells and the viability after 24h was found to be around ~42% assessed by the MTT assay. On the other hand, in the same experiment and same aggregation protocol but with PC12 cells, 2 $\mu$ M of aggregated A $\beta$ (40) gave viability of ~38% using the MTT assay after 24h. As there is no dose dependent study done on A $\beta$  toxicity, it is unclear why different A $\beta$  values that were very different apart were chosen in the same experiment for different cell cultures. In the next set of experiment with a modified shock protein, 100 $\mu$ M aggregated A $\beta$ (40) gave viability of ~50% after 24h treatment of SH-SY5Y cells. There are two important observations from this study: Different cell cultures give widely different toxicities towards A $\beta$  (2 $\mu$ M A $\beta$  to PC12 and 100 $\mu$ M A $\beta$  to SH-SY5Y gave

almost same viabilities). Secondly, in A $\beta$  studies, the range of A $\beta$  studies can vary from as low as 2 $\mu$ M to as high as 100 $\mu$ M A $\beta$  in the same publication. Additionally, same aggregation protocol, same cell type, same experimental methodology gave different set of viabilities at 100 $\mu$ M A $\beta$  (~42% and ~50%). In our work, the aggregation protocol has same methodology as in this publication. The cell culture experiments as well as A $\beta$  studies done in our work are also consistent with this publication.

The interactions of different heat shock proteins with A $\beta$ (40) was studied in a system of human neuroblastoma SH-SY5Y cells by Lee, Good et al [204]. To prepare aggregated A $\beta$ (40), lyophilized A $\beta$ (40) was dissolved in trifluoroacetic acid (TFA) and incubated for 20-30min to completely dissolve the A $\beta$ . Then, the TFA-A $\beta$  solution was directly added to the cell media to its final concentration and mixed at 37<sup>0</sup>C for different times. Different rotation times were used to get different aggregated A $\beta$ (40) species. The aggregated A $\beta$ (40) was added to SH-SY5Y for 2h and the viability determined using the Annexin-PE-7AAD dye. Viable cell exclude both dyes. In the first experiment in a system of hsp20, 100 $\mu$ M of aggregated A $\beta$ (40) gave ~45% of A $\beta$  control & hsp27, 100 $\mu$ M of aggregated A $\beta$ (40) gave ~47% of A $\beta$  control. Next, in a system of hsp17.7, 20 $\mu$ M A $\beta$ (40) had ~65% viability. As no dose dependent study was done, it is unclear why different concentrations of A $\beta$ (40) were used. Also, the time of aggregation of A $\beta$ (40) was varied. Specifically, 100 $\mu$ M A $\beta$ (40) was aged for 2h, 4d, 8h and 24h. These differently aged peptides were added to A $\beta$  and toxicity assessed after 2h. The viabilities are as follows: after 2h aggregation: ~66% viability. 4h aggregation time: ~62% viability, 8h aggregation time: ~53% viability and after 24h aggregation time: ~48% viability of SH-SY5Y was observed. Important points can be observed from this publication: 1) Different A $\beta$  concentrations (20 $\mu$ M and 100 $\mu$ M) of the same peptide are used in the same study without a dose-dependent study done beforehand.

2) Concentrations as high as 100 $\mu$ M are used for A $\beta$  toxicity studies. 3) With increased aging, A $\beta$  peptide shows increasing toxicity, whereas other studies show conflicting results for ageing and toxicity data [208, 209]. The aggregation methodology for A $\beta$  used in our work is consistent with this publication.

Yang et al studied the effect of citrate on the inhibition of A $\beta$ (40) peptide aggregation using SH-SY5Y cells [210]. Stock solution of A $\beta$ (40) peptide was prepared by solubilizing the lyophilized A $\beta$ (40) by shaking in NaOH solution. SH-SY5Y cell viability was assessed by the WST-1 assay. It is an assay in which viable cells metabolize tetrazolium salts to formazan that can be detected spectrophotometrically. When SH-SY5Y cells were incubated with 20 $\mu$ M A $\beta$ (40) for 3 days, cell viability of A $\beta$  control was ( $\sim 65.3\% \pm 5.2\%$ ) compared to live control of 100% cells.

In a system of cultured fetal rat cortical neurons, the effects of laminin 1 and laminin 2 on aggregated A $\beta$ (40) was investigated by Drouet et al [211]. Stock solutions of A $\beta$  were prepared by dissolving the A $\beta$  in hexafluoro-2-propanol. Then, fibrillar aggregated A $\beta$  was prepared by incubation the peptide in culture medium for 48h. For the A $\beta$  studies, 5 $\mu$ M aggregated A $\beta$  was added to the cultured neurons for 48h and the viability assessed by MTT assay. In this study, no dose-dependent study for aggregated A $\beta$  was done before other toxicity studies. The cortical neuron viability was  $\sim 38.1\%$  after 24h incubation and  $\sim 30.2\%$  after 48h incubation with 5 $\mu$ M A $\beta$ (40). In the next experiment (refer to Fig 1.A. in the publication), with 5 $\mu$ M A $\beta$ (40) aggregated by the same procedure and the same cell culture experiment, the neuronal viability was  $\sim 40\%$  of control (live control is 100%) after 48h incubation. In table 2 of the publication, in the experiment with laminin 2, the 5 $\mu$ M A $\beta$ (40) gave 34% viability compared to control after 48h. Further, in another experiment with different compound (see figure 4A in publication), the

A $\beta$  control value was ~20% viability compared to live control after 48h incubation. The aggregated protocol was the same, concentration of A $\beta$  was 5 $\mu$ M and the cortical neurons were used. In this publication, for the same peptide A $\beta$ (40), with the same aggregation protocol, same concentration of A $\beta$ (40) used (i.e. 5 $\mu$ M), and the same incubation time with cortical neurons (48h), the ranges of viability obtained are from ~20%, 30%, 34% and 40%. This may point to the fact that even with the same batch of A $\beta$ , in the same publication and similar conditions, the toxicities of the aggregated A $\beta$  formed could differ significantly. Also, it is interesting to note that a low concentration (5 $\mu$ M) of A $\beta$ (40) is showing about 20% to 40% viabilities.

To investigate the effect of mortalin overexpression on A $\beta$ (42) toxicity was investigated in a human neuroblastoma cell line SH-SY5Y[212]. A $\beta$  was dissolved in ice-cold cell culture medium and incubated for 24h to form aggregated A $\beta$ (42) and the supernatant used for subsequent experiments. The viability was assessed by the CCK-8 assay that gives spectrophotometric reading similar to the MTT assay. From a dose dependent study, SH-SY5Y viabilities at different concentrations of A $\beta$ (42) after 24h incubation were: 1 $\mu$ M A $\beta$ (42): ~92%, 5 $\mu$ M A $\beta$ (42): ~75%, 10 $\mu$ M A $\beta$ (42): 64%, 20 $\mu$ M A $\beta$ (42): 42% viability. Later experiments with 10 $\mu$ M A $\beta$ (42) gave ~65% viabilities.

Coenzyme Q10 was studied in a system of SH-SY5Y cells exposed to 5 $\mu$ M A $\beta$ (42) for 24h [213]. After 24h incubation of 5 $\mu$ M A $\beta$ (42) with SH-SY5Y cells, the viability of SH-SY5Y with MTT assay was ~63% compared to 100% viability for live control. In earlier publication [212], 10 $\mu$ M A $\beta$ (42) gave ~64% viability, whereas in this publication, 5 $\mu$ M A $\beta$ (42) gave ~63% viability. In another publication, use of the same 10 $\mu$ M A $\beta$ (42) gave ~12% viability of SH-SY5Y cells [194]. Thus, there are many variables in A $\beta$  studies that influence the toxicity profiles seen on cultured cells.

The neuroprotective effect of cannabidiol was investigated in a system of cultured rat pheochromocytoma PC-12 cells [214]. Briefly, 1µg/ml of Aβ(42) = 0.2215µM Aβ(42) was added to PC12 cells and incubated for 24h after which viability was determined by the MTT assay. It is interesting to note that incubation of PC12 cells with 0.2215µM Aβ(42) for 24h gave ~61.2% viability compared to 100% live control. This publication indicates that Aβ peptide values as low as 0.221µM are used and that such low concentration of Aβ peptide can give ~61% cell viability towards cells in culture.

The effect of genistein was investigated using aggregated Aβ(42) was studied in a system of SH-SY5Y cell cultures [215]. A dose-dependent study to determine the effective concentration (1µM, 2µM, 5µM, 10µM) and duration (24h, 48h, 72h) of Aβ(42) was assessed by using the MTT assay. After 24h incubation, 1µM, 2µM, 5µM, 10µM all gave around ~70% viability of SH-SY5Y using the MTT assay. After 72h, 5µM and 10µM of Aβ(42) gave ~50% viabilities of SH-SY5Y using the MTT assay. Following this study, a concentration of 5µM Aβ(42) was chosen with 72h incubation time. At the same conditions and same aggregation protocols, the viability of SH-SY5Y was ~62% using the MTT assay. This study indicates that performing a dose-dependent study with Aβ (~50% at 5µM Aβ) is not a very good predictor of the viabilities obtained in later experiments (~62% at 5µM Aβ) with the same experimental conditions. Also, at an incubation time of 24h, Aβ concentrations from 1µM till 10µM exhibited the same toxicity which is not seen in other studies [212, 213, 216].

Neuroprotective effects of salidroside against Aβ(25-35) were investigated in a system of SH-SY5Y cells *in vitro* using the trypan blue dye assay [216]. The assay is based on the exclusion of trypan dye from viable cells which can be counted on the hemocytometer as stained and unstained cells separately. The viable cell ratio is the non-stained cells divided by the total

cells (stained + unstained counted). A $\beta$ (25-35) was dissolved in DI water and then the stock solution was diluted to final concentration in the cell medium prior to use. Additionally, the CCK-8 assay was also used to measure cell viability by giving a spectrophotometric output corresponding to viable cells. In the dose dependent study with A $\beta$ (25-35), a concentration of 5 $\mu$ M, 15 $\mu$ M and 25 $\mu$ M was studied by incubating the peptide for 24h with SH-SY5Y and assessing the viability by the CCK-8 assay. The viabilities at 5 $\mu$ M = ~90%, 15 $\mu$ M= ~80% and 25 $\mu$ M= ~54.9% of the control. Later, using the same conditions with 25 $\mu$ M A $\beta$ (25-35) the viability was 50.0%. In another experiment, with different A $\beta$  fragment, namely A $\beta$ (42), the viabilities of SH-SY5Y cells assessed by CCK-8 assay after 24h incubation with A $\beta$ (42) are as follows: 5 $\mu$ M A $\beta$ (42): ~83% viability, 10 $\mu$ M A $\beta$ (42): ~58% viability, 25 $\mu$ M A $\beta$ (42): 42% viability. This indicates that even after a dose-dependent study, exact values of toxicity are difficult to achieve. Also, compared to other A $\beta$ (25-35) viability values to other publications, the viabilities are different at same concentration of A $\beta$  [217].

The role of N-truncated A $\beta$  oligomers was investigated in a system of primary mouse neurons [218]. Fresh peptide stock solutions were made by dissolving in hexafluoro-2-propanol. These stock solutions were dried under nitrogen and directly added to the culture medium and incubated for 1hr prior to use in the experiments. This procedure was used to generate A $\beta$  peptide oligomers. The toxicity of A $\beta$  peptides was assessed by the MTT assay after incubation of the mouse neurons for 24h and 48h with A $\beta$  peptides (see figure 6A in publication). After 24h incubation with 1 $\mu$ M A $\beta$ (40) the viability of SH-SY5Y with MTT assay was ~80% and that of 1 $\mu$ M A $\beta$ (42) was ~72%. After 48h, viability of SH-SY5Y with 1 $\mu$ M A $\beta$ (40) was ~60% while that of 1 $\mu$ M A $\beta$ (42) was ~53%. This study is interesting because, a lower concentration of A $\beta$

peptides (1 $\mu$ M) was used for all studies which showed significant toxicities towards mouse neurons.

The effect of cholesterol and A $\beta$ /A $\beta$ -metal complexes was investigated in human neuroblastoma cell line SH-SY5Y [219]. This study elucidates the use of a low concentration of A $\beta$  in toxicity studies *in vitro*. A $\beta$ (42) was dissolved in hexafluoroisopropanol (HFIP) for 40min and then HFIP removed. Finally, dialysis was performed with A $\beta$ (42) for 24h and used in toxicity studies for A $\beta$  control. After addition of 0.5 $\mu$ M A $\beta$ (42) for 24h to SH-SY5Y cells, the viability for A $\beta$  control was observed to be ~ 82% as assessed by the MTT assay. This is significant because the study uses a low concentration of A $\beta$  and 0.5 $\mu$ M concentration killed only ~18% cells which was their range of study.

The ability of pregnenolone and its ester to attenuate the toxicity of A $\beta$ (25-35) was investigated using a rat pheochromocytoma cell line PC-12 [217]. A concentration of 20 $\mu$ M A $\beta$ (25-35) was added to PC-12 cultures and viability assessed with the MTT assay after 24h, 48h and 72h treatment. After 24h, viability of PC-12 was ~96%, indicating no toxicity of the 20 $\mu$ M A $\beta$ (25-35) fragment. After 48h exposure time, viability decreased to ~65% and after 72h to ~55%. This no toxicity shown by A $\beta$ (25-35) after 24h exposure is inconsistent with other studies [216].

The effect of aggregation/incubation conditions on the toxicity of A $\beta$ (40) fibrils on SH-SY5Y cells was studied by T. Good et.al.[200]. A $\beta$ (40) solutions are prepared by dissolving lyophilized A $\beta$ (40) in trifluoroacetic acid (TFA) at room temperature and then adding the A $\beta$ -TFA to its final concentration in cell culture media. In this study, the incubation conditions are gentle agitation and no agitation for different periods of time to get aggregated A $\beta$ (40) species.

The viability of differentiated SH-SY5Y cells were examined after treatment with A $\beta$  samples prepared with and without agitation using the annexin-PE, 7-AAD cell assay. In this assay, viable cells are both annexin-PE and 7-AAD negative. When fresh 100 $\mu$ M A $\beta$ (40) was tested on SH-SY5Y, no toxicity was observed. This observation is in contrast with other studies [190, 196]. The assay was run after 2h incubation with aggregated A $\beta$ (40) peptides using flow cytometry. The study indicated that toxicity with 100 $\mu$ M A $\beta$ (40) aggregated with gentle agitation (24h) was significantly greater than the toxicity of fibrils formed under no agitation conditions (72h). The study shows that A $\beta$  fibrils formed via different methods do not have the same toxicity or even the same stability. Additionally, this study demonstrates the use of high concentration (100 $\mu$ M) of aggregated A $\beta$ (40) used on SH-SY5Y cells. The protocols and methods used in this study are similar to those used in our work.

**Table 5: SH-SY5Y viabilities assessed after 24h of addition of 100 $\mu$ M A $\beta$ (40) aggregated according to different conditions, from ref. [200]**

100 $\mu$ M aggregated A $\beta$ (40) prepared with gentle agitation		100 $\mu$ M aggregated A $\beta$ (40) prepared with no agitation	
Time of aggregation of A $\beta$	Approx. SH-SY5Y cell viability	Time of aggregation of A $\beta$	Approx. SH-SY5Y cell viability
Control (no A $\beta$ )	100%	Control (no A $\beta$ )	100%
0h (fresh A $\beta$ )	102%	0h (fresh A $\beta$ )	102%
2h	68%	1h	78%
4h	65%	4h	51%
8h	52%	8h	35%
24h	50%	24h	62%
		72h	75%

The ability of the oriental medicine, Jangwonhwan, to inhibit oxidative stress induced due to A $\beta$  peptides in human neuroblastoma cells SH-SY5Y was investigated by Seo, Han et al [220]. The viability of SH-SY5Y was assessed by the WST-1 assay spectrophotometrically to give the proportion of viable cells. A $\beta$ (42) was dissolved in DMSO after which they were diluted down in Phosphate buffered saline or cell media and incubated 24h before addition to cells. After addition of 80 $\mu$ M A $\beta$ (42) to SH-SY5Y and incubation for 24h, the viability of A $\beta$  control was observed to be ~30% compared to 100% live control from the WST-1 assay.

The neuroprotective potential of salvianolic acid B (Sal B) against A $\beta$ -induced toxicity human neuroblastoma SH-SY5Y and rat PC-12 cultures is explored using aggregated A $\beta$ (40), A $\beta$ (42) peptides [208]. Toxicity of the aggregated peptides was studied using the MTT assay. A $\beta$  was dissolved in DMSO prior to the assay and A $\beta$  aggregation was performed in PBS at 37<sup>0</sup>C. A $\beta$  seed samples in PBS were preincubated for 3-7days for fibril aging at 37<sup>0</sup>C. Differentiated SH-SY5Y cells were incubated with aggregated A $\beta$  for 24h after which the viability was assessed using the MTT assay. In the first experiment, using 15 $\mu$ M aggregated A $\beta$ (40), PC-12 cultures has ~15% viability of A $\beta$  control. The viability of differentiated SH-SY5Y when treated with 50 $\mu$ M aggregated preformed A $\beta$ (42) was ~25% assessed by the MTT viability assay. Finally, 15 $\mu$ M aggregated preformed A $\beta$ (42) added to PC-12 cells gave ~27% viability in MTT viability assay (see figure 2 for those results in the publication). In the next sets of experiments with SH-SY5Y cells, 50 $\mu$ M preformed A $\beta$ (42) gave ~21.1% viability, 50 $\mu$ M of 3 day aggregated A $\beta$ (42) gave 25.1% viability and 50 $\mu$ M of 7 day aggregated A $\beta$ (42) gave 28.1% viability. This study demonstrates that aggregated A $\beta$  shows different toxicity on different cultures. Also, it is interesting to note that 15 $\mu$ M A $\beta$ (40) gave ~15% viability whereas 15 $\mu$ M preformed A $\beta$ (42) gave ~27% viabilities in the same cell system of PC-12 cells. It is a well-established fact that

although A $\beta$ (40) constitutes to 90% A $\beta$  in the plasma, A $\beta$ (42) is significantly more toxic species compared to A $\beta$ (40), however this study is in contrast to that fact [184-187, 221].

The interaction of a A $\beta$ (39-42) fragment of A $\beta$  peptide with 10 $\mu$ M A $\beta$ (42) and 25 $\mu$ M A $\beta$ (40) to prevent toxicity in PC-12 cells was assessed using the MTT assay [222]. Peptides were dissolved in DMSO and diluted to their final concentration in the cell culture media. PC12 cells were incubated for 15h with the peptides [222, 223]. The PC-12 viability after treatment with 10 $\mu$ M A $\beta$ (42) and 25 $\mu$ M A $\beta$ (40) was ~78% of live control (100%). Here, an uncommon incubation time of 15h was used to assess toxicity of PC-12 cells. Also, viabilities of cells at same concentration in other studies were significantly different than this study. Another study using the same protocols and experimental conditions reported ~49% viability at 10 $\mu$ M A $\beta$ (42) [223].

The ability of different A $\beta$  fragments to protect rat pheochromocytoma PC-12 cells from toxicity was investigated using the MTT assay [223]. For the peptide A $\beta$ (42) incubated with PC-12 cells for 15h, concentration of 0.1 $\mu$ M gave ~90% viability, 1 $\mu$ M A $\beta$ (42) gave ~78% viability, 5 $\mu$ M A $\beta$ (42) gave ~60% viability and 10 $\mu$ M A $\beta$ (42) gave ~49% viability by the MTT assay. In another publication [222], using the same A $\beta$ (42) protocol, the viability of PC-12 cells was ~78% for 10 $\mu$ M A $\beta$ (42). Thus, in the same cell line, using same concentration of A $\beta$  peptide, different viabilities are observed from different publications.

Interesting results are presented in the study by Zhang et. al. where intracellular and extracellular A $\beta$  peptides were investigated with human neuronal cells [187]. A $\beta$  peptides were dissolved in sterile DI water and incubated at room temperature for 5days. The same batch of peptides when injected inside the neurons caused significant toxicity (100,000 times greater) for

the A $\beta$ (42) compared to extracellular incubation. The same human neurons were incubated with the same batch of aged 10 $\mu$ M A $\beta$ (40) and aged 10 $\mu$ M A $\beta$ (42) for 24h and they showed no toxicity to neurons at these conditions (a concentration known to induce cell death in a variety of cell lines). The results are in contrast to other studies where significant toxicity is observed from A $\beta$  peptides at these concentrations (or even lower). Almost all other studies show toxicity at these concentrations or even lower concentrations of A $\beta$ (40) and A $\beta$ (42). Also, A $\beta$ (42) is known to be more toxic to cells than A $\beta$ (40).

The protective effect of quinone compound against A $\beta$ (25-35) toxicity was investigated in an SH-SY5Y cell culture and viability assessed by the MTT assay [224]. A $\beta$ (25-35) was dissolved in DI water and incubated for 3 days to form aggregates. SH-SY5Y cells incubated with 25 $\mu$ M A $\beta$ (25-35) for 24h gave around ~65% of SH-SY5Y cells compared to live control (100% cells).

Human  $\alpha_2$ -macroglobulin was studied in an system of aggregated A $\beta$ (42) using human neuroblastoma SH-SY5Y cell line, SK-N-AS cell line, LAN5 cell line and SMS-KCNR cell line [225]. After incubation of 10 $\mu$ M A $\beta$ (42) for 24h the viability assessed by MTT assays is as follows: SH-SY5Y cells: ~65% viability, SK-N-AS cells : ~70% viability, LAN5 cell line: ~60% viability and SMS-KCNR: ~62% compared to 100% viability of the live control. This study demonstrates that a variety of cell culture systems are used in one publication for A $\beta$  studies.

Howlett, Roberts et al. investigated the neurotoxic behavior of two synthetic batches of A $\beta$ (1-40) peptide having > 99% purity by HPLC [199]. The A $\beta$ (40) was dissolved in pure water and ageing was carried out at 37<sup>0</sup>C to achieve aggregation. The two batches of A $\beta$ (40) as TFA salt, lot# ZK051 and lot#ZK600, were studied in rat PC-12 cultures. After ageing, the peptides

were added to PC-12 cells and viability was assessed with the MTT assay after 2h incubation with the peptides. A comparison between batches #ZK051 and #ZK066 of A $\beta$ (40) is given below from the publication. Neurotoxicity is assessed as the decrease in the conversion of MTT to a formazan product in the presence of 1 $\mu$ g/ml and 10 $\mu$ g/ml of A $\beta$ (40). Live control has 0% toxicity. For comparison, the PC-12 culture conditions, aggregation protocols, ageing times for different A $\beta$  batches were all consistent for comparison purposes.

**Table 6: PC-12 viabilities exposed to two batches to A $\beta$ (40) aggregated under similar conditions, from ref [199]**

Ageing of the A $\beta$ (40) peptide (h)	Neurotoxicity observed in PC-12 cultures in (%)	
	Batch ZK051 of A $\beta$ (40)	Batch ZK600 of A $\beta$ (40)
0h (No ageing)	10 $\pm$ 2 @ 10 $\mu$ g/ml	32 $\pm$ 1 @ 10 $\mu$ g/ml
24h ageing	36 $\pm$ 4 @ 10 $\mu$ g/ml	52 $\pm$ 7 @ 10 $\mu$ g/ml
	26 $\pm$ 4 @ 1 $\mu$ g/ml	53 $\pm$ 3 @ 1 $\mu$ g/ml
168h ageing	43 $\pm$ 4 @ 10 $\mu$ g/ml	51 $\pm$ 2 @ 10 $\mu$ g/ml
	42 $\pm$ 6 @ 1 $\mu$ g/ml	44 $\pm$ 5 @ 1 $\mu$ g/ml

The results from table 6 show that batch ZK600 produced significantly greater toxicity at 0 and 24h of ageing time. Thus, the use of fresh A $\beta$ (40) peptide (with no ageing) and the use of aged peptide (24h) shows very different toxic profiles between the two batches compared. In the ideal case, since they both are A $\beta$ (40), have >99% purity and are studied at the same culture/experimental conditions, the toxicity shown by both batches should be consistent. However, this is not true for these two batches of A $\beta$ (40) and neurotoxic behavior of A $\beta$ (40) varies between synthetic batches of A $\beta$ . The likely reason given by the researchers is that the differences result from conformational variations.

In this study, low concentrations of A $\beta$ (40) and A $\beta$ (42) were used to study neuronal apoptosis induced in human neuron primary cultures [209]. A control peptide with the reverse sequence A $\beta$ (40-1) is also included for comparison purposes as it is the in-active control against A $\beta$ (40). This reverse fragment is frequently used as the negative control in experiments. Fibrillar A $\beta$ (40) and A $\beta$ (42) were prepared by incubating freshly solubilized peptides in sterile DI water at 37<sup>0</sup>C for 5 days. The peptides were then diluted down to 100nM concentration in the cell media. Neurons were treated with 100nM of A $\beta$ (40) and A $\beta$ (42) for 6, 12, 24, 48 and 72h after which viability was assessed by the MTT assay. According to the study, the normal concentration of A $\beta$  in cerebrospinal fluid is 4nM which represents a 25X times concentration added to the cells. Compared to 100% control of live cells, viability after 12h treatment was ~100% for A $\beta$ (40), ~90% for A $\beta$ (42) and surprisingly, ~72% for A $\beta$ (40-1). At 24h, the viabilities are increases to ~100% for all the 3 types of A $\beta$  peptides. At 48h, the viability is ~90% for all the peptides. At 72h incubation, A $\beta$ (40) viability is 72%, A $\beta$ (42) viability is ~90% and A $\beta$ (40-1) is ~81%. This indicates highly irregular viabilities in contrast with trend observed [204]. There is strong evidence that A $\beta$ (42) is significantly more toxic than A $\beta$ (40). However, at most incubation times, A $\beta$ (42) toxicity was either equal to A $\beta$ (40) or lower. Also, it is interesting to see that A $\beta$ (40-1), the reverse control peptide is showing toxicity and also more than the active parts of A $\beta$  in some cases. This indicates that there are yet understood mechanisms involved in A $\beta$  toxicity. Also, 100nM is a low concentration that the researchers have used in this study.

New inhibitors were investigated on the A $\beta$ (1-39) fragment in a system of PC-12 cells [99]. A $\beta$ (39) was dissolved in trifluoroacetic acid (TFA) then diluted to PBS, incubated for 7 days, the diluted to the cell medium and incubated again for 1 day. PC-12 cells were incubated with 24 $\mu$ M concentration of above prepared A $\beta$ (39) and viability assessed after 24h using the

MTT assay. The viability of PC-12 cells was about ~65% of the live control (100%). This study indicates that A $\beta$  studies are done with a wide variety of fragments or different lengths of A $\beta$  peptides each having its own variability in biological and physical activity.

The role of G protein activation in A $\beta$  peptide toxicity was investigated using A $\beta$ (1-16) fragment, A $\beta$ (1-40) and A $\beta$ (25-25) in a system of PC-12 cell culture[226]. A $\beta$  peptide aggregates were formed by dissolving the peptides in trifluoroacetic acid (TFA) water solution. After incubation for 1h at 37<sup>0</sup>C, the dissolved peptides were diluted to their final concentration of 20 $\mu$ M in cell median and rotated for 24 hours prior to addition to cells. After 24h treatment of PC-12 cells with these peptides, the viability was determined by the MTT assay. Compared to 100% live control, 20 $\mu$ M of aggregated A $\beta$ (1-16) gave ~100% viability indicating that the A $\beta$ (1-16) was not biologically active. 20 $\mu$ M of aggregated A $\beta$ (40) gave ~52% viability and 20 $\mu$ M of A $\beta$ (25-35) gave ~45% PC-12 viabilities. The aggregation protocol used in our work is consistent with this publication except for the use of DMSO instead of TFA. In the same study, different A $\beta$  fragments are used and results compared.

Wang et al. investigated the effect of cholesterol and sialic acid content on the toxicity induced by A $\beta$ (40), A $\beta$ (25-35) and in-active A $\beta$ (1-16) in different cell lines[125]. The lyophilize peptide was treated dissolved in trifluoroacetic acid (TFA)-water solution. After incubation for 1h at 25<sup>0</sup>C, the peptide stock solutions were further diluted in PBS and rotated for 24h. Finally, the peptides were diluted to their final concentration of 20 $\mu$ M in cell media and rotated for 24h prior to addition to cells. The aggregated peptides were added to human neuroblastoma SH-SY5Y cells, C-6 glioma cells and rat pheochromocytoma PC12 cells and the viability assessed by the MTT assay after 24h of treatment. For rat PC-12 cells, the viabilities after 24h of treatment with 20 $\mu$ M A $\beta$ (40) were ~55%, 20 $\mu$ M A $\beta$ (25-35) were ~48% and 20 $\mu$ MA $\beta$ (1-16)

showed no toxicity. In case of SH-SY5Y cells, after 24h, viabilities were, 20 $\mu$ M A $\beta$ (40) = ~52% viability, 20 $\mu$ M A $\beta$ (25-35) = ~45% viability and A $\beta$ (1-16) showed no toxicity towards SH-SY5Y. However, when C6 glioma cells were treated with 20 $\mu$ M A $\beta$ (40), there was no toxicity induced by A $\beta$  peptides on C6 cells. However, this no toxicity seen in C6 glioma's is in contrast with other studies, where 25 $\mu$ M A $\beta$ (42) gave around 48% viability after 24h treatment as assessed by MTT assay [227]. This is significant as one study observes no toxicity in A $\beta$ -C6 cell study (this publication), whereas the other study has observed almost ~50% viability when A $\beta$  is exposed to C-6 cells [227]. Additionally, in the same publication, 3 different cell types and 3 different A $\beta$  fragments are used.

Patel and Good et al. investigated a new rapid viability assay to assess A $\beta$  induced neurotoxicity in SH-SY5Y cell cultures [183]. The new viability assay required an incubation time of 2h to see the toxic effects of A $\beta$  compared to the conventional viability assays such as MTT reduction assay, lactate dehydrogenase assay, trypan blue assay, propidium iodide assay and the TUNEL assay which require 24h or more to get toxicity profiles. Thus, a rapid apoptosis assay using annexin-PE and 7AAD was studied using 100 $\mu$ M A $\beta$  and SH-SY5Y cells. Lyophilized A $\beta$ (40) was dissolved in dimethyl sulfoxide (DMSO) or trifluoroacetic acid-water solution. After complete dissolution, the peptides were diluted to their final concentration in cell media and rotated for 24h at 25<sup>0</sup>C to get fibrillar aggregated A $\beta$ . To get different A $\beta$  aggregated intermediate species, samples of A $\beta$  were incubated at 37<sup>0</sup>C for different periods of time (0h, 4h, 8h, 24h or 72h). In the first experiment, 100 $\mu$ M A $\beta$ (40) was aggregated for 24h and then the viability of SH-SY5Y cells was assessed as a function of time of incubation with 100 $\mu$ M A $\beta$ (40). (the results are shown in table 7) For 6h incubation with 100 $\mu$ M A $\beta$ (40): viability was ~110%, 12h incubation: viability was ~84%, 24h incubation: viability was ~70% and 48h incubation:

viability was ~60%. In the same type of experiment but with different viability assay, annexin-PE+7AAD assay, the effect of different incubation times gave completely different viabilities. See figure 13. below (adapted from [183], with permission from Elsevier Inc.):

For the next result, A $\beta$ (40) was aggregated for 24h prior to the addition to SH-SY5Y cells. After aggregation, 100 $\mu$ M A $\beta$ (40) was added to the cells, and the viability measured using different assays, PI assay after 24 and 48h incubation and the new proposed assay, annexin-V+7AAD, which required 2h incubation of cells with A $\beta$ . So, 15min incubation with 100 $\mu$ M A $\beta$ (40) gave ~94% SH-SY5Y viability, 30min incubation gave ~89% viability, 1h incubation gave ~68% viability, 2h gave ~93% viability, 4h gave ~83% viability and 8h gave ~80% viability (results are shown in figure 13). The results adapted [183] (with permission from Elsevier Inc.) from the publication are shown below:

**Table 7: SH-SY5Y viability after 24h aggregation with different concentration of A $\beta$  and different viability assays, from ref. [183]**

24h aggregated A $\beta$ (40)	Normalized Viability of SH-SY5Y cells (%)		
Concentration of aggregated A $\beta$ (40) added to cells	24h incubation and PI assay used	24h incubation and PI assay used	2h incubation and annexin V-7-AAD assay used
10 $\mu$ M	~81%	~72%	~95%
20 $\mu$ M	~96%	~89%	~74%
50 $\mu$ M	~88%	~72%	~90%
75 $\mu$ M	~85%	~71%	~83%
100 $\mu$ M	~70%	~60%	~73%

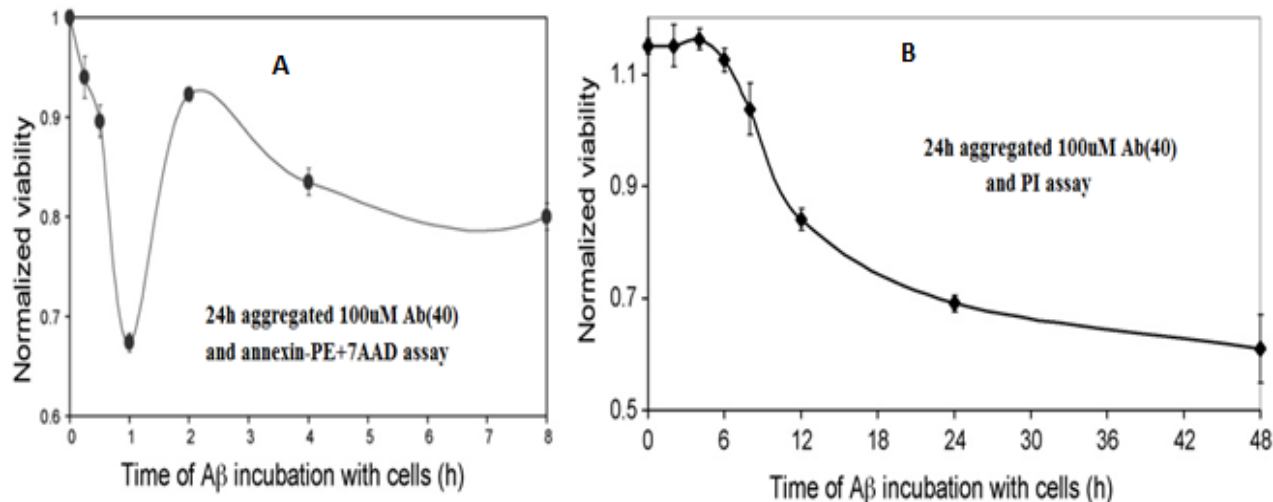


**Figure 13: Normalized viability of SH-SY5Y cells as a function of time of incubation of cells with 100µM Aβ(40), viability from different assays**

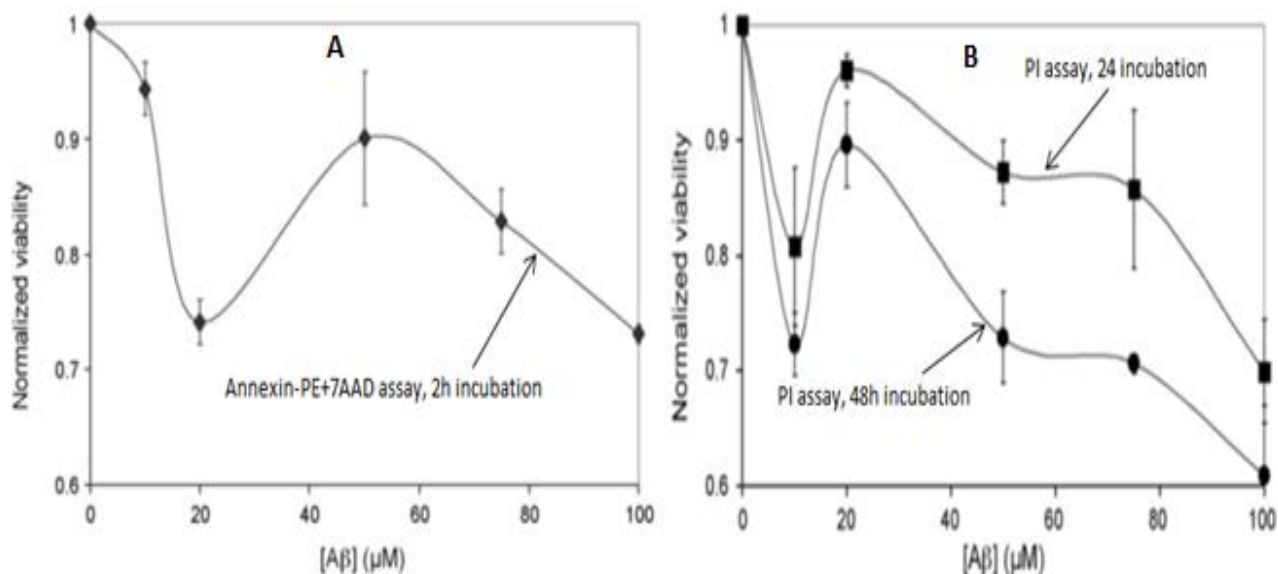
Figure 13 A: Normalized viability of SH-SY5Y cells as a function of time of incubation of cells with 100µM Aβ, as assessed by the Annexin-PE and 7AAD assay. Aβ was aggregated for 24 h with mixing prior to addition to cells. The mean viability of three or more measurements is plotted. Statistically significant changes in cell viability were detected at all times measured after 0 time ( $p < 0.05$ ).

Figure 13 B: Normalized viability of SH-SY5Y cells as a function of time of incubation with 100µM Aβ as assessed by the PI assay. Aβ was aggregated for 24 h with mixing prior to addition to cells. Mean viability measurements plus or minus their standard deviation (error bars) are shown for three or more independent measurements.

(results adapted from publication [183], with permission from Elsevier Inc.)

Also, from figure 14.B, it can be seen that in the PI assay, 10µM Aβ(40) concentration gave higher toxicity compared to 20µM, 30µM and 75µM in the 24h PI assay. Also, 10µM Aβ(40) gave higher toxicity compared to 20µM Aβ(40) in the 48h PI assay. Coming to the annexin-PE+7-AAD assay (figure 14.A.), the 20µM Aβ(40) showed deviations from normality. Thus, from the table 7 and figure 13, it can be seen that with the same solution of aggregated Aβ(40) at the same concentration (100µM) and the same culture conditions, just the use of different assays and different incubation times give completely different toxicity profiles. This possibly indicates that the dynamic structure of aggregated Aβ could be changing in solution and

the toxicity must be dependent on the concentration and the incubation time used. Hence, it is possibly the best if we shift our focus away from these assays. As such, the MTT assay is widely used and established for A $\beta$  studies.



**Figure 14: Normalized viability of SH-SY5Y cells as a function of A $\beta$  concentration assessed by different assays**

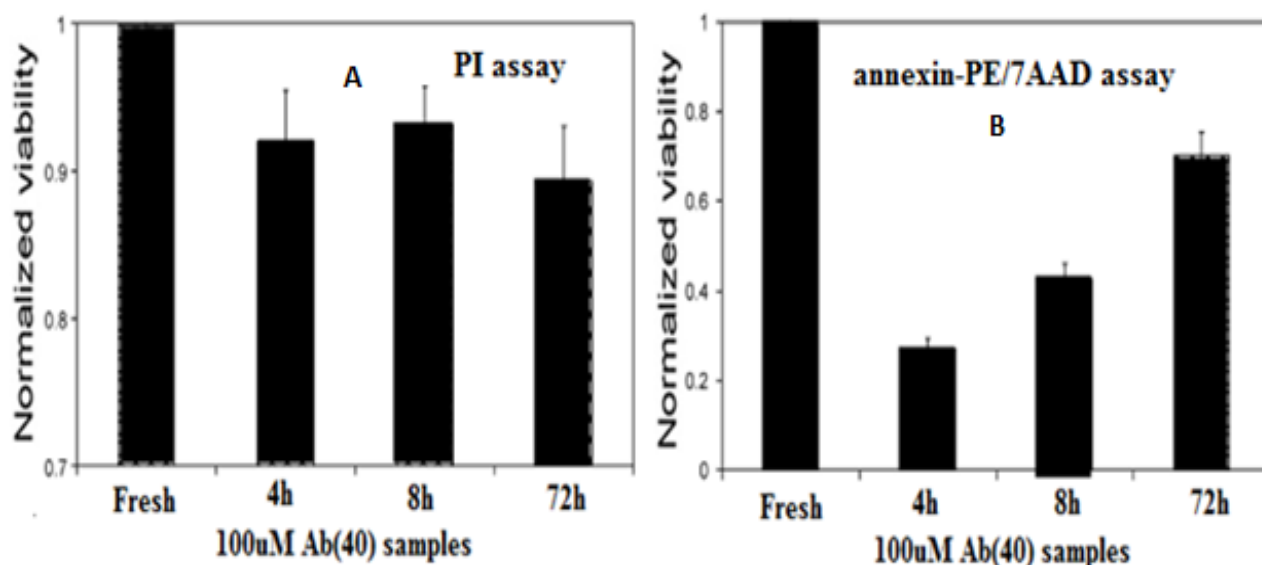
Figure 14.A: Normalized viability of SH-SY5Y cells assessed by the annexin-PE and 7AAD two-color assay as a function of A $\beta$  concentration. A $\beta$  samples were aggregated for 24 h with mixing prior to addition to cells. Cells were incubated with A $\beta$  for 2 h.

Figure 14.B: Normalized viability of SH-SY5Y cells as a function of A $\beta$  concentration as assessed by the PI assay. A $\beta$  samples were aggregated for 24 h with mixing prior to addition to cells. Cells were incubated with A $\beta$  for 24 h (■) and 48 h (●).

(results adapted from publication [183], with permission from Elsevier Inc.)

Additionally, when the two assays, PI and annexin-PE/7AAD are compared head-to-head, 100 $\mu$ M of A $\beta$ (40) samples were incubated for various periods of time (0h=fresh A $\beta$  sample, 4h, 8h, 72h incubation) and the toxicity assessed by the two assays. The results adapted from the publication are given in figure 15:

We can see that, sample 100 $\mu$ M A $\beta$  samples give different viability values from different assays even when all other conditions such as A $\beta$  concentration, cell culture, method of aggregation of A $\beta$ (40) were consistent. Additionally, in this publication, 100 $\mu$ M of fresh A $\beta$ (40) did not show any toxicity towards SH-SY5Y cells, whereas other publications show toxicity of the fresh, un-aggregated A $\beta$  peptide. See [190, 196, 199, 200] for conflicting reports on the toxicity of fresh A $\beta$ (40).



**Figure 15: Normalized viability of A $\beta$ (40) incubated for various periods of time as obtained from the PI (A) and annexin-PE/7AAD (B) assay**

Figure 15 A: Normalized viability of A $\beta$  species as assessed by PI assay. 100 $\mu$ M A $\beta$  was incubated at 37 $^{\circ}$ C without mixing for various periods of time (0, 4, 8, and 72 h) prior to addition to cells. Cells were exposed to A $\beta$  for 24 h prior to staining with PI. Only cell viability associated with the A $\beta$  sample that was aggregated for 72 h prior to cell addition was statistically different from that of the fresh peptide sample ( $p < 0.05$ ).

Figure 15B: Normalized viability of A $\beta$  species incubated at 37 $^{\circ}$ C without mixing for various periods of time as obtained from the annexin-PE and 7AAD two-color assay. 100 $\mu$ M A $\beta$  was used. Peptide was aggregated for 0, 4, 8 and 72 h in MEM prior to addition to cells without further dilution of peptide. Cells were exposed to A $\beta$  for 2 h prior to staining with annexin-PE and 7AAD. Cell viability associated with A $\beta$  species preincubated for 4 and 8 h prior to addition to cells were statistically different from viability associated with fresh and the 72 h fibrillar samples ( $p < 0.05$ ).

(results adapted from publication [183], with permission from Elsevier Inc.)

The ability of sialic acid conjugated dendrimers to attenuate the toxicity of A $\beta$ (40) was investigated in a model human neuroblastoma SH-SY5Y cell culture [8]. Lyophilized A $\beta$ (40) was dissolved in DMSO to make 10mg/ml stock solutions. After incubation for 1h to 30min, the stock were diluted to their final concentration to cell media and rotated for 24h to form aggregated A $\beta$  fibrils and other aggregated A $\beta$  species. Peptides were added to SH-SY5Y cells and toxicity assessed after 24h incubation by the PI toxicity assay. At a concentration of 5 $\mu$ M aggregated A $\beta$ (40), the viability after 24h was ~60%. At a concentration of 20 $\mu$ M aggregated A $\beta$ (40), the viability after 24h was ~90% in the same experiment (refer figure 2 in publication). In the next experiments with 50 $\mu$ M A $\beta$ (40), the A $\beta$  control viability observed was ~55% and ~60% in experiments after 24h (refer figure 4 in publication). This indicates that concentration of aggregated A $\beta$ (40) does not give proportional toxicity in SH-SY5Y cells, even if all other protocols are consistent in all experiments. Also, in the same publication, even though no dose-dependent study is done, a total of 3 different concentrations of A $\beta$ (40) are used to evaluate toxicity profiles for different compounds. The protocols in our work are consistent with this publication.

The ability of sialic acids attached to dendrimers via different functional groups to reduce the toxicity of A $\beta$ (40) was investigated in a model human neuroblastoma SH-SY5Y cell line [26]. Lyophilized A $\beta$ (40) was dissolved in DMSO to make 10mg/ml stock solutions. After incubation for 1h to 30min, the stock were diluted to their final concentration to cell media and rotated for 24h to forms aggregated A $\beta$  fibrils and other aggregated A $\beta$  species. Peptides were added to SH-SY5Y cells and toxicity assessed after 24h incubation by the PI toxicity assay. After incubation 50 $\mu$ M aggregated A $\beta$ (40) with SH-SY5Y cells for 24 hours, the A $\beta$  control values obtained were ~55% viability, ~60% viability and ~64% viability in three separate experiments.

Even if the toxicity given by same A $\beta$ (40) peptide, by the same aggregation protocol and same cell system, results for these experiments are compared to one another. This indicates that in spite of variability in A $\beta$  toxicity, results can be compared to one another (the difference in A $\beta$  toxicity these experiments was of 9%).

Photopolymerized sialic acid polymers were developed to protect mouse neuroblastoma N2A cells from neurotoxicity induced by aggregated A $\beta$ (40) by Cowan et al [162]. Lyophilized A $\beta$ (40) was dissolved in DMSO to make 10mg/ml stock solutions. After incubation for 1h to 30min, the stock were diluted to their final concentration to cell media and rotated for 24h to forms aggregated A $\beta$  fibrils and other aggregated A $\beta$  species. Peptides were added to N2A cells and toxicity assessed after 24h incubation by the PI toxicity assay. After incubation 20 $\mu$ M aggregated A $\beta$ (40) with N2A cells for 24 hours, the A $\beta$  control values obtained were ~70% viability and ~78% viability in the same experiments with different compounds. This indicates that even with the same batch of A $\beta$ (40) and same aggregation protocol and same cell culture experiments, different viabilities of N2A cell can be observed.

To address the conflicting results from neurotoxicity studies, May et al. investigated A $\beta$ (40) peptides from different sources for neurotoxicity expressed in rat hippocampal cell culture system [228]. Stock solutions of 1mM were prepared by dissolving in 10% DMSO and used in cell cultures studies at 10 $\mu$ M A $\beta$  concentrations. The viability of the cells after 4 days of incubation with A $\beta$ (40) was measured by the Lactate Dehydrogenase Assay (results from that publications are shown in figure 16). Lactate dehydrogenase (LDH) is a stable enzyme, present in all cell types, and rapidly released into the cell culture medium upon damage of the plasma membrane. Cell death or cytotoxicity can be quantified by the measurement of plasma membrane damage. Thus, amount of LDH released directly correlates to cytotoxicity observed. For this

study, all the cytotoxicity experiments were run at similar conditions to ensure consistency. A $\beta$ (40) lots investigated were #Z1682, #Z1960, #Z1424 from Bachem, Inc., 1 lot of A $\beta$ (40) was from Multiple Peptides System (MPS), one A $\beta$ (40) from Athena Lot # 164-OA-P232-1, one lot from Eli Lilly. Thus, in total 6 lots were investigated out of which 3 were from Bachem Inc. The results from the cytotoxicity assay for 10 $\mu$ M A $\beta$ (40) with cell cultures are given in the figure 16 below. Significant lot-to-lot variations were observed. The results show that only lot #Z1682 was toxic to hippocampal cultures. All other lots were non-toxic. Another significant mention in the publication was that their initial biochemical characterization by reverse phase HPLC, electrospray mass spectroscopy, and amino acid sequence analysis did not reveal any obvious differences in all these lots. This shows that some but not all preparations of A $\beta$  are neurotoxic even under identical *in vitro* culture conditions [228].

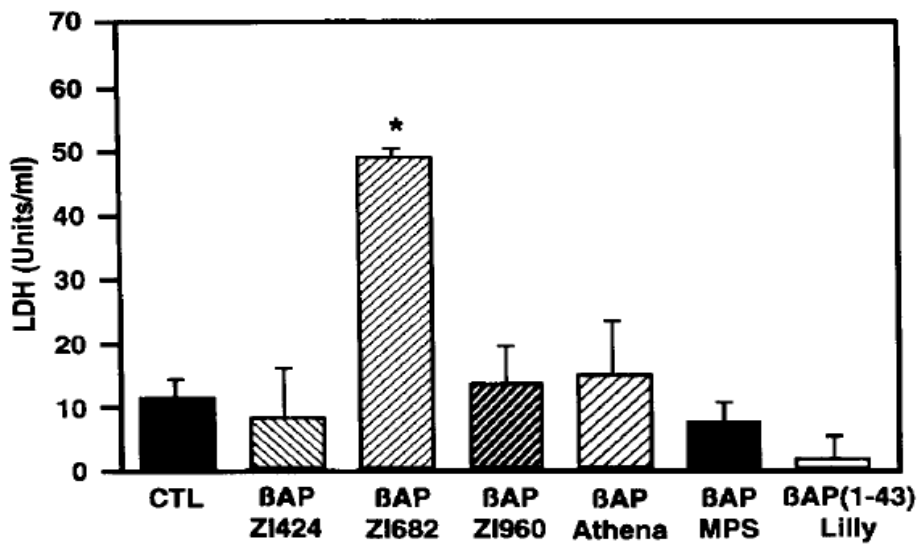


**Figure 16: Direct toxicity of A $\beta$ (40) in high density rat hippocampal cultures.**

A $\beta$ (40) from various sources was added at 10 $\mu$ M A $\beta$ (40) concentration to cultures and viability assessed after 4 days later by Lactate Dehydrogenase Assay. Results are expressed at units/ml of LDH (mean  $\pm$ SD). CTL represent the control LDH level. Result shows that only A $\beta$  lot # Z1682 showed toxicity to cultures. All other lots were non-toxic under identical *in vitro* conditions. (result adapted from publication [228], with permission from Elsevier Inc.)

### 2.15.2. Summary

In this section, almost 47-50 studies involving different fragments of A $\beta$ , namely, A $\beta$ (42), A $\beta$ (40), A $\beta$ (25-25), reverse peptide A $\beta$ (40-1), A $\beta$  fragments A $\beta$ (1-16) etc. have been reviewed. It is evident that there is a wide variability in experimental methodology, for example, on the type of peptide used, aggregation protocol used, concentration of the peptide used, cell culture model used, A $\beta$ -cell incubation time used, cytotoxicity assay used and most importantly, the viabilities reported from all these different studies.

Researchers have used aggregated as well as fresh A $\beta$  peptides in their toxicity studies. However, there are conflicting reports on the toxicity of fresh peptides (No ageing, No aggregation). In some studies, fresh peptides have shown non-toxicity whereas they have shown toxicity in other studies [183, 190, 196, 199, 200]. On the other hand, most of the studies reviewed in this section used aggregated A $\beta$  peptides. Also, there are a significant number of researchers working on the different A $\beta$  aggregates, their binding, physical characterization and so on (see section 2.7 and 2.8 in dissertation). Thus, in our study, we will use aggregated A $\beta$  peptides because there is a plethora to evidence to suggest that aggregated A $\beta$  is toxic to cells in culture.

From the different studies, it can be seen that there are multiple protocols used to induce aggregation in the A $\beta$  peptide. Reviewing the literature, the most used approach is to dissolve the lyophilized A $\beta$  powder in a strong polar solvent such as DMSO, HFIP or TFA[15, 88, 190, 193, 194, 197, 201]. The peptide stock is then diluted into the cell media or PBS or water depending on the type of study [8, 26, 161, 183, 190, 196, 201, 229]. Then, the A $\beta$ -cell media solution is incubated or rotated for different periods of time depending on the type of application or the type of aggregated A $\beta$  species desired. The time of incubation with cells as well as time of

aggregation before addition to cells is an important aspect in A $\beta$ -cell studies. Additionally, different incubation times and different aggregation times have shown different effects on different cell systems [201, 204, 205, 211].

The concentration of A $\beta$  used *in vitro* spans over the nanomolar to the micromolar range. Studies have used concentrations as low as 0.1 $\mu$ M A $\beta$  [191, 209], 0.5 $\mu$ M A $\beta$  [193]. Other groups have used concentration as high as 100 $\mu$ M [200, 202, 204, 207] A $\beta$  in cell studies with all concentrations in between. Looking at the literature reviewed, all the studies fall in the micromolar range, from 0.1 $\mu$ M to 100 $\mu$ M. There are publications that have used different concentrations of A $\beta$  in the same study and used the results for further comparisons.

It appears that several different cell lines can be used in A $\beta$  studies. A survey of literature shows that rat PC-12 and human neuroblastoma SH-SY5Y are the most commonly used cell lines. There are also studies on neuronal NT-2 [195], septal rat neurons [191], human neuroblastoma SK-N-SH [203], neuroblastoma N2A [229], neuroblastoma SJ-N-AS, LAN5, SMS-KCNR [225], cortical neurons etc. Out of these, human neuroblastoma SH-SY5Y was chosen as the model cell line as most of the studies reviewed here used SH-SY5Y in toxicity studies.

In most of the studies reviewed here, the cytotoxicity of the cells is measured by the MTT assay. Other assays such as lactate dehydrogenase assay, trypan blue assay, CCK-8 assay [212, 216], propidium iodide assay, WAST-1 assay [220] and the TUNEL assay are also popular. From these studies, it can be seen that the viabilities assessed from these assays vary among the different assays for the same concentration of A $\beta$  species. E.g. A $\beta$ (40) toxicity assessed by an assay in one study is different than the A $\beta$ (40) toxicity assessed in same study by the same assay

[8, 26, 183] or among different studies by the same assay. Additionally, the viabilities of the cells treated with the same A $\beta$  peptide gives different values if assessed by different assays [183].

There is a wide variability between the viabilities of the cultures treated with A $\beta$  under similar conditions. This is aptly explored by a study that investigated 18 batches of A $\beta$  and found 37% were non-toxic to PC-12 cells under similar conditions. Two experiments, done on two separate dates, with the same batch (ZK568) of A $\beta$ (40) and with the same number of cells gave very high toxicity (~24% viability of cells were in A $\beta$  control) in one experiment whereas no toxicity (~91% viability in A $\beta$  control) in the other [190]. In another study, only 1 out of 6 batches of A $\beta$ (40) evaluated showed toxicity to hippocampal cultures under consistent conditions [228]. This shows that some but not all preparations of A $\beta$  are neurotoxic even under identical *in vitro* culture conditions. Also, it appears that toxicity of A $\beta$  is not directly proportions to the concentration of A $\beta$  added to the cells [8, 183]. One study reported that 0.5 $\mu$ M A $\beta$ (42) gave ~56% viability compared to 5 $\mu$ M A $\beta$ (42) that gave ~77% viability of cells [193] under exact same conditions and aggregation protocols. Another study observed no toxicity towards cells at concentrations of A $\beta$ (40) from 1 $\mu$ M to 20 $\mu$ M, but observed ~22% viability at 30 $\mu$ M A $\beta$ (40) concentration [194]. Other studies have routinely used less than 20 $\mu$ M A $\beta$ (40) with high toxicities [196, 208, 214]. Higher concentration of 100 $\mu$ M A $\beta$  gave ~50% viability in SH-SY5Y cells, whereas the similar or even lower viabilities is observed in the low concentration range of A $\beta$  in other studies [194, 196, 215, 218, 223]. In a publication, 2 $\mu$ M A $\beta$ (40) on PC-12 cells and 100 $\mu$ M A $\beta$ (40) on SH-SY5Y cells gave almost the same viabilities (~50%) under similar A $\beta$  aggregation protocols. In one study, it was observed that 20 $\mu$ M A $\beta$ (40) induced no toxicity in C6 glioma cells whereas other study reported 25 $\mu$ M A $\beta$ (42) giving ~48% viability after 24h [125, 227]. Thus, it can be seen that in almost every publication, different viabilities are obtained for

concentrations depending on the type of model culture system used for the study. The viabilities of SH-SY5Y cells treated with the same 100 $\mu$ M A $\beta$  samples show completely different toxicities when evaluated with two different assays [183].

Finally, due to its amphiphilic nature, A $\beta$  peptide shows high unpredictability and high variability in toxicity profiles [190]. In 1997, a new method to predict toxicity of A $\beta$ (40) was investigated where the researcher found 33% of the 18 batches of synthetic A $\beta$  to be non-toxic to cells. This dual nature of A $\beta$  is the precise reason why there has been limited progress towards development of a therapeutic against AD.

Additionally, there are several more observations done from each done at the end of each reviewed publication. The main observation is that the toxicity behavior of the A $\beta$  peptide is dependent on multiple factors and hence it is very difficult to observe consistency across the studies. Also, this is the precise reason why even after 100 years since its discovery, the exact cause, exact mechanism, and exact diagnosis is still unclear or unknown. This has made developing therapeutics for AD very difficult.

### **2.15.3. Design of Experiments: Guidelines**

Since there are a vast number of variables when it comes to A $\beta$  studies, each part of the A $\beta$  toxicity experiments is considered separately.

#### **Choice of A $\beta$ Peptide**

Almost all A $\beta$  studies are done with A $\beta$ (40), A $\beta$ (42) or A $\beta$ (25-35) peptides. In our experiments, we chose A $\beta$ (40) for toxicity attenuation studies with SH-SY5Y cells. More than 90% of the A $\beta$  in the human CSF is A $\beta$ (40) compared to its other fragment A $\beta$ (42). Also, more than 90% of the A $\beta$  produced from the amyloid precursor protein is A $\beta$ (40) [11, 61]. Among the

reviewed papers, A $\beta$ (40) has been used in the following studies [8, 26, 125, 183, 190, 194-196, 200, 201, 206-208, 210, 226, 229].

### **Choice of A $\beta$ (40) Concentration for Toxicity Studies**

Multiple groups have used concentrations of A $\beta$  peptides ranging from 0.1 $\mu$ M [209], 0.5 $\mu$ M [219] to 100 $\mu$ M [200, 202, 207]. In most biological fluids, cerebrospinal fluid, plasma, A $\beta$  exists in the nanomolar concentrations [230, 231]. At lower concentrations of A $\beta$ (40) conflicting results were observed at 10 $\mu$ M and 20 $\mu$ M in a publication whose protocols with A $\beta$  were consistent to our own [183]. Hence, to avoid that range, a concentration of 50 $\mu$ M was chosen to study the toxic effects of A $\beta$  in cells. Also, 50 $\mu$ M falls within the biological range (0.1 $\mu$ M to 100 $\mu$ M) of A $\beta$  peptides that are studied *in vitro*. Additionally, the closest research publications that are parallel to this study used 50 $\mu$ M A $\beta$ (40) concentration for those studies. [8, 26]. Other publications have also used 50 $\mu$ M concentration of A $\beta$  are [183, 190, 194, 208].

### **Choice of 50 $\mu$ M A $\beta$ (40) Aggregation Protocol**

Stock solutions of A $\beta$ (1-40) at concentrations of 10mg/ml were prepared by dissolving the lyophilized peptide in anhydrous dimethyl sulfoxide (DMSO). A $\beta$  peptides are dissolved in a strong polar solvent to prevent any preexisting seeds that may affect aggregation. This protocol is consistent with other studies [15, 88, 190, 193, 194, 197, 200, 201, 204, 207, 222, 226, 229, 232]. After incubating for 30min to 1h at 25<sup>0</sup>C to ensure complete dissolution, the stock solutions of A $\beta$  were diluted directly to their final concentration in sterile cell culture media and rotated at 25<sup>0</sup>C for 24h prior to the addition to the cells. This protocol of diluting the stock directly to cell media is consistent with the following studies [8, 26, 161, 183, 190, 193, 196, 200, 201, 203, 204, 207, 222, 226, 229, 232].

### **Choice of Time of Incubation with SH-SY5Y Cells**

The time of incubation of the aggregated A $\beta$  peptide was chosen to be 24h after which the viability was assessed. Multiple groups have used 24h incubation time in their A $\beta$  toxicity studies [8, 26, 125, 190, 193, 195, 196, 200, 203, 205-208, 211-214, 216, 218, 219, 224, 226, 229].

### **Choice of Dose Dependent Study**

Out of around 50 publications reviewed, only a few studies [190-192, 198, 215, 216] have performed dose-dependent or cell-death calibration curves using different A $\beta$  peptide concentrations. In most cases, dose-dependent studies were done when a new aggregation protocol [194] or a new viability assay [183] was proposed. Studies have shown that viabilities from a dose-dependent curve are not a very good predictor of the viability obtained by using the same concentration and conditions in subsequent experiments [190-192, 198, 215, 216]. The general trend observed is that a suitable concentration of A $\beta$  peptide is picked and toxicity studies are done directly using that concentration. Also, there are studies that indicate lot-to-lot and within-lot variability in the toxicity shown by A $\beta$  peptides [190, 199]. Thus, in our work, we chose not to perform the dose-dependent studies with aggregated A $\beta$ (40).

### **Choice of Cytotoxicity assay**

The 3-(4,5-dimethylthiazol-2-yl)-2,5-diphenyl-2H-tetrazolium bromide (MTT assay) was chosen for evaluation of the viabilities of SH-SY5Y cells. As it can be seen from this document, MTT is a common viability assay that is routinely used in A $\beta$  studies by several research groups. As the MTT is a very established assay, the protocol used is consistent with literature. After 24h incubation with the peptides or test compounds, the media from the wells was replaced with

100µl of culture media without phenol red. 10µl of 5mg/ml MTT solution was freshly prepared in culture media without phenol red and added to all the wells. After incubation for 2h, the cells were checked for purple crystals and the media was replaced with 200µl of DMSO. After 20min on the shaker, absorbance at 570nm and 690nm was measured using a standard microplate reader. Normalized viability values were obtained by dividing the percentage of viable cells in the sample by that in the control samples with no A $\beta$  or other agent added.

### **Viabilities Observed from Toxicity Studies**

The issue with variable viabilities seen in A $\beta$  studies is discussed in detail in the summary section. Multiple groups have seen extremely wide range of viabilities with A $\beta$  peptides. There are entire publications which investigate the unpredictability of different batches of A $\beta$  [190, 199, 228] studied under consistent aggregation and *in vitro* conditions. The entire focus of this experimental design section was to illustrate and understand the differences in the studies done with A $\beta$  *in vitro*. From this document, it is evident that viability of a cell culture incubated with A $\beta$  depends upon multiple factors such as, A $\beta$  peptide chosen [99, 125, 187, 194, 196, 208], A $\beta$  concentration chosen [193, 194, 196, 201-203, 214, 215], A $\beta$  aggregation protocol chosen, time of A $\beta$  aggregation [196, 199-201, 204, 215], type of cell culture model used [125, 207, 208, 225], time of incubation with cells [192, 203, 222], type of viability assay used [183] and so on. In the same experiment, at the same conditions and same concentrations of A $\beta$ , different viabilities have been observed from A $\beta$  peptide treated cells [199, 205, 211, 223, 229]. Additionally, different concentrations of A $\beta$  peptides have been used in the same study giving different viabilities [8, 187, 204, 207]. In another study, 5µM A $\beta$ (42) gave viabilities ranging from 20% to 40% under exact same conditions [211]. Under the exact same conditions, different viabilities of cells treated with A $\beta$  have been reported [8, 26, 191, 202, 205, 207, 211, 229].

Thus, in our case, the different viabilities obtained from different batches of A $\beta$ (40) are within reasonable limit. In this work, A $\beta$  studies were run with different batches for A $\beta$ (40) for the two parts of this work. What is important is that the A $\beta$  control value does not vary within each part, i.e., within sialic acid-complex part and within biological-sugar-complex part. Even though the aggregation protocol and cell culture protocols are consistent, the difference in toxicity could be the result of different A $\beta$  batch or a difference in the aggregated species formed after 24h aggregation protocol. It is for this precise reason why we are treating the sialic acid complex study and sugar-analogs complex study as individual pieces of publications. Within each study, we still have just one A $\beta$  control value against which we are doing comparisons. The only link between the sialic acid-chitosan complex part and biological sugar-complex part is the 35% labeling we used as the labeling percentage of chitosan. Thus, we are not comparing any of the A $\beta$  results from sialic-acid chitosan complex study with that of the sugar-analog study. If the viabilities of A $\beta$  control from the two parts of this dissertation were close together, it would have made the comparison between sialic acid-complex and KDN-complex possible.

### **3. SIALIC ACID CONJUGATED CHITOSAN FOR THE ATTENUATION OF AMYLOID-BETA TOXICITY: DEGREE OF LABELING STUDY**

#### **3.1. Introduction**

Alzheimer's disease (AD) is the leading cause of neurodegeneration, affecting almost 37 million people worldwide with an estimated cost of healthcare of over \$600 billion, the bulk attributed to long-term care for patients unable to care for themselves[3, 4]. While there are numerous hallmarks of AD (including neurofibrillary tangles and amyloid plaques), we will focus on fibrils, whose main protein component is the amyloid-beta peptide ( $A\beta$ ). We chose this target as it is widely hypothesized that  $A\beta$  is the primary causative agent in AD-related neurodegeneration.

A number of investigators, including the ourselves, have suggested that  $A\beta$  binds to neuronal cell membranes through interaction with cell surface gangliosides or glycoproteins containing sialic acid [8, 114, 233-235]. Gangliosides are glycosphingolipids with one or more sialic acid moieties attached to a sugar chain. Numerous studies have shown that the binding affinity of  $A\beta$  to the membrane is higher when multiple sialic acids are present, either because of clustering of gangliosides or because of the degree of sialylation of the gangliosides. [8, 29, 113, 118, 234, 235]. Evidence suggests that  $A\beta$  interacts specifically with the sialic acids present on gangliosides such as GM1[4, 29, 112], and this GM1- $A\beta$  moiety can act as a seed for further amyloid deposition thus becoming the key step in the initiation of AD [29, 31, 129, 135, 236]. Additionally, reduction of cell surface sialic acids has been found to protect cells from  $A\beta$  toxicity[33].

Thus, it would be beneficial to develop membrane mimicking materials that could compete favorably with the cell surface for  $A\beta$  binding, thereby reducing the free  $A\beta$  that interacts with neurons thus protecting them from  $A\beta$  toxicity. The aim is recreate the clustered

sialic acid structure seen on cell membranes by the design of novel conjugated compounds that have antibody-like affinity towards A $\beta$ . Previously synthesized membrane mimetic multivalent sialic acid polymers were found to attenuate toxicity [8, 26]. These materials also bound to A $\beta$  with high affinity (on the order of  $10^7$  to  $10^8$  M $^{-1}$  association binding constants, compared to  $10^6$ - $10^7$  M $^{-1}$  for sialic acid containing neuronal membranes to A $\beta$ ) [8, 26, 237]. A major issue in those studies was core polymer toxicity and inflexibility. This shortcoming is addressed in this work using chitosan as the core backbone polymer, as chitosan is an FDA approved polymer for implantation. Chitosan is a natural amino-polysaccharide comprising of copolymers of D-glucosamine and N-acetyl glucosamine units linked together by  $\beta$ -(1-4) glycosidic bonds. Chitosan has an amino group present at C2 position, which allows for its modification using EDC chemistry. Detailed reviews on the chitosan, its host of biological properties, and chemical modifications have been published elsewhere [163, 164, 168, 169, 174, 175, 238].

In this study, we have designed several sialic acid (N-acetyl neuraminic acid) conjugated chitosan molecules of different valency, or different number of sialic acid residues per chitosan molecule, using EDC chemistry. By using chitosan, we will benefit from its biocompatibility and non-toxicity as a backbone. Also, chitosan is a flexible, linear molecule; hence, we expect better clustering effect when sialic acid is attached to it. Using a model cell-line SH-SY5Y, along with aggregated A $\beta$ (40) peptide, it will be possible to predict the clustering of sialic acids necessary to achieve optimum protection from A $\beta$  toxicity. Since other studies have seen binding of the A $\beta$  to sialic acid complexes, we hope to make a biomimetic that A $\beta$  can bind to, and therefore prevent A $\beta$ -cell interaction. Thus, sialic acid decorated chitosan will more closely mimic neuronal cell adhesion molecules (NCAM), providing another mimetic target for A $\beta$ .

## **3.2. Materials and Methods**

### **3.2.1. Materials**

A $\beta$ (1-40).HCl peptide was purchased from Anaspec Inc. (San Jose, CA). Human neuroblastoma SH-SY5Y cells were purchased from ATCC (Manassas, VA). Cell dissociation buffer and cell culture reagents were purchased from Gibco-Invitrogen (Grand Island, NY). Chitosan powder (MW~15000, DD~84%) was purchased from Polysciences Inc. (Warrington, PA). 1-Ethyl-3-(3-dimethylaminopropyl) carbodiimide hydrochloride (EDC) and *N*-hydroxysulfosuccinimide (Sulfo-NHS) were purchased from Pierce Biotechnology (Rockford, IL). Ultrafiltration membranes were purchased from Millipore (Billerica, MA). Human recombinant nerve growth factor- $\beta$  (NGF- $\beta$ ), (3-[4,5-dimethylthiazol-2-yl]-2,5-diphenyl tetrazolium bromide (MTT), Sialic acid (*N*-Acetylneuraminic acid), chemicals for Warren assay and all other reagents were purchased from Sigma-Aldrich (St. Louis, MO).

### **3.2.2. Peptide Preparation**

The A $\beta$  peptides were prepared analogously to established methods in structural and toxicity literature for forming  $\beta$ -sheet and A $\beta$  fibrils. A $\beta$ (1-40) stock solutions were prepared by dissolving the lyophilized peptide in anhydrous dimethyl sulfoxide (DMSO) to make 10mg/ml stock solutions. After incubating for 30 min to 1h at 25°C, stock solutions of A $\beta$  were diluted to their final concentrations in cell culture medium and rotated at 25°C for 24h prior to addition to the cells. This method of peptide preparation has been found to produce A $\beta$  fibrils that were consistently toxic to the cells in *in vitro* at concentrations between 20 $\mu$ M and 100 $\mu$ M [8, 226].

### **3.2.3. Cell Culture**

Human neuroblastoma SH-SY5Y cells were cultured in a humidified 5% CO<sub>2</sub>/air incubator at 37°C in Minimum Essential Media (MEM), supplemented with 10% (v/v) fetal

bovine serum, 2.2 mg/ml NaHCO<sub>3</sub>, 100 U/ml penicillin, 100 µg/ml streptomycin and 2.5 µg/ml amphotericin-B (fungizone). SH-SY5Y cells were NGF differentiated prior to use in toxicity experiments by addition of 20ng/ml NGF to cells for 5-7 days in 96 well plates. All the cells used in experiments were under the 10<sup>th</sup> passage to ensure consistent metabolic response and stability.

#### **3.2.4. Synthesis and Purification of Sialic Acid Labeled Chitosan**

Sialic acid was conjugated with chitosan using EDC chemistry following the manufacturer's suggested protocol with minor modifications. Chitosan (MW~ 15000, DD~ 84%) at concentration of 8 mg/ml, was dissolved in 1X Phosphate Buffer Solution (PBS) and 5% HCl solution. The molar concentrations of sialic acid and EDC were based on the theoretical calculation of the number of primary amines in one mole of chitosan calculated from the number of glucosamine units. To achieve different percentage labeling, the ratio of the amount of sialic acid added to primary amines in reaction was varied in each case. For the conjugation experiment, sialic acid at different molar concentrations was dissolved in 1ml of activation buffer (0.1M of 2-[morpholino]ethanesulfonic acid (MES) and 0.5M NaCl at pH 6.0). To this activated buffer solution, 0.3626mM of EDC (10 Fold excess to the moles of primary amines in chitosan) and 5mM of Sulfo-NHS (1.1mg) were added. The pH was maintained in between 5.0 to 6.0 by the use of 0.1M phosphate buffer (at pH 7.2). The reaction mixture was continuously rotated at room temperature for 15 min. Thereafter, 1.4µl of 2-mercaptoethanol was added to deactivate the unreacted EDC. The reaction mixture was stirred for 2min and then, 1 ml of chitosan solution was added; pH increased to 7.0 by the use of phosphate buffer and mixture allowed to react overnight. After 24h, the reaction mixture was checked for precipitation. If observed, the

resulting precipitate was dissolved by drop-wise addition of 10% (v/v) acetic acid solution before purification.

To remove the unreacted sialic acid and EDC, the reaction volume was ultrafiltered using 10000 NMWL cutoff Amicon Ultra Centrifugal filter unit. Six washes of DI water were done each time, assuming that the final concentration of the free sialic acid in the mixture was less than 6% of the total sialic acid (free and covalently bound to chitosan) [8]. After purification, the sialic acid labeled chitosan was stored at -4°C for later use.

### **3.2.5. Verification and Quantification of the Extent of Sialic Acid Conjugation**

The verification of the presence of sialic acid on chitosan was performed using Thermo Electron Nicolet 380 FTIR with Smart Orbit attachment (Thermo Electron Corporation, Waltham, MA). For the FTIR analysis, samples of sialic acid-chitosan conjugates (called complex) were lyophilized using Labconco FreeZone 1 Liter Benchtop Freeze Dry Systems. Dry lyophilized complex powders were stored at -4°C before and after use in the FTIR. For the FTIR analysis of chitosan, dry powder obtained directly from the manufacturer was used.

The extent of sialic acid labeling was determined by a procedure described by Warren [239]. In this method, the free sialic acid undergoes periodic oxidation resulting in the formation of  $\beta$ -formylpyruvic acid. This acid reacts with 2 molecules of thiobarbituric acid to give a red chromophore with a maximum absorbance at 549nm [240]. The Warren assay uses the following reagents, Solution A) 0.2M Sodium (meta) periodate in 9M phosphoric acid (prepared fresh each time); Solution B) 10% (w/v) Sodium arsenite in a solution of 0.5M sodium sulphate-0.1M H<sub>2</sub>SO<sub>4</sub> and Solution C) 0.6% (w/v) Thiobarbituric acid in a solution of 0.5M sodium sulphate

The procedure to determine the extent of sialic acid labeling is as follows [241]. Assuming that the complex synthesized was 100% labeled, a sample containing 0.3mM of sialic acid concentration was hydrolyzed by 0.1N hydrochloric acid at 80°C for 1h. Then, to a 0.2ml hydrolyzed sample, 0.1ml of periodate solution (A) was added, tubes shaken and allowed to stand for 20min. After that, 1ml of arsenite solution (B) was added and the tube vortexed till the yellow-brown color disappeared. Care was taken to completely make the yellow-brown color disappear. This was done by immediately vortexing after adding the arsenite, allowing the solution to stand for a few minutes and again vortexing. Thiobarbituric acid solution (C), 3ml was added, the solution intensely mixed and the sample immersed in a vigorously boiling water bath for 15min. Samples which showed the presence of white coloration were discarded as it indicated that the yellow-brown color was not completely removed in the earlier step. Next, the sample was placed in cold water for 5min to develop the chromophore. Then, 4.3ml of cyclohexanone was added and then tubes shaken vigorously. The sample was then centrifuged at 1500g for 7min at 25°C to extract the resulting chromophore into the cyclohexanone. The precipitate-free upper organic phase was taken in a 10mm path-length quartz fluorometer cell (Starna Cells Inc.) and the absorbance measured at 549nm. Each reading was repeated four times.

Using the same procedure, the assay was performed on pure sialic acid samples to get the standard curve and on pure chitosan to determine whether chitosan interfered with the chromophore production. The standard curve will allow us to calculate the degree of labeling of our compounds. Three independent measurements were taken in each case.

### **3.2.6. MTT Toxicity Assay**

SH-SY5Y cells were plated at a density of  $2 \times 10^4$  cells/well in 96 well plates and NGF differentiated. After 5-7 days differentiation, culture medium was replaced with medium containing NGF to which the compound to be tested was added, either A $\beta$ , chitosan, sialic acid conjugated chitosan complex, or a combination of the above. A $\beta$  peptide at a concentration of 50 $\mu$ M was prepared by methods described in earlier sections. In all experiments, A $\beta$  was added to the cells approximately 30min prior to the addition of chitosan or conjugated complex. A gradient of chitosan and conjugated complex from 30 $\mu$ M to 1 $\mu$ M was applied on the 96 well plate. After 24h, of the addition of A $\beta$ , chitosan, sialic acid conjugated chitosan; the viability of cells was determined by using the MTT assay. The media from the wells was replaced with 100 $\mu$ l of culture media without phenol red. 10 $\mu$ l of 5mg/ml MTT solution was freshly prepared in culture media without phenol red and added to all the wells. After incubation for 2h, the cells were checked for purple crystals and the media was replaced with 200 $\mu$ l of DMSO. After 20min on the shaker, absorbance at 570nm and 690nm was measured using a standard microplate reader. Normalized viability values were obtained by dividing the percentage of viable cells in the sample by that in the control samples with no A $\beta$  or other agent added[242, 243].

### **3.2.7. Statistical Analysis**

We used ANOVA followed by the Tukey's test for the complete analysis of the intrinsic toxicity and A $\beta$  studies data. The results were significant if  $p < 0.05$ . Detailed statistical analysis of the results is presented after the results and discussion section. The p-values for every comparison are given in the appendix. The detailed analysis of the results with statistical analysis is provided in later sections.

### 3.3. Results and Discussion

#### 3.3.1. Verification of Sialic Acid Conjugation to Chitosan

Figure 17 shows the FTIR results for complex B (moles of primary amines in chitosan/ moles of sialic acid = 1), Figure 18 shows spectra for complex F (moles of primary amines in chitosan/ moles of sialic acid = 4) and figure 19 shows complex G (moles of primary amines/moles of sialic acid =10) spectra. The FTIR result for pure chitosan is also included for comparison purposes. The dashed line indicates the sialic acid-chitosan complex spectra whereas the solid line shows the pure chitosan spectra.

In the region from  $3000$  to  $3500\text{cm}^{-1}$ , the FTIR of pure chitosan shows two weak peaks that are indicative of the primary amines present in chitosan. These two peaks are absent in complex spectra and instead a broad band for amide  $\text{-NH}$  stretching frequency is observed. A strong peak around  $\sim 1650\text{cm}^{-1}$  for the complex spectra, indicates the presence of amide bond. The loss of primary amines and the formation of amide bonds confirm the complex of SA with chitosan. Sialic acid has carboxylic acid group which is used to couple with the amine in chitosan. In the complex spectra, the characteristic strong peak of  $\text{C=O}$  of carboxylic acid in between  $1700$  to  $1725\text{cm}^{-1}$  is not observed. The complex also shows peaks at  $\sim 1030\text{cm}^{-1}$  and  $\sim 1380\text{cm}^{-1}$  that indicates the presence of alcohols and acids consistent with sugar molecule attached to chitosan. Thus, all the three spectra indicate the presence of sialic acid on chitosan. The spectra for intermediate concentrations of sialic acid (i.e. Complex A, C, D, E) are not shown (but verified). From these results, we can qualitatively say that the EDC chemistry was successful for the synthesis of sialic acid conjugated chitosan. This is significant as it validates EDC as a crosslinking technique for future works.

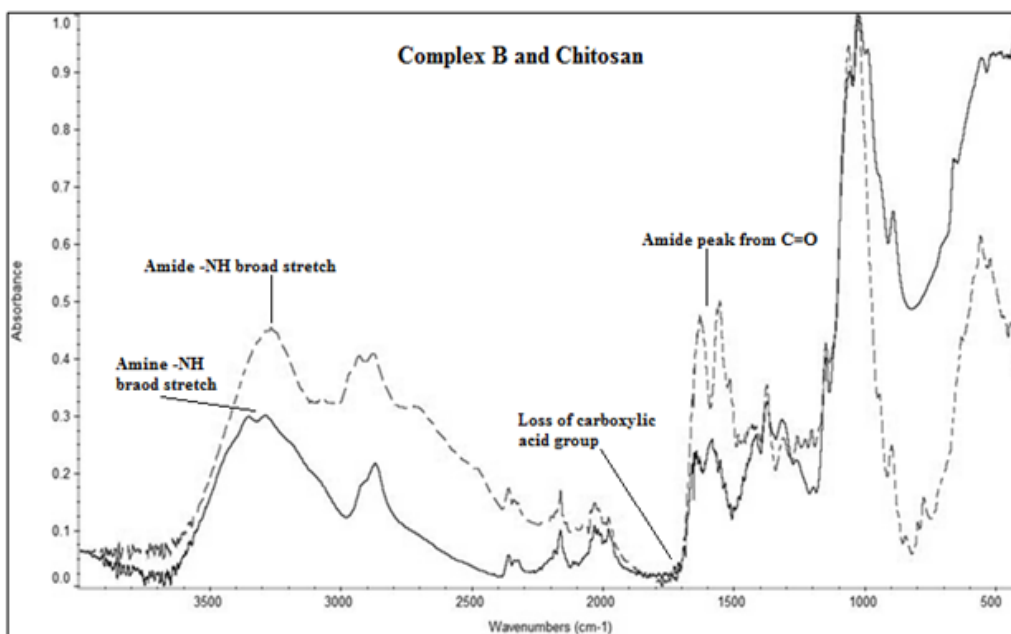


**Figure 17: FTIR results of sialic acid conjugated chitosan complex B (dashed line) and pure chitosan (solid line).**

Complex B (having ratio of moles of primary amines in chitosan/ moles of sialic acid = 1). The x-axis is wavenumber ( $\text{cm}^{-1}$ ) and the y-axis is normalized absorbance.

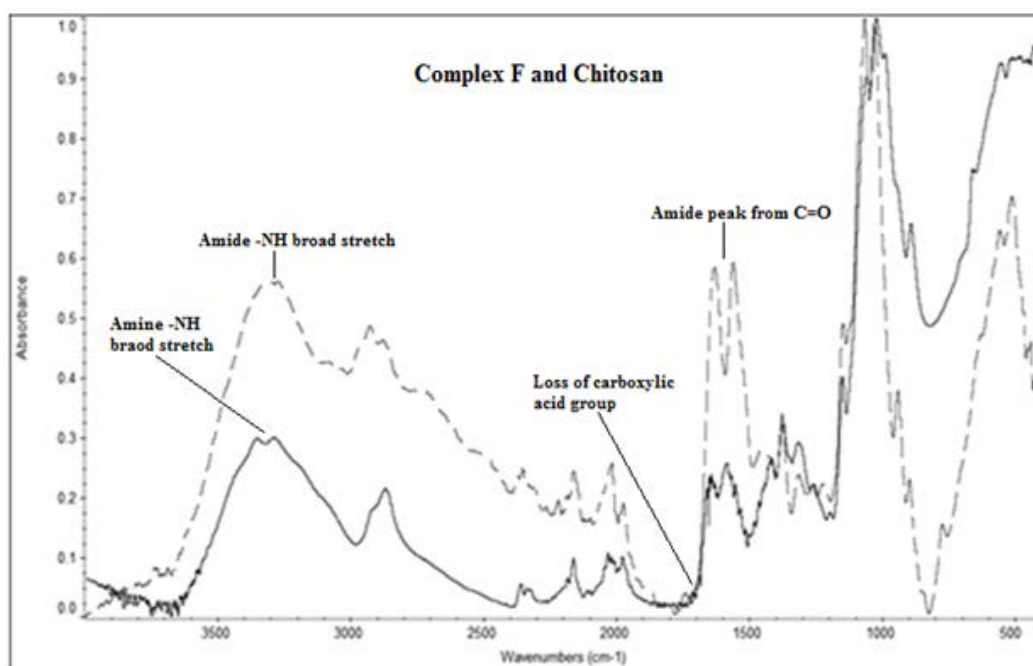


**Figure 18: FTIR results of sialic acid conjugated chitosan complex F (dashed line) and pure chitosan (solid line)**

Complex F (having ratio of moles of primary amines in chitosan/ moles of sialic acid = 4), The x-axis is wavenumber ( $\text{cm}^{-1}$ ) and the y-axis is normalized absorbance.

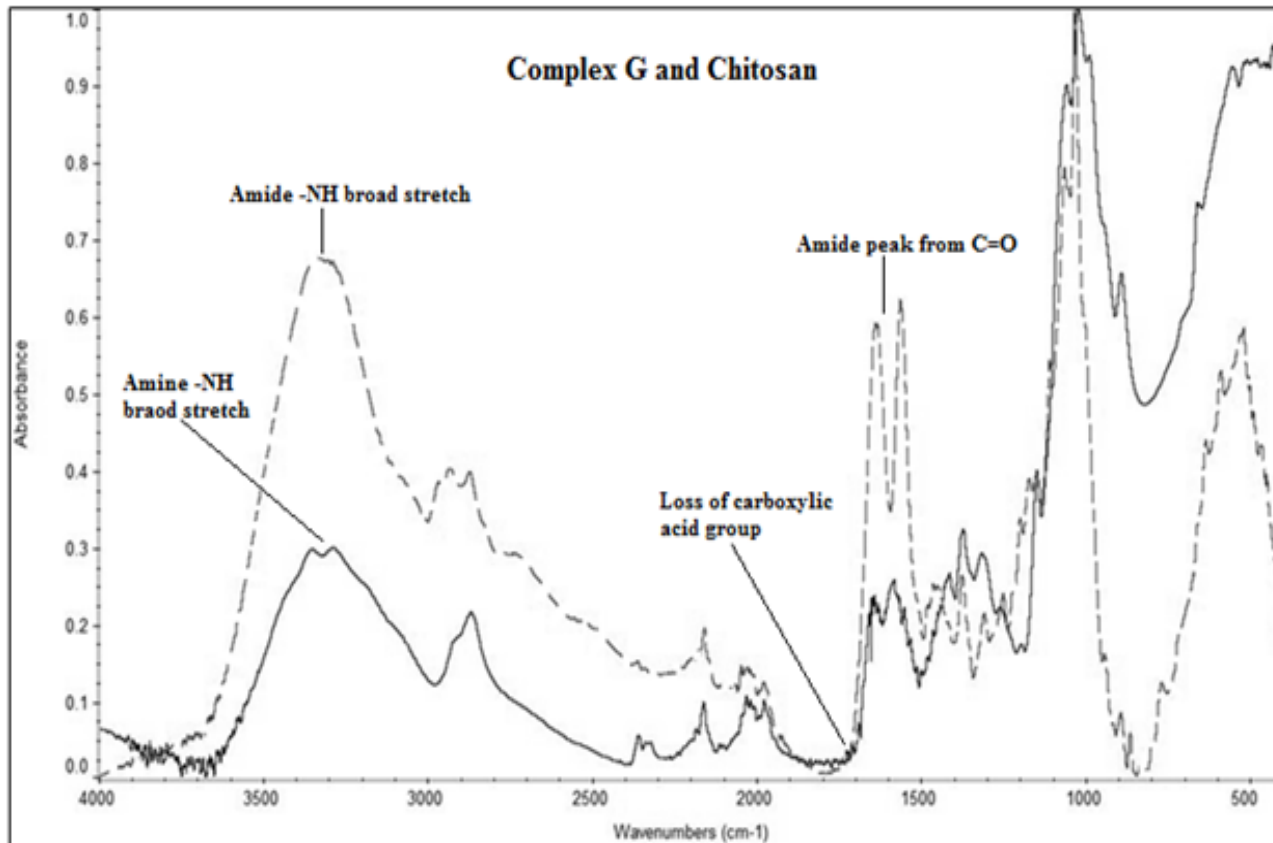


**Figure 19: FTIR results of sialic acid conjugated chitosan complex G (dashed line) and pure chitosan (solid line)**

Complex G (having ratio of moles of primary amines in chitosan/moles of sialic acid = 10). The x-axis is wavenumber (cm<sup>-1</sup>) and the y-axis is normalized absorbance.

### 3.3.2. Quantification of Sialic Acid Conjugation to Chitosan

The Warren assay was performed on pure sialic acid to generate the standard curve. As seen from figure 20, the Warren assay gives very accurate, linear and reproducible results with very low standard deviation. The standard curve was useful in the calculation of the degree of labeling of chitosan. The assay gave accurate results if the concentration of sialic acid (SA) in the sample was in between 0.05mM to 0.3mM. The assay was also performed on higher SA concentrations, but the curve saturated limiting the highest concentration that can be tested to

0.3mM (results not shown). Pure chitosan was also evaluated using the Warren assay but the results were negative (results not shown) indicating that chitosan did not interfere with the assay. The moles of primary amines in reaction mixture were determined theoretically from the degree of deacetylation of the chitosan sample. The extent of sialic acid (SA) labeling was effectively determined by using the Warren assay as the FTIR results were insufficient for the quantitative estimate of the amount of SA present on chitosan. The percentage of SA labeling was calculated by dividing the absorbance of the sample by the estimated absorbance for 100% labeling of the amine terminals of the chitosan with sialic acid. The percentage of sialic acid conjugation for different samples of complex synthesized by the EDC chemistry is shown in Table 8. Using EDC chemistry, it was possible to achieve 8% to 48% labeling (sample A to sample G) of the amines of chitosan by sialic acid.

**Table 8: Percentage labeling of chitosan by sialic acid from EDC chemistry**

Sample	[Sialic Acid]:[Primary Amines] in reaction solution	Degree of Labeling (%)
A	1:4	7.8 ± 1.1
B	1:1	14.1 ± 1.9
C	1.33:1	17.6 ± 0.4
D	1.66:1	24.5 ± 0.5
E	2:1	37.3 ± 1.5
F	4:1	40.7 ± 1.4
G	10:1	48.0 ± 2.5

From figure 21, we observe that the conjugation chemistry follows a classic saturation curve for sialic acid labeling. As the concentration of sialic acid increases, the degree of labeling increases until the curve starts saturating. The results also indicate that the saturation characteristic appear after sample E (with ratio of moles of amines to moles of SA =2). It may be

possible that as more and more sialic acids get attached to chitosan via amine groups, it becomes increasingly difficult to accommodate additional sialic acids due to steric hindrance. It seems unlikely that we would achieve a higher degree of labeling of chitosan by sialic acid (SA) as the bulk of SA's already present on the chitosan would prevent free SA from interacting with the amines on chitosan. The different percentage labeling of chitosan will allow us to study the effect of SA concentration on A $\beta$  binding. It will also allow us to predict the labeling at which optimum protection will be achieved. Now, our compounds range from unlabeled chitosan (0% labeled, flexible and linear) to complex G (48% labeled, saturated SA concentration on the surface, rigid and inflexible). This will allow us to test the A $\beta$  attenuating properties of the labeled compounds on all ends of the spectrum.

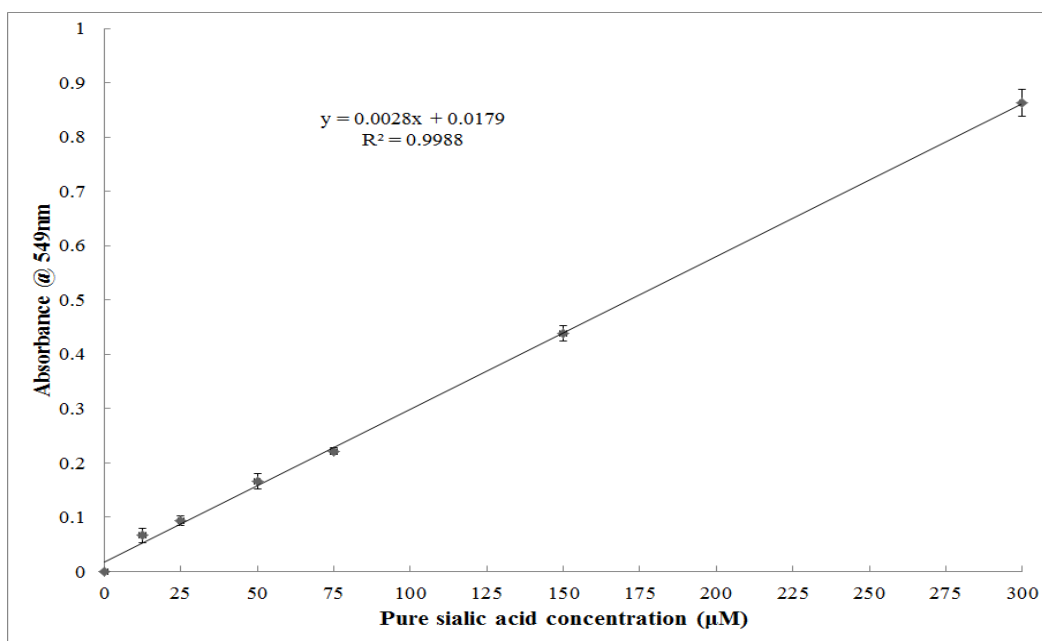


**Figure 20: Results of Warren assay on pure sialic acid – standard curve**

Data is represented as mean  $\pm$  SD, n=3

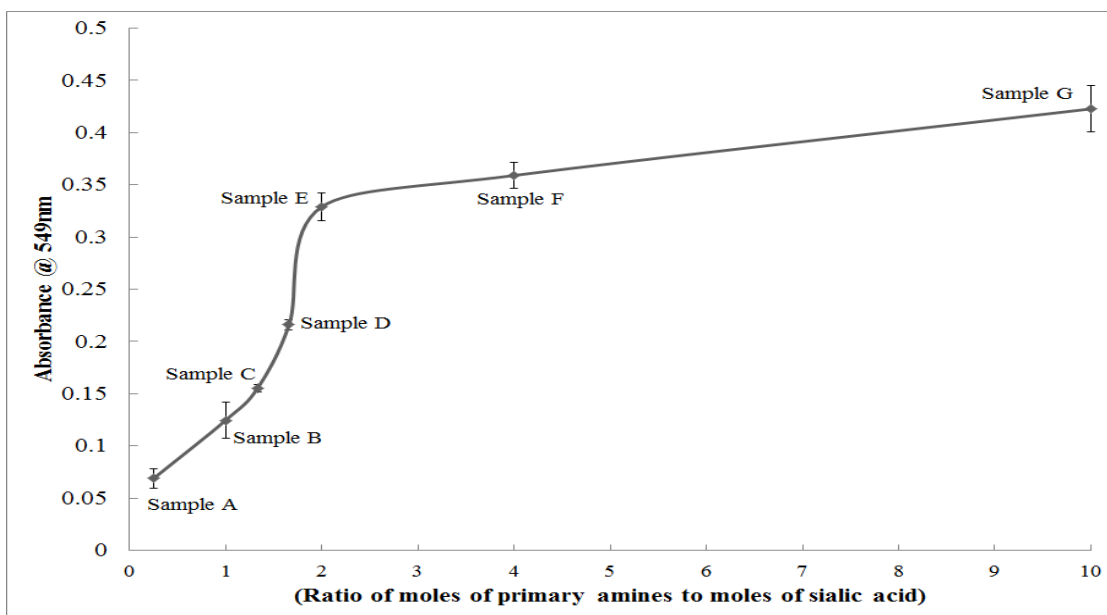


**Figure 21: Saturation curve for EDC labeling of chitosan**

Data is represented as mean  $\pm$  SD, n=4

### 3.3.3. Intrinsic Toxicity of Sialic Acid-Chitosan Complexes and Unlabeled Chitosan

The compounds, unlabeled chitosan and sialic acid-chitosan complexes A to G, were tested for intrinsic toxicity using the MTT assay described earlier by varying the concentration of the compounds from  $1\mu\text{M}$  to  $30\mu\text{M}$ . This will allow us to determine the toxicity of the compounds compared to chitosan toxicity in the absence of  $\text{A}\beta$ . The toxicity values are normalized to live control containing no complex or chitosan. The results for toxicity studies are shown in Figure 22. The statistical analysis is presented later. The bar at  $0\mu\text{M}$  complex concentration represents the normalized control viability with no complex or chitosan in the system. It can be observed that chitosan, complex A (1/4Fold), complex B (1 Fold), complex C (1.33Fold), complex D (1.66Fold) and complex E (2 Fold) show little to no toxicity towards SH-SY5Y cultures. The range of toxicity for the compounds tested range from no apparent toxicity

(chitosan and complexes A,B,C,D,E) to 20% toxicity for complex F (4 Fold) to 40% toxicity for complex G (10 Fold). For detailed analysis of the results see the statistical analysis section.

As no toxicity is observed for chitosan at even higher concentrations (30 $\mu$ M), it supports the fact that the backbone selected is biocompatible and non-toxic to cells in culture. This is an improvement over earlier works where the issue was core backbone toxicity [8, 26]. As it is apparent from figure 22, there is a distinct increase in toxicity that occurs between complex E (2 Fold) and complex F (4 Fold). This follows the transition to saturation found from the labeling evaluation (refer figure 21).

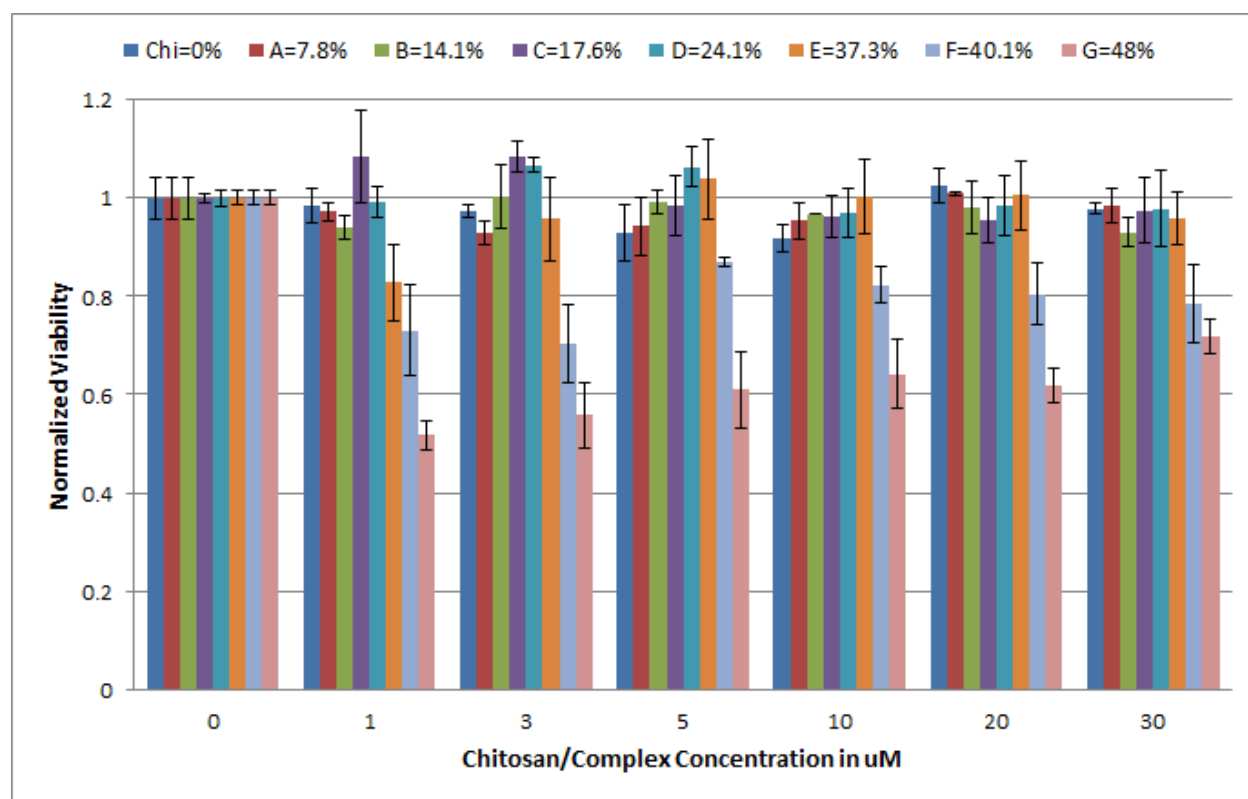


**Figure 22: Intrinsic toxicity of sialic acid chitosan complexes (A to G) and naïve chitosan exposed to SH-SY5Y**

The bar charts are labeled according to the sialic acid-chitosan complexes and their respective sialic acid labeling. Viability at 0 $\mu$ M represents the normalized control viability with no complex or chitosan in the system. Data is represented as mean  $\pm$ SD, n=4 in each case.

This indicates that there is likely a link between compound toxicity and molecular rigidity. We know this from EDC chemistry that it was difficult to achieve higher degree of labeling of chitosan by sialic acid. We believe this might be the factor affecting the transition into toxicity. There is a direct relation between intrinsic toxicity and molecular weight of the compound. Thus, the 40% toxicity of complex G (10 Fold) can be as a result of the high molecular weight due to higher number of sialic acid molecules present on the chitosan backbone (48% labeling shown by Warren assay).

#### **3.3.4. A $\beta$ Toxicity Attenuation Studies of Sialic Acid-Chitosan Complexes and Unlabeled Chitosan**

The ability of chitosan and complexes to attenuate the toxicity of aggregated A $\beta$  peptide was investigated *in vitro* using the MTT assay. A gradient of 0 $\mu$ M to 30 $\mu$ M of chitosan and complexes was applied and the results with 50 $\mu$ M A $\beta$  can be found in figure 23. The statistical analysis is given later. The toxicity attenuation values are normalized to control containing 50 $\mu$ M A $\beta$  with no chitosan or complex added. The bars at 0 $\mu$ M concentration represents the A $\beta$  control value (i.e. wells with only A $\beta$  in media but no compounds added) used for normalization. Looking at the results, all compounds (including chitosan) showed significant protective properties against A $\beta$ . The levels of A $\beta$  toxicity attenuation by the compounds are as follows: Complex A (1/4 Fold) shows the least protective effect against A $\beta$  toxicity. The reason can be explained by the fact that due to least sialic acid labeling, there is a loss of the protective effect shown by naïve chitosan plus there is insufficient sialic acid present to effectively cluster. Earlier studies have shown that free sialic acid did not show any significant protective properties [8]. . Now, as the degree of labeling increases, higher viabilities in SH-SY5Y cells are observed. The highest protection can be seen for labeling from ~17.6% to ~37.6% of chitosan (i.e. complex C,

D, E). This transition may indicate that the mechanism of protection has now shifted to our complex sequestering A $\beta$  away from the cells. This is a strong possibility, as the biomimetics were synthesized with sialic acids labeled on chitosan. On the neuronal membrane, A $\beta$  has affinity towards clustered sialic acids and binds to them. If our complexes are showing toxicity attenuation, it is most likely that the protection is due to binding of A $\beta$  to the complex. In the study with sialic acid labeled dendrimers, A $\beta$  had binding affinities to the sialic acid dendrimers complexes on the order of  $10^{-7}$ M to  $10^{-9}$ M [8, 26], which were at least an order of magnitude higher than A $\beta$  binding to gangliosides ( $10^{-6}$ M [8, 26, 156]) on neuronal membranes. Looking at the data, it is difficult to predict whether one or multiple mimics bind to A $\beta$ . Binding studies should be done to prove the exact mechanism of protection (e.g. to prove binding of complex with A $\beta$ ). This sequestering of the A $\beta$  away from the cell is the mechanism of protection that we aimed for. It is difficult to elucidate whether the complex acts via competitive or non-competitive mechanism in attenuating the toxicity of A $\beta$ . It is also possible that the complex binds with A $\beta$ , and alters the rate at which A $\beta$  interacts with the cells, and induces toxic effect. This may be the reason why we see protection at all concentrations studied but not complete protection (or 100% cell survival). Additionally, we do not see any type of dose-dependent behavior from the complexes. Thus, the mechanism of protection needs to be investigated in much more detail in later studies. While all compounds (including chitosan) showed protective properties (in all cases,  $p < 0.05$ , by Tukey's test), there was a distinct transition between complex E (2 Fold) and complex F (4 Fold). This indicates that an optimum can be achieved that balances the degree of sialation and backbone flexibility (which is critical in the effectiveness of the sialic acid to 'cluster'). Similar transition was also seen in figure 17 in the case of intrinsic toxicity of the complexes E and F. Even of more interest is the effectiveness of chitosan to

exhibit protective properties similar to that for sialic acid complexes. It also suggests that the sialic acid mimic interaction with A $\beta$  and cells must be more than just competitive binding or electrostatic interactions. It has been suggested that lysine or histidine residues on the toxic A $\beta$  species interact with the negatively charged groups on the cell membranes, possibly sialic acids[162]. Thus, the presence of another charged species in solution could shield the cell from the harmful interactions with A $\beta$ . This could possibly explain the protective effect shown by chitosan in solution. The results from this study indicate that the sugar structure could play a critical role in A $\beta$  binding, thus raising the possibility that other biological sugars could prove to be equally or even more effective than sialic acid in binding and sequestering the pathogenic A $\beta$  peptide.

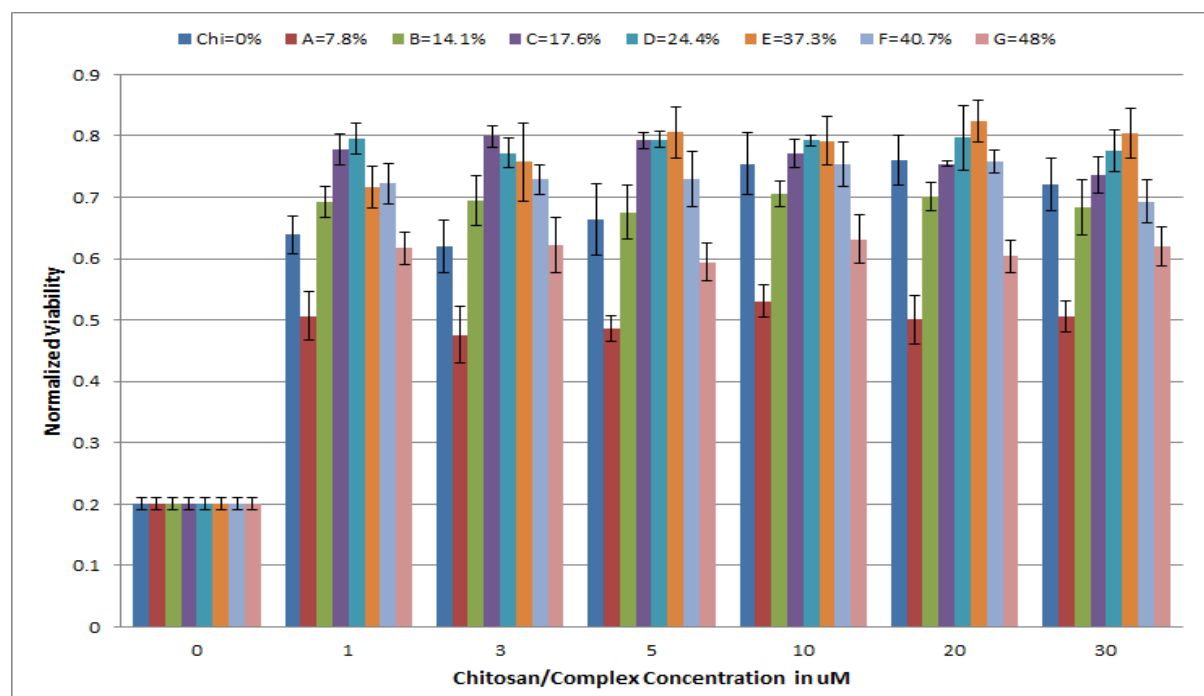


**Figure 23: Attenuation of 50μM A $\beta$  toxicity by sialic acid chitosan complexes (A to G) and Naïve chitosan**

The bar charts are labeled according to the sialic acid-chitosan complexes and their respective sialic acid labeling. Viability at 0μM represents the system with 50μM A $\beta$ (40) with no complex or chitosan in the system. Data is represented as mean  $\pm$ SD, n=4 in each case.

Nevertheless, this type of protection also works in our favor, that if we can delay or alter the rate of toxicity of A $\beta$  towards neurons, we can essentially aim to delay the age of onset or the time of progression of Alzheimer's disease. This the reason why we need to investigate structural analogs of sialic acid, to understand which groups or subgroups of sialic acid are interacting with or have higher affinity towards A $\beta$ . This information coupled with binding studies will prove beneficial from the therapeutic point of view.

### **3.4. Statistical Analysis of Intrinsic Toxicity and A $\beta$ Toxicity Attenuation Data**

Every value in the bar charts are expressed as normalized viabilities plotted on the y-axis with the test compound concentration on the x-axis. Each mean is calculated from the average of the viabilities observed from at least four replicates of each complex/compound concentration. For the statistical analysis, we are interested to understand how each compound performed at all the concentrations we tested. Hence, each compound, starting with 0 $\mu$ M concentration, the viabilities obtained at all concentrations is compared to one another. This is the statistical analysis for each compound. Similarly, at each concentration, we wanted to compare the viabilities obtained from all compounds tested at that concentration. This will allow us to compare the effects of different compounds at the same concentration. This is the statistical analysis for each concentration.

As this is a case of multiple comparisons, we use ANOVA followed by a suitable post-hoc test. For the post-hoc test, Tukey's Honest Significant Difference (HSD) test (shorthand "Tukey's test" in later texts) is used. For every case or comparison, we are keeping the constant error rate of  $\alpha$  equal to 0.05. All our measurements are done independently. The two important assumptions of ANOVA test is that the population is normally distributed and the variances for

all populations are equal. A sample dataset was run with the Levene's test in SAS to check for equality of variances. The output from Levene's test is attached in the Appendix. Thus, the homogeneity of the variance is verified and our data fits the requirements for ANOVA. However, this is a common assumptions in such kind of toxicity studies [8, 26, 162, 203, 229]. Furthermore, as a post hoc test, the analysis is done by Tukey's test. The null hypothesis is that the two means (i.e. the means of the two normalized viabilities being compared) are equal. When the null hypothesis is rejected, post hoc comparisons are done using Tukey's test to investigate further which groups/means differ.

### **Tukey's Test**

Tukey's test allows for all possible pairwise tests and is based on the studentized range statistics. It also keeps a constant experimental error rate ( $\alpha$ ) for all possible pairwise tests. The sample size is equal in Tukey's method. The differences between the means is calculated and compared to the critical value to see if the difference is significant. This critical value is the "Honestly Significant Difference" and that value is computed from SAS. The adjusted p-values for all pairwise comparisons are given in the output.

### **Guide to Interpreting the Statistical Information on the Bar Chart**

Data for normalized viability is presented as mean  $\pm$ SD of at least four replicates on the bar chart. The statistical significance of differences between groups was estimated by ANOVA. Further, any differences between the means group were analyzed by Tukey's test. Each graph shows the results and the statistical outputs obtained from the Tukey's test. Different letters across the graphs indicate statistically-significant differences ( $p < 0.05$ ); the same letter indicates no statistical difference between those groups. This assignment of letters is done using a macro

for SAS program developed by Saxton M.A [244]. This macro is run after the analysis by Tukey's test. The macro groups similar means together and assigns a letter. The figure 24 shows the statistical analysis of the KDN-Chitosan complex intrinsic toxicity data. The table (24.A) in the figure 24 below shows the output from the macro by the Tukey's test (at  $p < 0.05$ ). The means are sorted and ranked starting with the highest to the lowest mean. Each mean represents the normalized viability at each concentration of the compound studied. Using SAS, the calculation for the critical value of the "Least Significant Difference" (LSD) is done. When the analysis is done by the Tukey's test, SAS applies the adjustment on the LSD based on Tukey's test and the critical value is adjusted. The highest mean is assigned the letter group A. If the critical value of the LSD = "X", then means below that differ by less than "X" do not differ statistically. This is represented by giving them a common letter so that they share a letter.

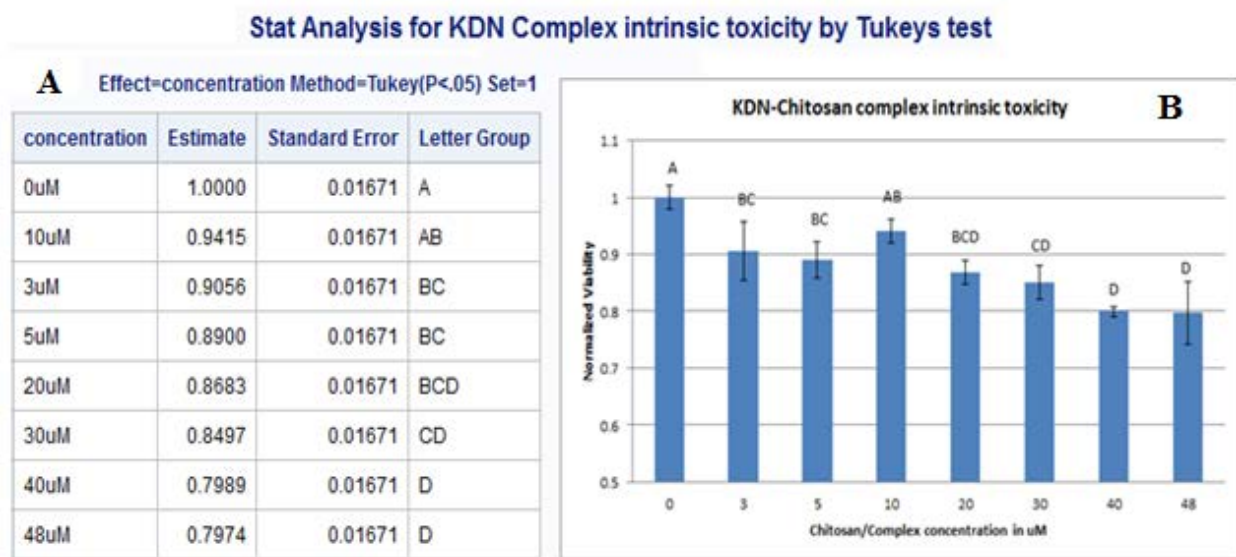


**Figure 24: Grouping example- Statistical analysis and graph for KDN complex intrinsic toxicity data**

The table 24.A. represents the output using the macro which gives letter grouping for the means by Tukey's test. The figure 24.B represents the normalized viabilities of KDN-complex plotted as a function of concentration. The similar letters above the bar indicate no statistical difference. Different letters indicates statistical difference at  $p < 0.05$  by Tukey's test.

As seen in figure 24-A, the difference between the means of 0 $\mu$ M and 10 $\mu$ M is not statistically significant. This is indicated by same letter A on 0 $\mu$ M and 10 $\mu$ M in figure 24.B. Here, each mean is the normalized viability obtained at each concentration. Hence, they both are assigned the letter A. However, the mean of 10 $\mu$ M is less than that of the mean at 0 $\mu$ M. Hence, 10 $\mu$ M is assigned A and B (i.e. “AB”). Thus, 10 $\mu$ M indicated by “AB” is statistically the same as all other means that have the letter A or B above them. Moving on after 10 $\mu$ M, the next highest mean is 3 $\mu$ M. SAS determined that the mean of 10 $\mu$ M and 3 $\mu$ M were statistically different (working with the adjusted critical value for Tukey’s) and hence it is assigned a separate letter group “BC”. Looking at the output data in the appendix, the comparison between the 0 $\mu$ M and 10 $\mu$ M gives the p-value of 0.0106 using Tukey’s test. Coming back to 3 $\mu$ M, the letter “B” and “C” is shared with 10 $\mu$ M, 5 $\mu$ M, 20 $\mu$ M, 30 $\mu$ M. All these means do not differ statistically even if one is lower in value than the other. Looking back at the table, the normalized viability at 0 $\mu$ M is statistically different from all the viabilities at all other concentrations. Thus, means that share a letter are not statistically different. Example: As seen from figure 24.A, the normalized viability at 3 $\mu$ M (indicated by letter group “BC” is statistically different from the normalized viabilities at 0 $\mu$ M (indicated by A), 40 $\mu$ M (indicated by D) and 48 $\mu$ M (indicated by D) as given by Tukey’s test (at  $p < 0.05$ ). The comparison between each data point and the p-values obtained by Tukey’s test are attached in the appendix. Also, the output from macro is included along with the means compared in the appendix.

### **3.4.1. Intrinsic Toxicity of Sialic Acid-Chitosan Complexes and Unlabeled Chitosan**

The following plots show the result of the intrinsic toxicity of the complexes and chitosan evaluated without A $\beta$  in media. In all results, a gradient of 1 $\mu$ M to 30 $\mu$ M chitosan or complex concentration are applied and the viabilities evaluated. The viability at 0 $\mu$ M concentration

represents the untreated cells, i.e. live control with no test/experimental compound added to the control well. The normalized viability is calculated by dividing the viable cells in a sample by that of the live control, which represents 100% cells. Each point is represented as mean  $\pm$  SD of the normalized viability values (with four replicates each). The statistical significance of differences between the means is estimated by ANOVA followed by the post hoc comparisons by the Tukey's test. Different letters above the groups indicates statistically different means at  $p < 0.05$  as given by Tukey's test. Similar letter or group of letter indicates no statistical significance between those groups. A macro in SAS programing was used to convert similar means into letter groups [244].

### **Statistical Analysis Done for Each Compound**

The next set of graphs show the statistical analysis of each complex or compound done at all the concentrations studied. Thus, for this analysis each compound is considered separately.

The graph below (figure 25) shows the analysis for the intrinsic toxicity of unlabeled chitosan compared at all concentrations from 1 $\mu$ M to 30 $\mu$ M. Essentially, it can be seen that unlabeled chitosan does not show any toxicity (statistically relevant) at all concentrations. Thus, unlabeled chitosan as a backbone is non-toxic to the cells. This is a significant improvement over previous works. Also, as chitosan has shown no toxicity, it will be possible to isolate the effects of just sialic acid in further results.

In the result (figure 26) for sialic acid-chitosan complex A, which has around ~7.8% labeling of chitosan, we see that the non-toxic nature of the chitosan is maintained even after ~7.8% labeling of the amine terminals by sialic acid moieties. At all concentrations studied, addition of the complex A shows no statistical difference from control at 0 $\mu$ M.

When the normalized viability means from complex B (having ~14.1% labeling) are compared to one another by Tukey's test, we see no statistical differences in viabilities at all concentrations. Since, none of the compounds shows any statistical change from control viability, it indicates that complex B is non-toxic to the SH-SY5Y cells, see figure 27.

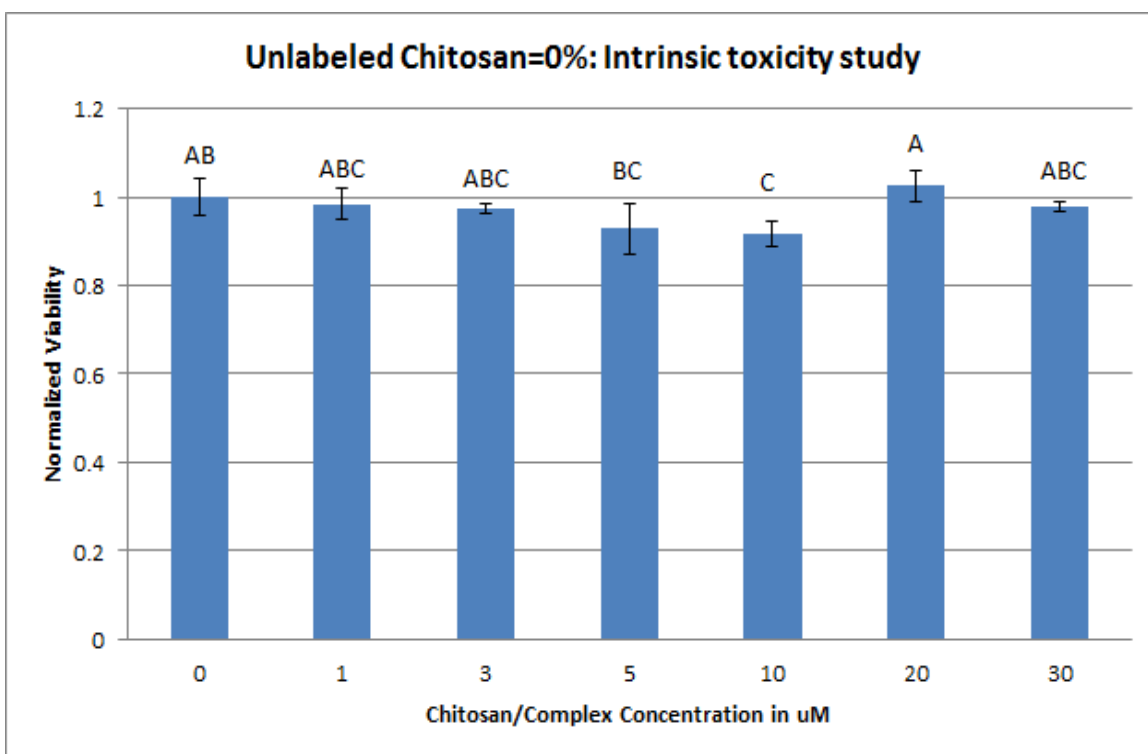


**Figure 25: Unlabeled chitosan=0%: Intrinsic toxicity studies**

Similar letters or group of letters above the bar chart indicates no statistical difference between the normalized viabilities of those concentrations as given by Tukey's test at  $p < 0.05$

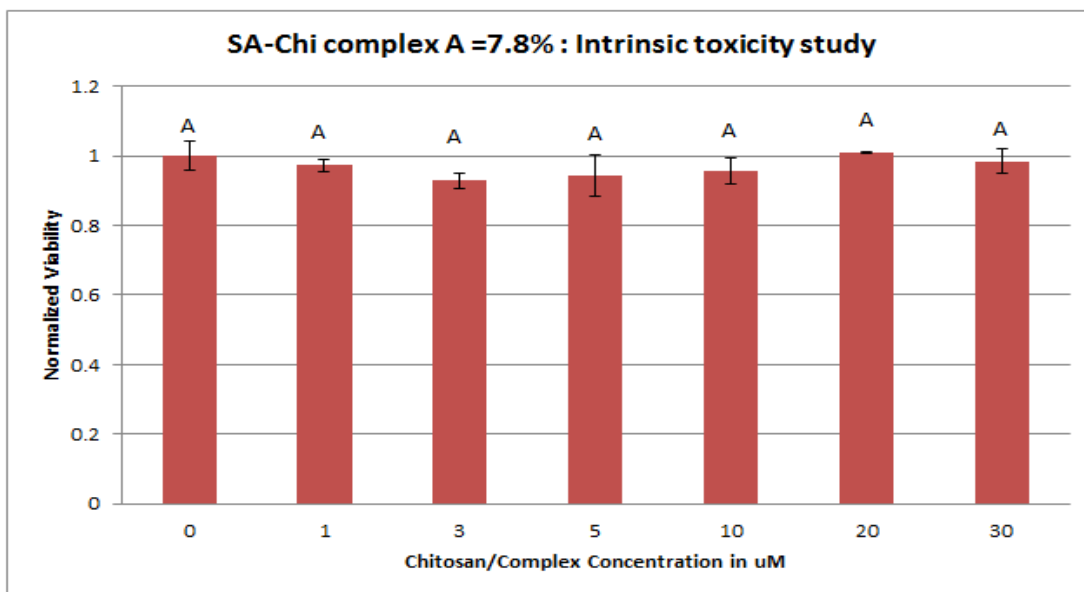


**Figure 26: Sialic acid-chitosan complex A =7.8% labeling: Intrinsic toxicity studies**

Similar letters or group of letters above the bar chart indicates no statistical difference between the normalized viabilities of those concentrations as given by Tukey’s test at  $p < 0.05$

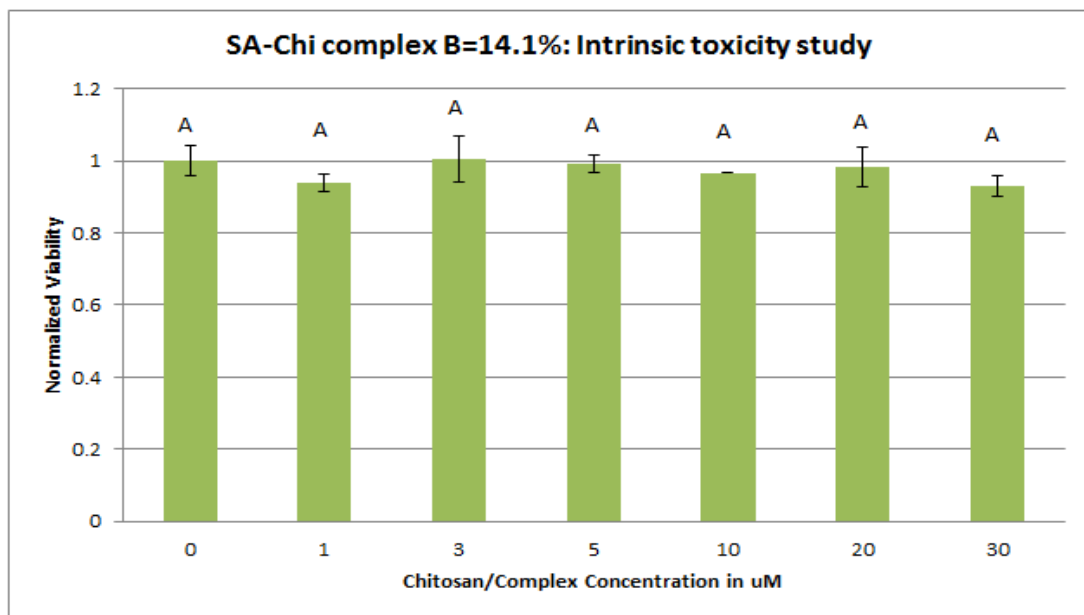


**Figure 27: Sialic acid-chitosan complex B =14.1% labeling: Intrinsic toxicity studies**

Similar letters or group of letters above the bar chart indicates no statistical difference between the normalized viabilities of those concentrations as given by Tukey’s test at  $p < 0.05$

Sialic acid complex C with 17.6% labeling also shows no toxicity towards SH-SY5Y cells at all the concentrations studied. Similarly, no statistical difference was found at all concentrations (in all cases,  $p > 0.05$ ). (Refer to figure 28).

Sialic acid complex D (~24.1% labeling) is non-toxic as seen from the figure 29 as none of the concentrations differ significantly than live control. Thus, complex D is non-toxic at all concentrations.

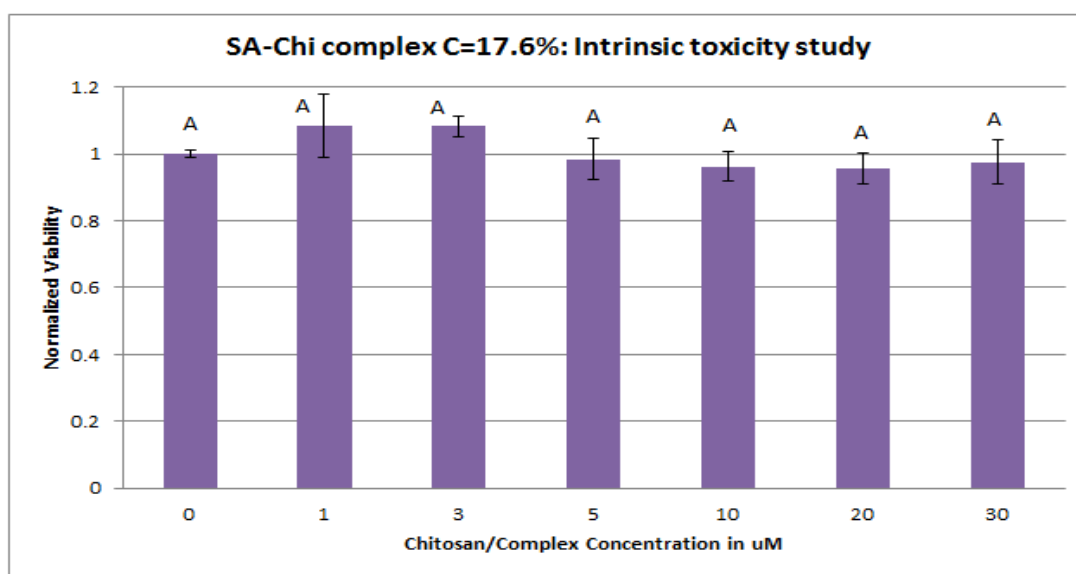


**Figure 28: Sialic acid-chitosan complex C =17.6% labeling: Intrinsic toxicity studies**

Similar letters or group of letters above the bar chart indicates no statistical difference between the normalized viabilities of those concentrations as given by Tukey's test at  $p < 0.05$

Looking at Figure 30, there is no toxicity seen from the sialic acid complex E. There is a dip observed at 1 $\mu$ M point that is inconsistent with the observed trend. However, the most likely explanation is biological variability as none of the other complexes show any statistically significant toxicity at 1 $\mu$ M concentration compared to control. This indicates that the complex E is non-toxic to SH-SY5Y cells.

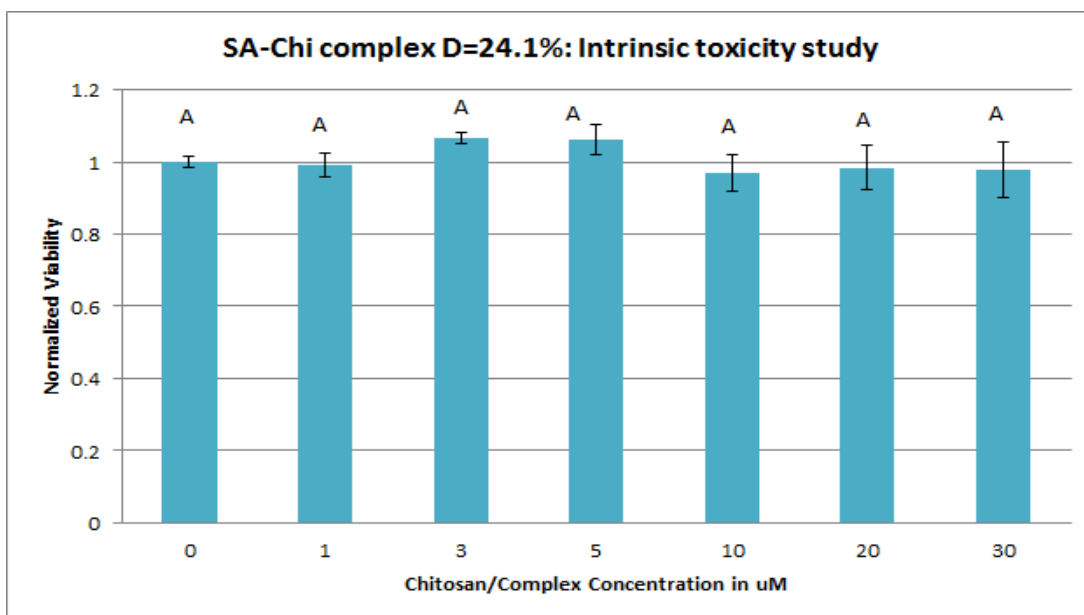


**Figure 29: Sialic acid-chitosan complex D = 24.1% labeling: Intrinsic toxicity studies**

Similar letters or group of letters above the bar chart indicates no statistical difference between the normalized viabilities of those concentrations as given by Tukey's test at  $p < 0.05$

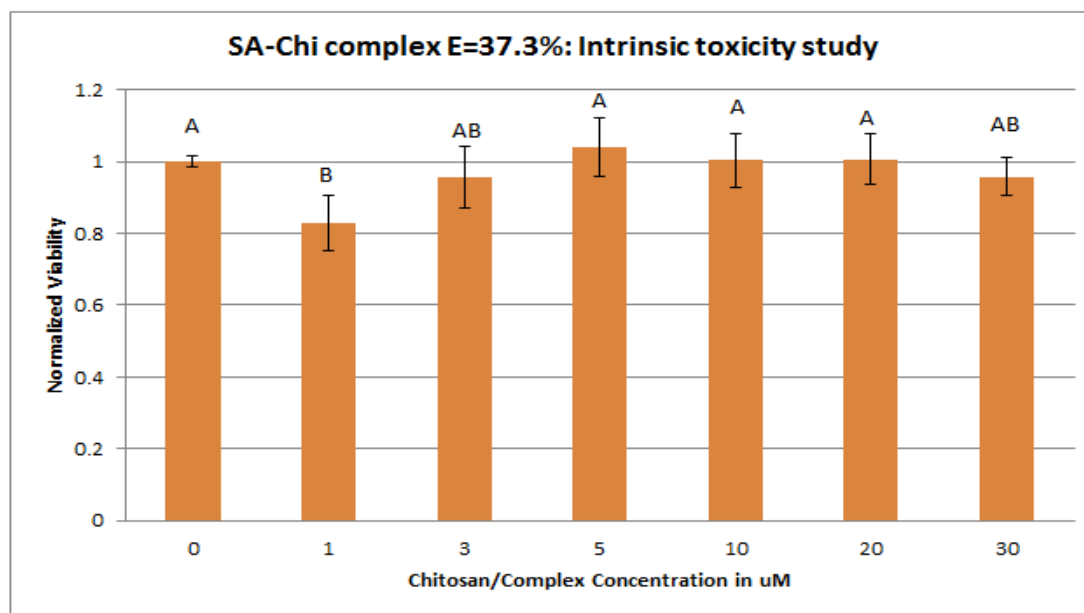


**Figure 30: Sialic acid-chitosan complex E = 37.3% labeling: Intrinsic toxicity studies**

Similar letters or group of letters above the bar chart indicates no statistical difference between the normalized viabilities of those concentrations as given by Tukey's test at  $p < 0.05$

From the analysis of the intrinsic toxicity of sialic acid complex F (~40.1% labeling) we start observing toxicity towards SH-SY5Y cells (refer to figure 31). At all concentrations except 5 $\mu$ M, the viabilities are statistically different compared to control. The range of toxicity appears to be around ~20% toxicity. This toxicity was not seen from any other compounds with less sialic acid labeling than complex F. This also corresponds to the transition seen from increasing sialic acid labeling to saturation in labeling as seen from the EDC chemistry curve. Also, at this point, we are approaching the limit of sialic acid labeling, which may indicate a likely link between molecule rigidity and toxicity. However, no further studies were done to confirm the molecule rigidity or its effect on toxicity.

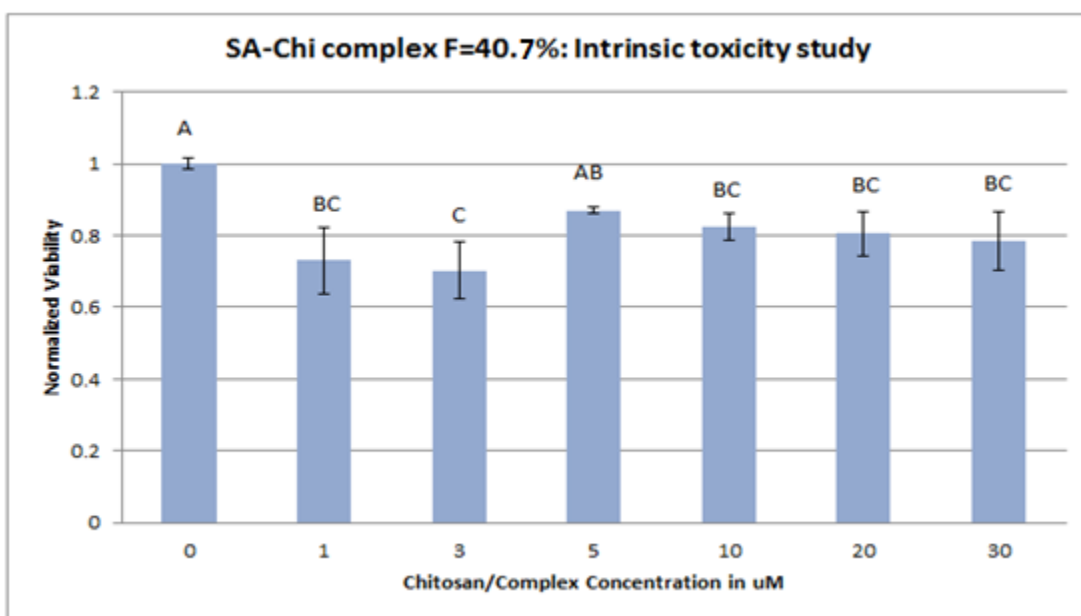


**Figure 31: Sialic acid-chitosan complex F = 40.7% labeling: Intrinsic toxicity studies**

Similar letters or group of letters above the bar chart indicates no statistical difference between the normalized viabilities of those concentrations as given by Tukey's test at  $p < 0.05$

Sialic acid complex G has ~48% labeling which is the maximum we could achieve from the EDC chemistry. It seems unlikely that any higher labeling of chitosan could be achieved as the saturation characteristics were seen from the EDC chemistry curve. This complex is the most

bulky among all the other compounds tested and also shows the highest toxicity among all complexes. We see that at all concentrations, the viability of cell treated with complex G is statistically lower compared to the live control (figure 32). We see viability in the range of ~60% after the addition of complex G. This indicates a likely link between higher molecular weight of the compound and high toxicity observed to cells in culture. Also, another plausible explanation could be that molecular rigidity may be the contributing factor towards toxicity. This issue of molecular rigidity was also observed in the case of star-burst shaped dendrimers that exhibited high toxicity [8, 26, 160]. However, this needs to be investigated from further studies.

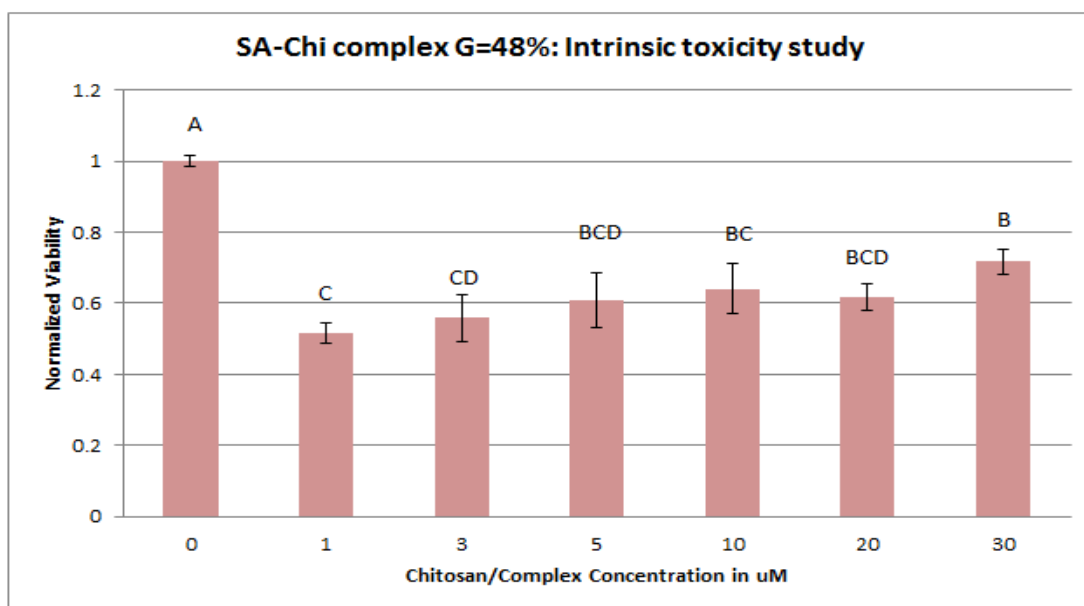


**Figure 32: Sialic acid-chitosan complex G=48% labeling: Intrinsic toxicity studies**

Similar letters or group of letters above the bar chart indicates no statistical difference between the normalized viabilities of those concentrations as given by Tukey's test at  $p < 0.05$

#### **Statistical Analysis Done for Each Concentration**

In this section, the complexes are compared to one another at each concentration. This will help us to understand the effect of each complex at a particular concentration. Similar letters on complexes on different concentrations are not compared. E.g.: in Figure 33, Chitosan at  $1\mu\text{M}$

has “AB” letter group, which is same as that on chitosan at 3 $\mu$ M. However, those two are not to be compared in this section. The letter grouping only refers to comparison at one concentration.

The results from figure 33 show the statistical analysis for each particular concentration 1 $\mu$ M, 3 $\mu$ M and 5 $\mu$ M. All complexes are compared among each other at a particular concentration. At 1 $\mu$ M, we see that chitosan and complexes A to D shows no significant difference. The highest toxicity is observed from complex G followed by complex F at 1 $\mu$ M. At 3 $\mu$ M and 5 $\mu$ M, unlabeled chitosan and complexes A to E have similar effect on viability of SH-SY5Y cells. Lower viabilities are observed for sialic acid complex F (~40.1% labeling) and complex G (~48% labeling) at these concentrations. Thus, at lower concentrations, it is observed that complex F and G consistently have higher toxicities compared to other labeled compounds.

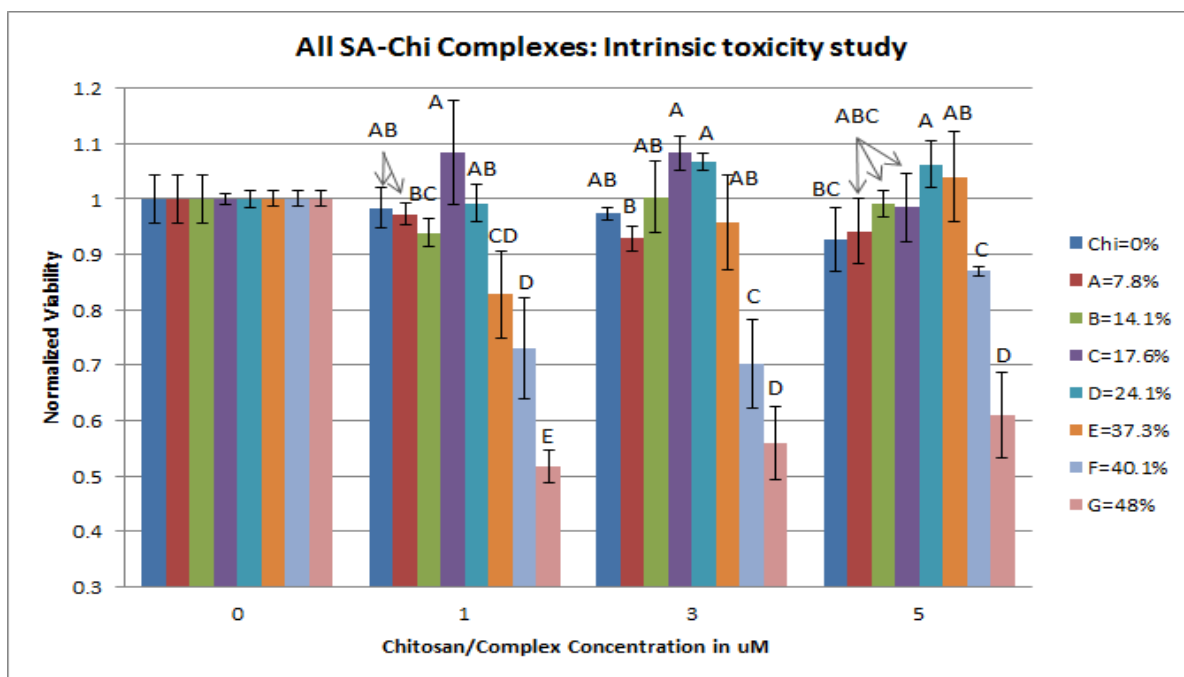


**Figure 33: All sialic acid-chitosan complexes: Intrinsic toxicity compared at 1 $\mu$ M, 3 $\mu$ M, 5 $\mu$ M**

Similar letters or group of letters above the bar chart indicates no statistical difference between the normalized viabilities of those concentrations as given by Tukey’s test at  $p < 0.05$

At lower concentrations from 1 $\mu$ M to 5 $\mu$ M, a broader trend is observed where complexes A to E fall in one group which show almost no toxicity and very less variability in between each other when the viabilities are compared. On the other hand, complex F and G consistently show higher toxicities at these concentrations, and hence this from the other group which is consistently different compared to complexes A to E at these concentrations. This analysis indicates that, at lower concentrations, chitosan and complexes A to E are non-toxic and show the same effect whereas complexes F and G show toxicity.

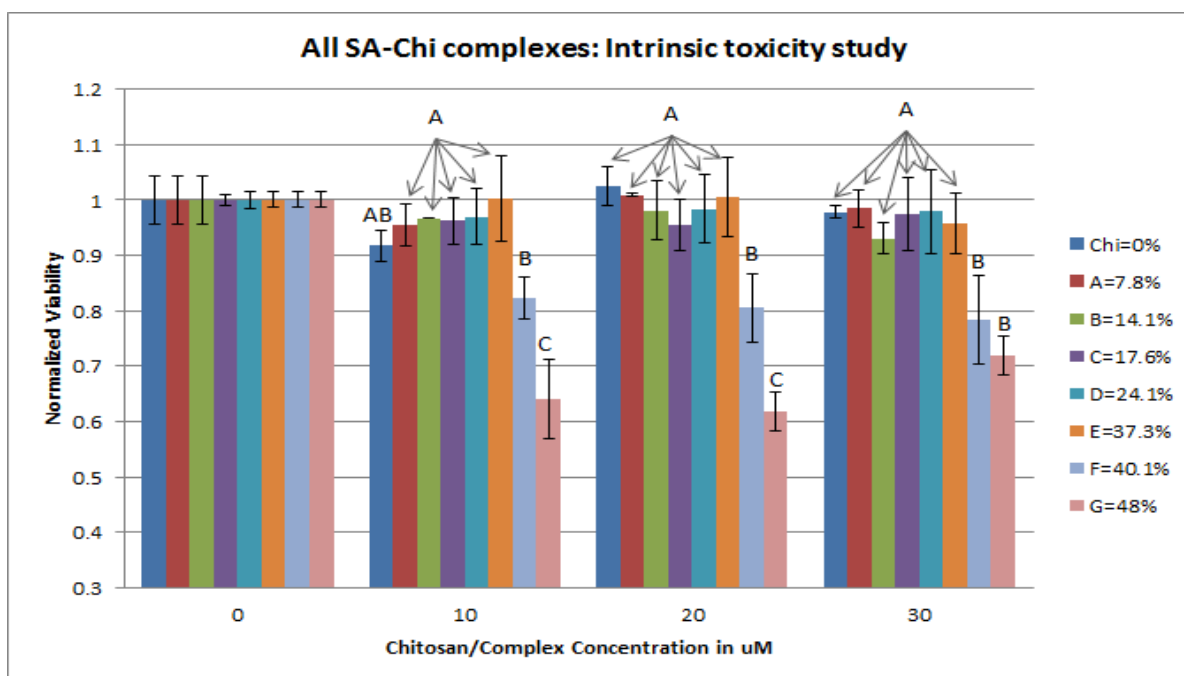


**Figure 34: All sialic acid-chitosan complexes: Intrinsic toxicity compared at 10 $\mu$ M, 20 $\mu$ M, 30 $\mu$ M**

Similar letters or group of letters above the bar chart indicates no statistical difference between the normalized viabilities of those concentrations as given by Tukey's test at  $p < 0.05$

The comparison for higher concentrations is shown in the figure 34. At 10 $\mu$ M, 20 $\mu$ M and 30 $\mu$ M unlabeled chitosan and labeling from ~7.8% to ~37.3% show similar effects on SH-SY5Y viability. This works in our favor because these complexes are not toxic to cells at even higher concentrations. Similar to the trend observed at lower concentrations, complex F (~80%

viability) and complex G (~60% to ~70% viability) show higher toxicities compared to all other compounds.

At higher concentrations from 10 $\mu$ M to 30 $\mu$ M, unlabeled chitosan and complexes A to E show no difference from live control indicating that they are non-toxic at even higher concentrations. Similar grouping can be done for chitosan and complexes A to E (all p-values > 0.05). Complexes F and G differ significantly from the above group (in all cases, p < 0.05). This is not the case for complexes F and G which show higher toxicities at all the concentrations compared to other labeled complexes.

These results indicate that intrinsic toxicity is not observed from 7.8% to 37% of sialic acid labeling to chitosan. Studies have shown that ligand has higher affinity to receptor that is multivalent or high in labeling. So, the optimum between intrinsic toxicity to SH-SY5Y and higher labeling of chitosan by sialic acid can be seen from complex E (has ~37.3% labeling).

### **3.4.2. A $\beta$ Toxicity Attenuation Studies of Sialic Acid-Chitosan Complexes and Unlabeled Chitosan**

The results in this section show the statistical analysis for unlabeled chitosan, sialic acid chitosan complexes (A to G) with 50 $\mu$ M aggregated A $\beta$  in the media. Aggregated A $\beta$  is prepared according to established protocols and added to cells in culture and viability assessed after 24h. After addition of 50 $\mu$ M aggregated A $\beta$  and no other experimental/test compound/complex, the normalized viability obtained is ~20%. This is indicated on the bar chart by point 0 $\mu$ M chitosan/complex concentration. This value represents the A $\beta$  control value, so, if our complexes are effective, we should see an increase in viability after the addition of the synthesized complexes.

In each case, viability is represented as mean  $\pm$  SD with four replicates. Statistical analysis was performed by ANOVA followed by Tukey's test in SAS program. Statistically similar means are grouped together and indicated by the same letter or same groups of letters. Different letters across the graphs indicate statistically different means as indicated by Tukey's test (at  $p < 0.05$ ). The macro used to analyze this data is kindly provided by Saxton M.A [244].

### Statistical Analysis Done for Each Compound

The next set of plots shows the statistical analysis for the A $\beta$  studies with each complex/chitosan compared at all concentrations from 1 $\mu$ M to 30 $\mu$ M. Each complex is presented separately so that multiple comparisons can be done at all doses studied.

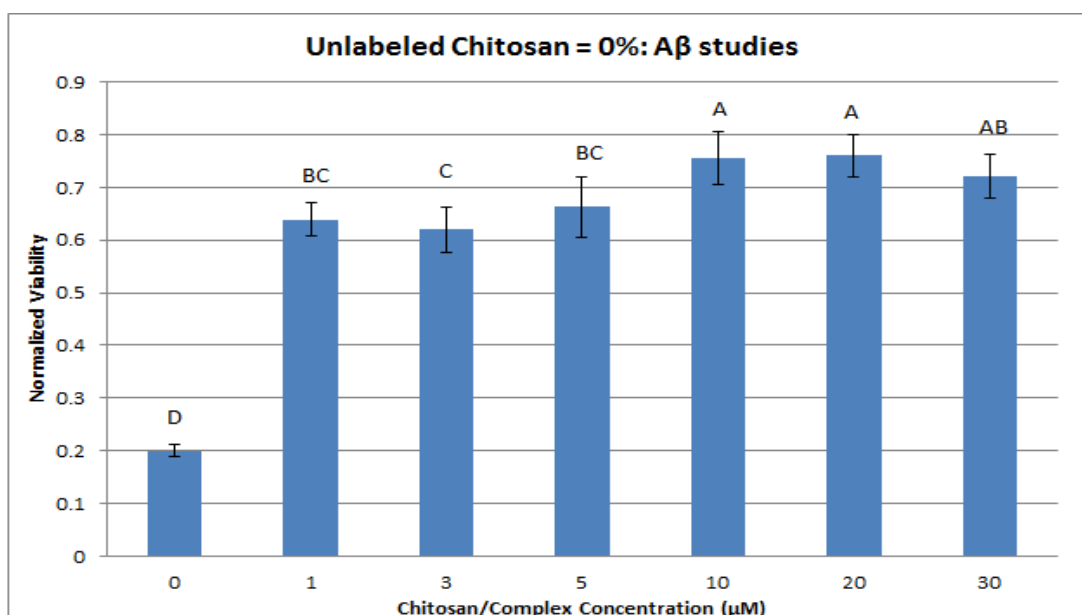


**Figure 35: Unlabeled chitosan = 0% labeling: A $\beta$  toxicity attenuation studies**

Similar letters or group of letters above the bar chart indicates no statistical difference between the normalized viabilities of those concentrations as given by Tukey's test at  $p < 0.05$

The results in figure 35 show the A $\beta$  toxicity attenuation properties for unlabeled chitosan. It is evident that chitosan shows significant protection from A $\beta$  at all concentrations

studied. Statistically highest protection can be seen from concentrations of 10 $\mu$ M to 30 $\mu$ M where there is almost ~75% cell viability compared to ~20% at A $\beta$  control. As we have already discussed earlier, A $\beta$  toxicity is a combination of the effects of electrostatic interactions, hydrophobic interactions and binding with sialic acids on cell membranes. Chitosan is a very strong polycation due to its protonation of amine groups as physiological pH. Thus, it is likely that the protection seen is due to the shielding of the cell from the harmful electrostatic interactions of A $\beta$ . This effect of a polycation protection is not uncommon and many studies has demonstrated that a strong polycation shows protection from toxic A $\beta$  [8, 26, 162]. In spite of the protection shown by chitosan, the mechanism of protection is not a viable option for long term effects. Although we see protection in 24h, this shielding of the cells may prove more detrimental later on. Additionally, electrostatic protection is unspecific. As we are sequestering the cell away, there is a possibility of inhibiting cellular functions due to unspecific electrostatic shielding. Our aim is to sequester the A $\beta$  away from the cell (and not vice versa) and that is the precise reason why we need sialic acid labeling on chitosan even if chitosan shows protective behavior.

From the above results of A $\beta$  attenuation properties of complex A (figure 36), having ~7.8% labeling, we see enhanced protection at all concentrations of complex A. The viabilities of SH-SY5Y are around ~50% compared to A $\beta$  only at ~20% viability. As it is evident, complex A shows less protection than unlabeled chitosan. The most plausible explanation is that only a minimum labeling of the amine terminals in chitosan by sialic acid was sufficient to disrupt the electrostatic protective effect shown by chitosan.

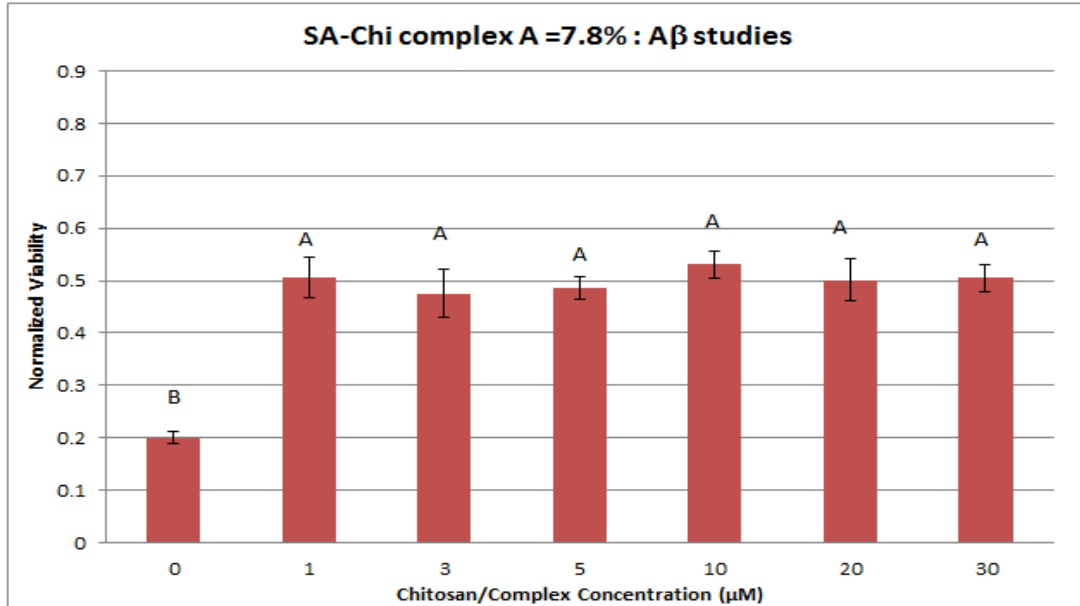


**Figure 36: Sialic acid-chitosan complex A = 7.8% labeling: Aβ toxicity attenuation studies**

Similar letters or group of letters above the bar chart indicates no statistical difference between the normalized viabilities of those concentrations as given by Tukey's test at  $p < 0.05$

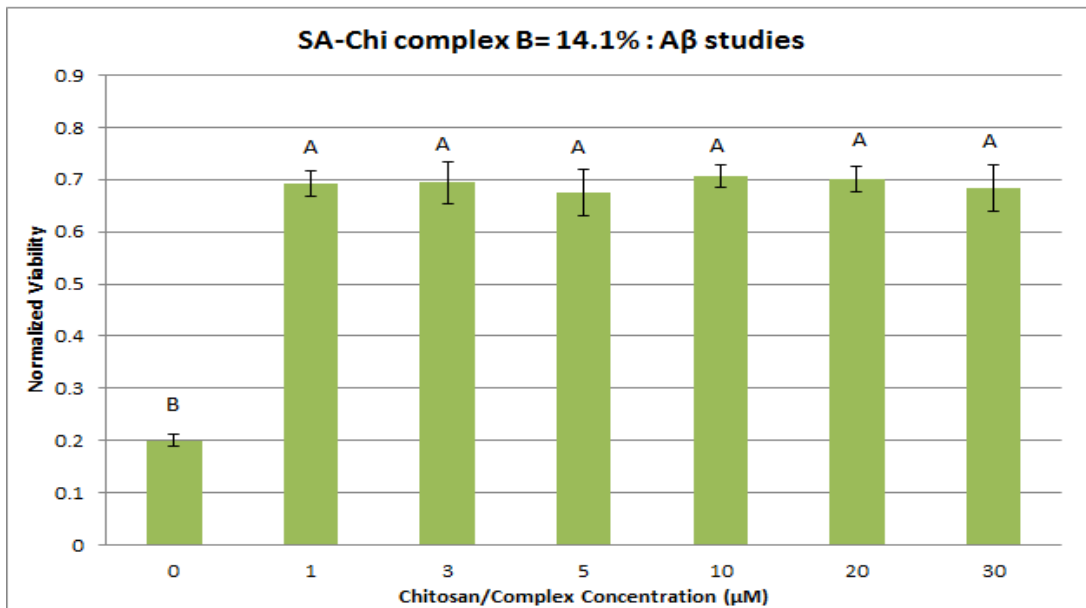


**Figure 37: Sialic acid-chitosan complex B = 14.1% labeling: Aβ toxicity attenuation studies**

Similar letters or group of letters above the bar chart indicates no statistical difference between the normalized viabilities of those concentrations as given by Tukey's test at  $p < 0.05$

The results for Aβ toxicity attenuation by complex B having ~14.1% labeling is shown in the figure 37. Compared to Aβ control, addition of complex B shows around ~70% viability of

SH-SY5Y cells. All concentrations of complex B show similar protection from toxic A $\beta$ . This is interesting because unlabeled chitosan was showing highest protection at higher concentrations. Also, complex B is showing higher protection compared to complex A at each concentration.

From the results of A $\beta$  toxicity studies with sialic acid complex C (~17.6% sialic acid labeling) we see excellent protective properties at all concentrations studied compared to A $\beta$  control (refer figure 38). We see that the highest viability is ~80% and the range of protection is ~72 to ~80%.

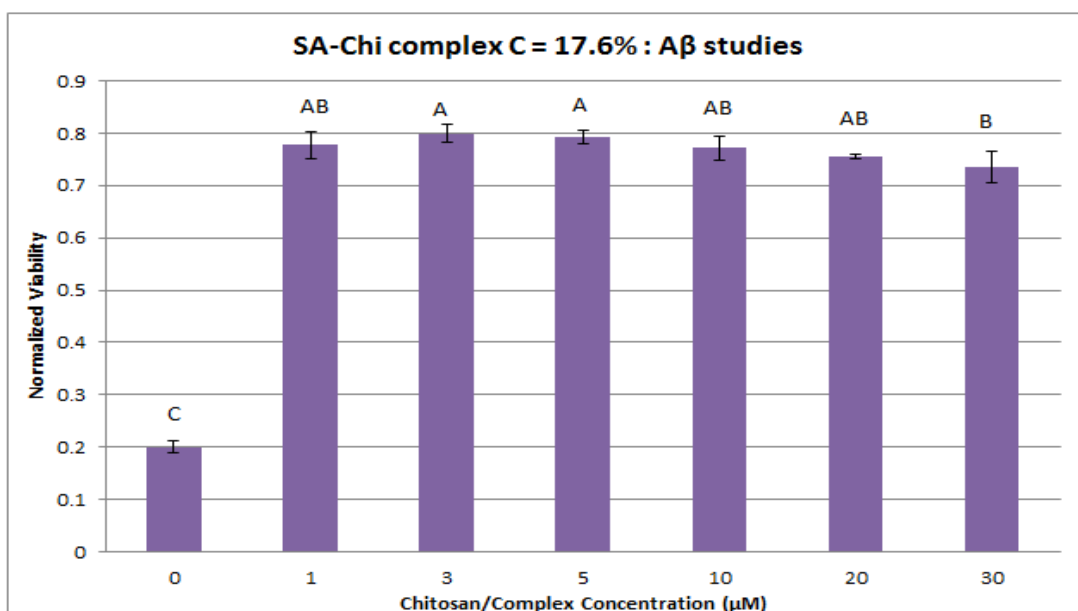


**Figure 38: Sialic acid-chitosan complex C = 17.6% labeling: A $\beta$  toxicity attenuation studies**

Similar letters or group of letters above the bar chart indicates no statistical difference between the normalized viabilities of those concentrations as given by Tukey's test at  $p < 0.05$

Sialic acid complex D (~24.1% labeling) also shows significant protective properties compared to control. The data is presented in figure 39. The average protection shows around ~80% SH-SY5Y cell survival after addition of complex to A $\beta$  treated cells.

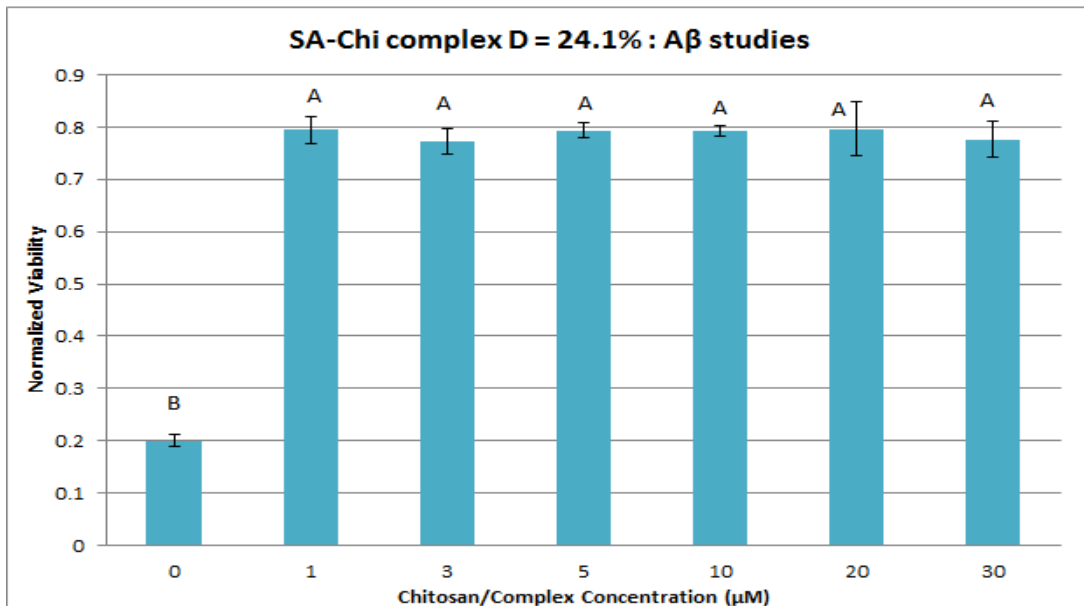


**Figure 39: Sialic acid-chitosan complex D = 24.1% labeling: Aβ toxicity attenuation studies**

Similar letters or group of letters above the bar chart indicates no statistical difference between the normalized viabilities of those concentrations as given by Tukey's test at  $p < 0.05$

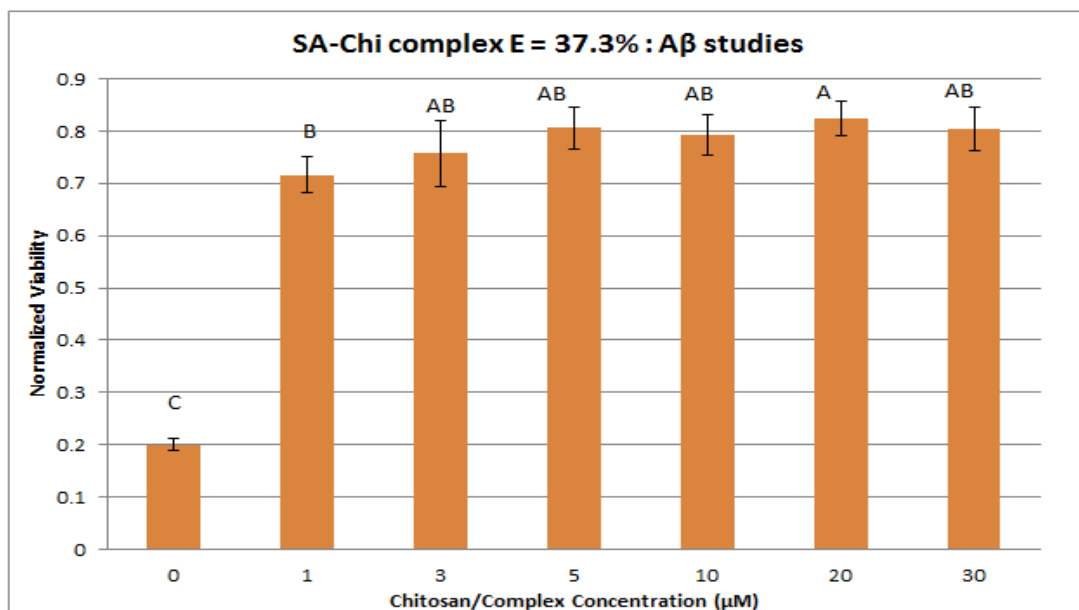


**Figure 40: Sialic acid-chitosan complex E = 37.3% labeling: Aβ toxicity attenuation studies**

Similar letters or group of letters above the bar chart indicates no statistical difference between the normalized viabilities of those concentrations as given by Tukey's test at  $p < 0.05$

In figure 40, the A $\beta$  toxicity attenuation properties of complex E (~37.3% labeling) are presented. At all concentrations tested, SH-SY5Y cells have significantly more survival compared to A $\beta$  control cells. At concentration of 1 $\mu$ M we see around ~71% protection which increases to ~82% around 20 $\mu$ M. Thus, complex E gives a good balance between intrinsic toxicity and high A $\beta$  attenuation properties. This also represents the transition seen in sialic acid labeling from the EDC saturation curve, which we believe is the transition to less flexibility of the molecule. This observation further supports our theory of a flexible backbone with sialic acid labeling, which will present the necessary clustering towards A $\beta$  in solution and therefore attenuate toxicity of A $\beta$  *in vitro*.

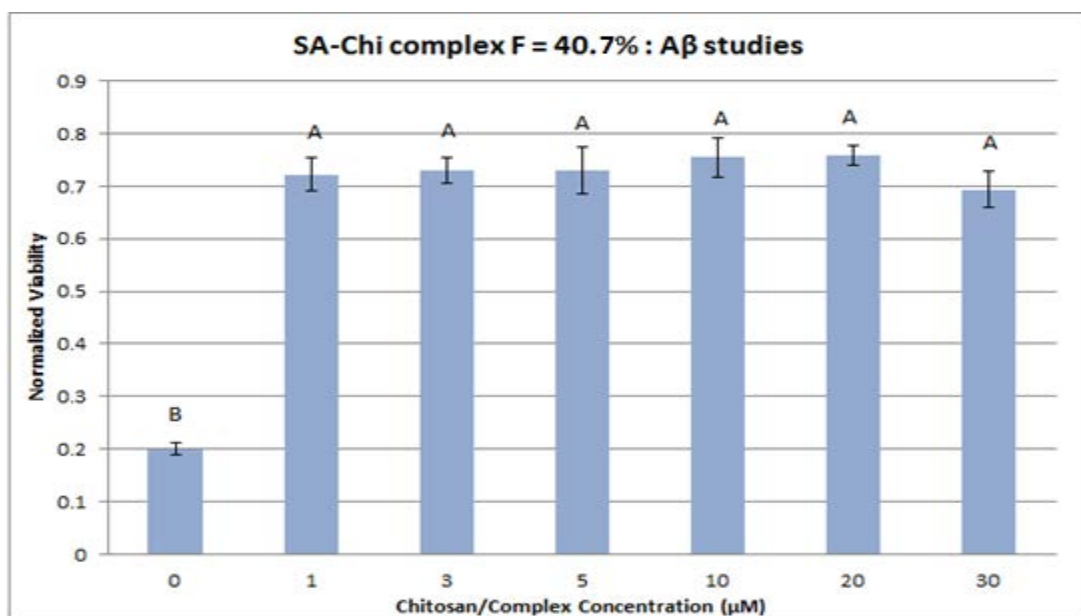


**Figure 41: Sialic acid-chitosan complex F = 40.7% labeling: A $\beta$  toxicity attenuation studies**

Similar letters or group of letters above the bar chart indicates no statistical difference between the normalized viabilities of those concentrations as given by Tukey's test at  $p < 0.05$

Sialic acid-chitosan complex F (has ~40.7% labeling) also protects SH-SY5Y cells significantly from A $\beta$  at all concentrations tested. See figure 41 for the result of complex F. However, now, this protection is around ~70 to ~75%, which is less compared to complex E

(~37% labeling) which shows around ~82% viability. Now, in spite of the degree of labeling increase, we start seeing a decrease in viability of SH-SY5Y cells.

It can be seen that sialic acid complex G (see figure 42), with 48% labeling of chitosan, shows significant protection if compared to A $\beta$  control (at 0 $\mu$ M complex concentration). Also, we do not see any significant difference between the protections offered at concentrations from 1 to 30 $\mu$ M. However, the protection offered by complex G gives around ~60% viability, which is less than the protection from complex D, E. One likely explanation that fits the data is that our complex backbone is saturated with sialic acid labeling and hence, essentially, it is a bulky higher molecule weight molecule that shows sub-optimum sialic acid clustering towards A $\beta$  that gives less protection compared to other less percentage labeled chitosan complexes. However, it is difficult to address the issue of molecule rigidity or even flexibility in a complex of sialic acid and chitosan.

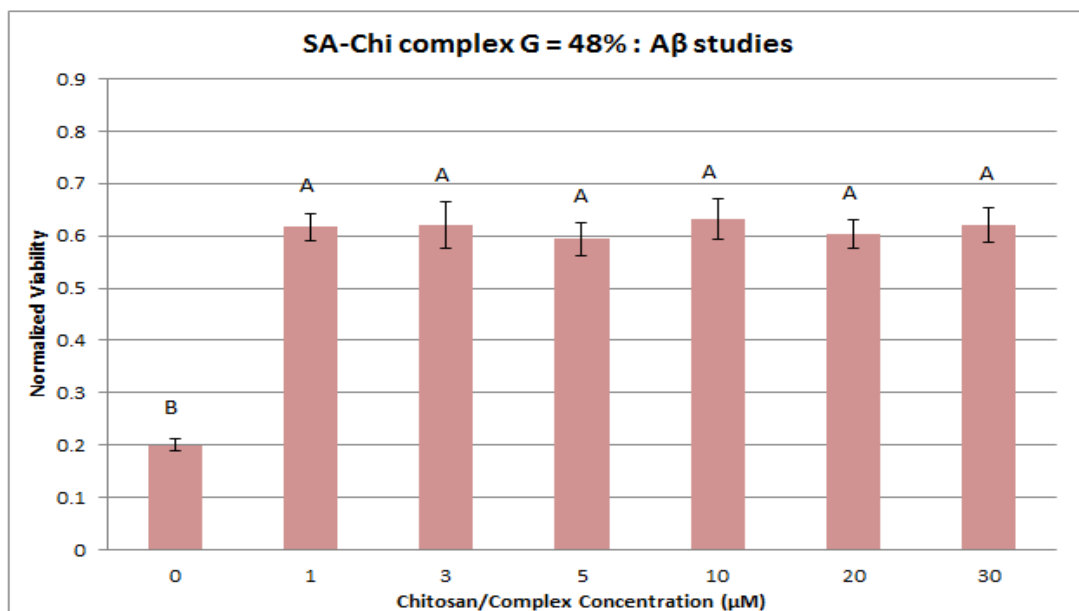


**Figure 42: Sialic acid-chitosan complex G = 48% labeling: A $\beta$  toxicity attenuation studies**

Similar letters or group of letters above the bar chart indicates no statistical difference between the normalized viabilities of those concentrations as given by Tukey's test at  $p < 0.05$

## Statistical Analysis Done for Each Concentration

In the next set of plots, each compound tested, unlabeled chitosan and the different sialic acid-chitosan complexes, are compared among each other at every concentration studied. We are interested to analyze which compound offers what level of protection at each concentration. Similar letters on adjacent concentration do not mean that those viabilities are statistically similar. Each complex is only compared at each concentration separately. The A $\beta$  control at 0 $\mu$ M chitosan/complex concentration is given for better understanding of the results only.

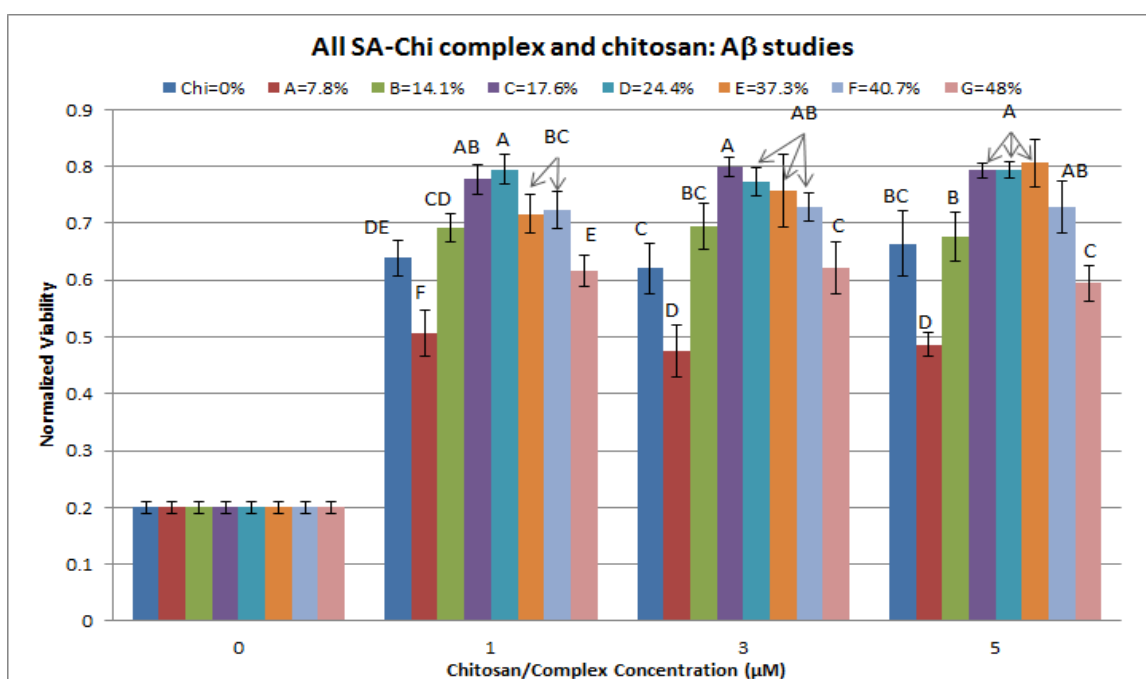


**Figure 43: All sialic acid-chitosan complexes at 1 $\mu$ M, 3 $\mu$ M, 5 $\mu$ M: A $\beta$  toxicity attenuation studies**

Similar letters or group of letters above the bar chart indicates no statistical difference between the normalized viabilities of those concentrations as given by Tukey's test at  $p < 0.05$

The results for all complexes at lower concentrations (i.e. 1 $\mu$ M, 3 $\mu$ M and 5 $\mu$ M) are given in figure 43. At a concentration of 1 $\mu$ M, complex D shows the highest protection followed by complex C. Chitosan also shows protection, but it is statistically lower compared to protection from sialic acid complexes C, D, E, F. Compared to unlabeled chitosan (0% labeling), we see a

sharp drop in viability from complex A. This supports our theory that even small percentage labeling of chitosan by sialic acid is sufficient to disrupt the electrostatic protection offered from electrostatic shielding. Increasing the labeling from ~7.8% to ~14.1% also increases the protection with maximum observed from complex D (~24.4% labeling). After that, as the labeling increases, the protection decreases which the least being observed from complex G. At 5 $\mu$ M complexes C, D, E, F shows the highest protection from 50 $\mu$ M A $\beta$  toxicity. Chitosan offers protection, albeit statistically lower compared to complexes C, D, E, F. Again, similar trend is observed where complex A shows much lower protection after minimum sialic acid labeling. The protection starts increasing with sialic acid labeling and reaches the highest for ~17.6 to ~37.3% labeling of chitosan. After that, the protection decreases even after the percentage labeling (on complexes F and G) of chitosan increases. At 5 $\mu$ M, similar trends are observed with highest protection from 17.6 to 37.3% labeling. Chitosan also shows statistically lower protection compared to complexes C, D, E.

Again, broader trends can be observed from the data, at lower concentrations (1 $\mu$ M, 3 $\mu$ M, 5 $\mu$ M), we see complexes C (17.6%), D (24.2%) and E (37.3%) show no statistical difference between one another ( $p > 0.05$ ) and offer the highest protection from A $\beta$ . Thus, this is the highest protection group of complexes. The next highest protective group is unlabeled chitosan, complex B (14.1%) and F (40.7). At all concentrations, they are statistically similar protection from A $\beta$ . Finally, complexes A (7.8%) and G (48%) show the least protection from A $\beta$ .

In figure 44, the analysis of A $\beta$  studies at higher concentrations, 10 $\mu$ M, 20 $\mu$ M and 30 $\mu$ M of chitosan/complex concentration are presented (figure 44). Again, each compound is compared to other at a single concentration, with similar letter indicating no statistical difference between

the means of the groups. Again, means refer to the normalized viability values. At 10 $\mu$ M as well as 20 $\mu$ M, we see highest protection from unlabeled chitosan and complexes C, D, E (~17.6% to ~37.3%). Only statistical difference is observed from complex A and G compared to the other compounds. This trend is also observed at lower concentrations. At 30 $\mu$ M, highest protection is observed from complex D, E (~24.5% and ~37% labeling) followed by complex C. Other complexes show lower protection.

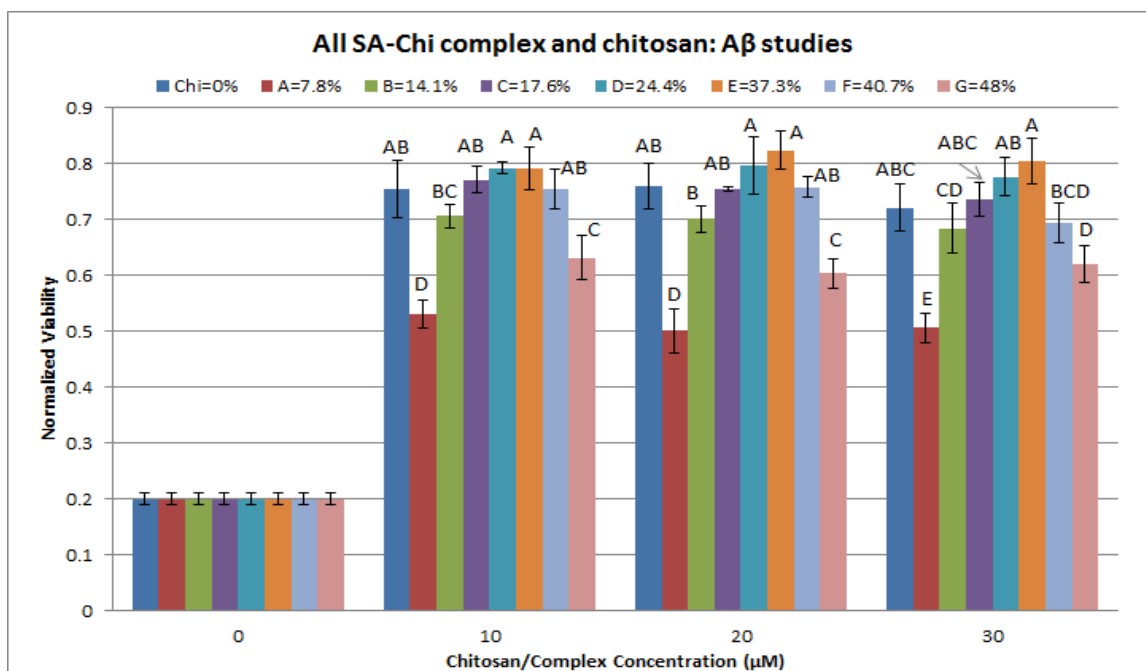


**Figure 44: All sialic acid-chitosan complexes at 10 $\mu$ M, 20 $\mu$ M, 30 $\mu$ M: A $\beta$  toxicity attenuation studies**

Similar letters or group of letters above the bar chart indicates no statistical difference between the normalized viabilities of those concentrations as given by Tukey's test at  $p < 0.05$

At higher concentrations (10 $\mu$ M, 20 $\mu$ M, 30 $\mu$ M) again, the trend continues but with an exception. Here, the protection seen from chitosan is similar to the highest protection seen from sialic acid complexes C, D, E respectively. Earlier, we have seen that chitosan offer higher protection at higher concentration. Next highest protection is from group of complexes B and F

followed by the least shown by the group of complex A (in all cases,  $p < 0.05$  compared to other groups) and complex G.

### **3.4.3. Our Hypothesis for the Observed Results**

Looking at the entire picture, we see similar trends in all the data from A $\beta$  toxicity attenuation studies. Below are the likely explanations from these trends. Chitosan being a strong polycation (amino groups become protonated at pH 7.0) shows protection due to strong electrostatic interactions with the negatively charged cell surface. This interaction of strong polycations with the cell surface is well documented in literature. Thus, we believe, chitosan is sequestering the cell away from A $\beta$  and that is not the ideal effect/protection. At an extended period of time, this unspecific shielding of the cell will actually prove detrimental as this protection will start interfering with other intracellular processes of the cell (metabolites, hormones, amino acid transport) that depend on the electrostatic interactions with their host receptors. Also, as a therapeutic, it is unrealistic to protect each and every cell from the toxic effects of A $\beta$ . Our next result also supports our argument. When we label chitosan with just ~7.8% sialic acid, the protection shown by complex A decreases compared to unlabeled chitosan. This decreased protection is seen at all the concentrations of complex A. This may be due to the disruption of the protection seen from the electrostatic interactions. This is why A $\beta$  kills more cells when complex A is added compared to unlabeled chitosan. Now, as the degree of labeling increases, higher viabilities in SH-SY5Y cells are observed. The highest protection can be seen for labeling from ~17.6% to ~37.6% of chitosan (i.e. complex C, D, E). This transition may indicate that the mechanism of protection has now shifted to our complex sequestering A $\beta$  away from the cells. This is a strong possibility, as the biomimetics were synthesized with sialic acids labeled on chitosan. On the neuronal membrane, A $\beta$  has affinity towards clustered sialic acids

and binds to them. If our complexes are showing toxicity attenuation, it is most likely that the protection is due to binding of A $\beta$  to the complex. In the study with sialic acid labeled dendrimers, A $\beta$  had binding affinities to the sialic acid dendrimers complexes on the order of  $10^{-7}$ M to  $10^{-9}$ M [8, 26], which were at least an order of magnitude higher than A $\beta$  binding to gangliosides ( $10^{-6}$ M [8, 26, 156]) on neuronal membranes. Looking at the data, it is difficult to predict whether one or multiple mimics bind to A $\beta$ . Binding studies should be done to prove the exact mechanism of protection (e.g. to prove binding of complex with A $\beta$ ). This sequestering of the A $\beta$  away from the cell is the mechanism of protection that we aimed for. It is difficult to elucidate whether the complex acts via competitive or non-competitive mechanism in attenuating the toxicity of A $\beta$ . It is also possible that the complex binds with A $\beta$ , and alters the rate at which A $\beta$  interacts with the cells, and induces toxic effect. This may be the reason why we see protection at all concentrations studied but not complete protection (or 100% cell survival). Additionally, we do not see any type of dose-dependent behavior from the complexes. Thus, the mechanism of protection needs to be investigated in much more detail in later studies. Nevertheless, this type of protection also works in our favor, that if we can delay or alter the rate of toxicity of A $\beta$  towards neurons, we can essentially aim to delay the age of onset or the time of progression of Alzheimer's disease.

This the reason why we need to investigate structural analogs of sialic acid, to understand which groups or subgroups of sialic acid are interacting with or have higher affinity towards A $\beta$ . This information coupled with binding studies will prove beneficial from the therapeutic point of view.

#### **3.4.4. Summary of the Statistical Analysis**

We used ANOVA followed by Tukey's test (at  $p < 0.05$ ) for the statistical analysis of the toxicity studies. A macro was used to group statistically similar means together and assign letter groups to them. Thus, similar letters above the bar indicates no statistical difference between those means (as given by Tukey's test at  $p < 0.05$ ). Each mean the normalized viability at that concentration. This grouping allows for multiple comparisons between each and every data point on the bar chart. We studied a gradient of  $1\mu\text{M}$  to  $30\mu\text{M}$  of unlabeled chitosan and sialic acid-chitosan complexes A (~7.8% labeling), B (~14.1%), C (~17.6%), D (~24.5%), E (~37.3%), F (~40.7%) to G (~48% labeling) on SH-SY5Y cells. For the sake of understanding, we will treat  $1\mu\text{M}$  to  $5\mu\text{M}$  as low concentrations and  $10\mu\text{M}$  to  $30\mu\text{M}$  as high concentrations of compounds for this study. The comparison between each data point and the p-values obtained by Tukey's test are attached in the appendix. Also, the output from macro is included along with the means compared in the appendix.

#### **Intrinsic Toxicity Data**

##### **Statistical Analysis Done for Each Compound**

It is observed that unlabeled chitosan does not show any significant toxicity at towards SH-SY5Y cells. The only case where difference was observed was at  $10\mu\text{M}$  when compared to live control ( $p=0.0459$ ). This is a significant improvement over other studies where the issue was high intrinsic backbone toxicity towards cultured cells [8, 26].

For complexes A, B, C, D, E, from the statistical analysis, none (except, complex E at  $1\mu\text{M}$ ) of the viabilities at any concentration of the complexes differ significantly from the live control (in all cases,  $p > 0.05$ ). Thus, complexes A (~7.8%) to E (~37.3%) do not show any

intrinsic toxicity towards SH-SY5Y cells at all concentrations studied. This indicates that we were successful in developing complexes that were non-toxic towards cells. Again, this is an improvement over previous works where the issue was high intrinsic toxicity of the complexes towards cultured neurons[8, 26, 229].

Toxicity is observed starting with complex F (40.7%) and the viability range is around ~80% at all concentrations of complex F. Viabilities at all concentrations of complex F, except 5 $\mu$ M, differ significantly from the 0 $\mu$ M live control (in all cases  $p < 0.05$ ). This follows the transition to saturation in sialic acid labeling found from the EDC chemistry curve for chitosan (see figure 20 in dissertation). Sialic acid complex G (~48%) is the most toxic and the range of viability of cells is around ~60% at higher concentrations of complex G (compared to live control, all viabilities for all concentrations are statistically different, in all cases,  $p < 0.001$ ).

### **Statistical Analysis Done for Each Concentration**

At lower concentrations from 1 $\mu$ M to 5 $\mu$ M, a broader trend is observed where complexes A to E fall in one group which show almost no toxicity and very less variability in between each other when the viabilities are compared. On the other hand, complex F and G consistently show higher toxicities at these concentrations, and hence, these two complexes from the other group which is consistently more toxic compared to group of complexes A to E at lower concentrations. This analysis indicates that, at lower concentrations, chitosan and complexes A to E are non-toxic and show the same effect whereas complexes F and G show toxicity towards cells in culture.

At higher concentrations from 10 $\mu$ M to 30 $\mu$ M, unlabeled chitosan and complexes A to E show no difference from live control indicating that they are non-toxic at even higher

concentrations. Similar grouping can be done for chitosan and complexes A to E (all p-values > 0.05). Complexes F(40.7%) and G(48%) differ significantly from the above group (in all cases, p < 0.05) and show consistent higher toxicity at all concentrations.

This trend of higher toxicity seen above 40% labeling indicates a likely link between higher labeling and higher toxicity or higher molecular weight of the complex and higher toxicity.

### **A $\beta$ Toxicity Attenuation Data**

In this study, along with a gradient of 1 $\mu$ M to 30 $\mu$ M of unlabeled chitosan and complexes A to G, a concentration of 50 $\mu$ M aggregated A $\beta$  is added to the cells. The A $\beta$  control value is ~20% viability compared to live control (100%).

### **Statistical Analysis Done for Each Compound**

When viabilities of cells treated with unlabeled chitosan or any of the complexes at any concentration (1 $\mu$ M to 30 $\mu$ M) is compared to the A $\beta$  control viability, we see that in all cases the p-value is < 0.001. This indicates that all the cells treated with the sialic acid-chitosan complexes and unlabeled chitosan have statistically higher viabilities compared to A $\beta$  control. This proves that all the complexes synthesized show A $\beta$  toxicity attenuation properties. Unlabeled chitosan shows lower protection from 1 $\mu$ M till 5 $\mu$ M after which the protection increases and is statistically the same from 10 $\mu$ M to 30 $\mu$ M.

In all the A $\beta$  studies with sialic acid complexes, a typical dose dependent response is not seen. All the complexes, from 1 $\mu$ M to 30 $\mu$ M, do not show any statistical difference between each other for all doses. This indicates that the mechanism of protection is not just competitive

binding or electrostatic interactions. It is possible that due to strong polycations strength of chitosan, electrostatic dominance could be higher. It may be that the binding to A $\beta$  is non-competitive and the complex of (A $\beta$ )-(sialic acid-chitosan) is still toxic to cells but at a reduced rate. A recent publication developed mathematical models to investigate this theory[162].

### **Statistical Analysis Done for Each Concentration**

Unlabeled chitosan shows significant protection from A $\beta$  and the protection is higher at 10 $\mu$ M to 30 $\mu$ M concentration of chitosan added with A $\beta$ . A likely reason for this protection is that the chitosan polycation interacts with the negatively charged cell membrane. This effect of a polycation compound protecting cells is seen in other studies with toxic A $\beta$  [8, 26, 162]. Further evidence supporting this hypothesis is that complex A (~7.8%) treated cells have ~50% viability compared to ~65% in chitosan. This indicates that minimum labeling of the chitosan cations were sufficient to disrupt the protection and hence complex A shows less protection.

As the labeling increases, we see an increase in viabilities and the highest protection is seen from complexes C (~17.6%) to E (37.3%) labeling. From intrinsic toxicity studies, the toxicity of the complexes are non-existent up to complex E. Thus, the optimum between higher sialic acid labeling and non-toxicity can be seen from complex E. After that, the protection starts decreasing with the least from complex G.

Again, broader trends can be observed from the data, at lower concentrations (1 $\mu$ M, 3 $\mu$ M, 5 $\mu$ M), we see complexes C (17.6%), D (24.2%) and E (37.3%) show no statistical difference between one another ( $p > 0.05$ ) and offer the highest protection from A $\beta$ . Thus, this is the highest protection group of complexes. The next highest protective group is unlabeled chitosan, complex B (14.1%) and F (40.7). At all concentrations, they are statistically similar

protection from A $\beta$ . Finally, complexes A (7.8%) and G (48%) show the least protection from A $\beta$ .

At higher concentrations (10 $\mu$ M, 20 $\mu$ M, 30 $\mu$ M) again, the trend continues but with an exception. Here, the protection seen from chitosan is similar to the highest protection seen from sialic acid complexes C, D, E respectively. Earlier, we have seen that chitosan offer higher protection at higher concentration. Next highest protection is from group of complexes B and F followed by the least shown by the group of complex A (in all cases,  $p < 0.05$  compared to other groups) and complex G.

## **4. EVALUATION OF SIALIC ACID-ANALOGS FOR THE ATTENUATION OF AMYLOID-BETA TOXICITY**

### **4.1. Introduction**

Alzheimer's disease (AD) is the most common neurodegenerative disorder that affects almost 5.4 million individuals in the United States alone [245]. The brains of AD patients are characterized by the presence of extracellular senile plaques and neurofibrillary tangles. The senile plaques are composed primarily of the beta-amyloid peptide ( $A\beta$ ), and it is hypothesized that  $A\beta$  plays a crucial role in the neurodegeneration associated with AD [84, 246]. To that end, agents which either sequester  $A\beta$  or interfere with  $A\beta$  interaction/binding to cells have been sought after as a means to reduce the pathological effects of  $A\beta$  [8, 26, 156, 247].

It is generally accepted that  $A\beta$  binding to extracellular membranes is a critical step in the development of amyloidoses, including AD. There is a variety of evidence suggesting that  $A\beta$  binds to cell membranes through interaction with cell surface gangliosides or glycoproteins containing sialic acids [21, 112-114, 134, 234]. Furthermore, numerous studies have shown that  $A\beta$  binding affinity is higher when multiple sialic acids are present, either because of clustering of the gangliosides or because of the degree of sialylation of the gangliosides [8, 26, 28, 113, 118, 248]. There is increasing evidence which proves that  $A\beta$  binds to gangliosides on the neuronal membrane forming a ganglioside- $A\beta$  moiety, which further acts as an endogenous seed for amyloid fibril formation [21, 23, 31, 32, 129, 236]. However, to design smart biomimetic therapeutics for AD, it is crucial to understand which groups or subgroups within the sialic acid have the highest affinity towards  $A\beta$ . It is this kind of information that this study will try to address. In a related work, we synthesized membrane mimicking sialic acid conjugated chitosan complexes having different degrees of labeling of sialic acid and tested the ability of those

complexes to attenuate A $\beta$  toxicity in a neuroblastoma cell line. It was observed that along with the labeled compounds, naïve chitosan showed similar protective properties [249]. Therefore, the evaluation of unique sialic acid-analogs may prove to be more effective in attenuating A $\beta$  toxicity.

In the current study, four unique biological sugars (see figure 10) were conjugated to chitosan via EDC chemistry and the interactions of these complexes with A $\beta$  were studied *in vitro*. Chitosan was used as a backbone to benefit from its protective properties and the sugars selected are substructures of sialic acid (N-acetylneuraminic acid). This work addresses whether other biological sugars other than sialic acid are effective for use in the design of therapeutics for AD. Also, it will help to identify and isolate the unique –R group, or the substructure of sialic acid, which is most likely responsible for A $\beta$  toxicity attenuation. By addressing how differences in sugar structure alter the binding affinity, mechanism of A $\beta$  binding and differences in toxicity, we can contribute to develop a new class of therapeutics aimed at preventing A $\beta$  toxicity associated with AD.

## **4.2. Materials and Methods**

### **4.2.1. Materials**

A $\beta$ (1-40).HCl peptide was purchased from Anaspec Inc. (San Jose, CA). Human neuroblastoma SH-SY5Y cells were purchased from ATCC (Manassas, VA). Cell dissociation buffer and other cell culture reagents were purchased from Gibco-Invitrogen (Grand Island, NY). Chitosan powder (MW~15000, DD~84%) was purchased from Polysciences Inc. (Warrington, PA). 1-Ethyl-3-(3-dimethylaminopropyl) carbodiimide hydrochloride (EDC) and N-hydroxysulfosuccinimide (Sulfo-NHS) were purchased from Pierce Biotechnology (Rockford,

IL). The ultra-filtration membranes were purchased from Millipore (Billerica, MA). Tetrahydropyran-2-carboxylic acid (Pyran) was purchased from Ryan Scientific Inc. (Mt. Pleasant, SC). Human recombinant nerve growth factor (NGF- $\beta$ ) for SH-SY5Y, MTT (3-(4,5-dimethylthiazol-2-yl)-2,5-diphenyltetrazolium bromide), Sialic acid (N-acetylneuraminic acid), Keto-deoxynonulosonic acid (KDN), D(+)-galacturonic acid (GA), Cyclohexanecarboxylic acid (CHC), chemicals and all other reagents were purchased from Sigma-Aldrich (St. Louis, MO).

#### **4.2.2. Peptide Preparation**

Stock solutions of A $\beta$ (1-40) at concentrations of 10mg/ml were prepared by dissolving the lyophilized peptide in anhydrous dimethyl sulfoxide (DMSO). After incubating for 30min to 1h at 25<sup>0</sup>C to ensure complete dissolution, the stock solutions of A $\beta$  were diluted directly to their final concentration in sterile cell culture media and rotated at 25<sup>0</sup>C for 24h prior to the addition to the cells. This method of preparing aggregated A $\beta$  peptide has been found to yield A $\beta$  fibrils and other aggregated species that were consistently toxic to cells *in vitro* at concentrations ranging from 20 $\mu$ M to 100 $\mu$ M [8, 249, 250].

#### **4.2.3. Cell Culture**

Human neuroblastoma SH-SY5Y cells were cultured in a humidified 5% CO<sub>2</sub>/air incubator at 37<sup>0</sup>C in Minimum Essential Media (MEM), supplemented with 10% (v/v) fetal bovine serum, 2.2mg/ml NaHCO<sub>3</sub>, 100U/ml penicillin, 100 $\mu$ g/ml streptomycin and 2.5 $\mu$ g/ml amphotericin B (fungizone). SH-SY5Y cells were NGF differentiated prior to use in toxicity studies by the addition of 20ng/ml of NGF- $\beta$  to cells for 5-7 days in a 96 well plate. All the cells used in toxicity studies were under the 10<sup>th</sup> passage to ensure consistent metabolic response and stability.

#### 4.2.4. Synthesis and Purification of Sugar-Chitosan Complexes

KDN, GA, CHC, and Pyran were conjugated to chitosan using EDC chemistry following the manufacturer's suggested protocol with minor modifications. Chitosan (MW~15000, DD~84%) at a concentration of 8mg/ml, was dissolved in 1X phosphate buffer solution (PBS) and 5% HCl solution. The molar concentrations of the conjugating sugars, EDC and Sulfo-NHS were based on the theoretical calculation of the number of primary amines calculated using the degree of deacetylation (DD) and the number of glucosamine units in chitosan. In an earlier related paper, the EDC chemistry for different percentage labeling of chitosan by sialic acid was presented [249]. From that data, saturation characteristics were observed for sialic acid labeling of chitosan for the chemistry using two-fold excess of sialic acid to primary amines in chitosan with significant decrease in complex toxicity and improved protective properties. Additionally, the observed difference in labeling for four-fold chemistry and two-fold chemistry was nominal, with drastic decreased in protective properties for chemistries greater than four-fold excess[249]. Hence, for all subsequent sugars, four-fold excess of sugars were used compared to the number of primary amines in chitosan to ensure consistent degree of labeling. Thus, four fold excess molar concentration of each sugar was dissolved in 1ml of activation buffer (0.1M 2-(morpholino)ethanesulfonic acid (MES) and 0.5M NaCl at pH 6.0). To this solution, 0.362mM EDC (10 fold molar excess to the moles of primary amines in chitosan) and 5mM of Sulfo-NHS was added. The pH was maintained in-between 5.0 to 6.0 by the use of 0.1M phosphate buffer. After rotating the reaction mixture for 30min at room temperature, 1.4 $\mu$ l of 2-mercaptoethanol was added to deactivate the unreacted EDC. After stirring the mixture for 2min, 1ml of chitosan solution (8mg/ml) was added and the pH increased again by using phosphate buffer. The total reaction mixture was allowed to rotate overnight. After 24h, sample was checked for

precipitation. If observed, the resulting precipitate was dissolved by the addition of 10% (v/v) of acetic acid solution before purification.

To remove the unreacted sugars and EDC, the reaction volume was filtered using 10000 NMWL cutoff Amicon Ultra centrifugal filter unit. At least six washes of de-ionized water were performed. This ensured that the final concentration of the free sugars in the reaction mixture was less than 6% of the total sugars (free and covalently bound to chitosan). After purification, the sugar-chitosan complexes were stored at minus 4°C for later use.

#### **4.2.5. Quantification of KDN Present in KDN-Chitosan Complex**

The extent of KDN labeling of chitosan was done by the method proposed by Aminoff [251]. The following reagents were used for the test: Solution A: 25mM periodic acid in 0.125N concentrated H<sub>2</sub>SO<sub>4</sub> at pH 1.2, Solution B: 2% (w/v) solution of sodium arsenite in 0.5N HCl. Solution C: 0.1M solution of 2-thiobarbituric acid at pH 9.0 (adjusted with NaOH) in water. Solution D: 5% (v/v) solution of 12N HCl in acid butanol. Briefly, the method is as follows: In a 0.5ml sample of complex, blank or pure chitosan, 0.25ml of periodate reagent (solution A) was added, tube shaken and incubated at 37°C for 30min. Then, 0.2ml of arsenite reagent (solution B) was added and the sample stirred until the yellow color of liberated iodine disappeared. Afterwards, 2ml of thiobarbituric acid reagent (solution C) was added, the tube mixed and incubated in a boiling water bath for 7.5min. After cooling to room temperature in an ice-bath, 5ml of acid butanol (solution D) was added and the contents mixed vigorously. The sample was then centrifuged 2000g for 7min at 25°C, to extract the resulting chromophore into butanol. The absorbance of the butanol layer was measured at 549nm using a spectrophotometer within 1h.

The Aminoff procedure was performed with pure KDN solution to generate a standard curve. Pure chitosan solution was also tested to determine whether chitosan interfered with the color production. Assuming the KDN-chitosan complex was 100% labeled, a sample containing 0.3mM of KDN concentration was hydrolyzed with 0.1N HCl at 80°C for 1h before the assay. This assumption of 100% labeling was necessary to ensure that the amount of KDN in the assayed “KDN-complex sample” would fall under the range of the Aminoff assay. Three or more independent measurements were taken in each case.

#### **4.2.6. Quantification of GA Present in GA-Chitosan Complex**

The quantification of GA present on chitosan was done by the carbazole-sulfuric acid method. The following reagents were made fresh each time. Solution E: 4M sulfamic acid-potassium sulfamate at pH 1.6 (made by adding saturated KOH to sulfamic acid in water), Solution F: 0.1% (w/v) of carbazole in ethanol. The protocol is as follows: To a 0.4ml sample of complex, blank or chitosan, 40µl of sulfamic acid reagent (solution E) was added. Sample was mixed and 2.4ml of concentrated H<sub>2</sub>SO<sub>4</sub> was carefully added. After the sample reached room temperature, 100µl of carbazole reagent (solution F) was added and mixed thoroughly. Then, the open tube was placed in a boiling water bath for 20min. After cooling to room temperature, the absorbance of the sample was measured at 525nm using a spectrophotometer.

The assay was run with pure GA for the standard curve. Also, pure chitosan was tested for the interference with the assay. Similar assumption about 100% GA labeling was made to ensure that the amount of GA in the “GA-complex” sample would fall within the range of the carbazole-sulfuric acid assay. Hydrolysis of the GA-complex was done with 0.1N HCl at 80°C for 1h prior to its use in the assay. Three or more independent readings were taken in each case.

#### **4.2.7. MTT Toxicity Assay**

SH-SY5Y cells were plated at a density of  $2 \times 10^4$  cells/well in 96 well plates and then NFG differentiated for 5-7 days. After differentiation, the cell medium was replaced with medium containing NGF to which the compounds to be tested was added, either A $\beta$ , chitosan, sugar-chitosan complex or a combination of the above. Aggregated A $\beta$  peptide at a concentration of 50 $\mu$ M was prepared as per the methods described earlier and fresh stock solutions were used each time. In all experiments, A $\beta$  was added to the cells approximately 30min prior to the addition of chitosan or sugar-chitosan complexes. A gradient of chitosan and sugar-chitosan complexes from 0 $\mu$ M to 50 $\mu$ M was applied on the 96 well plates. The plates were incubated in a humidified 5% CO<sub>2</sub>/air incubator at 37<sup>0</sup>C for 24h. The viability of the cells were determined by using the MTT (3-(4,5-dimethylthiazol-2-yl)-2,5-diphenyltetrazolium bromide) assay. The media in the wells was then replaced with 100 $\mu$ l of culture media without phenol red. 10 $\mu$ l of freshly prepared MTT solution in culture media without phenol red (5mg/ml) was added to all the wells. After incubation for 2h, the wells were checked for purple crystals and the media replaced with 200 $\mu$ l of DMSO. After 20min on the shaker, absorbance at 570nm and 690nm was measured using a standard microplate reader. Normalized viability values were obtained by dividing the percentage of viable cells in the sample by that of in the control samples with no A $\beta$  or other compound added [249, 252, 253].

#### **4.2.8. Verification of Sugar Conjugation to Chitosan**

The presence of sugars on chitosan was verified using Thermo Electron Nicolet 380 FTIR with Smart Orbit attachment (Thermo Electron Corporation, Waltham, WA). All of the sugar-chitosan complexes synthesized were lyophilized using a Labconco FreeZone 1 Liter Benchtop Freeze

Dry system. The lyophilized powders were stored at  $-4^{\circ}\text{C}$  for further use. For the FTIR of chitosan, lyophilized powder obtained directly from the manufacturer was used.

#### **4.2.9. Statistical Analysis**

We used ANOVA followed by the Tukey's test for the complete analysis of the intrinsic toxicity and  $\text{A}\beta$  studies data. The results were significant if  $p < 0.05$ . Detailed statistical analysis of the results is presented after results and discussion section. The p-values for every comparison are given in the appendix.

### **4.3. Results and Discussion**

#### **4.3.1. Verification of Sugar Conjugation to Chitosan**

Multibounce FTIR was used to verify successful attachment of sialic acid-analog to the chitosan backbone. The solid blue line in each FTIR spectra represents pure chitosan, while the dashed red line represents sugar chitosan complex. Each Figure represents a different analog-chitosan complex, Figure 45: Keto-deoxynonulosonic acid (KDN) complex and unlabeled chitosan, Figure 46: D(+)-galacturonic acid (GA) complex and unlabeled chitosan, Figure 47: Tetrahydropyran-2-carboxylic acid (Pyran) complex and unlabeled chitosan and Figure 48: Cyclohexanecarboxylic acid (CHC) complex and unlabeled chitosan, respectively. The spectra indicate successful conjugation of chitosan by all complexes. This is evident by the loss of the amine doublet at  $3300\text{ cm}^{-1}$  due to amide bond formation, the presence of broad amide stretch at  $3300\text{ cm}^{-1}$  and the appearance of strong double peaks at  $1500 - 1700\text{ cm}^{-1}$  due to the formation of the amide linkage. Also, loss of carboxylic acid group which shows a peak around  $\sim 1800\text{ cm}^{-1}$  is not seen indicating that the sugars have coupled to chitosan via formation of amide linkage.

Other spectral changes are unique to each compound and are used for qualitative verification only.

The FTIR spectra verify that the conjugation was successful in the conjugation of sugars to chitosan. This is significant in that it validates the EDC technique for future works. While FTIR is not quantitative as performed, the qualitative use of FTIR for this technique supports the assertion that the conjugation chemistry was successful.

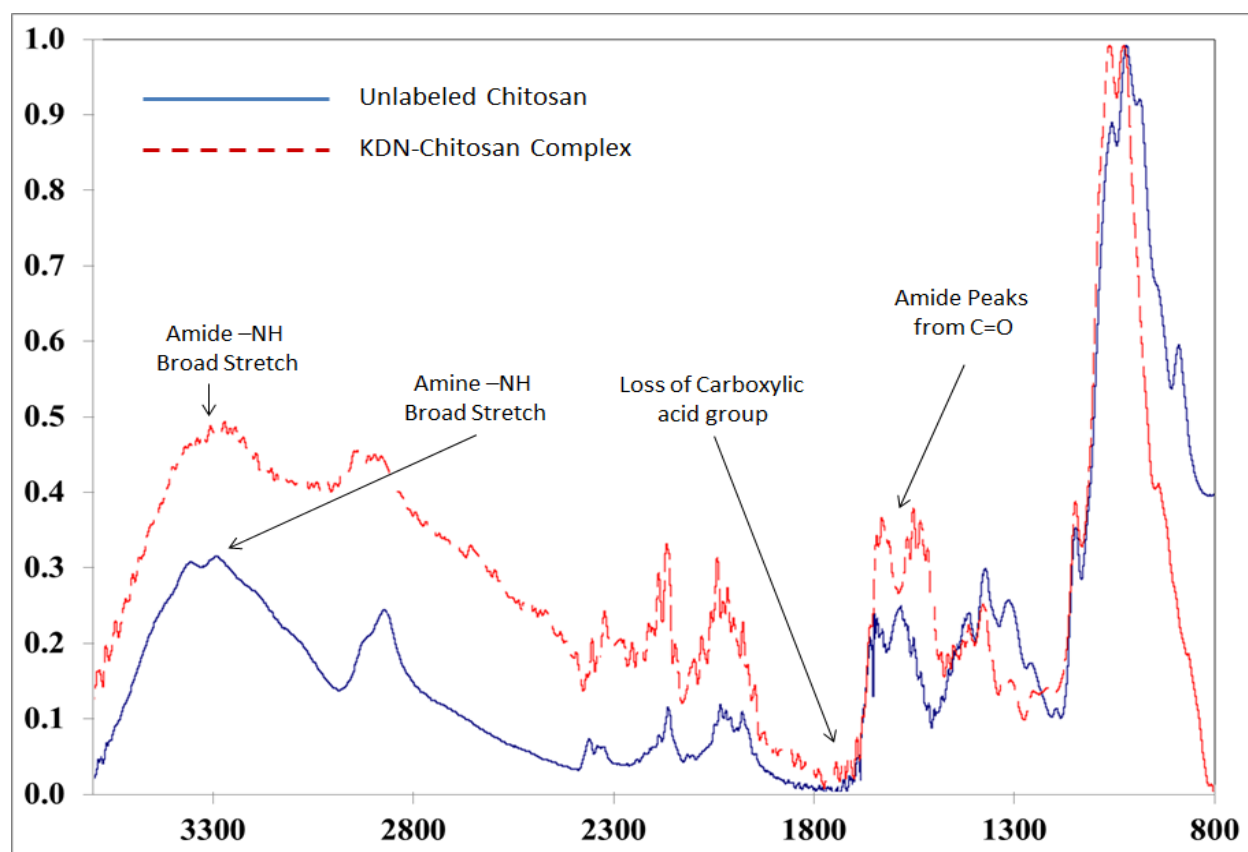


**Figure 45: FTIR spectra for unlabeled chitosan (solid blue line) and KDN-chitosan complex (dashed red line)**

Spectral regions of interest: Increases at 1500 to 1700 cm<sup>-1</sup> indicates formation of amide linkage, loss of doublet at 3300cm<sup>-1</sup> indicates disappearance of amines, broad stretch around 3300cm<sup>-1</sup> indicates presence of amide linkage

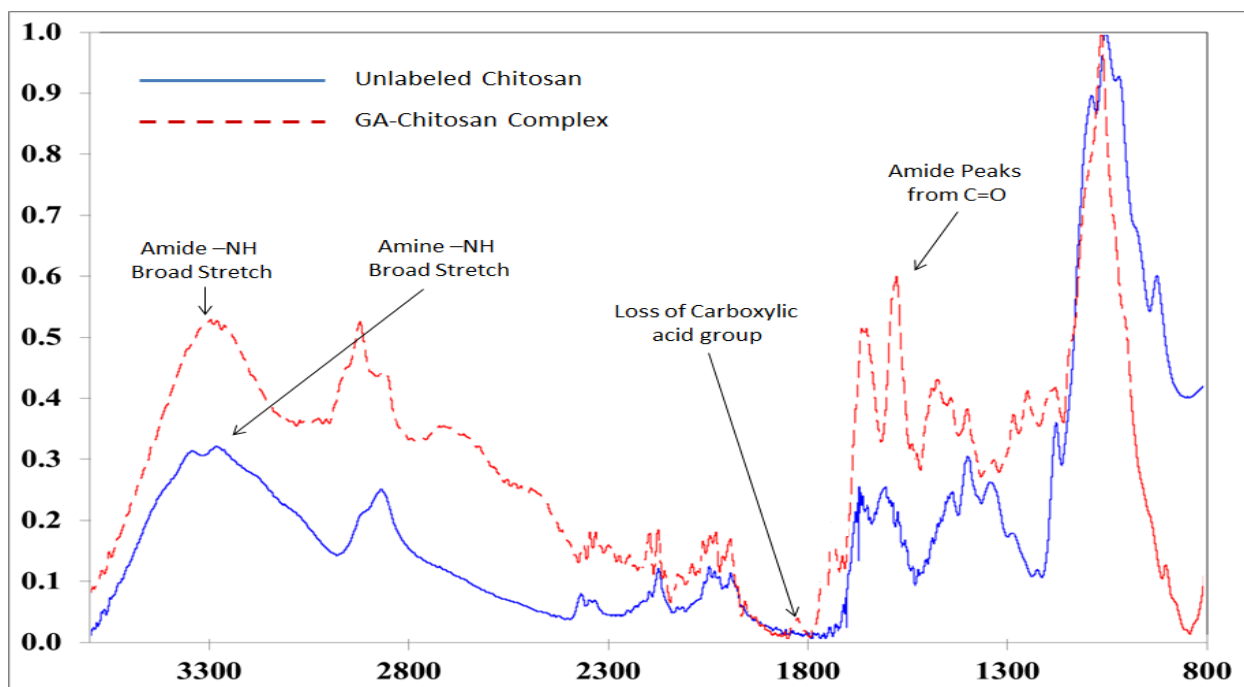


**Figure 46: FTIR spectra for unlabeled chitosan (solid blue line) and GA-chitosan complex (dashed red line)**

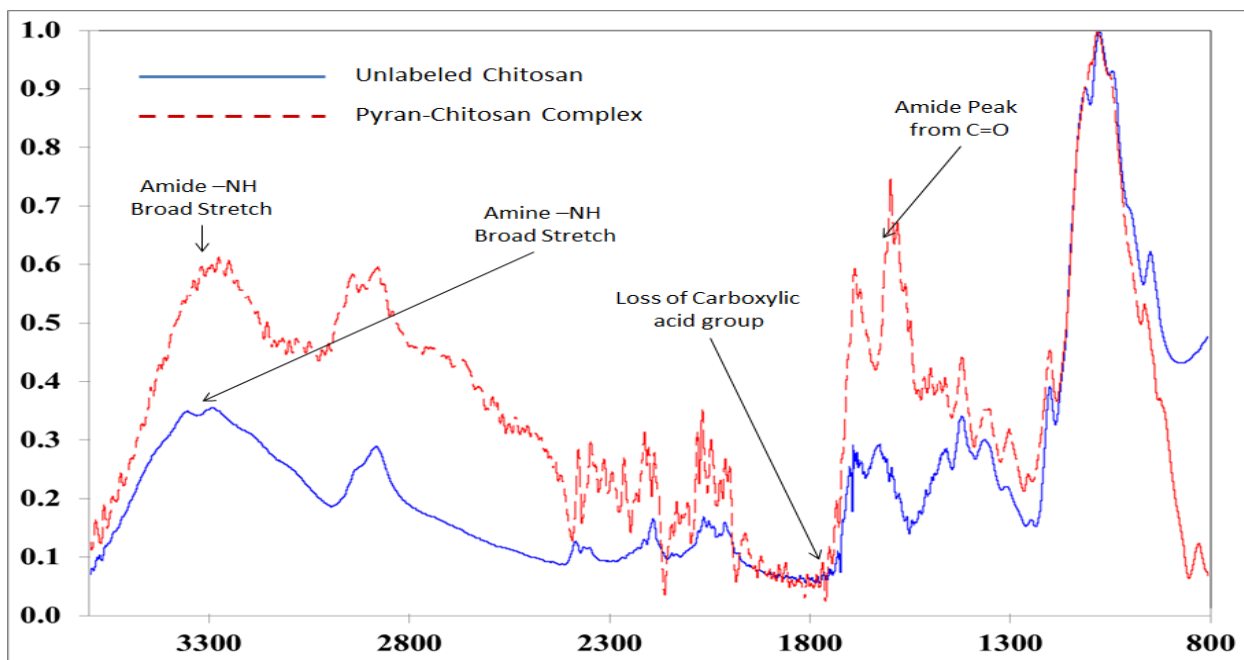


**Figure 47: FTIR spectra for unlabeled chitosan (solid blue line) and Pyran-chitosan complex (dashed red line)**

Spectral regions of interest: Increases at 1500 to 1700  $\text{cm}^{-1}$  indicates formation of amide linkage, loss of doublet at  $3300\text{cm}^{-1}$  indicates disappearance of amines, broad stretch around  $3300\text{cm}^{-1}$  indicates presence of amide linkage

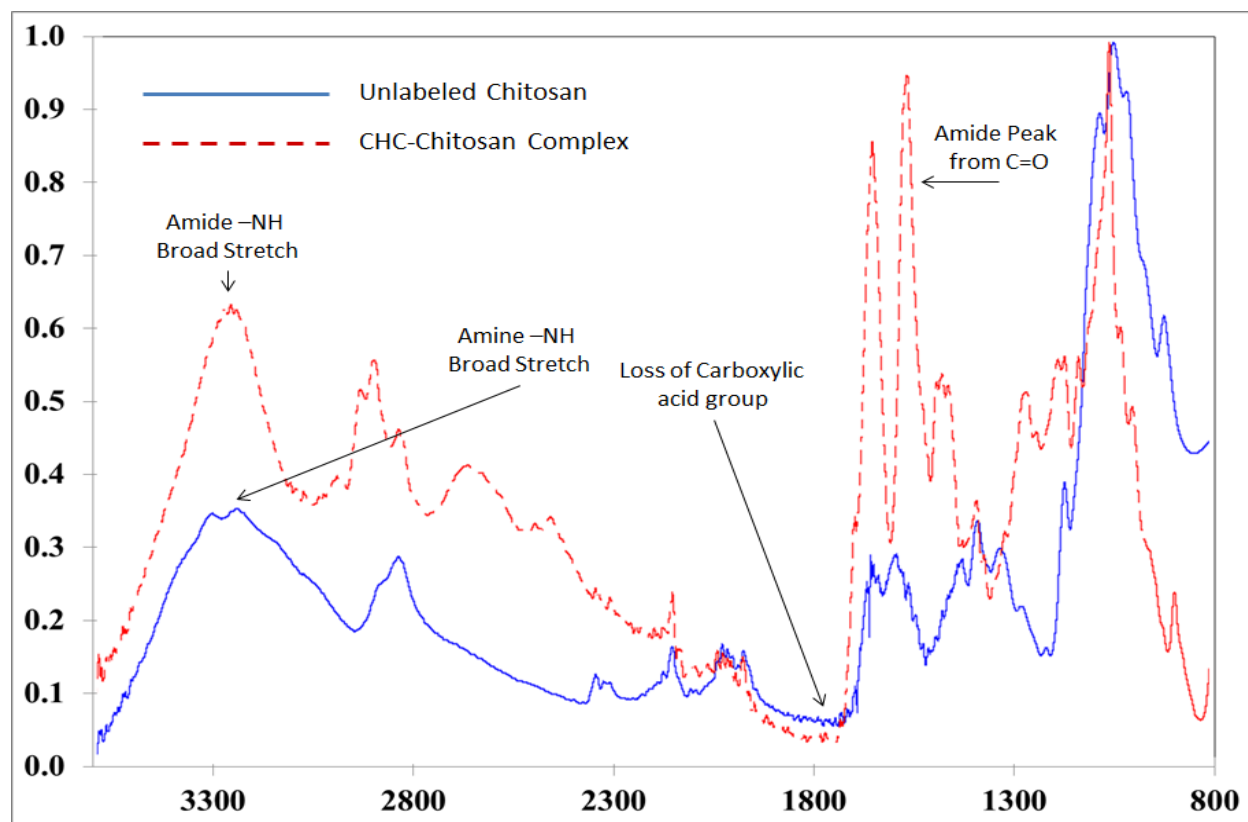


**Figure 48: FTIR spectra for unlabeled chitosan (solid blue line) and CHC-chitosan complex (dashed red line)**

Spectral regions of interest: Increases at 1500 to 1700  $\text{cm}^{-1}$  indicates formation of amide linkage, loss of doublet at 3300  $\text{cm}^{-1}$  indicates disappearance of amines, broad stretch around 3300  $\text{cm}^{-1}$  indicates presence of amide linkage

#### 4.3.2. Quantification of Sugar Conjugation to Chitosan

The results for pure chitosan in the carbazole-sulfuric acid assay and Aminoff assay were negative implying that chitosan did not interfere with the assays (results not shown). Figure 49 shows the results of the Aminoff assay for KDN quantification. Solid diamonds indicate the standard curve from pure KDN whereas an open crossmarker shows the quantification of KDN present in the 4-fold KDN-chitosan complex. Figure 50 represents the results for the GA quantification using the Carbazole-sulfuric acid assay. Solid diamonds represent the standard curve of pure GA and open cross marker indicates the sample of GA-chitosan complex

quantified. The standard curves are useful to calculate the degree of labeling of chitosan by KDN and GA. The degree of labeling was calculated by dividing the observed absorbance of the complex sample by the calculated absorbance of the sample with 100% labeling of the amine terminals of chitosan by the sugars assayed (based on the standard curve). The Warren assay was used to quantify sialic acid labeled to chitosan [241]. The percentage labeling of chitosan by sialic acid, KDN and GA by EDC chemistry is shown in Table 9.

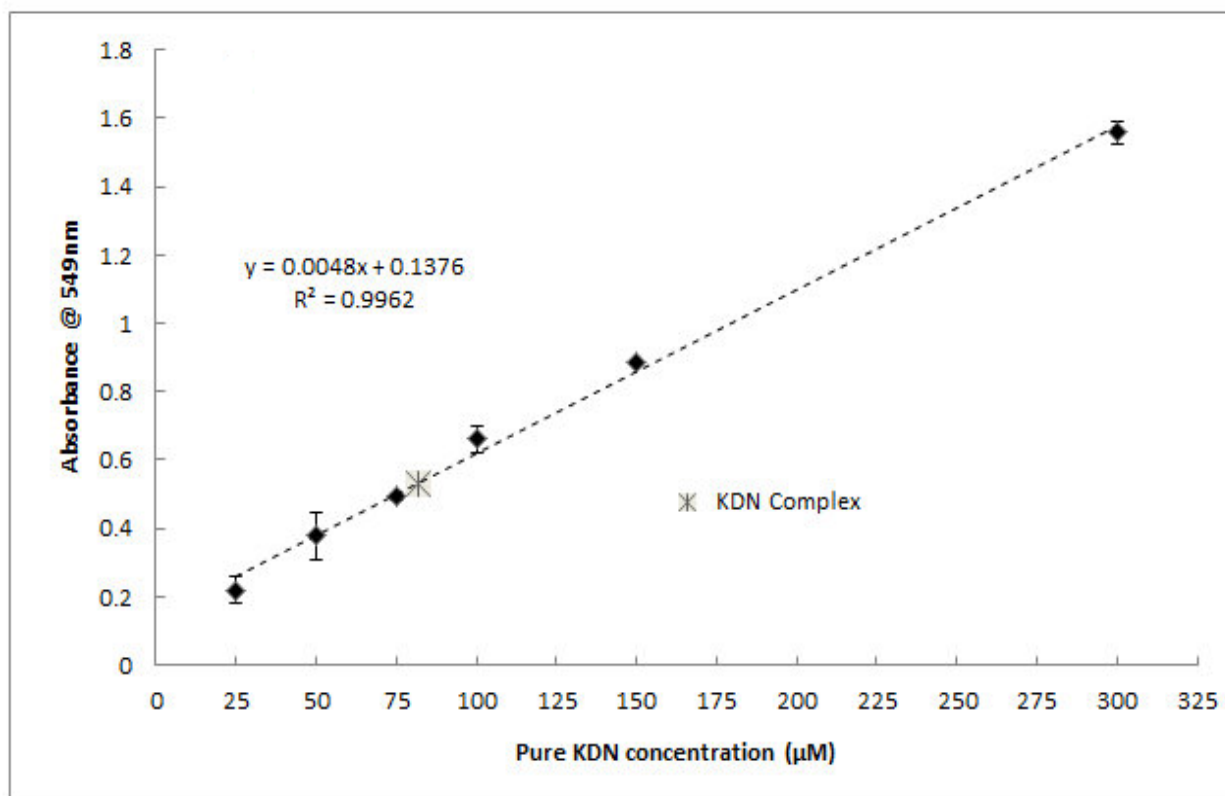


**Figure 49: Results for the quantification of Keto-deoxynonulosonic acid (KDN)-chitosan complex**

The Aminoff assay is used for KDN quantification. Filled diamonds represent the standard curve from pure KDN assay. Open cross marker represents the KDN-complex quantified using Aminoff assay. Data is represented as mean  $\pm$  SD, n=3

**Table 9: Percentage labeling of chitosan by different sugars**

Complex	[Sugar]:[Primary Amine] in reaction solution	Degree of labeling of chitosan
Sialic acid-chitosan[249]	4:1	40.70 ± 1.4
KDN-chitosan	4:1	34.13 ± 2.23
GA-chitosan	4:1	35.69 ± 1.766

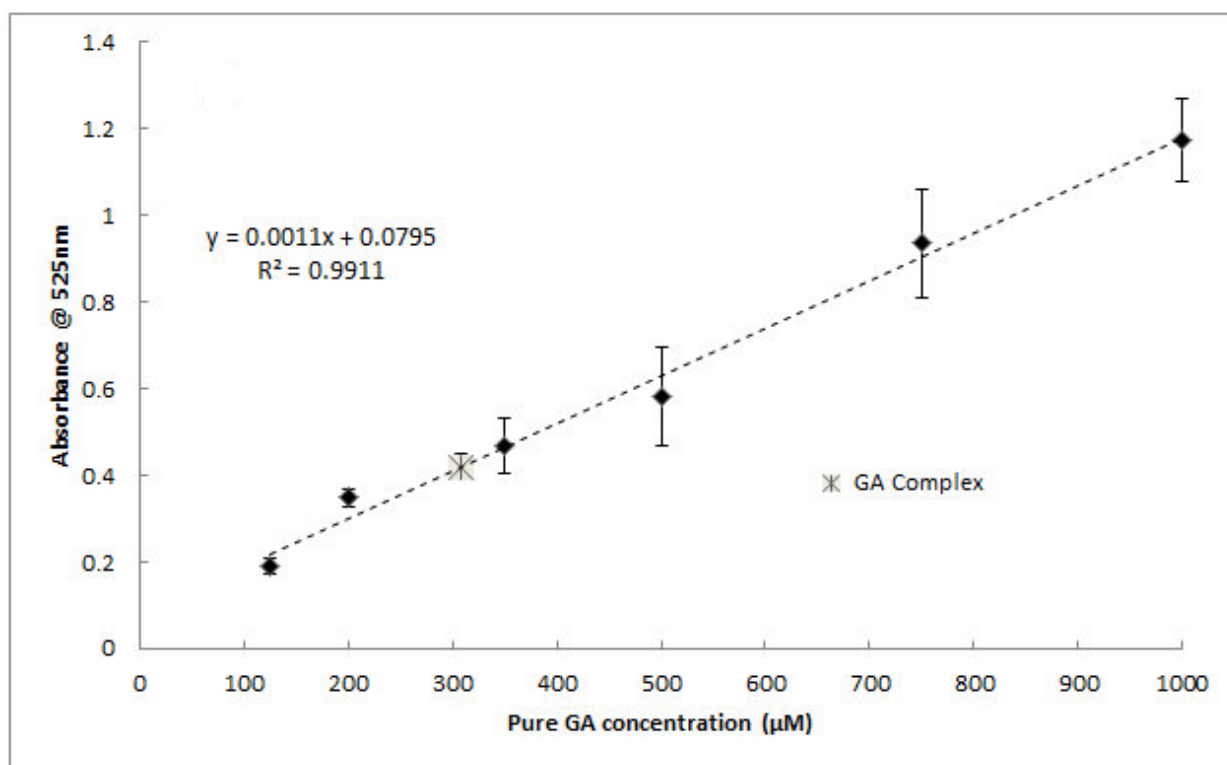


**Figure 50: Results for quantification of Galacturonic acid (GA)-chitosan complex**

The carbazole-sulfuric acid assay is used for GA quantification. Filled diamonds represent the standard curve from pure GA assay. Open cross marker indicates GA-complex quantified. Data is represented as mean ± SD, n=3.

The results from Table 9 indicate that all the three sugars quantified show around 35-40% labeling of chitosan when using the 4:1 ratio of sugars to primary amines in the reaction mixture. It is also evident that EDC chemistry can be used with sufficient accuracy to achieve the desired percentage labeling of chitosan primary amines. For the CHC and Pyran complexes, all attempts to verify the 35%-40% labeling have met with little to no success. Techniques that were attempted include colorimetric (total carbohydrate) assays, MALDI-TOF, NMR, Flame elemental analysis, HPLC-MS and XPS. Nevertheless, as seen from figure 10, the structures of CHC and Pyran attached to chitosan are very similar to that of GA that has been quantified. Thus, a reasonable assumption can be made that the remaining two complexes, CHC and Pyran, have around 35% to 40% labeling.

#### **4.3.3. Intrinsic Toxicity of Sugar Analogs and Sugar-Chitosan Complexes**

MTT was used to determine the toxicity of analogs and complexes developed. The intrinsic toxicity of pure sugar analogs on SH-SY5Y viability are shown in figure 51. The intrinsic toxicity of various sugar-chitosan complexes on SH-SY5Y viability are shown in figure 52. The toxicity values were normalized to the live control containing no analog or complex. The bar at 0 $\mu$ M represents the live control with 100% cells. We observed that KDN and CHC display no toxicity, but, GA and Pyran exhibit toxicity towards SH-SY5Y cells. The range of toxicity for analogs ranged from no apparent toxicity (CHC) to 40% toxicity (GA). From these results, it is difficult to predict the exact mechanism of toxicity as such sugars have not been studied with neuronal cultures to the best of our knowledge.

The results of the toxicity studies for the complexes are in figure 52. CHC, KDN, and GA showed very little change in toxicity from complexation. However, Pyran showed a

significant improvement in toxicity upon complexation (decrease in toxicity). The complex toxicities are as follow:  $\text{CHC} = \text{Pyran} < \text{KDN} < \text{GA}$ . The range of complex toxicity ranged from no apparent toxicity (CHC and Pyran) to 40% toxicity (GA). More detailed explanation for these results is presented in the statistical analysis section.

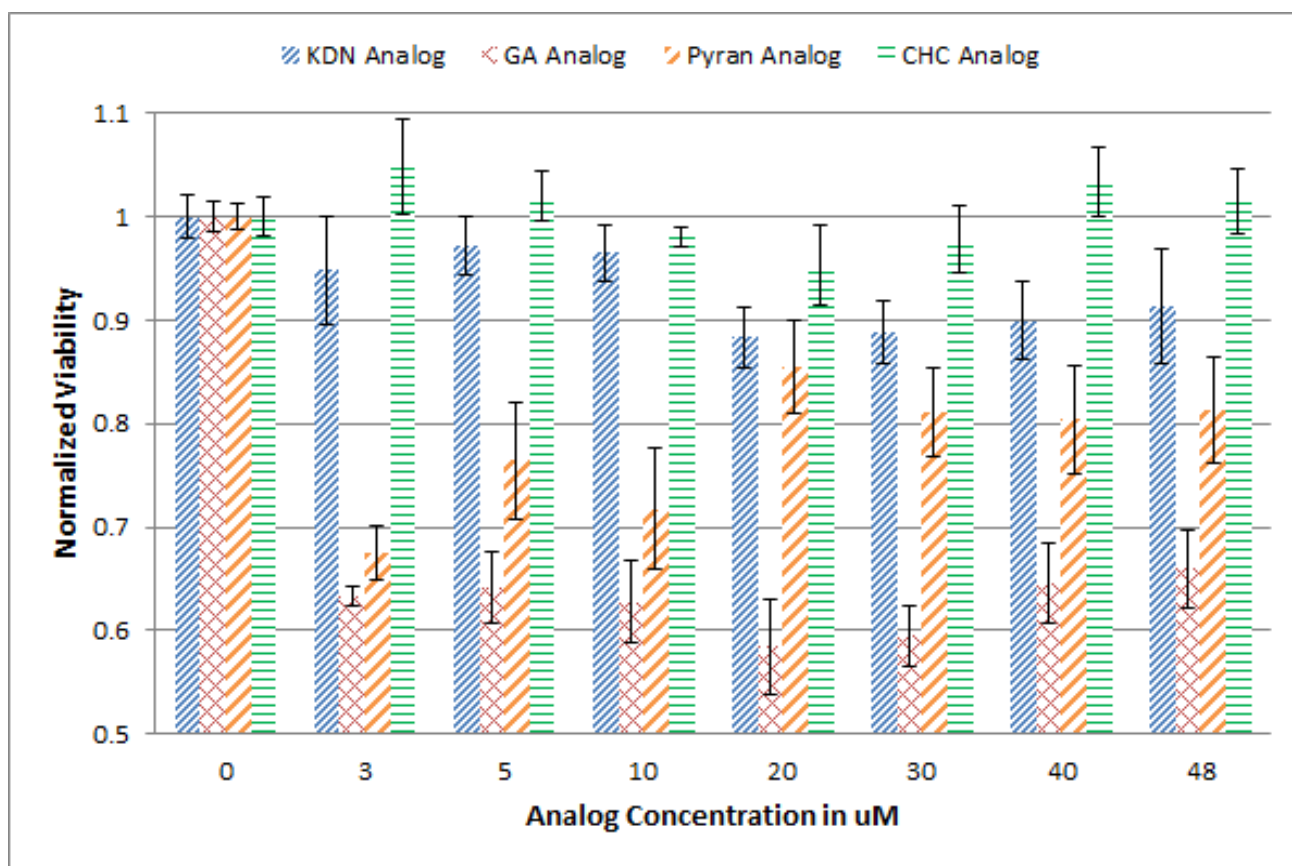


**Figure 51: Toxicity of sugar-analogs exposed to SH-SY5Y**

Results of SH-SY5Y viability when exposed to pure sugar analogs. Figure contains results for pure compounds, Keto-deoxynonulosonic acid (diagonal bar), D(+)-galacturonic acid (open diamond bar), Tetrahydropyran-2-carboxylic acid (wide diagonal bar), Cyclohexanecarboxylic acid (horizontal bar). The 0 $\mu$ M concentration represents the normalized control viability with no analogs in the system. Error bars represent mean  $\pm$ SD and n=4 in each case.

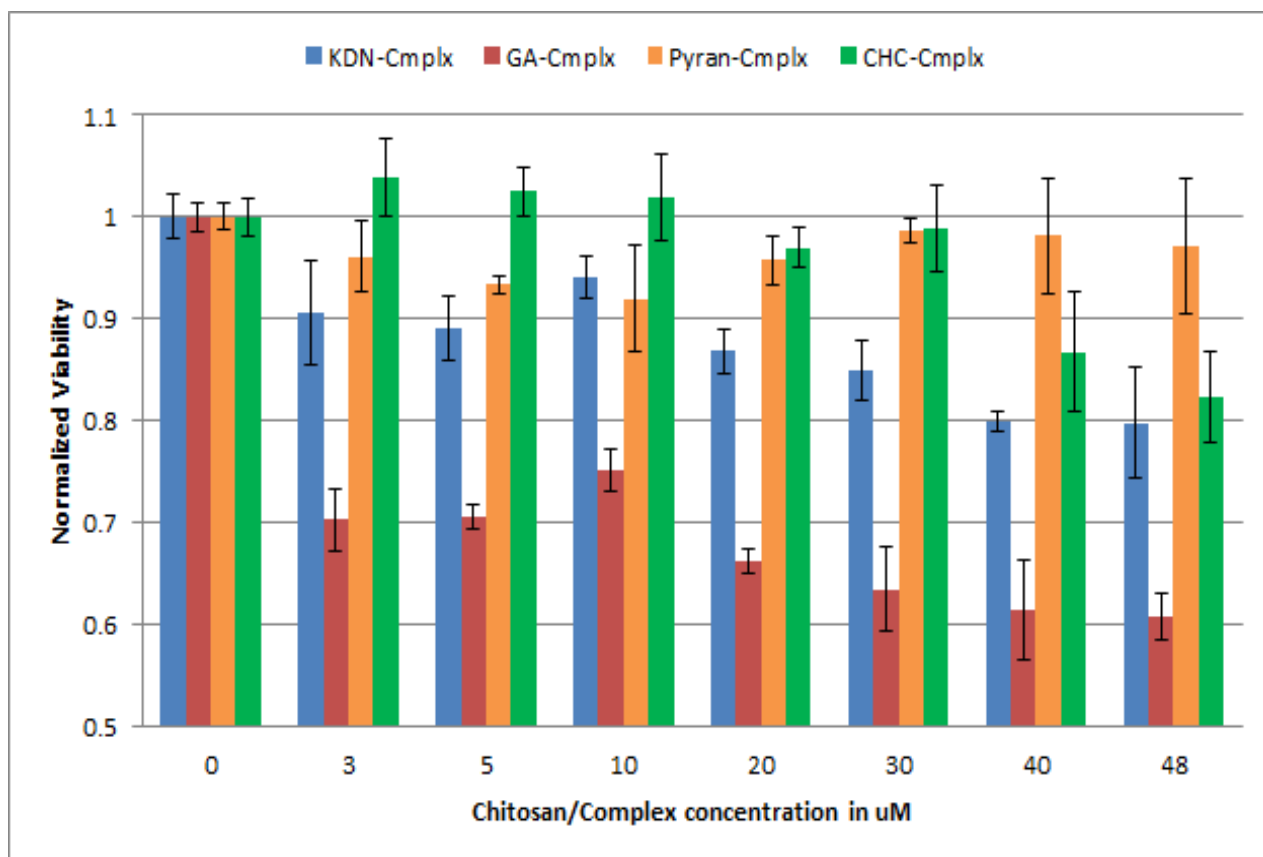
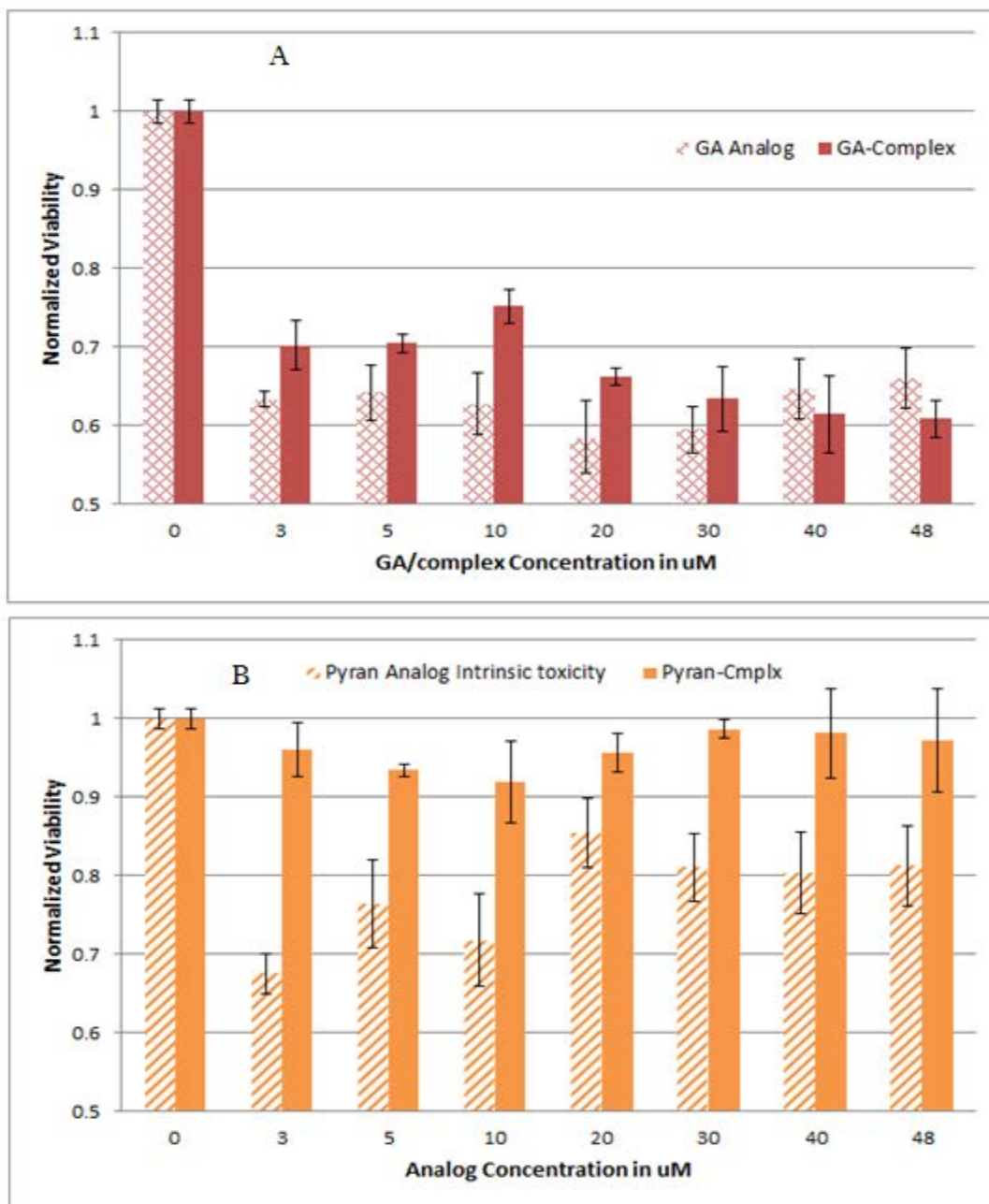


**Figure 52: Toxicity of sugar-chitosan complexes exposed to SH-SY5Y**

Results of SH-SY5Y viability when exposed to sugar-complexes, Figure contains results for pure compounds, Keto-deoxynonulosonic acid (Blue bar), D(+)-galacturonic acid (red bar), Tetrahydropyran-2-carboxylic acid (orange bar), Cyclohexanecarboxylic acid (green bar). The 0 $\mu$ M concentration represents the normalized control viability with no complex in the system. Error bars represent mean  $\pm$ SD and n=4 in each case.

When comparison is made to the control values, only CHC showed no intrinsic toxicity. This is significant in that the CHC and Pyran only differ by the presence of the oxygen substitution in the ring structure (present in Pyran), indicating that this oxygen substitution is an important factor in toxicity. Another comparison between GA and KDN shows a similar phenomenon with respect to the multi-OH tail. The loss of -OH tail found in KDN but not in GA leads to a significant increase in intrinsic toxicity. This indicates that such decoration of a therapeutic may be necessary to prevent toxicity and address its therapeutic effects. The same

argument can be made for avoiding the oxygen substitution in the core ring. It is this type of structural impact information that we were attempting to understand and elucidate.



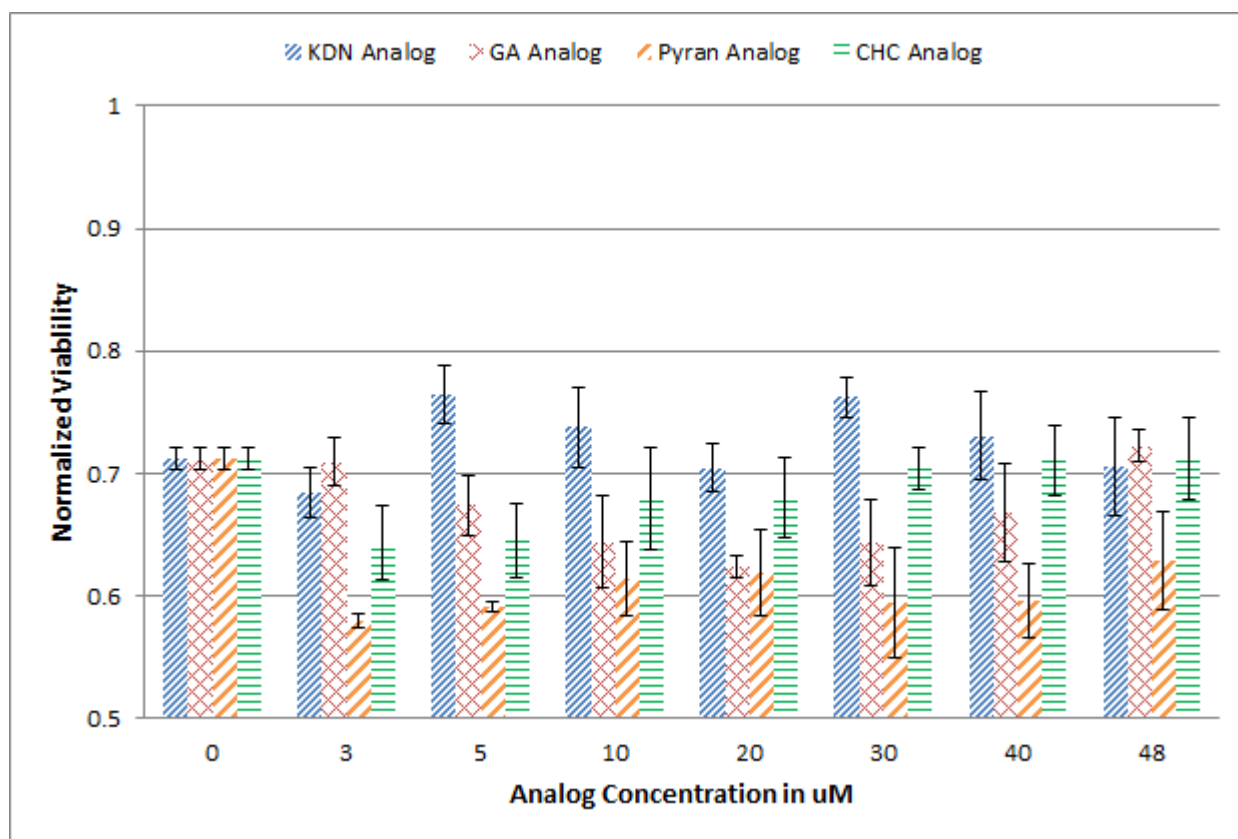
**Figure 53: Comparison of the intrinsic toxicity before and after complexation of sugars**

Figure (53.A.) show the results of the intrinsic toxicity of GA analog and GA-chitosan complex compared together. Figure (53.B.) shows the result of the intrinsic toxicity of Pyran analog and Pyran-chitosan complex compared together. Results show toxicity of Pyran analog is attenuated in the Pyran-chitosan complex after conjugation.

Another interesting observation was seen when the intrinsic toxicities of the sugar were compared before and after complexation. As seen from the figure below (figure 53), GA analog is toxic to SH-SY5Y cells and so is the GA-chitosan complex. This indicates that the toxicity of GA is maintained even after complexation. We have already tested chitosan toxicity and seen that chitosan is a non-toxic backbone. On the other hand, comparing the intrinsic toxicities of Pyran analog before and after complexation presents us with a different picture. It is observed that the viabilities of Pyran-complex are higher than the viabilities of Pyran-analog at all concentrations studied (in all cases,  $p < 0.05$ ). As it is evident, Pyran analog was toxic to cells, whose toxicity is attenuated after complexation with chitosan backbone. This provides an important observation that the toxicity of compounds could be attenuated after complexation. This also indicates that we are not limited to just biological sugars and it is possible that a potentially know toxic compound can now the complexed and the toxicity attenuated.

#### **4.3.4. Efficacy of Sugar Analogs and Sugar-Chitosan Complexes to Attenuate A $\beta$ Toxicity**

MTT was used to determine the ability of the compounds to attenuate A $\beta$  toxicity of analogs and complexes developed. The toxicity values were normalized to the control containing 50 $\mu$ M A $\beta$  with no analog or complex. The dashed line represents the A $\beta$  control value used for normalization. Figure 54 shows the ability of the pure sugar analogs to attenuate the toxicity of 50 $\mu$ M aggregated A $\beta$ (40). The analogs, as a group, showed no significant ability to attenuate A $\beta$  toxicity. The results of the attenuation studies for the sugar-chitosan complexes are in Figure 55.



**Figure 54: Attenuation of 50 $\mu$ M A $\beta$  toxicity by sugar analogs**

Results of SH-SY5Y viability when exposed to sugar analogs and 50 $\mu$ M A $\beta$  in media. Figure contains results for pure compounds, Keto-deoxynonosonic acid (diagonal bar), D(+)-galacturonic acid (open diamond bar), Tetrahydropyran-2-carboxylic acid (wide diagonal bar), Cyclohexanecarboxylic acid (horizontal bar). The 0 $\mu$ M analog concentration represents the viability with 50 $\mu$ M A $\beta$ (40) and no analogs in the system. Error bars represent mean  $\pm$ SD and n=4 in each case.

The result from the KDN analog A $\beta$  attenuation study indicate that, statistically, none of the viabilities at any concentrations studied are significantly different from the viability obtained from A $\beta$  control (71% viability). This analysis indicates that KDN-analog does not have any protective effect on cells from the toxic A $\beta$ . From the study of Pyran analog with 50 $\mu$ M A $\beta$ , it can be seen that the viabilities of the wells treated with Pyran are statistically lower compared to the A $\beta$  control. Similarly, at all concentration of GA analog studied, we see a decrease in viabilities and thus, no protection can be seen from A $\beta$ . The toxicity towards the cells is most

likely the combination of aggregated A $\beta$  and GA together. The addition of CHC analog at any concentration does not show any protective effect on SH-SY5Y viability. At all concentrations, the means were not statistically different from the A $\beta$  control (in all cases,  $p > 0.05$ ).

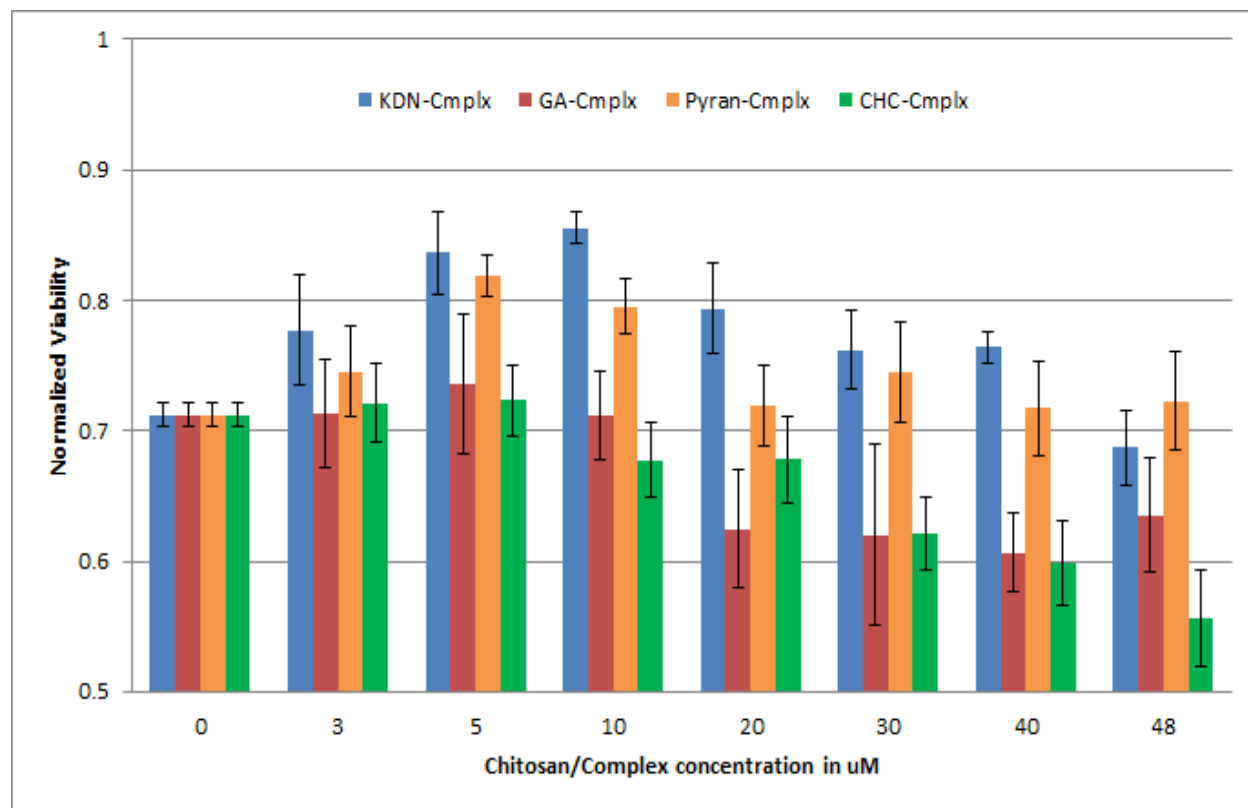


**Figure 55: Attenuation of 50 $\mu$ M A $\beta$  toxicity by sugar-chitosan complexes**

Results of SH-SY5Y viability when exposed to sugar-complexes and 50 $\mu$ M A $\beta$  in media. Figure contains results for pure compounds, Keto-deoxynonulosonic acid (Blue bar), D(+)-galacturonic acid (red bar), Tetrahydropyran-2-carboxylic acid (orange bar), Cyclohexanecarboxylic acid (green bar), The 0 $\mu$ M chitosan/complex concentration represents the viability with 50 $\mu$ M A $\beta$ (40) and no complex in the system. Error bars represent  $\pm$ SD and  $n=4$  in each case.

It can be seen that the viability of SH-SY5Y cells increase after the addition of KDN-chitosan complex which indicates protection from the complex. For the KDN-complex, the highest protection can be seen at concentrations of 5 $\mu$ M, 10 $\mu$ M and 20 $\mu$ M. Other concentrations also show protection and the protection increases and then decreases at higher concentrations. It is difficult to compare KDN-complex with sialic acid complex as there is a difference in the

values of A $\beta$  control. GA-complex does not show any protective properties at all concentrations studied. At 3 $\mu$ M to 10 $\mu$ M, the viabilities are not different than that of A $\beta$  control and then the viability decreases. From the results of Pyran-chitosan complex shown in figure 38, we can see that the complex offers protection from A $\beta$ . Highest protection can be seen from 5 $\mu$ M and 10 $\mu$ M concentration of the complex. CHC-complex offers no protection from A $\beta$  and the viability decreases as the concentration of complex increases. None of the viabilities at any concentrations are statistically higher compared to those of the A $\beta$  control.

The two complexes, KDN-complex and Pyran-complex showed significant protective properties, while CHC and GA complexes showed no attenuation. Levels of toxicity attenuation of complexes were as follows: KDN > Pyran > GA = CHC. The statistical analysis and detailed explanation for the results are in the statistical analysis section.

Since, none of the sugar analogs by themselves showed any significant levels of A $\beta$  toxicity attenuation, it supports the works of previous investigators including ourselves that the clustering of sugars in the cellular membrane plays a significant role in A $\beta$  binding [8, 26, 162, 235, 248, 249, 254]. However, the effectiveness of complexes is more pronounced. Using the same KDN/GA comparison from the previous section, the role the multi -OH tail plays in the binding of A $\beta$  becomes clear. While GA complex shows no protective properties, the KDN complex exhibits the highest levels of protection. Thus, we hypothesize that the multi-OH tail is that differentiating factor and this is the target that A $\beta$  recognizes. Revisiting the Pyran/CHC comparison displays a contradictory result from the toxicity studies. While it is apparent that the oxygen substitution significantly increases toxicity, it also leads to a significant level of toxicity attenuation. These two pieces of information lead us to the belief that the oxygen ring substitution allows for either cellular or A $\beta$  binding in a competitive, interfering manner.

However, the –OH tail shows similar crossreactivity with the cells (indicated by the level of neuroprotection and toxicity). In comparison of the two compounds, it is likely that oxygen structures are the best target for future therapeutic development. Again, increasing evidence suggests that lipid-protein interactions play a crucial role in the aggregation of various amyloidogenic proteins. Thus, such kind of structural information will be useful as a general guideline for researchers involved in further therapeutic development. Binding studies performed on complex will yield definite information on the affinity of A $\beta$  to these –R groups.

#### **4.4. Statistical Analysis of Intrinsic Toxicity and A $\beta$ Toxicity Attenuation Data**

Every value in the bar charts are expressed as normalized viabilities plotted on the y-axis with the test compound concentration on the x-axis. Each mean is calculated from the average of the viabilities observed from at least four replicates of each complex/compound concentration. For the statistical analysis, we are interested to understand how each compound performed at all the concentrations tested. Hence, for each compound, starting with 0 $\mu$ M concentration, the viabilities obtained at all concentrations is compared to one another. This is the statistical analysis for each compound. Similarly, at each concentration, we wanted to compare the viabilities obtained from all compounds tested at that concentration. This will allow us to compare the effects of different compounds at the same concentration. This is the statistical analysis for each concentration.

As this is the case of multiple comparisons, we use ANOVA followed by a suitable post-hoc test. For the post-hoc test Tukey's Honest Significant Difference (HSD) test (shorthand "Tukey's test" in later texts) is used. For every case or comparison, we are keeping the constant error rate of  $\alpha$  equal to 0.05. All our measurements are done independently. The two important

assumptions of ANOVA test is that the population is normally distributed and the variances for all populations are equal. A sample dataset was run with the Levene's test in SAS to check for equality of variances. The output from a sample dataset is presented in the appendix. The output from Levene's test is attached in the Appendix. Thus, the homogeneity of the variance is verified and our data fits the requirements for ANOVA. However, this is a common assumptions in such kind of toxicity studies [8, 26, 162, 203, 229]. Furthermore, as a post hoc test, the analysis is done by Tukey's test. The null hypothesis is that the two means (i.e. the means of the two normalized viabilities being compared) are equal. When the null hypothesis is rejected, post hoc comparisons are done using Tukey's test to investigate further which groups/means differ.

### **Tukey's Test**

Tukey's test allows for all possible pairwise tests and is based on the studentized range statistics. It also keeps a constant experimental error rate ( $\alpha$ ) for all possible pairwise tests. The sample size is equal in Tukey's method. The differences between the means is calculated and compared to the critical value to see if the difference is significant. This critical value is the "Honestly Significant Difference" and that value is computed from SAS. The adjusted p-values for all pairwise comparisons are given in the output.

### **Guide to Interpreting the Statistical Information on the Bar Chart**

Data for normalized viability is presented as mean  $\pm$ SD of at least four replicates on the bar chart. The statistical significance of differences between groups was estimated by ANOVA. Further, any differences between the means group were analyzed by Tukey's test. Each graph shows the results and the statistical outputs obtained from the Tukey's test. Different letters across the graphs indicate statistically-significant differences ( $p < 0.05$ ); the same letter indicates

no statistical difference between those groups. This assignment of letters is done using a macro for SAS program developed by Saxton M.A [244]. This macro is run after the analysis by Tukey’s test. The macro groups similar means together and assigns a letter. The figure 56 shows the statistical analysis of the KDN-Chitosan complex intrinsic toxicity data. The table (Figure 56.A.) in the figure below shows the output from the macro by the Tukey’s test (at  $p < 0.05$ ). The means are sorted and ranked starting with the highest to the lowest mean. Each mean represents the normalized viability at each concentration of the compound studied. Using SAS, the calculation for the critical value of the “Least Significant Difference” (LSD) is done. When the analysis is done by the Tukey's test, SAS applies the adjustment on the LSD based on Tukey's test and the critical value is adjusted. The highest mean is assigned the letter group A. If the critical value of the  $LSD = “X”$ , then means below that differ by less than “X” do not differ statistically. This is represented by giving them a common letter so that they share a letter.

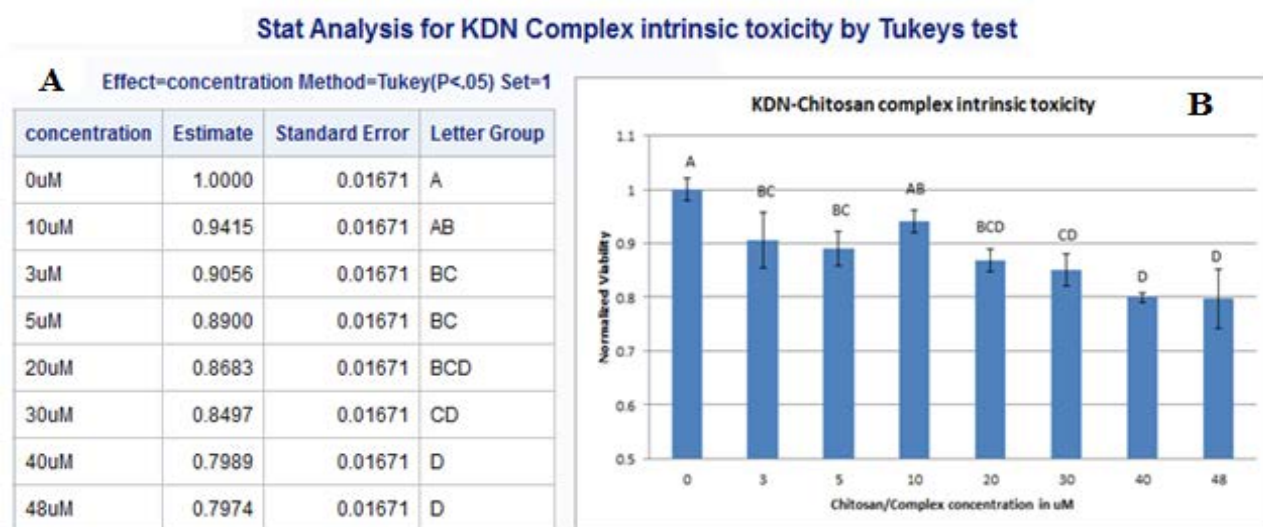


**Figure 56: Grouping example: Statistical analysis and graph for KDN-complex intrinsic toxicity data.**

The table (56.A.) represents the output using the macro which gives letter grouping for the means by Tukey’s test. The figure (56.B.) represents the normalized viabilities of KDN-complex plotted as a function of concentration. The similar letters above the bar indicate no statistical difference. Different letters indicates statistical difference at  $p < 0.05$  by Tukey’s test.

As seen from figure 56.A, the difference between the means of 0 $\mu$ M and 10 $\mu$ M is not statistically significant. This is illustrated by same letter A on 0 $\mu$ M and 10 $\mu$ M in Figure 56.B. Here, each mean is the normalized viability obtained at each concentration. Hence, they both are assigned the letter A. However, the mean of 10 $\mu$ M is less than that of the mean at 0 $\mu$ M. Hence, 10 $\mu$ M is assigned A and B (i.e. “AB”). Thus, 10 $\mu$ M indicated by “AB” is statistically the same as all other means that have the letter A or B above them. Moving on after 10 $\mu$ M, the next highest mean is 3 $\mu$ M. SAS determined that the mean of 10 $\mu$ M and 3 $\mu$ M were statistically different (working with the adjusted critical value for Tukey’s) and hence it is assigned a separate letter group “BC”. Looking at the output data in the appendix, the comparison between the 0 $\mu$ M and 10 $\mu$ M gives the p-value of 0.0106 using Tukey’s test. Coming back to 3 $\mu$ M, the letter “B” and “C” is shared with 10 $\mu$ M, 5 $\mu$ M, 20 $\mu$ M, 30 $\mu$ M. All these means do not differ statistically even if one is lower in value than the other. Looking back at the table, the normalized viability at 0 $\mu$ M is statistically different from all the viabilities at all other concentrations. Thus, means that share a letter are not statistically different. Example: As seen from figure 1-A, the normalized viability at 3 $\mu$ M (indicated by letter group “BC” is statistically different from the normalized viabilities at 0 $\mu$ M (indicated by A), 40 $\mu$ M (indicated by D) and 48 $\mu$ M (indicated by D) as given by Tukey’s test (at  $p < 0.05$ ). The comparison between each data point and the p-values obtained by Tukey’s test are attached in the appendix. Also, the output from macro is included along with the means compared in the appendix.

#### **4.4.1. Intrinsic Toxicity of Pure Sugar Analogs**

The graphs below show the intrinsic toxicity studies for pure analogs KDN, GA, Pyran and CHC tested without A $\beta$  in media. In all the graphs below, the normalized viability of 1 at 0 $\mu$ M analog concentration represents the live control with 100% cells and no other

test/experimental compound added to them. Normalized viability values at each concentration were obtained by dividing the percentage of viable cells in the sample by that in the live control samples. The results are represented as the mean  $\pm$ SD of at least four replicates. The statistical significance of differences between groups was estimated by ANOVA. Further, any differences between the means group were analyzed by Tukey's test. Different letters across the graphs indicate statistically-significant differences ( $p < 0.05$ ); the same letter indicates no statistical difference between those groups. As an example, in the plot for KDN analog intrinsic toxicity, the statistical significance of the live control at 0 $\mu$ M indicated by letter (A). All other concentrations which have the letter (A) above them are not statistically significant from one another. Thus, in this case, 3 $\mu$ M, 5 $\mu$ M 10 $\mu$ M and 48 $\mu$ M are not statistically different from 0 $\mu$ M as all those concentrations have the letter A above each of those concentrations. However, 0 $\mu$ M point is statistically different (given by Tukey's test with  $p < 0.05$ ) from viabilities at 20 $\mu$ M, 30 $\mu$ M and 40 $\mu$ M (as they do not contain the letter A). Two or more groups of letters (e.g. AB) mean that those means are statistically similar to group A as well as B (although A only and B only groups are statistically different from one another). A macro was used in SAS programming to convert similar means into groups of letters using the Tukey's test[244]. In all cases, each concentration group is compared to each other. The comparison between each data point and the p-values obtained by Tukey's test are attached in the appendix. Also, the output from macro is included along with the means compared in the appendix.

### **Statistical Analysis Done for Each Compound**

Looking at figure 57, it can be seen that KDN analogs kills no more than 12% cells at all concentrations shows compared to control. This low toxicity from KDN is expected as KDN is a biological sugar and is a member of the sialic acid family of compounds. Additionally, KDN is

also found throughout the human body. The viability is higher at lower concentrations (from 3 $\mu$ M to 10 $\mu$ M) whereas it decreases from 20 $\mu$ M to 48 $\mu$ M concentration of pure KDN.

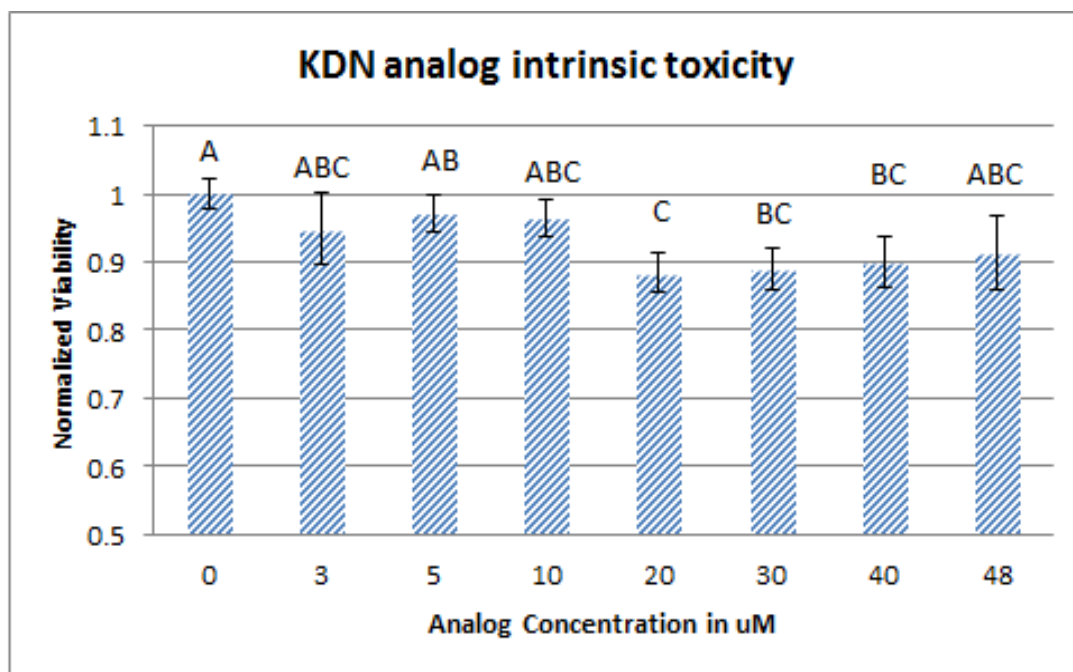


**Figure 57: KDN analog- Intrinsic toxicity studies**

Similar letters or group of letters above the bar chart indicates no statistical difference between the normalized viabilities of those concentrations as given by Tukey's test at  $p < 0.05$

From the figure 58, cells treated with GA analog at all concentrations show around ~60% viability compared to live control. The exact mode of toxicity cannot be asserted from the performed experiments. While GA has not been studied specifically with respect to a neuronal cell culture to the best of our knowledge, it is difficult to ascertain the exact mode of toxicity from this data. One interesting possibility is the significant difference between KDN and GA with respect to the multi-OH tail. Thus, the increased toxicity could be most likely attributed to the loss of multi-OH tail in GA.

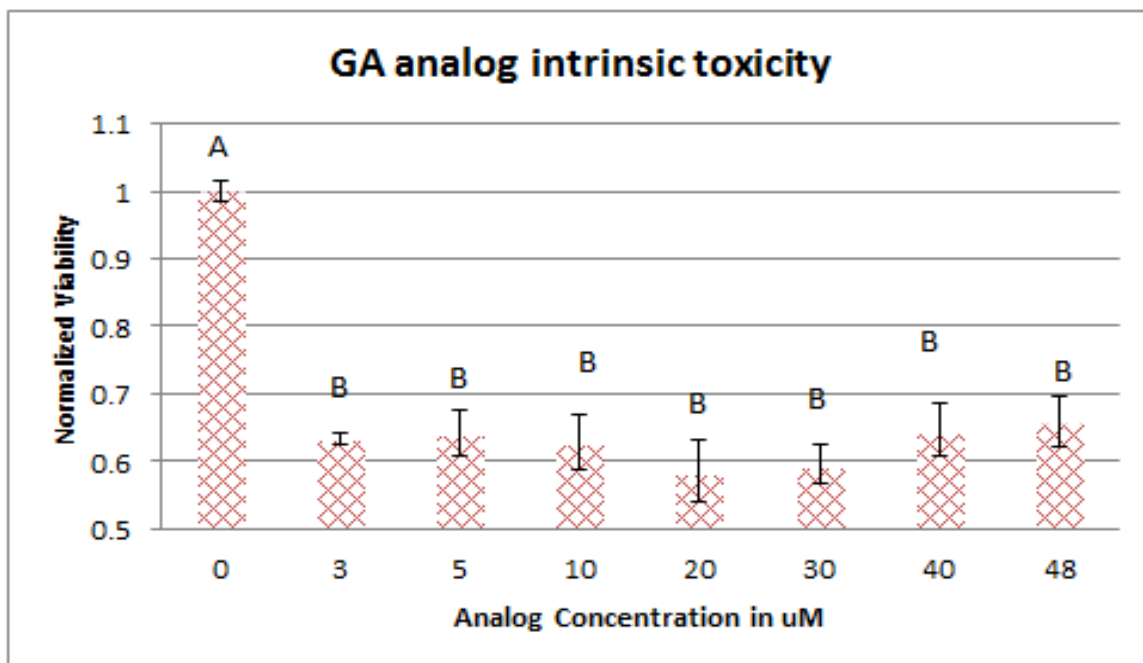


**Figure 58: GA analog- Intrinsic toxicity studies**

Similar letters or group of letters above the bar chart indicates no statistical difference between the normalized viabilities of those concentrations as given by Tukey's test at  $p < 0.05$

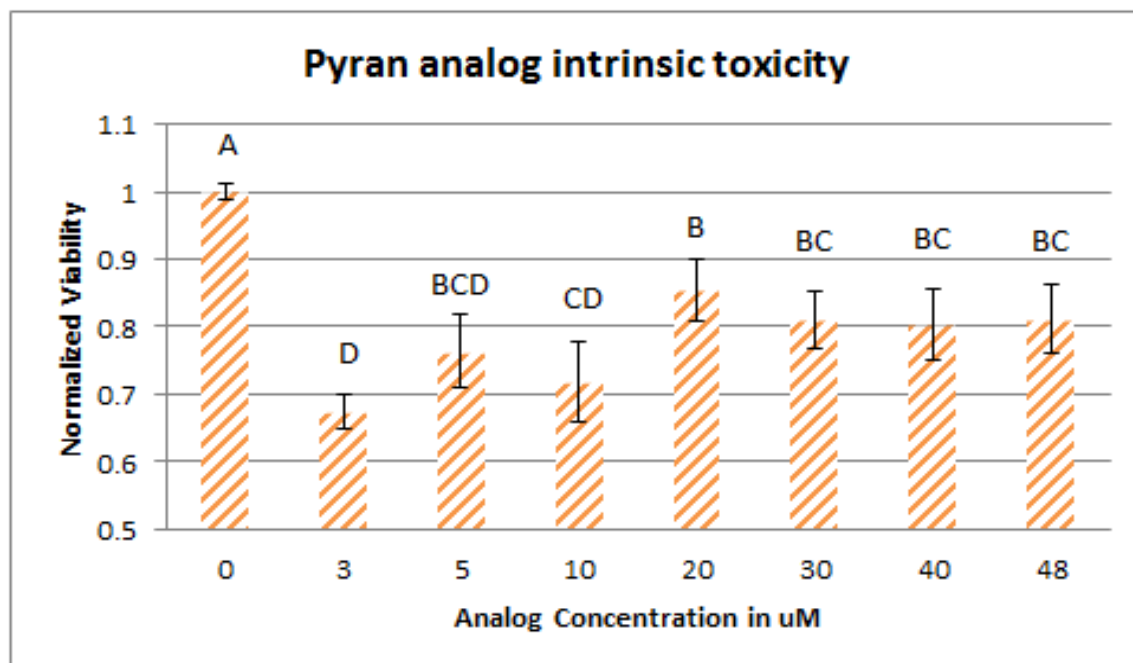


**Figure 59: Pyran analog- Intrinsic toxicity studies**

Similar letters or group of letters above the bar chart indicates no statistical difference between the normalized viabilities of those concentrations as given by Tukey's test at  $p < 0.05$

From the intrinsic toxicity of Pyran analog (figure 59), we can see that there is a drop in viability after addition of pure Pyran at all concentrations studied. The range of viability observed is from ~70% to 80%. Lowest viability is obtained at 3 $\mu$ M whereas highest is seen at 20 $\mu$ M. Again, the interaction of Pyran structure with respect to neuronal culture has not been investigated yet. One possibility is the significant similarity is the presence of oxygen substitution between the GA structure and Pyran structure (see figure 10). Also, since CHC does not show any toxicity at all concentrations, the only difference being the absence of oxygen substitution, the Pyran toxicity can be attributed to the oxygen substitution in the ring structure.

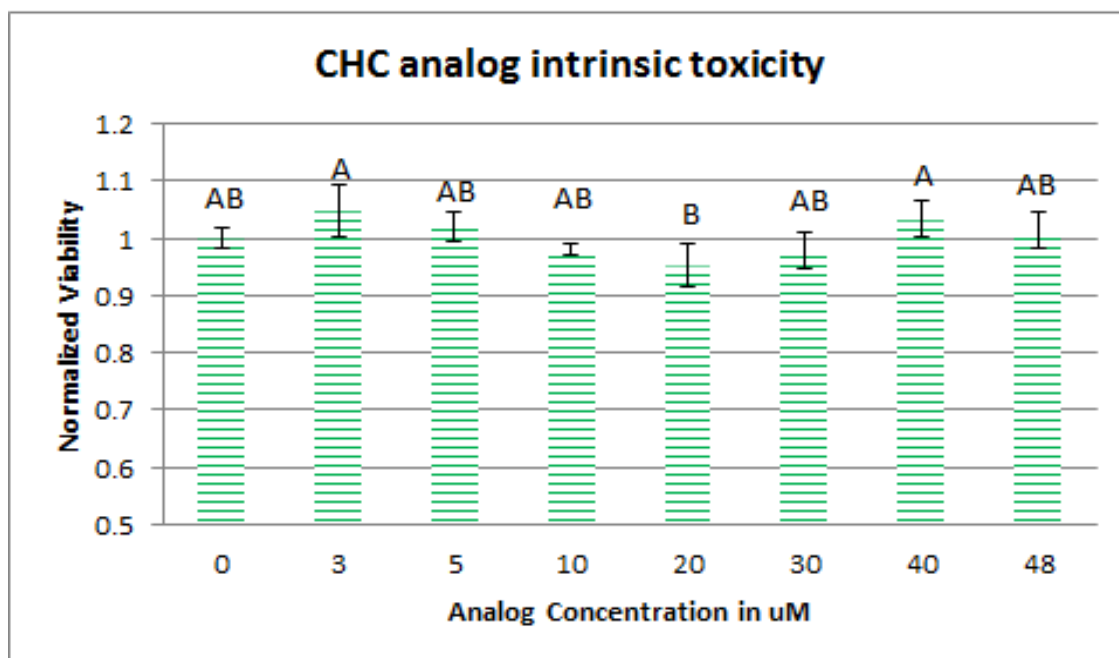


**Figure 60: CHC analog- Intrinsic toxicity studies**

Similar letters or group of letters above the bar chart indicates no statistical difference between the normalized viabilities of those concentrations as given by Tukey's test at  $p < 0.05$

The addition of pure CHC analog (figure 60) shows no toxicity towards SH-SY5Y cell culture at all concentrations studied. Again revisiting the plausible structural difference-activity explanation, the only difference in structure between CHC and Pyran is the oxygen substitution

in the ring structure. As all other conditions are the same between the two experiments, one possibility for lower viability in Pyran analog study could be that oxygen substitution in the ring structure contributes to the intrinsic toxicity.

### Statistical analysis done for each concentration

The next sets of figures (figures 61 and 62) give the statistical comparison between the four sugar analogs at a particular concentration. Thus, the four analogs are compared at concentrations from 3 $\mu$ M to 48 $\mu$ M.

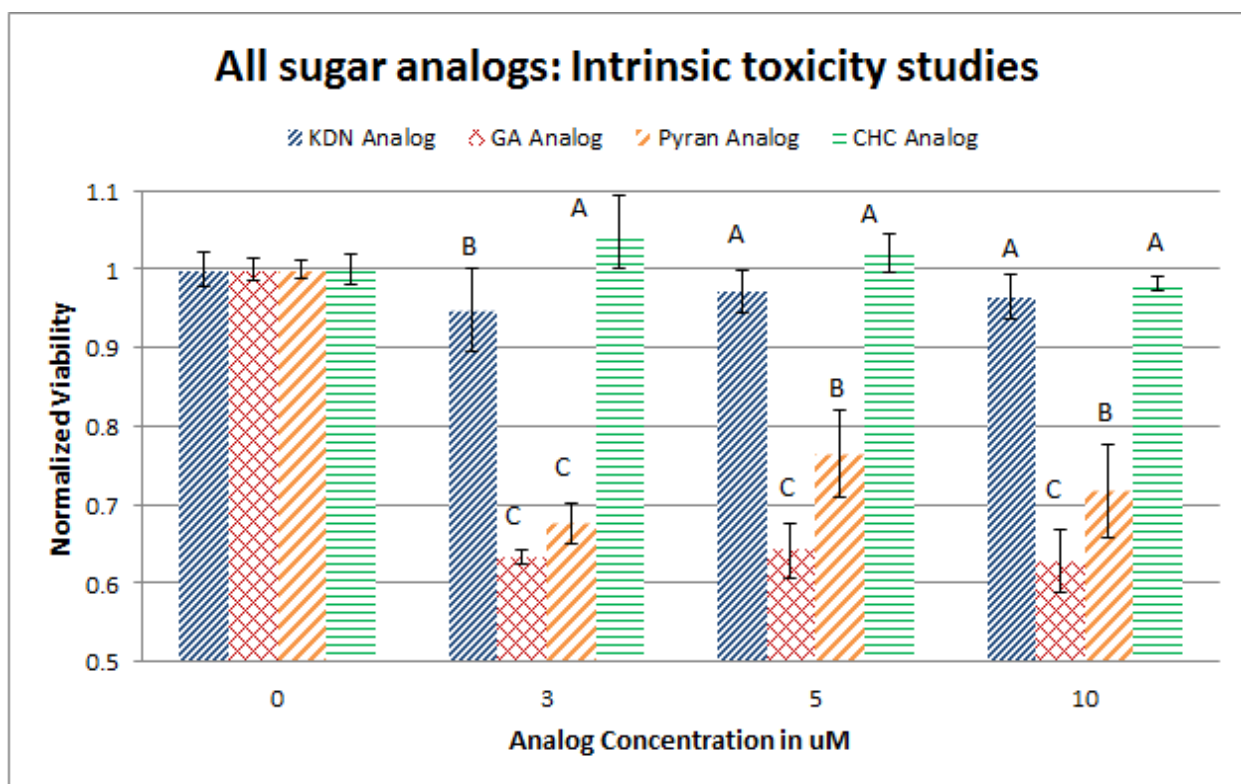


**Figure 61: All sugar analogs at 3 $\mu$ M, 5 $\mu$ M, 10 $\mu$ M- Intrinsic toxicity studies**

Similar letters or group of letters above the bar chart indicates no statistical difference between the normalized viabilities of those concentrations as given by Tukey's test at  $p < 0.05$

The figure 61 shows the statistical analysis for pure analogs KDN, GA, Pyran and CHC at the concentration of 3 $\mu$ M, 5 $\mu$ M and 10 $\mu$ M. Each sugar analog is compared among themselves

at each concentration studied by ANOVA followed by Tukey's test (at  $p < 0.05$ ). Analogs are not compared between two different concentrations although the graph output shows similar letters between adjacent concentrations. Means that do not share the same letters above the error bars are statistically different as given by Tukey's test ( $p < 0.05$ ) at that particular concentration only. At least four replicates were done for each concentration for each compound tested. At  $3\mu\text{M}$ , CHC and KDN show no toxicity whereas higher toxicity is observed from Pyran (~67% viability) and GA (64% viability). Such a trend is also seen in the other concentrations  $5\mu\text{M}$  and  $10\mu\text{M}$ . The results indicate that at lower concentrations, CHC and KDN shows greater than 95% viability whereas at the same concentrations, Pyran (less than 74% viability) and GA (less than 64% viability) show decreased viabilities.

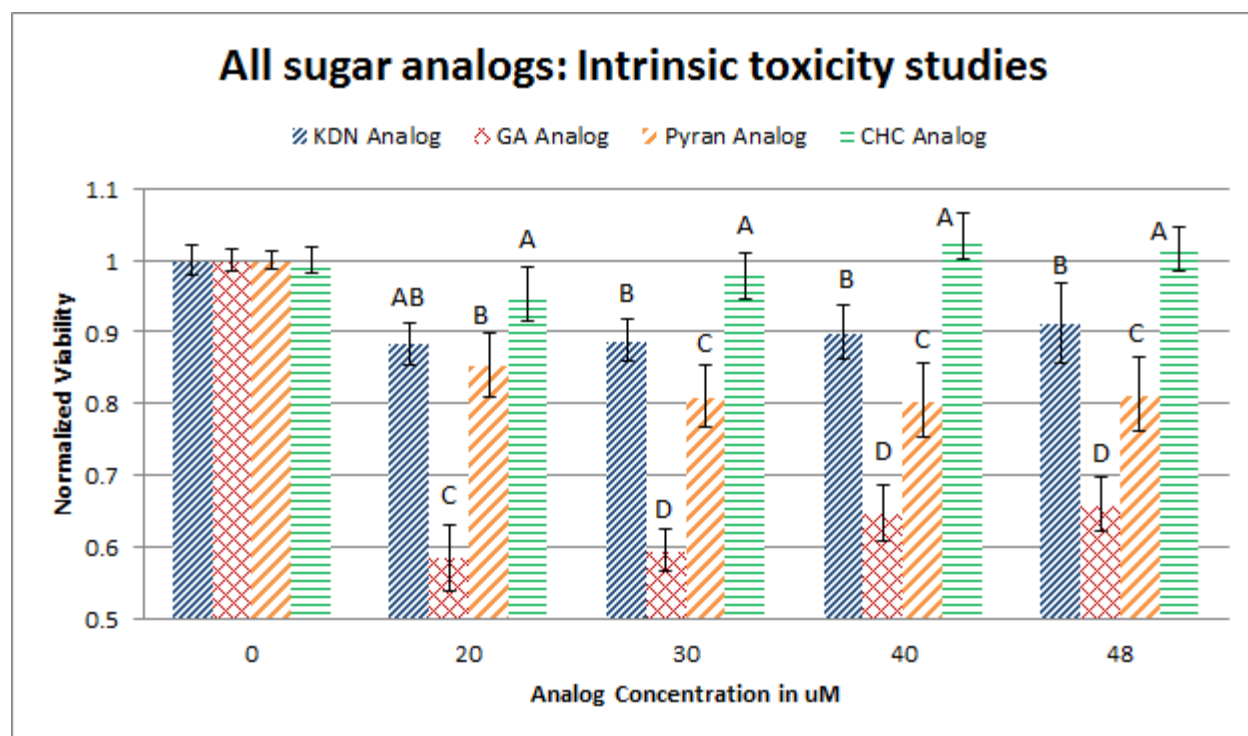


**Figure 62: All sugar analogs at  $20\mu\text{M}$ ,  $30\mu\text{M}$ ,  $40\mu\text{M}$ ,  $48\mu\text{M}$ - Intrinsic toxicity studies**

Similar letters or group of letters above the bar chart indicates no statistical difference between the normalized viabilities of those concentrations as given by Tukey's test at  $p < 0.05$

The sugar analogs were also tested for their intrinsic toxicity at higher concentrations (20 $\mu$ M, 30 $\mu$ M, 40 $\mu$ M and 48 $\mu$ M) and the results are given in figure 62. Each sugar analog is compared among themselves at each concentration studied by ANOVA followed by Tukey's test (with  $p < 0.05$ ). Means that do not share the same letters above error bars are statistically different as given by Tukey's test ( $p < 0.05$ ). Similar observations can be seen as compared to the results from lower concentrations. Cells treated with pure GA shows lower viability than the cells treated with all other pure analogs. Thus, among the four analogs tested, GA shows the highest intrinsic toxicity. However, at this point, we are interested in testing the toxicity of each complex after conjugation with chitosan. So, since GA is the best structural analog we could find that fit our criteria, GA is continued for further A $\beta$  attenuation studies.

#### **4.4.2. Intrinsic Toxicity of Sugar-Chitosan Complexes**

The graphs show the statistical analysis for the intrinsic toxicity results of KDN-Chitosan complex, GA-Chitosan complex, Pyran-Chitosan complex and CHC-Chitosan complex. In all the below graphs, the normalized viability of 1 at 0 $\mu$ M represents the 100% live cells and no other test/experimental compound added to them. Normalized viabilities are obtained by dividing the viable cells in a sample with that of the live control (untreated cells). In each case, viability is represented as mean  $\pm$  SD with four replicates. Statistical analysis was performed by ANOVA followed by Tukey's test in SAS program. Similar means are grouped together and indicated by the same letter or same groups of letters. Different letters across the graphs indicates statistically different means as indicated by Tukey's (at  $p < 0.05$ ) test. The macro used to analyze this data is provided by Saxton M.A [244]. The individual p-values are provided in the appendix along with the output for the macro.

## Statistical Analysis Done for Each Compound

The graphs of the intrinsic toxicity of each sugar-chitosan complex show statistical comparisons between all concentrations for that particular complex studied. Each complex is presented separately so that multiple comparisons can be done at all the doses.

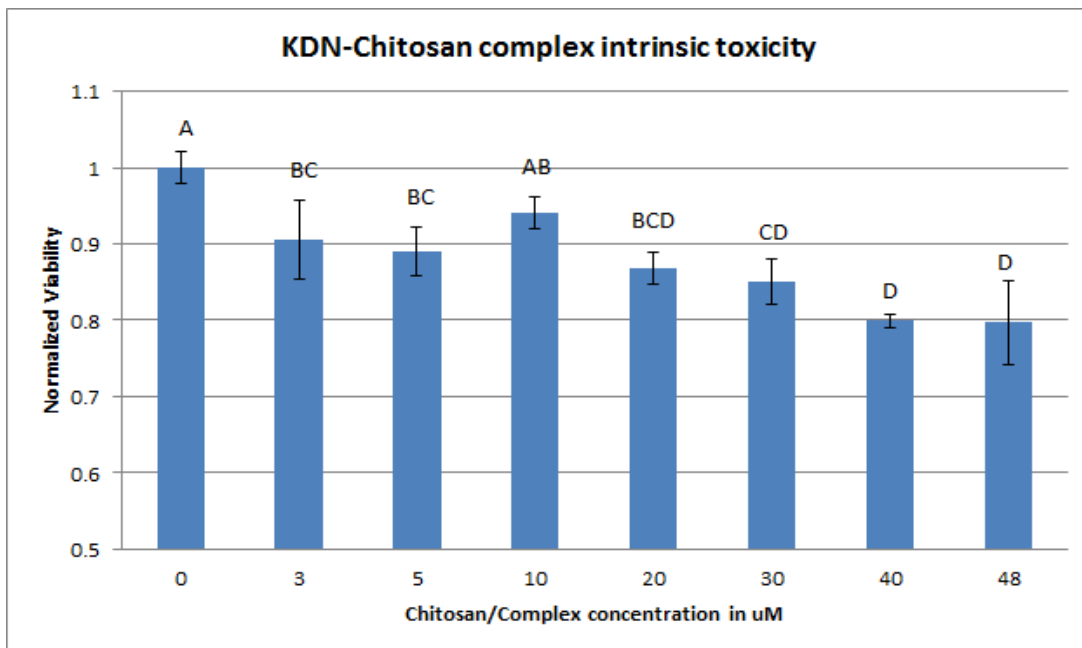


**Figure 63: KDN-chitosan complex- Intrinsic toxicity studies**

Similar letters or group of letters above the bar chart indicates no statistical difference between the normalized viabilities of those concentrations as given by Tukey's test at  $p < 0.05$

Figure 63 shows the intrinsic toxicity of KDN-Chitosan complex. At concentrations from  $3\mu\text{M}$  to  $10\mu\text{M}$ , we see viability in the range of  $\sim 90\%$ . At higher concentrations, the viability decreases with the lowest seen at  $40\mu\text{M}$  and  $48\mu\text{M}$ , with the lowest being  $\sim 80\%$  viability. Of note is the fact that, KDN sugar has the highest molecular weight as compared to the other sugars studied in this work. This seems to indicate that there is a possible link between high molecular weight of the complex and higher toxicity. Also, there is likely a link between higher toxicity

observed at higher concentration of these high M.W complexes applied to cells in culture [8, 255].

In the result of GA-Chitosan complex (refer to figure 64), we see viability in the range of ~70% at lower concentrations (3 $\mu$ M to 10 $\mu$ M) and around ~60% viability towards 48 $\mu$ M concentration. However, all the viabilities are statistically different compared to live control. Comparing to the KDN structure, the only significant difference between the two complexes is the multi -OH tail in KDN. From the analog data and complex data, we can see that GA analog and GA-Chitosan complex exhibit higher toxicities compared to KDN analog and KDN-Chitosan complex. Also, there is no change in toxicity after complexation. This also supports our earlier explanation that the loss of multi -OH tail can be the possible cause of intrinsic toxicity towards neuronal cells in culture.

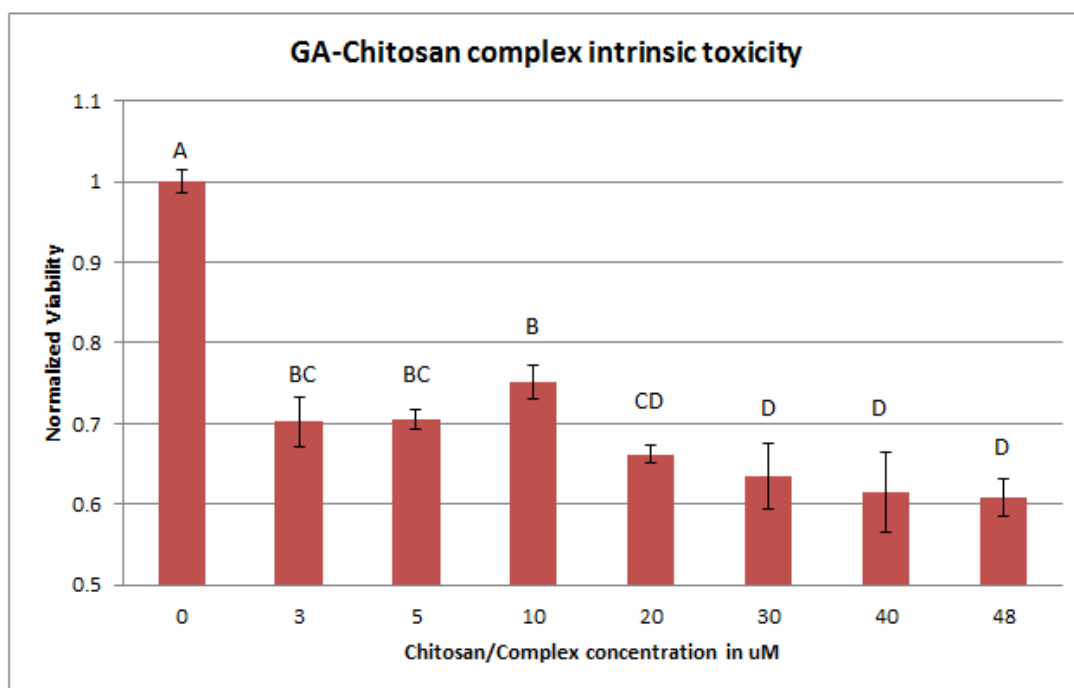


**Figure 64: GA-chitosan complex- Intrinsic toxicity studies**

Similar letters or group of letters above the bar chart indicates no statistical difference between the normalized viabilities of those concentrations as given by Tukey's test at  $p < 0.05$

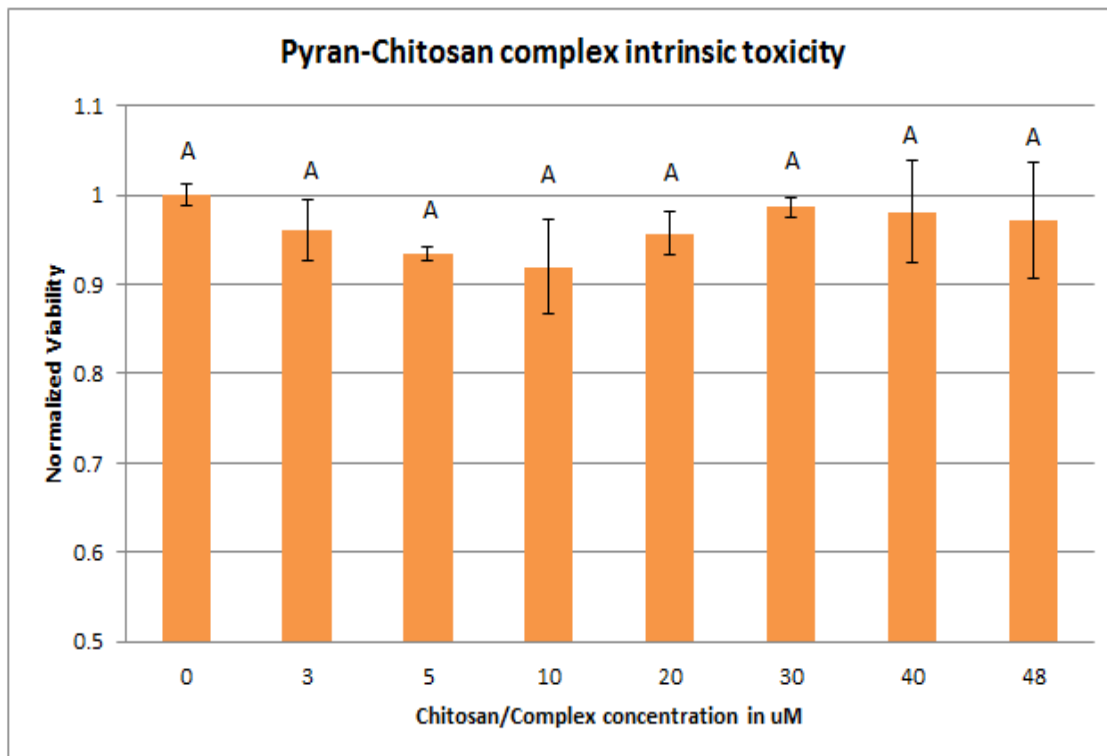


**Figure 65: Pyran-chitosan complex- Intrinsic toxicity studies**

Similar letters or group of letters above the bar chart indicates no statistical difference between the normalized viabilities of those concentrations as given by Tukey's test at  $p < 0.05$

Figure 65 shows the intrinsic toxicity of Pyran-Chitosan complex. Means are compared between all the concentrations applied in the work. We see that Pyran-complex is non-toxic (lowest viability is  $\sim 92\% \pm 0.05\%$  at  $10\mu\text{M}$ ) at all the concentrations applied, as it is evident that none of the means at any concentration are statistically different compared to control. This result is significant as Pyran-analog by itself showed viability in the range of  $\sim 70\%$  to  $\sim 80\%$ . This increase in viability seen in Pyran-chitosan indicates that the toxicity of the biological sugar is attenuated after complexation. This result indicates that it is possible to evaluate and consider compounds that are known to be potentially toxic as their toxicity after complexation could be attenuated.

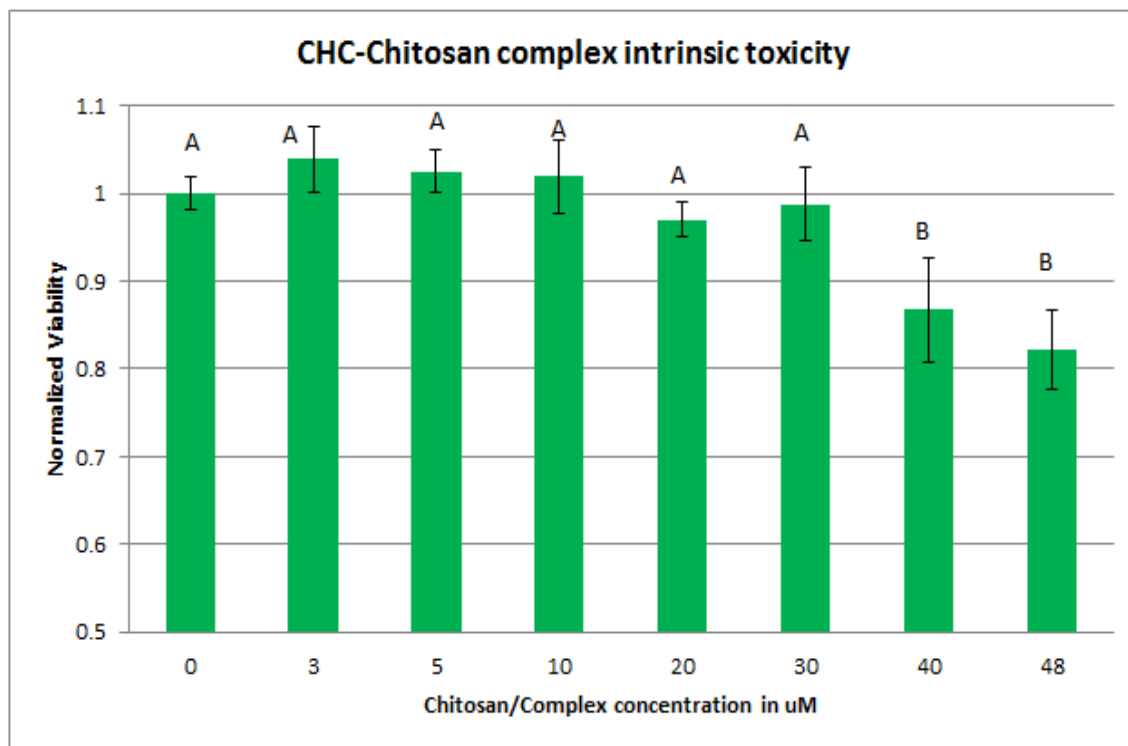


**Figure 66: CHC-chitosan complex- Intrinsic toxicity studies**

Similar letters or group of letters above the bar chart indicates no statistical difference between the normalized viabilities of those concentrations as given by Tukey's test at  $p < 0.05$

From the figure 66 showing the intrinsic toxicity of CHC-Chitosan complex, we see that from concentrations of  $3\mu\text{M}$  to  $30\mu\text{M}$ , the normalized viabilities are not statistically different compared to control. This indicates that the CHC complex shows no significant (statistically) toxicity at concentration up to  $30\mu\text{M}$ . At higher concentrations, the viability decrease to  $\sim 82\%$  at  $48\mu\text{M}$ .

### **Statistical Analysis Done for Each Concentration**

The next set of figures show the comparison between the sugar-chitosan complexes at each individual concentration studied. Thus, the effects of the four complexes are compared at each concentration from  $3\mu\text{M}$  to  $48\mu\text{M}$ .

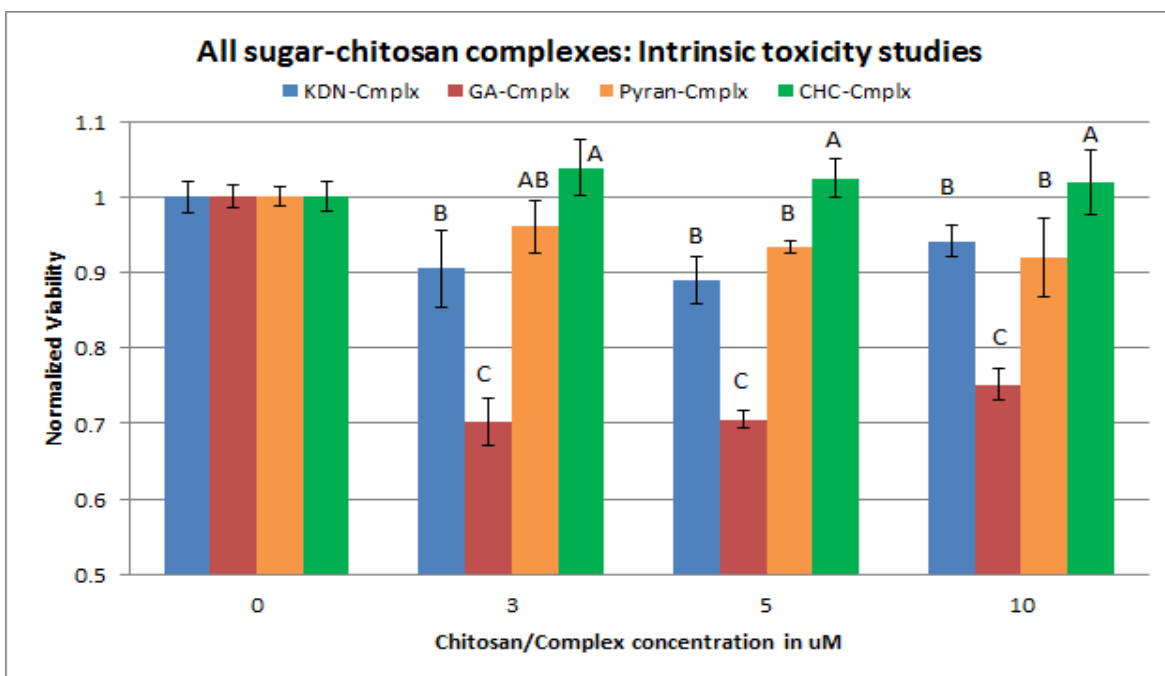


**Figure 67: All sugar-chitosan complexes at 3µM, 5µM, 10µM- Intrinsic toxicity studies**

Similar letters or group of letters above the bar chart indicates no statistical difference between the normalized viabilities of those concentrations as given by Tukey's test at  $p < 0.05$

At viability at 0µM represents the live control (untreated cells) and is provided for comparison purposes only. From the figure 67, at 3µM, CHC-complex shows no toxicity, whereas almost 30% toxicity is observed from GA-complex. Similar trend is seen at the other concentrations of 5µM and 10µM. Thus, at all these concentrations, the range of toxicity (from highest to lowest toxic) is as follows: GA-complex > KDN-complex = Pyran-complex > CHC-complex.

At higher concentrations (20µM to 48µM), the results show that Pyran-complex show no toxicity compared to control at all concentrations studied (refer figure 68). At 20µM and 30µM, statistically, the order of toxicities (from highest to lowest toxicity) is as follows: GA-complex > KDN-complex > CHC-complex = Pyran-complex. At concentrations of 40µM and 48µM, statistically, order of toxicities is: GA-complex > KDN-complex = CHC-complex > Pyran-

complex. It is interesting to note that at all concentrations (3 $\mu$ M to 48 $\mu$ M), GA-complex always shows higher toxicity compared to all other complexes.

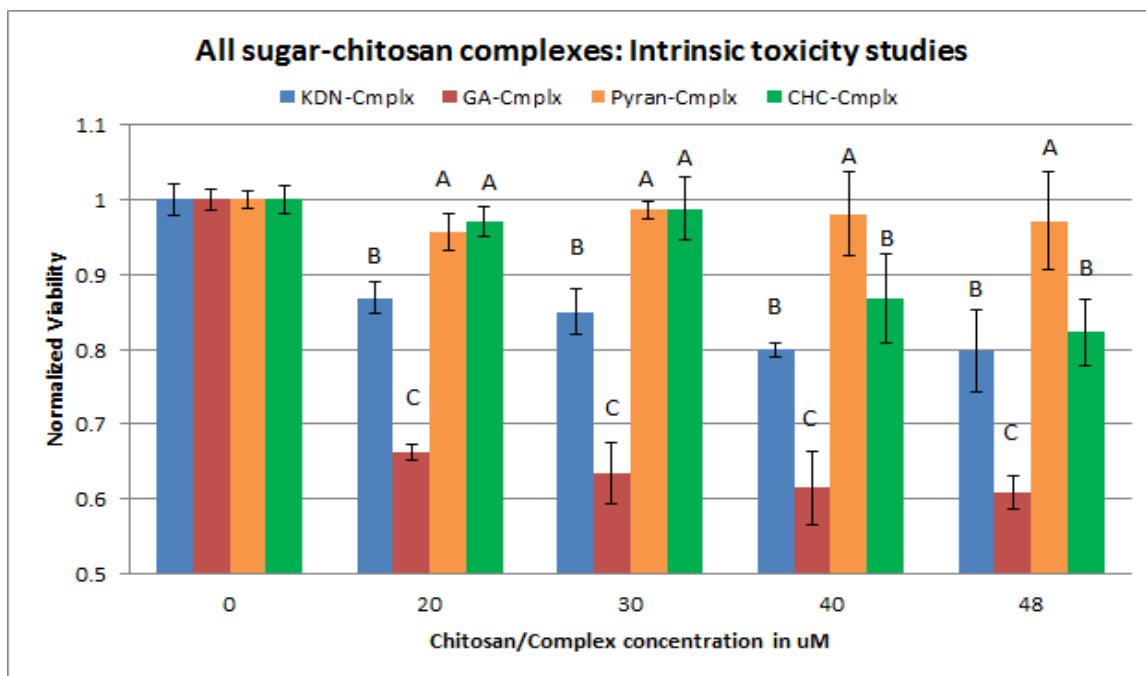


**Figure 68: All sugar-chitosan complexes at 20 $\mu$ M, 30 $\mu$ M, 40 $\mu$ M, 48 $\mu$ M- Intrinsic toxicity studies**

Similar letters or group of letters above the bar chart indicates no statistical difference between the normalized viabilities of those concentrations as given by Tukey's test at  $p < 0.05$

#### 4.4.3. A $\beta$ Toxicity Attenuation Properties of Pure Sugar Analogs

The results below show the A $\beta$  toxicity attenuation properties of the pure sugar analogs. The concentration of A $\beta$  studied is 50 $\mu$ M. In all the graphs, the normalized viability at 0 $\mu$ M analog concentration is the A $\beta$  control value, i.e. viable cells after treatment with only 50 $\mu$ M aggregated A $\beta$  with no analog/sugar added. For this study, A $\beta$  control viability was found to be 71% ( $\pm 0.01\%$ ). In all cases, a gradient of pure analogs from 3 $\mu$ M to 48 $\mu$ M was applied and four replicates were done for each concentration. Values on graph are represented as means  $\pm$  SD of the normalized viability values. The statistical analysis between the groups was done by

ANOVA followed by Tukey's test in SAS program. Different letters above each bar indicates statistically significant difference between the means as given by Tukey's test at  $p < 0.05$ . Same letter above the bar chart indicates no statistical difference between those means. To get the grouping of letters for similar means, a macro developed by Saxton M.A. was used in SAS [244].

### Statistical Analysis Done for Each Compound

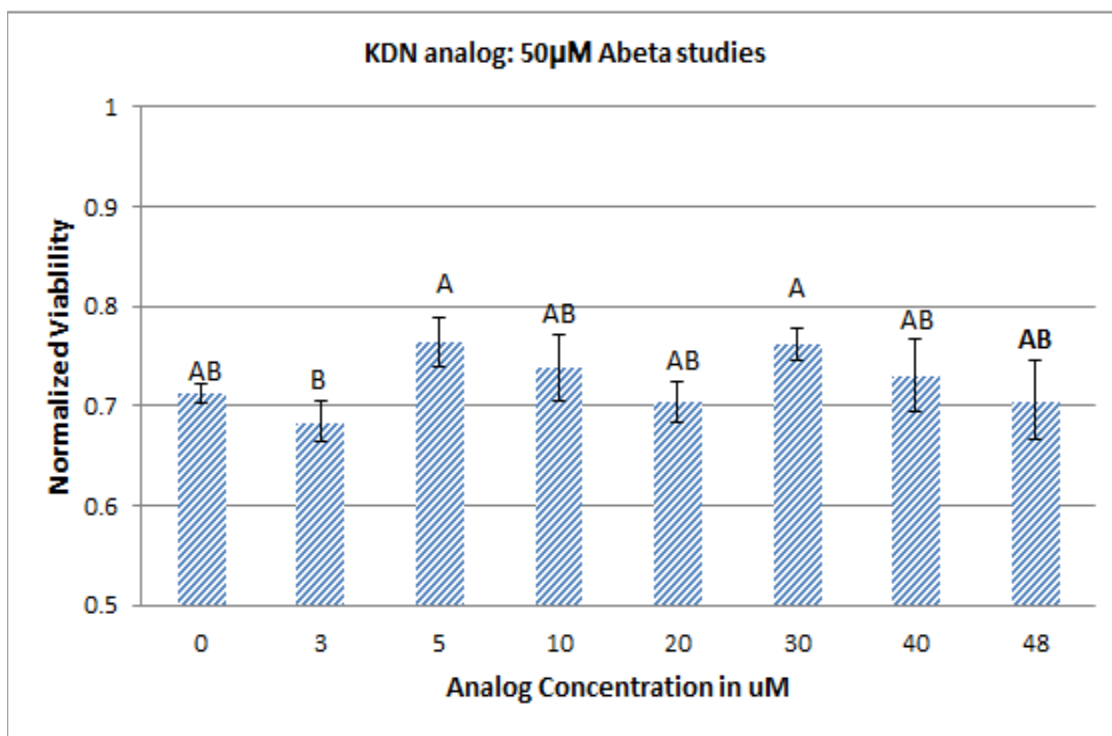


**Figure 69: KDN analog:  $A\beta$  toxicity attenuation studies**

Similar letters or group of letters above the bar chart indicates no statistical difference between the normalized viabilities of those concentrations as given by Tukey's test at  $p < 0.05$

The result from the KDN analog  $A\beta$  attenuation study (Figure 69) indicate that, statistically, none of the viabilities at any concentrations studied are significantly different from the viability obtained from  $A\beta$  control (71% viability). This analysis indicates that KDN-analog does not have any protective effect on cells from the toxic  $A\beta$  (figure 69).

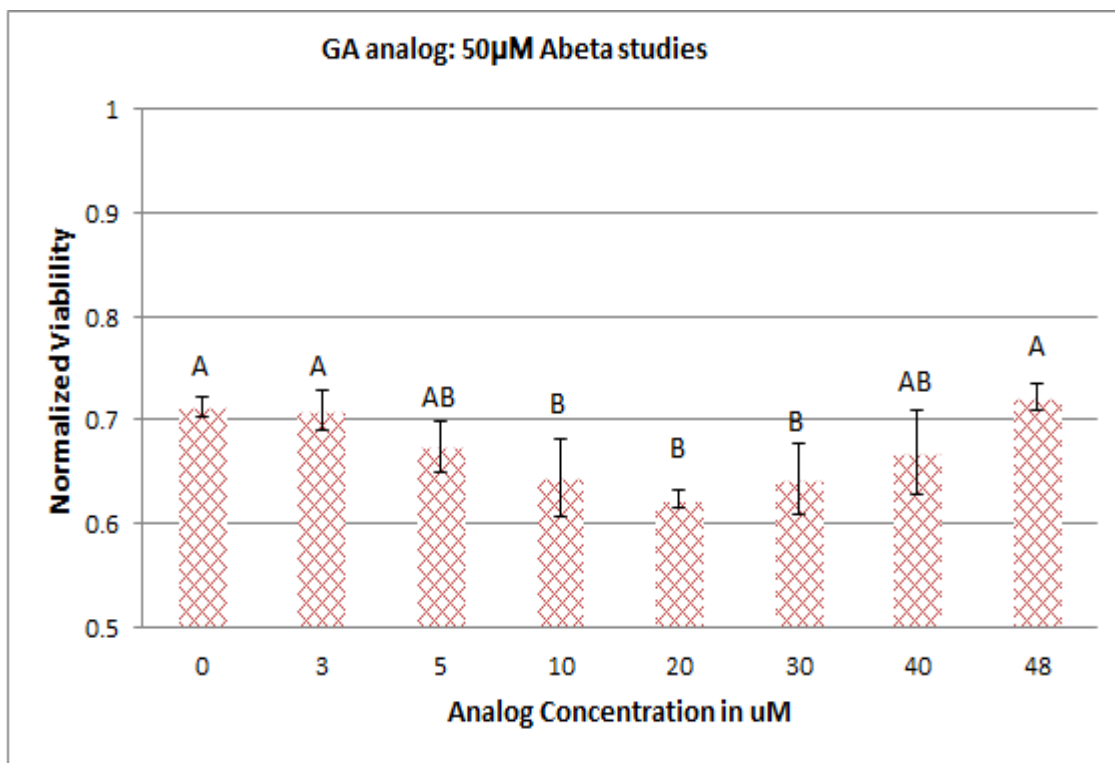


**Figure 70: GA analog: A $\beta$  toxicity attenuation studies**

Similar letters or group of letters above the bar chart indicates no statistical difference between the normalized viabilities of those concentrations as given by Tukey's test at  $p < 0.05$

Similarly, at all concentration of GA analog studied, we see a decrease in viabilities and thus, no protection can be seen from A $\beta$ . The toxicity towards the cells is most likely the combination of aggregated A $\beta$  and GA together (figure 70).

From the study of Pyran analog with 50µM A $\beta$  (figure 71), it can be seen that the viabilities of the wells treated with Pyran are statistically lower compared to the A $\beta$  control. In between 3µM and 48µM, Pyran monomer does not show any type of dose-response relationship. The result also indicates that Pyran monomer by itself does not show any A $\beta$  attenuation properties.

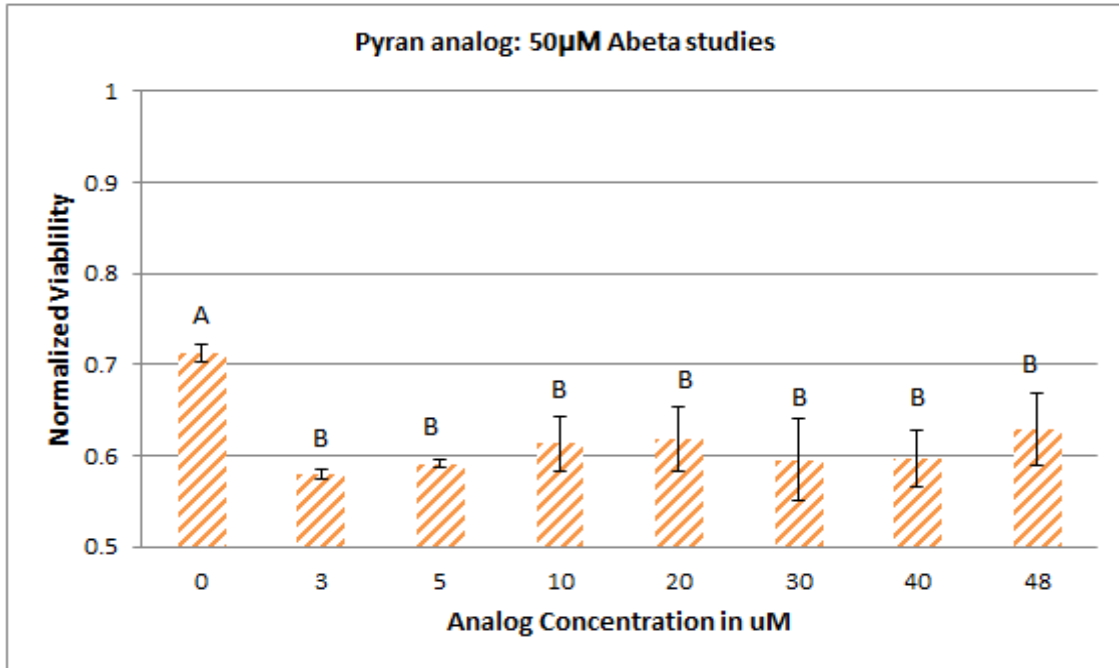


**Figure 71: Pyran analog: A $\beta$  toxicity attenuation studies**

Similar letters or group of letters above the bar chart indicates no statistical difference between the normalized viabilities of those concentrations as given by Tukey's test at  $p < 0.05$

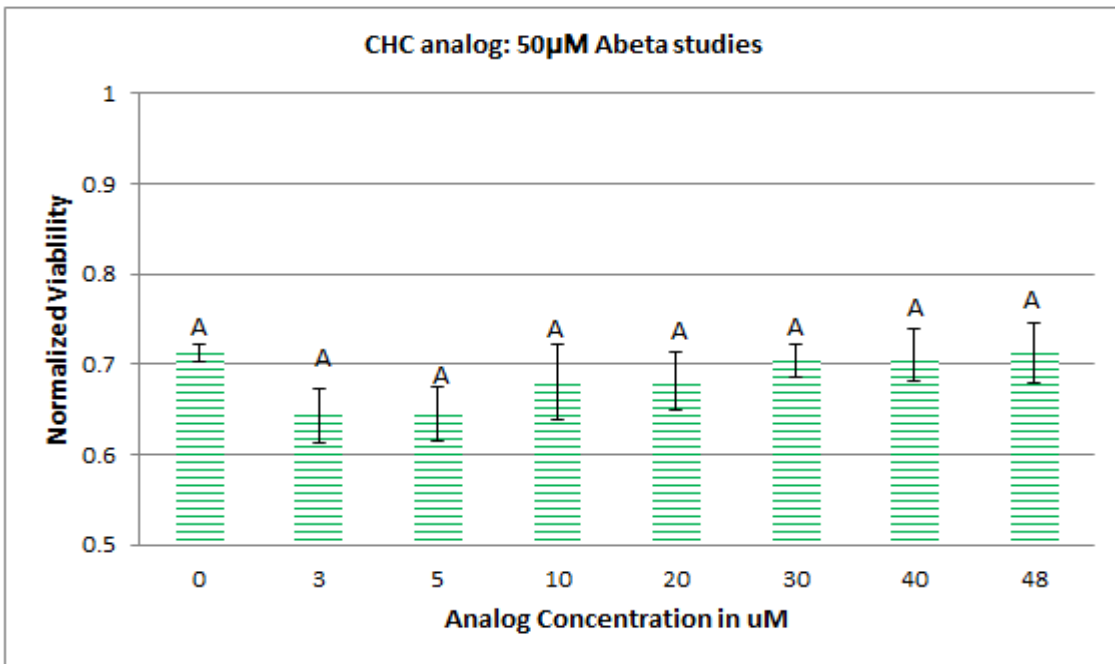


**Figure 72: CHC analog: A $\beta$  toxicity attenuation studies**

Similar letters or group of letters above the bar chart indicates no statistical difference between the normalized viabilities of those concentrations as given by Tukey's test at  $p < 0.05$

The addition of CHC analog at any concentration does not show any protective effect on SH-SY5Y viability (figure 72). At all concentrations, the means were not statistically different from the A $\beta$  control.

### Statistical Analysis Done for Each Concentration

The following plots show the statistical analysis done for each concentration with comparison among the four different sugars studied (figures 73, 74). Thus, here, we are comparing each sugar at a particular concentration. Significant here is that none of the sugar analogs show any protective effects from toxic A $\beta$ . These results indicates that clustering of the sugars in the neuronal membrane play a critical role in A $\beta$  toxicity attenuation and that free monomer in solution is insufficient to achieve the necessary clustering. Also, this result justifies the need of a suitable backbone that can allow the sugars to effectively cluster.

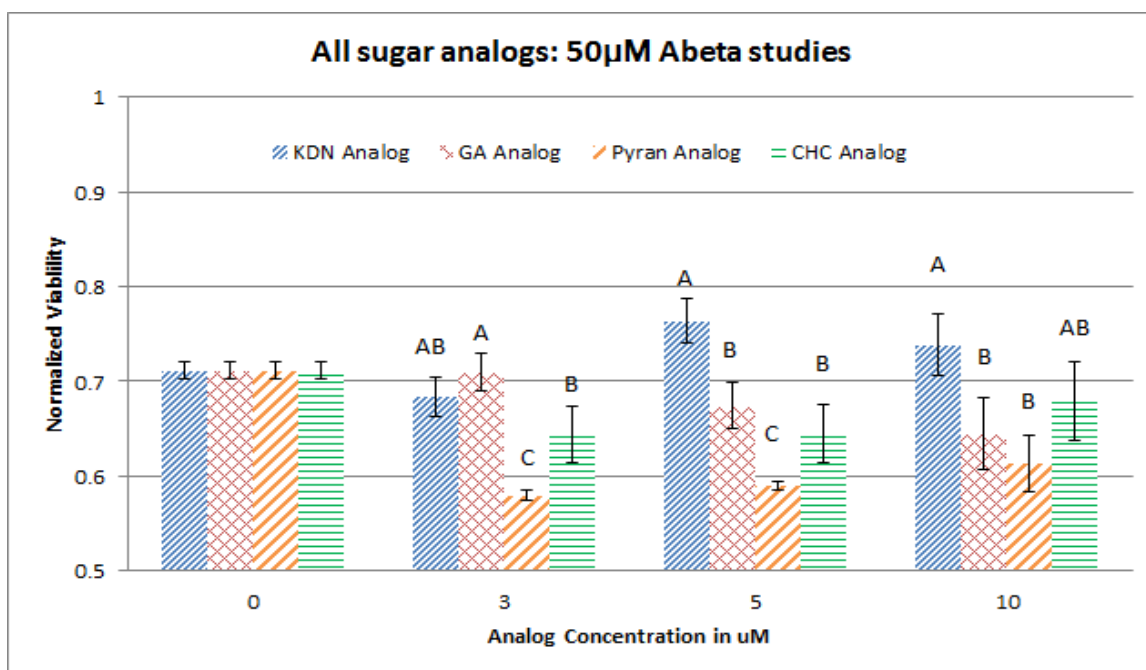


**Figure 73: All sugar analogs at 3µM, 5µM, 10µM: A $\beta$  toxicity attenuation studies**

Similar letters or group of letters above the bar chart indicates no statistical difference between the normalized viabilities of those concentrations as given by Tukey's test at  $p < 0.05$

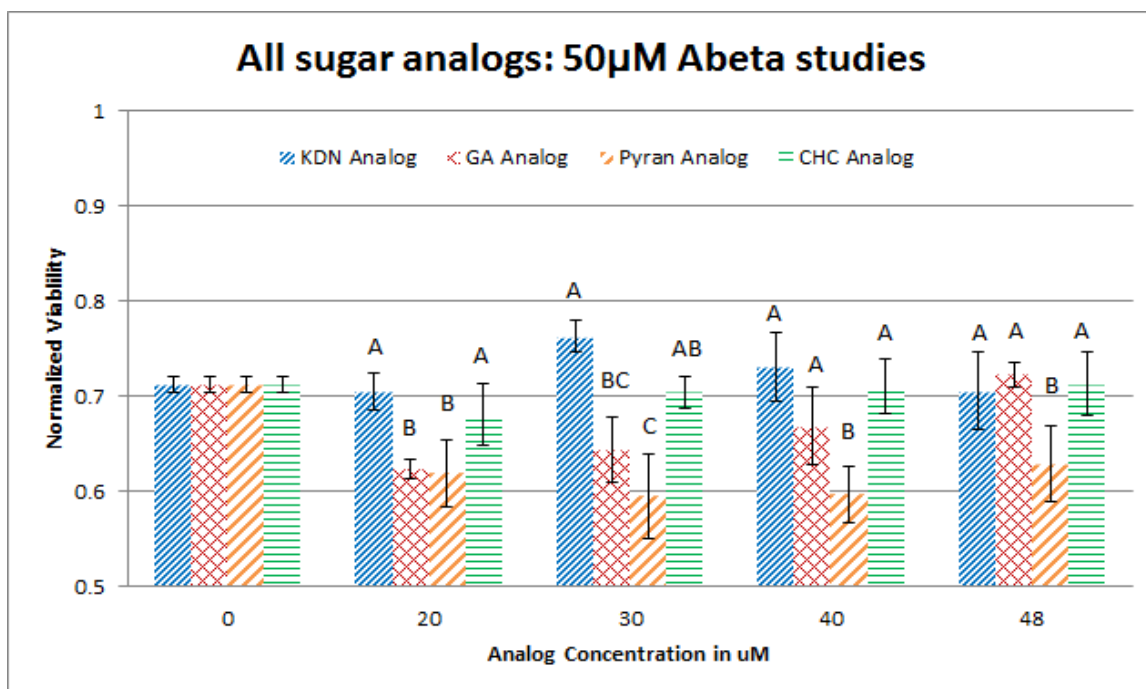


**Figure 74: All sugar analogs at 20µM, 30µM, 40µM, 48µM: Aβ toxicity attenuation studies**

Similar letters or group of letters above the bar chart indicates no statistical difference between the normalized viabilities of those concentrations as given by Tukey's test at  $p < 0.05$

#### 4.4.4. Aβ Toxicity Attenuation Properties of the Sugar-Chitosan Complexes

In the following section, all the sugars are conjugated with a chitosan backbone and their ability to attenuate the toxicity of 50µM aggregated Aβ is investigated. Aggregated Aβ is prepared according to established protocols and added to cells in culture and viability assessed after 24h. After addition of 50µM aggregated Aβ and no other experimental/test compound/complex, the normalized viability obtained around ~71%. This is indicated on the plots by the bar chart at point 0µM chitosan/complex concentration. This value represents the Aβ control value, so, if the complexes are effective in protection, an increase in viability should be observed after the addition of the synthesized complexes.

In each case, viability is represented as mean  $\pm$  SD with four replicates. Statistical analysis was performed by ANOVA followed by Tukey's test in SAS program. Statistically

similar means are grouped together and indicated by the same letter or same groups of letters. Different letters across the graphs indicates statistically different means as indicated by Tukey's (at  $p < 0.05$ ) test. The macro used to analyze this data is provided by Saxton M.A [244].

### Statistical Analysis Done for Each Compound

The next set of plots shows the statistical analysis for the  $A\beta$  studies with each sugar-complex or unlabeled chitosan compared at all concentrations from  $1\mu\text{M}$  to  $30\mu\text{M}$ . Each complex is plotted separately so that multiple comparisons can be done at all doses studied.

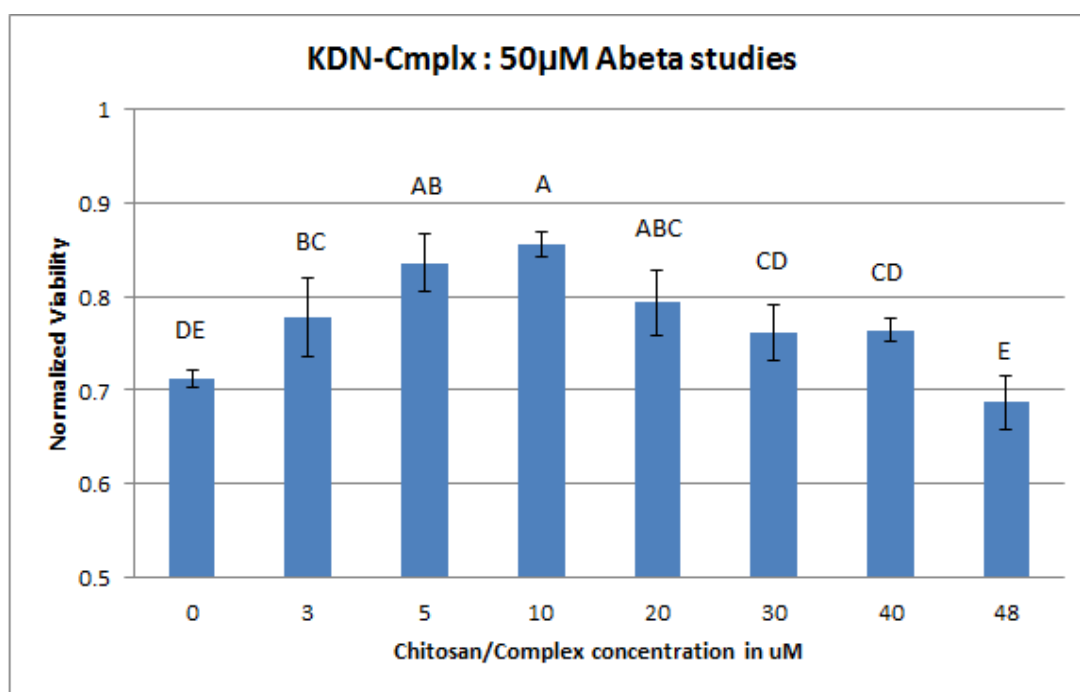


**Figure 75: KDN-chitosan complex:  $A\beta$  toxicity attenuation studies**

Similar letters or group of letters above the bar chart indicates no statistical difference between the normalized viabilities of those concentrations as given by Tukey's test at  $p < 0.05$

The above plot, figure 75, shows the result for the  $A\beta$  toxicity attenuation by KDN-chitosan complex. KDN differs from sialic acid at the C-5 position. It can be seen that the viability of SH-SY5Y cells increase after the addition of KDN-chitosan complex which indicates

protection from the complex. For the KDN-complex, the highest protection can be seen at concentrations of 5 $\mu$ M, 10 $\mu$ M and 20 $\mu$ M. Other concentrations also show protection and the protection increases and then decreases at higher concentrations. It is difficult to compare KDN-complex with sialic acid complex as there is a difference in the values of A $\beta$  control. Also, it should be noted that KDN is just a substructure of sialic acid, so it is likely that A $\beta$  only recognizes a part of the substructure which gives the toxicity attenuation from KDN-complex. The difference between GA-complex and KDN-complex is the presence of the multi-OH tail. So, the most likely explanation for the protection shown by KDN-complex and none shown by GA-complex is that the multi-OH chain is involved in A $\beta$  interactions.

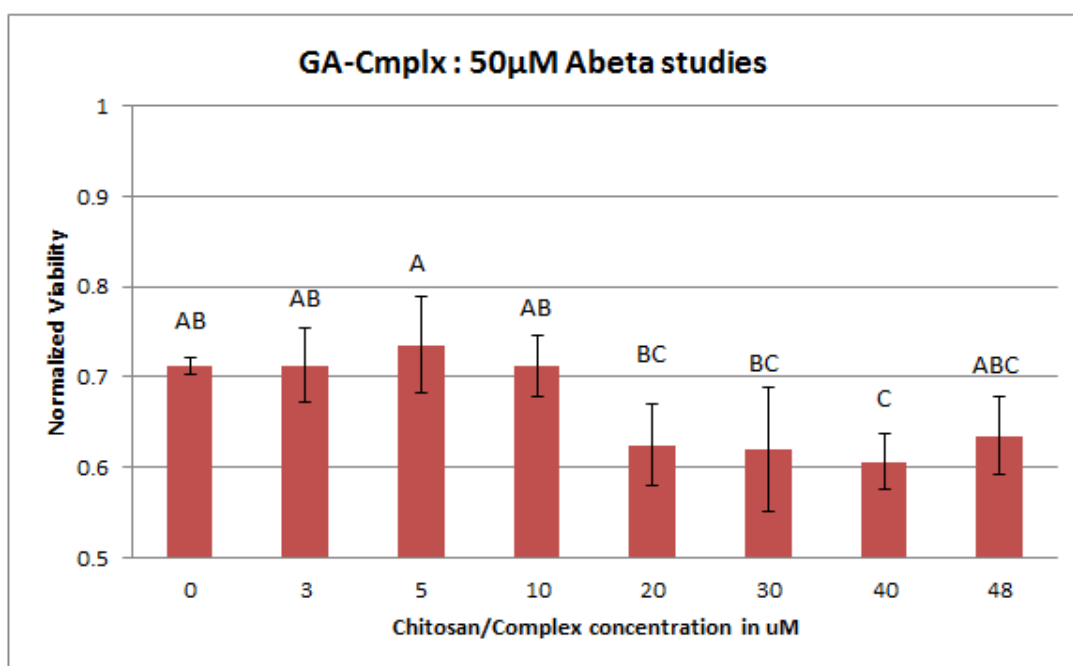


**Figure 76: GA-chitosan complex: A $\beta$  toxicity attenuation studies**

Similar letters or group of letters above the bar chart indicates no statistical difference between the normalized viabilities of those concentrations as given by Tukey's test at  $p < 0.05$

From the above result, figure 76, it can be seen that GA-complex does not shown any protective properties at all concentrations studied. At 3 $\mu$ M to 10 $\mu$ M, the viabilities are not

different than that of A $\beta$  control and then the viability decreases. The difference in the structure of KDN and GA is the multi –OH tail. As no protection from GA-complex can be seen, it is likely that the loss of –OH tail is the reason for loss of protection. Thus, it is plausible that the multi –OH tail of sialic acid is the target that A $\beta$  recognizes.

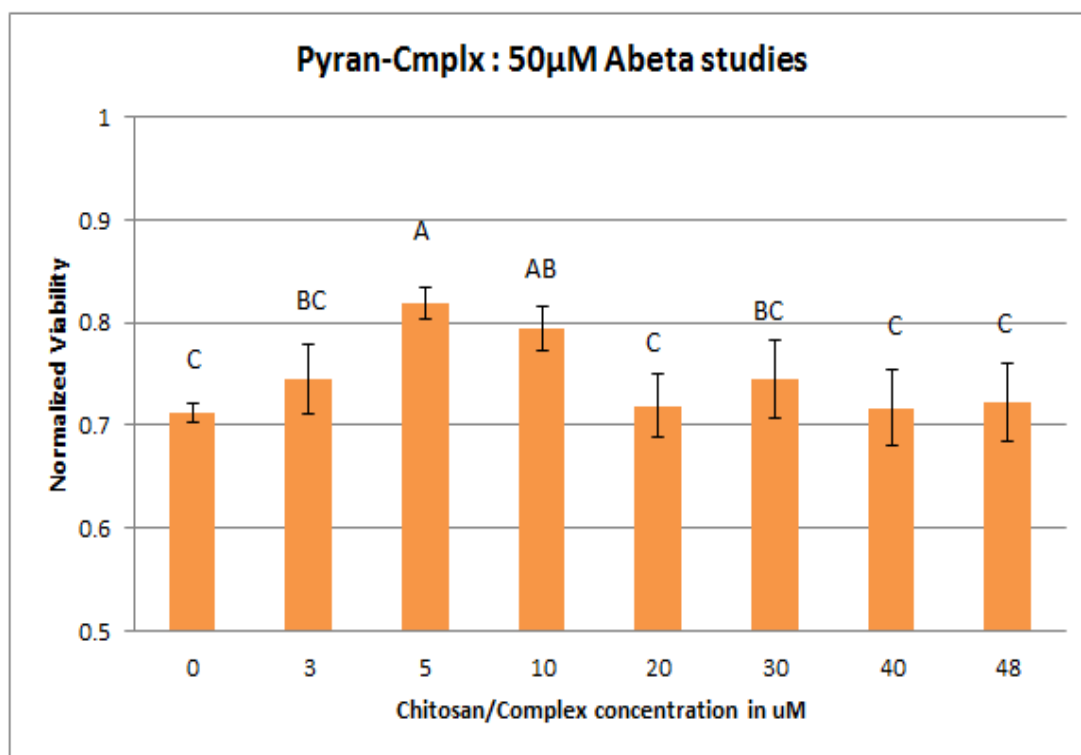


**Figure 77: Pyran-chitosan complex: A $\beta$  toxicity attenuation studies**

Similar letters or group of letters above the bar chart indicates no statistical difference between the normalized viabilities of those concentrations as given by Tukey's test at  $p < 0.05$

From the results of Pyran-chitosan complex shown in figure 77, we can see that the complex offers protection from A $\beta$ . Highest protection can be seen from 5 $\mu\text{M}$  and 10 $\mu\text{M}$  concentration of the complex. The Pyran structure consists of the oxygen substitution in the ring structure. The results indicate the possible role of Pyran substitution in A $\beta$  interactions. Such type of structural information will be useful in the development of a therapeutic based on polysaccharide structures.

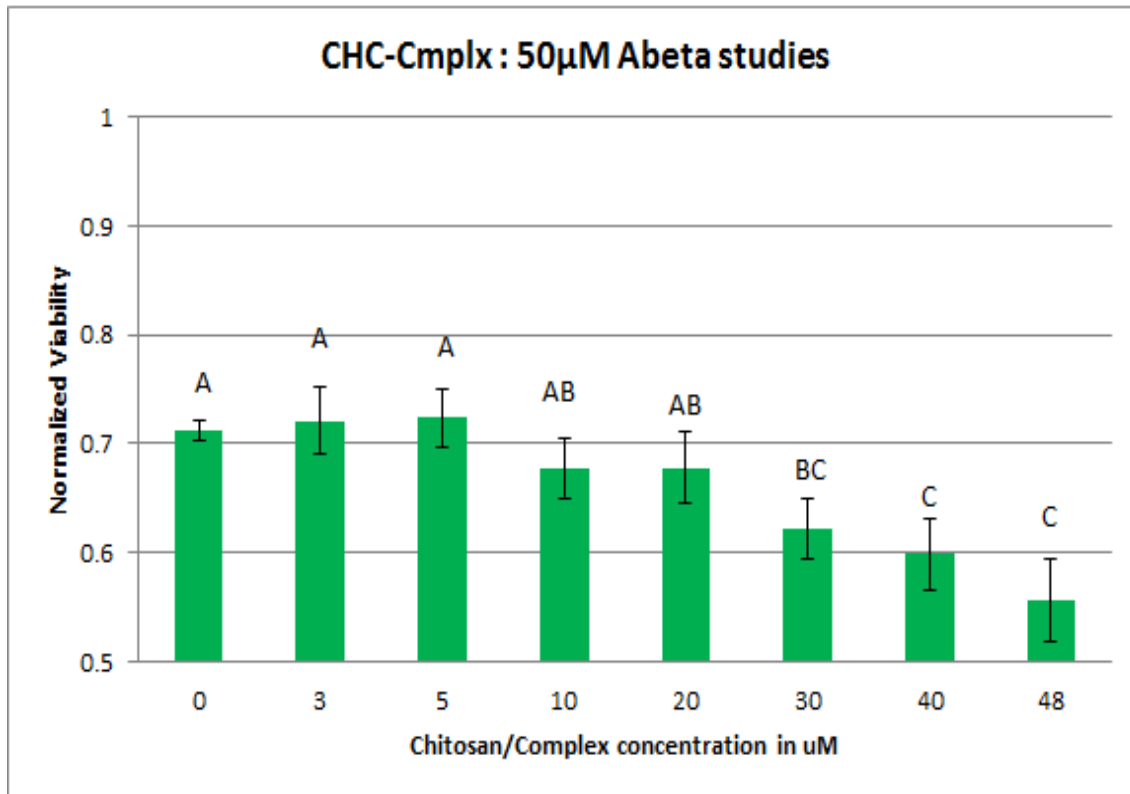


**Figure 78: CHC-chitosan complex:  $A\beta$  toxicity attenuation studies**

Similar letters or group of letters above the bar chart indicates no statistical difference between the normalized viabilities of those concentrations as given by Tukey's test at  $p < 0.05$

From the above results, figure 78, we see that CHC-complex offers no protection from  $A\beta$  and the viability decreases as the concentration of complex increases. None of the viabilities at any concentrations are statistically higher compared to those of the  $A\beta$  control. Again, the difference between Pyran-complex and CHC-complex is the presence of oxygen substitution. Making the same argument, it can be seen that the ring structure does not contribute to  $A\beta$  toxicity attenuation; whereas the same ring structure with the presence of oxygen substitution contributes to  $A\beta$  toxicity attenuation. This indicates a possible role of oxygenated saccharide structure in  $A\beta$  showing affinity towards cell surface sialic acids. Such type of comparisons can be made as the backbone chitosan has approximately similar labeling for all sugars.

## Statistical Analysis Done for Each Concentration

In this section, each compound tested, the different sugar-chitosan complexes are compared among each other at every concentration studied. We are interested to analyze which complex offers what level of protection at every concentration applied to the plate with 50 $\mu$ M aggregated A $\beta$  added to them. Similar letters on adjacent concentration do not mean that those viabilities are statistically similar. Each complex is only compared at each concentration separately. The A $\beta$  control at 0 $\mu$ M complex concentration is given for understanding only.

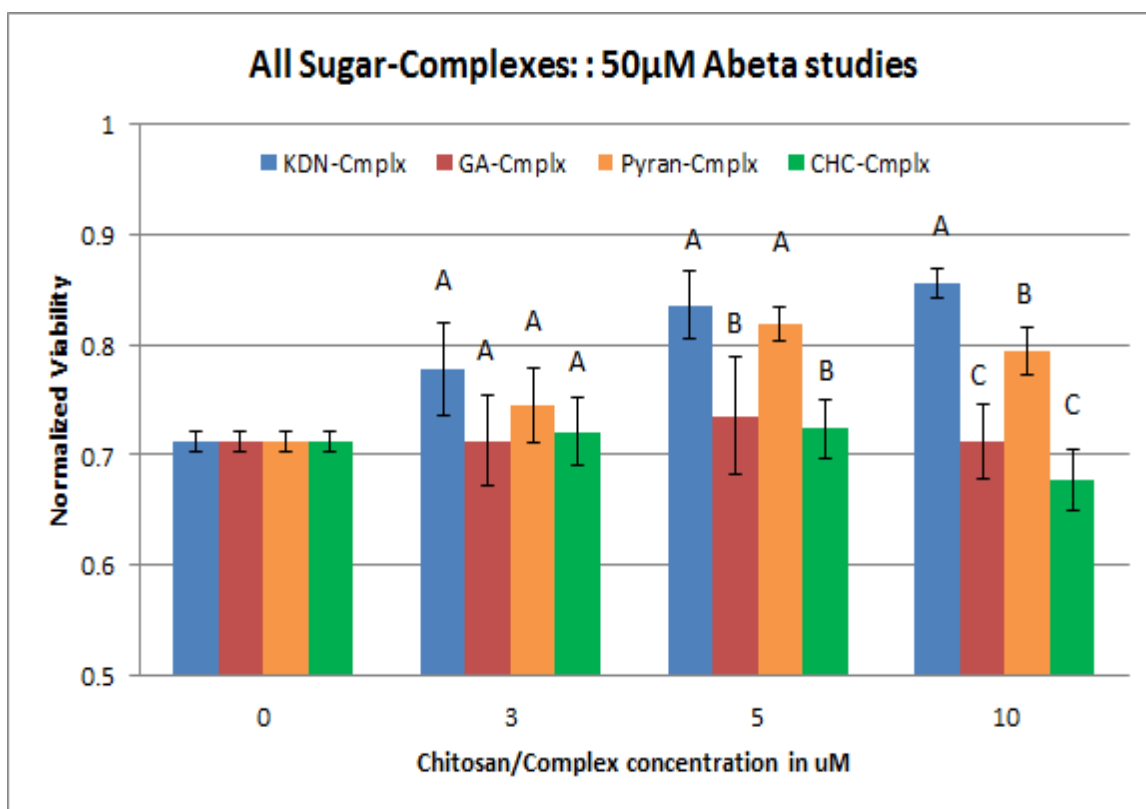


**Figure 79: All sugar-chitosan complexes at 3 $\mu$ M, 5 $\mu$ M, 10 $\mu$ M: A $\beta$  toxicity attenuation study**

Similar letters or group of letters above the bar chart indicates no statistical difference between the normalized viabilities of those concentrations as given by Tukey's test at  $p < 0.05$

In the above plot, each complex (with A $\beta$  media) is compared at 3 $\mu$ M, 5 $\mu$ M and 10 $\mu$ M separately (refer figure 79). At 3 $\mu$ M, it can be seen that the viability is higher from KDN-

complex and Pyran-complex although all the complexes do not differ statistically. But, compared to control, KDN-complex shows higher viabilities followed by Pyran-complex. Moving on to 5 $\mu$ M, we can see that statistically highest viabilities are seen from KDN-complex and Pyran complex compared to GA-complex and CHC-complex. This difference in viabilities between the two groups is even more pronounced at 10 $\mu$ M. Also, viability with GA-complex did not decrease immediately at lower concentrations, which can most likely be attributed to the oxygen substitution in GA. Our results indicate that, at all concentrations from 3 $\mu$ M to 10 $\mu$ M, KDN-complex followed by Pyran-complex show A $\beta$  toxicity attenuation properties.

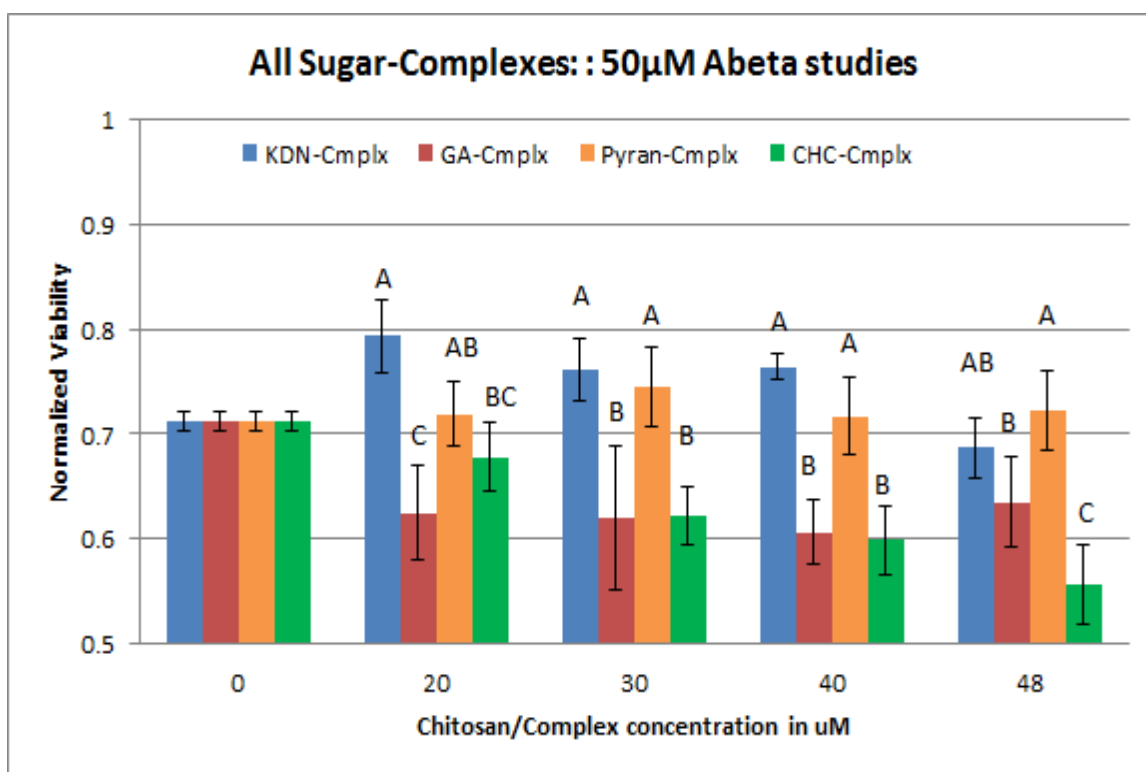


**Figure 80: All sugar-chitosan complexes at 20 $\mu$ M, 30 $\mu$ M, 40 $\mu$ M, 48 $\mu$ M: A $\beta$  toxicity attenuation study**

Similar letters or group of letters above the bar chart indicates no statistical difference between the normalized viabilities of those concentrations as given by Tukey's test at  $p < 0.05$

In figure 80, the viabilities of each complex are compared among themselves at 20 $\mu$ M, 30 $\mu$ M, 40 $\mu$ M and 48 $\mu$ M. Starting at 20 $\mu$ M, we see that KDN-complex shows the highest

protection followed by Pyran-complex. Lower viability is seen from GA-complex and CHC-complex. At 30 $\mu$ M, KDN-complex and Pyran-complex show toxicity attenuation whereas loss of viabilities can be seen from GA-complex and CHC-complex. Similar trends are seen at 40 $\mu$ M and 48 $\mu$ M. Overall, the results show that KDN-complex and Pyran-complex show higher viabilities at all concentration studied compared to GA-complex and CHC-complex.

Even if we do not expect the same level of protection as sialic acid-labeled chitosan, the results show the importance of the structures or –R groups of sialic acid that contribute to A $\beta$  toxicity attenuation. This has significance with respect to the understanding of the A $\beta$ -sialic acid interaction that takes place in-vivo. The information from such structure-activity experiments will aid in the development of smarter therapeutics since we know which groups contribute to intrinsic toxicity and which groups are important in A $\beta$  toxicity attenuation.

#### **4.4.5. Summary of the Statistical Analysis**

We used ANOVA followed by Tukey's test (at  $p < 0.05$ ) for the statistical analysis of the toxicity studies. A macro was used to group statistically similar means together and assign letter groups to them. Thus, similar letters above the bar indicates no statistical difference between those means (as given by Tukey's test at  $p < 0.05$ ). This allows for multiple comparisons between each and every data point on the bar chart. We studied a gradient of 3 $\mu$ M to 48 $\mu$ M of the pure sugar analogs or the sugar-chitosan complexes on SH-SY5Y cells. For the sake of understanding, we will treat 3 $\mu$ M to 10 $\mu$ M as low concentrations and 20 $\mu$ M to 48 $\mu$ M as high concentrations of compound in this study. The comparison between each data point and the  $p$ -values obtained by Tukey's test are attached in the appendix. Also, the output from macro is included along with the means compared in the appendix.

## **Intrinsic Toxicity of Pure Sugar Analogs**

### **Statistical Analysis Done for Each Compound**

KDN analog shows no statistical difference from live control ( $p > 0.05$ ) at lower concentrations whereas the viability decreases at higher concentrations of KDN compared to live control ( $p < 0.05$ ). Around ~90% cell survival is seen at higher concentrations of pure KDN.

In case of GA analog and Pyran analog, all the viabilities at all concentrations tested are statistically less compared to live control (in all cases,  $p < 0.05$ ). This indicates that pure GA and pure pyran are toxic to cells at all concentrations. The exact mode of toxicity cannot be discerned as such compounds have not been evaluated in a system of neuronal cultures to be best of our knowledge.

For CHC analog, none of the viabilities at any concentration are different from live control (in all cases,  $p > 0.05$ ). This indicates that CHC is a non-toxic compound.

### **Statistical Analysis Done for Each Concentration**

At lower concentrations, two distinct groups can be seen. Pure KDN and pure CHC show no toxicity and the highest viabilities. There is no statistical difference in their viabilities except at 3 $\mu$ M concentration (in all other cases,  $p > 0.05$ ). In the second group, pure GA and pure Pyran consistently show the lower viabilities. Thus, compared to the KDN-CHC group, all viabilities of GA and Pyran are statistically different (in all cases,  $p < 0.05$ ).

At higher concentrations, similar groups can be observed with KDN and CHC showing highest viabilities. In this, CHC is the least toxic. The second group, GA and Pyran analogs, show lower viabilities at higher concentrations. In all cases, the viabilities of CHC and KDN are

statistically higher compared to the GA and Pyran group ( $p < 0.05$ ). The toxicity of pure GA is the highest at all concentrations compared to other sugars.

## **Intrinsic Toxicity of Sugar-Chitosan Complexes**

### **Statistical Analysis Done for Each Compound**

At concentrations from  $3\mu\text{M}$  to  $10\mu\text{M}$ , for KDN-complex, we see viability in the range of  $\sim 90\%$ . At higher concentrations, the viability decreases with the lowest seen at  $40\mu\text{M}$  and  $48\mu\text{M}$ . This seems to indicate that there is a possible link between high molecular weight of the complex and higher toxicity. Also, it is possible that higher toxicity is observed at higher concentration due to the higher molecular weight of these complexes.

GA-complex is consistently toxic to the cells with viabilities in the range of  $\sim 70\%$  to  $60\%$ . Compared to live control, the viabilities at all concentrations of GA-complex are lower (in all cases,  $p < 0.0001$ ). Again, at higher concentration, higher toxicity is seen from GA-complex.

Interestingly, after complexation, the toxicity of Pyran analog is attenuated. The viabilities at all concentrations of Pyran-complex are statistically similar to that of live control (in all cases,  $p > 0.05$ ). This indicates that the toxicity of a potentially toxic sugar could be attenuated after its complexation.

CHC-chitosan complex is non-toxic at concentrations from 3 to  $30\mu\text{M}$ , whereas toxicity is seen at the remaining concentrations. Again, this can be the result of a high MW complex showing toxicity at higher concentrations.

### **Statistical Analysis Done for Each Concentration**

At lower concentrations, 3 $\mu$ M, 5 $\mu$ M and 10 $\mu$ M, the range of toxicity (from highest to lowest toxic) is as follows: GA-complex > KDN-complex = Pyran-complex > CHC-complex. At these concentrations, the viability shown by GA-complex at all concentrations is the lowest compared to the rest of the complexes (in all cases,  $p < 0.05$ ).

At higher concentrations (20 $\mu$ M to 48 $\mu$ M), the results show that Pyran-complex show no toxicity compared to control at all concentrations studied. At 20 $\mu$ M and 30 $\mu$ M, statistically, the order of toxicities (from highest to lowest toxicity) is as follows: GA-complex > KDN-complex > CHC-complex = Pyran-complex. At concentrations of 40 $\mu$ M and 48 $\mu$ M, statistically, order of toxicities is: GA-complex > KDN-complex = CHC-complex > Pyran-complex. It is interesting to note that at all concentrations (3 $\mu$ M to 48 $\mu$ M), GA-complex always shows higher toxicity compared to all other complexes (in all cases,  $p < 0.05$ ).

### **A $\beta$ Attenuation Properties of Pure Sugar Analogs**

In this study, along with a gradient of 3 $\mu$ M to 48 $\mu$ M of analogs, a concentration of 50 $\mu$ M aggregated A $\beta$  is added to the cells. The A $\beta$  control value is ~71% viability compared to live control (100%).

### **Statistical Analysis Done for Each Compound**

From the analysis, none of the pure sugars at any concentration show viabilities that are statistically higher compared to the A $\beta$  control. This proves that none of the sugars by themselves show any A $\beta$  toxicity attenuation properties. These results indicates that clustering of the sugars in the neuronal membrane play a critical role in A $\beta$  toxicity attenuation and that free

monomer in solution is insufficient to achieve the necessary clustering. Also, this result justifies the need of a suitable backbone that can allow the sugars to effectively cluster.

### **Statistical Analysis Done for Each Concentration**

None of the sugars show any significant protective property at attenuate A $\beta$  toxicity. Again, it indicates that a backbone structure is important for A $\beta$  toxicity attenuation.

### **A $\beta$ Attenuation Properties of the Sugar-Chitosan Complexes**

In this study, along with a gradient of 3 $\mu$ M to 48 $\mu$ M of sugar-chitosan complexes, a concentration of 50 $\mu$ M aggregated A $\beta$  is added to the cells. The A $\beta$  control value is ~71% viability compared to live control (100%).

### **Statistical Analysis Done for Each Compound**

It can be seen that the viability of SH-SY5Y cells increase after the addition of KDN-chitosan complex which indicates protection from the toxic A $\beta$ . For the KDN-complex, the highest protection can be seen at concentrations of 5 $\mu$ M, 10 $\mu$ M and 20 $\mu$ M concentration. The protection increases from 3 $\mu$ M to 10 $\mu$ M and then again starts decreasing at higher concentrations. It is difficult to compare KDN-complex with sialic acid-complex as there is a difference in the values of A $\beta$  control.

For the GA-complex and CHC-complex, at 3 $\mu$ M to 20 $\mu$ M, the viabilities are not different than that of A $\beta$  control ( $p > 0.05$ ) and then the viability decreases. Thus, GA-complex and CHC-complex shows no protection from A $\beta$ .

In case of Pyran-complex, we see that statistically highest protection is seen at 5 $\mu$ M, 10 $\mu$ M concentrations when compared to A $\beta$  control. Above 20 $\mu$ M, the viabilities are not statistically different from A $\beta$  control (in all cases,  $p > 0.05$ ).

### **Statistical Analysis Done for Each Concentration**

This data is explained better based on the structures of the sugars and these are the trends observed from the data.

At all concentrations, KDN-complex and Pyran-complex offer the highest protection from A $\beta$ . In all cases, except at 10 $\mu$ M, the effect seen by KDN-complex and Pyran-complex are statistically similar ( $p > 0.05$ ).

Now, the difference in the structure of KDN and GA is the multi –OH tail present in KDN. In all cases, except at 3 $\mu$ M, all the viabilities of KDN-complex are statistically higher than the viabilities of GA-complex (in all cases,  $p < 0.05$ ). As no protection from GA-complex can be seen, it is likely that the loss of –OH tail is the reason for loss of protection. Based on this result, we postulated that that the multi-OH group in sialic acid is the likely target that A $\beta$  recognizes on the neuronal membrane.

The difference in the structure of Pyran and CHC is the oxygen substitution in the ring structure. Comparing the results of Pyran-complex with CHC-complex, viabilities of Pyran-complex are statistically higher compared to all concentrations (in all cases,  $p < 0.05$ ), except 3 $\mu$ M and 20 $\mu$ M. Based on this result, we postulate that the oxygen atom in the ring structure is also a factor in A $\beta$  having affinity towards clustered sialic acids.

Even if we do not expect the same level of protection as sialic acid-labeled chitosan, the results show the importance of the structures or –R groups of sialic acid that contribute to A $\beta$  toxicity attenuation. This has significance with respect to the understanding of the A $\beta$ -sialic acid interaction that takes place in-vivo. Also, this will be of importance to groups investigating polysaccharide structures for therapeutic development.

## 5. CONCLUSIONS

### 5.1. Introduction

Despite over a century of research, the world's most prominent neurodegenerative disease, Alzheimer's disease (AD), still does not have clearly defined mechanisms, causes or cures. The work presented in this dissertation is a step towards understanding the missing pieces. One of the fundamental hallmarks of AD brain is the presence of aggregated amyloid-beta peptide ( $A\beta$ ) deposits and hence  $A\beta$  is posited to play a central role in the pathology of the disease. One theory is that  $A\beta$  toxicity is linked to the formation of toxic species, others believe that  $A\beta$  acts via association with the cell membrane causing toxicity. There are also several theorized environmental conditions that lead to the development of AD. However, it is generally agreed upon that, the first step in any of the mechanisms of  $A\beta$  action on the cell is  $A\beta$  binding to the cell membrane. To put this in a different context, there can be several different mechanisms or a combination of mechanisms that are causes neurotoxicity, but if the toxic species cannot interact with the neurons, there cannot be neurotoxicity associated with it. The understanding is that,  $A\beta$  has to interact with the cell to cause neurotoxicity, and this interaction occurs through the cell membrane in a still unexplained manner. It is precisely this theoretical bottleneck region that we plan to target.

One of the many goals of this project was to design biomimetic compounds to which  $A\beta$  will have higher affinity compared to its affinity towards cell membranes. Thus, in an *in-vitro* system with a model neuroblastoma cell line, we can expect excellent toxicity attenuation properties from the compounds against  $A\beta$ . One of the important observations that made this approach feasible is that  $A\beta$  shows affinity or binds to the sialic acids that are present on the gangliosides in the cell membranes. Particularly, this affinity of  $A\beta$  was higher when these

surface sialic acid moieties on the gangliosides are clustered together. Another important observation in favor of this approach was the observation that removal of cell surface sialic acids have been found to attenuate A $\beta$  toxicity. To this end, the dissertation focuses on the synthesis of such biomimetics compounds that are multivalent in sugars or sialic acid and the ability of such complexes to preferentially interfere with cell-A $\beta$  interactions. Another goal of this project was to identify the concentration or the clustering of sialic acids that show the highest toxicity attenuation. This will help us to understand the mechanisms behind A $\beta$ -cell membrane interactions.

Earlier works with sialic acid labeled dendrimer complexes [8, 26] have shown limited success in attenuating the toxicity of A $\beta$ . However, it was clear that A $\beta$  had higher affinity to these labeled dendrimers. As the dendrimers structure was rigid, it would be possible that labeling of sialic acids was suboptimum for A $\beta$  binding. Also, the different dendrimers tested had different levels of intrinsic toxicity towards the cells, which affected the toxicity attenuating properties of these constructs.

## **5.2. Sialic Acid Labeled Chitosan for the Attenuation of A $\beta$ Toxicity**

Chitosan is a versatile polysaccharide that has excellent biological properties with host of applications. The use of chitosan is a definite improvement over earlier works since chitosan is a non-toxic, biocompatible and a FDA approved biopolymer. Also, chitosan provided the amine functional group that could be modified without affecting the fundamental linear substructure of chitosan, thereby retaining its linearity, flexibility and act as a carrier for sialic acid molecules which is critical in order to mimic neuronal membranes and to attenuate toxicity of A $\beta$ .

Another important conclusion is the effectiveness of EDC chemistry with Sulfo-NHS to successfully couple the carboxylic acid group of sialic acid with the amine group present in the chitosan molecule. The amide linkage formed was successfully proved using FTIR results which showed the loss of primary amines and the presence of amide linkage in complex spectra that could only come from the coupling of sialic acid to chitosan via amide bonds. Thus, by varying the ratio of moles of sialic acid added to the reaction mixture compared to the moles of primary amines of chitosan, we succeeded in synthesizing sialic acid labeled chitosan complexes with varying degree of labeling of sialic acid or varying number of sialic acid residues on chitosan. The quantification of the amount of sialic acid present on chitosan was done using the Warren Assay which gave a red chromophore whose absorbance could be correlated to the amount of sialic acid. This important achievement of different amount of SA labeling (8% to 48%) table 3, allowed us to test the effectiveness of the complexes with different amounts of sialic acid on a linear flexible backbone to attenuate toxicity of A $\beta$  in a system of differentiated SH-SY5Y cells.

We have shown that a linear polysialiated structure that mimics the NCAM of a neuron shows significant ability to attenuate A $\beta$  toxicity *in vitro*. This indicates that to achieve the clustering effects shown in previous works does not require an a priori clustered backbone (like starburst dendrimers) and that a linear structure with sufficient flexibility will naturally achieve the clustered state when interacting with A $\beta$  (based on equivalent protective properties). Based on the toxicity attenuation results, it can be concluded that all complexes as well as naïve chitosan were effective in attenuating the toxicity of A $\beta$  (in all cases,  $p < 0.01$ ). Using a flexible backbone, it was observed that 37% labeling of chitosan by sialic acid shows the optimum protective properties, indicating a balance between the degree of sialic acid labeling and backbone flexibility (which will allow the sialic acid molecules to effectively cluster). Of more

interest is the fact that chitosan showed similar protective properties to the labeled compounds, thus indicating that there are other biological cyclic sugars that could prove to be equally or more effective than sialic acid in preventing A $\beta$  toxicity. It also suggests that the sialic acid-chitosan mimic interaction with A $\beta$  peptide and cells must be more than just competing with each other or simply electrostatic interactions. It has been suggested that either the lysines or histidines on the toxic A $\beta$  peptide species interact with the negatively charged sugars present on the cell membrane which are detrimental to cell health. Thus, we believe that the introduction of our complex with sialic acid residues creates another charged species that attracts A $\beta$  and this could shield the cell from the harmful interactions with A $\beta$ . This postulate could explain the toxicity attenuation shown by unlabeled chitosan in solution in addition to the complexes. With the technique we have developed to control the degree of labeling of a polyamine using EDC chemistry with high repeatability, we will be able to move forward and investigate other sugars in a similar way to the study presented here.

This work thus addresses the question whether biomimetics could be applied successfully to reduce the toxicity of A $\beta$  peptide. The use of chitosan made it possible to have a backbone that allowed the labeled sialic acids to effectively cluster, which was critical in toxicity attenuation. A significant number of studies have demonstrated the importance of clustering of sugars; our work is successful in predicting the optimum sialic acid concentration that shows highest protective properties.

### **5.3. Evaluation of Sialic Acid Analogs for the Attenuation of A $\beta$ Toxicity**

From the results of Chapter 3, it is clear that sialic acid (N-acetylneuraminic acid) labeled chitosan was effective in attenuating toxicity without the toxicity associated with the backbone

molecule. Since, chitosan showed protective properties, it was retained as the backbone molecule and the ability of other sugars (than sialic acid) to attenuate the toxicity was investigated keeping sialic acid as the benchmark for comparison with other sugars.

Since we are certain that A $\beta$  binds to sialic acids on the neuronal membrane in the brain, the most effective method to design a biomimetic (as a potential therapeutic) would be to understand which part of the sialic acid structure does A $\beta$  show the highest affinity or binds to. Thus, one of the goals of this work was to identify the core structures or the unique –R groups of sialic acid which are critical for toxicity association. Second goal was to determine whether other sugars show better or similar protective properties than sialic acid. The selection of different sugars was done keeping these criteria in mind.

We were successful in using EDC chemistry with high accuracy in conjugation of different sugars with chitosan. Also, this work demonstrates how EDC chemistry with Sulfo-NHS can be used with sufficient accuracy to achieve different percentage labeling of carboxylic acid containing molecules with an amine containing species. The verification of all conjugated complexes was done using FTIR which showed the presence of amide linkage in the complex spectra. Quantification of the amount of KDN and GA present on chitosan was done calorimetrically using the Aminoff and the carbazole assay methods.

From the intrinsic toxicity studies, it was evident that oxygen substitution in the ring structure (between CHC and Pyran) led to an increase in toxicity. Similar increase in toxicity for GA compared to KDN implied the importance of multi –OH tail in the intrinsic toxicity. All these point to the conclusion that decoration of therapeutics with such –OH tails may be necessary to prevent toxicity and address its therapeutic effects.

Since none of the analogs by themselves showed none protective properties, it reinforces the conclusion that clustering of sialic acid in the neuronal membranes is a necessary condition for A $\beta$  binding. Also, it concludes that simple addition of monomeric sialic acid moieties or GM1 molecules to aggregated A $\beta$  *in-vitro* will not be sufficient to achieve the protection desired from A $\beta$ .

For the complexes, KDN and Pyran complexes showed significant protective properties. As GA complex did not show any protection, we can believe that the multi –OH tail is the –R group that is involved in A $\beta$  interactions. Similarly, from the Pyran-CHC comparison, we found that oxygen substitution leads to increased toxicity attenuation indicating the possible role of oxygen in A $\beta$ -sialic acid interactions. This work elucidates the impact that certain structures of sialic acid and its analogs can have on A $\beta$  binding. It will allow for more specific and detailed improvements in the therapeutic polysaccharide structures that can be developed and modified to overcome other shortcomings of AD therapeutic development, particularly of penetrating the blood-brain barrier. Now that we know which or what structures are important, molecules could be developed that will be small enough the cross the Blood Brain Barrier.

The most followed approach in therapeutic development is to synthesize hundreds, thousands of structures or their analogs and test them brute force against the targets, out of which, a promising few advance for further testing. On an average, 5000 -10000 compounds are synthesized and tested over a period of several years out of which a select few make it to preclinical trials. Thus, there is no standard roadmap for drug synthesis that is being followed in this regard. This approach is costing millions in terms of man hours and money. The method we have used to design a therapeutic is focused towards developing the therapeutic in an efficient step-by-step way by understanding the role of each structure or functional group involved. This

way, we can design a novel drug that has just the structures or groups that are necessary in treating the disease. Using the method demonstrated in this research, i.e. to determine which substructure or core structure is effective as a possible therapeutic, will help to design therapeutic against a number of diseases and disorders more efficiently and smartly. Although we have just investigated this approach in the case of aggregated A $\beta$  in Alzheimer's disease, we can extent this approach to a wide variety of disease and applications. For example, there are several human protein diseases caused by misfolded or aggregated peptides which form fibrils with morphology similar to that observed in AD (see table 1). Most of the mechanisms behind these diseases involve membrane, lipid interactions. This is a dedicated approach that can be used for specific and targeted therapeutic development against such diseases.

## 6. FUTURE WORK

As with any research work with time limitations, there are several areas where the work done in this dissertation can be extended.

One of the immediate extensions of the current work is to develop small molecule therapeutics for A $\beta$  toxicity attenuation. Focus can be shifted to other more toxic A $\beta$  species such as ADDL's. Based on results from chapter 4, we will have a catalog of sugars or -R groups ready, that have shown the highest binding to A $\beta$  or protective effects from A $\beta$ . We can use this information to then design small molecule therapeutics which will show highest affinity towards A $\beta$  and A $\beta$  toxicity attenuation properties. Since we know the structures that exhibit intrinsic toxicity, we can avoid those when developing such a therapeutic. Additionally, we can move away from the need of a bulk backbone structure and focus on small molecules. These smart low MW biomimetic's could prove more effective in toxicity attenuation than the bulky polysialated materials. Also, based on the success of earlier work we could be able to shift from cyclic sugars to aliphatic compounds (such as poly-L-lysine) for the backbone. Other ideas for the backbone include diamino-alkanes such as 1,2 Diaminoethane (CAS 107-15-7) or 1,3 Diaminopropane (CAS 109-76-2). Other alkanes are available with 2-carbons to 19 carbons in their chains which will allow us to investigate the effect of sugar separation and backbone flexibility and how it affects therapeutic effectiveness. We have already shown that EDC chemistry can be used with sufficient accuracy to conjugate compounds which can be extended here. For other constructs, conjugation chemistries such as Thiol, Dicyclohexylcarbodiimide etc. can be investigated. Another area to explore can be to use double bonded alkenes instead of the alkanes to examine effect of backbone flexibility. This backbone will be more rigid due to the presence of a double

bond. This work can help researcher involved in development of polysaccharide molecules as possible therapeutic applications.

There has been no attempt in this work to understand the sites where these molecules are binding to the toxic A $\beta$  peptide. Also, we have not quantified the binding affinities of our biomaterials to the toxic A $\beta$  species. The binding of A $\beta$  to the complex synthesized should be investigated by the use of radiochemical techniques. One such technique, the Bolton Hunter method has been described for A $\beta$  in earlier works [8]. This would help in the estimation of the equilibrium dissociation constants for our complexes which can be compared with other works.

Additional area to pursue is to determine which species of A $\beta$ , protofibrils, oligomers are toxic to cells in culture. This is an critical missing piece of information in the AD puzzle. Using the information from chapter 3, we know which structures show the highest affinity. By attaching the novel compounds to an immobilized surface (most commonly used are gold surfaces), different species of A $\beta$  can tested to analyze their binding characteristics by techniques such as Surface Plasmon Resonance. Results from the binding constants using Bolton Hunter method and with particular A $\beta$  species will help us to determine the most toxic species that is neurotoxic to the cells.

One huge avenue that can be explored based on this work is the possibility of testing these constructs in-vivo on mouse models. Most of the therapeutics targeting the brain fails due to their bulky MW and its inability to cross the blood brain barrier. A small MW compound will be much easier to transport across the BBB to target the A $\beta$ A $\beta$  in the brain. This will provide the perfect set for *in vivo* tests later on. Our molecules can be attached to lipid or protein moieties that can easily cross the BBB. The efficacy of these constructs can be evaluated *in vivo*.

Extensive studies can be performed with mouse models that will help identify and further narrow the structures that show promise *in vivo*.

The work described in this dissertation provides a distinct roadmap to follow while investigating other diseases (see table 1). The next logical disease to investigate will be the aggregation and toxicity of  $\alpha$ -synuclein which is implicated in Parkinson's disease (PD). There is a major overlap in the mechanism between the two diseases, AD and PD. Also,  $\alpha$ -synuclein toxicity is postulated to be the result of the interactions between the aggregated peptide and neuronal membranes. Thus the same systematic development of therapeutic can be applied to investigate PD. Additionally, table 1 provides a number of diseases that are a result of protein aggregation or misfolding. This dissertation will provide the directions to investigate these diseases from a targeted therapeutic point-of-view.

## REFERENCES

1. Dahm, R., *Alois Alzheimer and the beginnings of research into Alzheimer's disease*, in *Alzheimer: 100 years and beyond*, M. Jucker, et al., Editors. 2006, Springer. p. 37-49.
2. Castellani, R.J., R.K. Rolston, and M.A. Smith, *Alzheimer Disease*. *Disease-a-month : DM*, 2010. **56**(9): p. 484-546.
3. Prince, M., R. Bryce, and C. Ferri, *World Alzheimer Report 2011, The benefits of early diagnosis and intervention*. Alzheimer's Disease International, 2011.
4. Rushworth, J.V. and N.M. Hooper, *Lipid Rafts: Linking Alzheimer's Amyloid-beta, Production, Aggregation, and Toxicity at Neuronal Membranes*. *International Journal of Alzheimer's Disease*, 2011. **2011**.
5. Grundke-Iqbal, I., et al., *Abnormal phosphorylation of the microtubule-associated protein tau (tau) in Alzheimer cytoskeletal pathology*. *Proceedings of the National Academy of Sciences of the United States of America*, 1986. **83**(13): p. 4913-4917.
6. Iqbal, K. and I. Grundke-Iqbal, *Opportunities and challenges in developing Alzheimer disease therapeutics*. *Acta Neuropathologica*, 2011. **122**(5): p. 543-549.
7. K. Iqbal, I.G.-I., *Alzheimer neurofibrillary degeneration: significance, etiopathogenesis, therapeutics and prevention*. *Journal of Cellular and Molecular Medicine*, 2008. **12**(1): p. 38-55.
8. Patel, D., J. Henry, and T. Good, *Attenuation of [beta]-amyloid induced toxicity by sialic acid-conjugated dendrimeric polymers*. *Biochimica et Biophysica Acta (BBA) - General Subjects*, 2006. **1760**(12): p. 1802-1809.
9. Pimplikar, S.W., *Reassessing the amyloid cascade hypothesis of Alzheimer's disease*. *The International Journal of Biochemistry & Cell Biology*, 2009. **41**(6): p. 1261-1268.
10. Parihar, M.S. and T. Hemnani, *Alzheimer's disease pathogenesis and therapeutic interventions*. *Journal of Clinical Neuroscience*, 2004. **11**(5): p. 456-467.

11. Minati, L., et al., *Reviews: Current Concepts in Alzheimer's Disease: A Multidisciplinary Review*. American Journal of Alzheimer's Disease and Other Dementias, 2009. **24**(2): p. 95-121.
12. Re, F., et al., *Beta Amyloid Aggregation Inhibitors: Small Molecules as Candidate Drugs for Therapy of Alzheimer's Disease*. Current Medicinal Chemistry, 2010. **17**(27): p. 2990-3006.
13. Hardy, J. and D.J. Selkoe, *Medicine - The amyloid hypothesis of Alzheimer's disease: Progress and problems on the road to therapeutics*. Science, 2002. **297**(5580): p. 353-356.
14. Hardy, J.A. and G.A. Higgins, *Alzheimer's disease: The amyloid cascade hypothesis*. Science, 1992. **256**(5054): p. 184.
15. Walsh, D.M., et al., *Amyloid beta -Protein Fibrillogenesis. Detection of a Protofibrillar Intermediate*. J. Biol. Chem., 1997. **272**(35): p. 22364-22372.
16. Walsh, D.M., et al., *Amyloid beta -Protein Fibrillogenesis. Structure and Biological Activity of Protofibrillar Intermediates*. J. Biol. Chem., 1999. **274**(36): p. 25945-25952.
17. M.Hoozemans, J.J., et al., *Always Around, Never the Same: Pathways of Amyloid Beta Induced Neurodegeneration Throughout the Pathogenic Cascade of Alzheimer's Disease*. Current Medicinal Chemistry, 2006. **13**(22): p. 2599-2605.
18. Zubenko, G., et al., *Platelet membrane fluidity in Alzheimer's disease and major depression*. Am J Psychiatry, 1987. **144**(7): p. 860-868.
19. Yanagisawa, K., et al., *GM1 ganglioside-bound amyloid beta-protein (Abeta): A possible form of preamyloid in Alzheimer's disease*. Nat Med, 1995. **1**(10): p. 1062-1066.
20. Yanagisawa, K. and Y. Ihara. *GM1 ganglioside-bound amyloid beta-protein in Alzheimer's disease brain*. 1998: Elsevier Science Inc.
21. Yanagisawa, K., *Role of gangliosides in Alzheimer's disease*. Biochimica et Biophysica Acta (BBA) - Biomembranes, 2007. **1768**(8): p. 1943-1951.

22. Hayashi, H., et al., *A seed for Alzheimer amyloid in the brain*. Journal of Neuroscience, 2004. **24**(20): p. 4894-4902.
23. Bucciantini, M., et al., *Toxic effects of amyloid fibrils on cell membranes: the importance of ganglioside GM1*. FASEB journal : official publication of the Federation of American Societies for Experimental Biology, 2012. **26**(2): p. 818-31.
24. Cantù, L., et al., *Gangliosides and the multiscale modulation of membrane structure*. Chemistry and Physics of Lipids, 2011. **164**(8): p. 796-810.
25. Sonnino, S., et al., *Gangliosides as components of lipid membrane domains*. Glycobiology, 2007. **17**(1): p. 1R-13.
26. Patel, D.A., J.E. Henry, and T.A. Good, *Attenuation of [beta]-amyloid-induced toxicity by sialic-acid-conjugated dendrimers: Role of sialic acid attachment*. Brain Research, 2007. **1161**: p. 95-105.
27. Kakio, A., et al., *Cholesterol-dependent Formation of GM1 Ganglioside-bound Amyloid beta -Protein, an Endogenous Seed for Alzheimer Amyloid*. J. Biol. Chem., 2001. **276**(27): p. 24985-24990.
28. Kakio, A., et al., *Interaction between amyloid beta-protein aggregates and membranes*. Journal of Peptide Science, 2004. **10**(10): p. 612-621.
29. Kakio, A., et al., *Interactions of Amyloid  $\beta$ -Protein with Various Gangliosides in Raft-Like Membranes: Importance of GM1 Ganglioside-Bound Form as an Endogenous Seed for Alzheimer Amyloid-beta*. Biochemistry, 2002. **41**(23): p. 7385-7390.
30. Matsuzaki, K., *Formation of Toxic Amyloid Fibrils by Amyloid-beta Protein on Ganglioside Clusters*. International Journal of Alzheimer's Disease, 2011. **2011**.
31. Yanagisawa, K., *Pathological significance of ganglioside clusters in Alzheimer's disease*. Journal of Neurochemistry, 2011. **116**(5): p. 806-812.
32. Ikeda, K., et al., *Mechanism of Amyloid  $\beta$ -Protein Aggregation Mediated by GM1 Ganglioside Clusters*. Biochemistry, 2011. **50**(29): p. 6433-6440.

33. Wang, S.S.-S., D.L. Rymer, and T.A. Good, *Reduction in Cholesterol and Sialic Acid Content Protects Cells from the Toxic Effects of  $\beta$ -Amyloid Peptides*. Journal of Biological Chemistry, 2001. **276**(45): p. 42027-42034.
34. Soto, C., *Plaque busters: strategies to inhibit amyloid formation in Alzheimer's disease*. Molecular Medicine Today, 1999. **5**(8): p. 343-350.
35. Association, A.s., *2011 Alzheimer's disease facts and figures*. Alzheimer's & dementia : the journal of the Alzheimer's Association, 2011. **7**(2): p. 208-244.
36. Rauk, A., *Why is the amyloid beta peptide of Alzheimer's disease neurotoxic?* Dalton Transactions, 2008(10): p. 1273-1282.
37. Terry, R., R. Katzman, and K. Bick, *Diagnosis, in Alzheimer's Disease*. 1994: Raven Pr. 9-25.
38. Honig LS, M.R., *Natural History of Alzheimer's disease*. Aging (Milano), 2001. **13**: p. 171-182.
39. Harvey, R.J., M. Skelton-Robinson, and M.N. Rossor, *The prevalence and causes of dementia in people under the age of 65 years*. J Neurol Neurosurg Psychiatry, 2003. **74**(9): p. 1206-1209.
40. Luchsinger, J.A. and R. Mayeux, *Dietary factors and Alzheimer's disease*. The Lancet Neurology, 2004. **3**(10): p. 579-587.
41. Mayeux, R., *Epidemiology of Neurodegeneration*. Annual Review of Neuroscience, 2003. **26**(1): p. 81-104.
42. Mayeux, R., et al., *Utility of the Apolipoprotein E Genotype in the Diagnosis of Alzheimer's Disease*. N Engl J Med, 1998. **338**(8): p. 506-511.
43. Blennow, K., M.J. de Leon, and H. Zetterberg, *Alzheimer's disease*. The Lancet, 2006. **368**(9533): p. 387-403.
44. Snowdon, D.A., et al., *Linguistic ability in early life and cognitive function and Alzheimer's disease in late life. Findings from the Nun Study*. JAMA, 1996. **275**(7): p. 528-532.

45. Alphonse Probst, D.L., Jürg Ulrich,, *Alzheimer's Disease: A Description of the Structural Lesions*. Brain Pathology, 1991. **1**(4): p. 229-239.
46. Iqbal, K., et al., *Tau pathology in Alzheimer disease and other tauopathies*. Biochimica et Biophysica Acta (BBA) - Molecular Basis of Disease, 2005. **1739**(2-3): p. 198-210.
47. Villemagne, V.L., et al., *The A $\beta$ centric Pathway of Alzheimer's Disease*, in *Abeta Peptide and Alzheimer's Disease: Celebrating a Century of Research*, C.J. Barrow and D.H. Small, Editors. 2007.
48. Roland Jakob-Roetne, H.J., *Alzheimer's Disease: From Pathology to Therapeutic Approaches*. Angewandte Chemie International Edition, 2009. **48**(17): p. 3030-3059.
49. Glenner, G.G. and C.W. Wong, *Alzheimer's disease: Initial report of the purification and characterization of a novel cerebrovascular amyloid protein*. Biochemical and Biophysical Research Communications, 1984. **120**(3): p. 885-890.
50. Li, B., et al., *Disruption of microtubule network by Alzheimer abnormally hyperphosphorylated tau*. Acta Neuropathologica, 2007. **113**(5): p. 501-511.
51. Ishiguro, K., et al., *A serine/threonine proline kinase activity is included in the tau protein kinase fraction forming a paired helical filament epitope*. Neuroscience Letters, 1991. **128**(2): p. 195-198.
52. Martin, L., X. Latypova, and F. Terro, *Post-translational modifications of tau protein: Implications for Alzheimer's disease*. Neurochemistry International, 2011. **58**(4): p. 458-471.
53. Pritchard, S.M., et al., *The toxicity of tau in Alzheimer disease: turnover, targets and potential therapeutics*. Journal of Cellular and Molecular Medicine, 2011. **15**(8): p. 1621-1635.
54. Noble, W., A.M. Pooler, and D.P. Hanger, *Advances in tau-based drug discovery*. Expert Opinion on Drug Discovery, 2011. **6**(8): p. 797-810.
55. Miyata, Y., et al., *Molecular chaperones and regulation of tau quality control: strategies for drug discovery in tauopathies*. Future Medicinal Chemistry, 2011. **3**(12): p. 1523-1537.

56. Gotz, J., et al., *Modes of Amyloid-beta toxicity in Alzheimer's disease*. Cellular and Molecular Life Sciences, 2011. **68**(20): p. 3359-3375.
57. Cappai, R. and A.R. White, *Amyloid  $\beta$* . The International Journal of Biochemistry & Cell Biology, 1999. **31**(9): p. 885-889.
58. Masters, C.L., et al., *Amyloid plaque core protein in Alzheimer disease and Down syndrome*. Proceedings of the National Academy of Sciences of the United States of America, 1985. **82**(12): p. 4245-4249.
59. Wilquet, V. and B.D. Strooper, *Amyloid-beta precursor protein processing in neurodegeneration*. Current Opinion in Neurobiology, 2004. **14**(5): p. 582-588.
60. Kremer, J.J. and R.M. Murphy, *Kinetics of adsorption of beta-amyloid peptide A beta(1-40) to lipid bilayers*. Journal of Biochemical and Biophysical Methods, 2003. **57**(2): p. 159-169.
61. Nathalie, P. and O. Jean-Noël, *Processing of Amyloid Precursor Protein and Amyloid Peptide Neurotoxicity*. Current Alzheimer Research, 2008. **5**(2): p. 92-99.
62. Grimm, M.O.W., H.S. Grimm, and T. Hartmann, *Amyloid beta as a regulator of lipid homeostasis*. Trends in Molecular Medicine, 2007. **13**(8): p. 337-344.
63. Vardy, E.R.L.C., A.J. Catto, and N.M. Hooper, *Proteolytic mechanisms in amyloid-beta metabolism: therapeutic implications for Alzheimer's disease*. Trends in Molecular Medicine, 2005. **11**(10): p. 464-472.
64. Cole, S.L. and R. Vassar, *BACE1 Structure and Function in Health and Alzheimer's Disease*. Current Alzheimer Research, 2008. **5**(2): p. 100-120.
65. Bateman, D., J. McLaurin, and A. Chakrabarty, *Requirement of aggregation propensity of Alzheimer amyloid peptides for neuronal cell surface binding*. BMC Neuroscience, 2007. **8**(1): p. 29.
66. Maltsev, A.V., S. Bystryak, and O.V. Galzitskaya, *The role of  $\beta$ -amyloid peptide in neurodegenerative diseases*. Ageing Research Reviews, 2011. **10**(4): p. 440-452.

67. Praticò, D., *Oxidative stress hypothesis in Alzheimer's disease: a reappraisal*. Trends in Pharmacological Sciences, 2008. **29**(12): p. 609-615.
68. Grundman, M. and P. Delaney, *Antioxidant strategies for Alzheimer's disease*. Proceedings of the Nutrition Society, 2002. **61**(02): p. 191-202.
69. Lin, H., R. Bhatia, and R. Lal, *Amyloid {beta} protein forms ion channels: implications for Alzheimer's disease pathophysiology*. FASEB J., 2001. **15**(13): p. 2433-2444.
70. Du Yan, S., et al., *An intracellular protein that binds amyloid-[beta] peptide and mediates neurotoxicity in Alzheimer's disease*. Nature, 1997. **389**(6652): p. 689-695.
71. Yankner, B.A. and T. Lu, *Amyloid {beta}-Protein Toxicity and the Pathogenesis of Alzheimer Disease*. J. Biol. Chem., 2009. **284**(8): p. 4755-4759.
72. Hardy, J. and D.J. Selkoe, *The Amyloid Hypothesis of Alzheimer's Disease: Progress and Problems on the Road to Therapeutics*. Sci. Aging Knowl. Environ., 2002. **2002**(29): p. or8-.
73. Scheuner, D., et al., *Secreted amyloid [beta]-protein similar to that in the senile plaques of Alzheimer's disease is increased in vivo by the presenilin 1 and 2 and APP mutations linked to familial Alzheimer's disease*. Nat Med, 1996. **2**(8): p. 864-870.
74. Tansley, G.H., et al., *The cholesterol transporter ABCG1 modulates the subcellular distribution and proteolytic processing of {beta}-amyloid precursor protein*. J. Lipid Res., 2007. **48**(5): p. 1022-1034.
75. Kaye, R., et al., *Common Structure of Soluble Amyloid Oligomers Implies Common Mechanism of Pathogenesis*. Science, 2003. **300**(5618): p. 486-489.
76. Multhaup, G., et al., *Reactive oxygen species and Alzheimer's disease*. Biochemical Pharmacology, 1997. **54**(5): p. 533-539.
77. Selkoe, D.J., *Alzheimer's Disease Is a Synaptic Failure*. Science, 2002. **298**(5594): p. 789-791.

78. Braak, F., H. Braak, and E. Mandelkow, *A sequence of cytoskeleton changes related to the formation of neurofibrillary tangles and neuropil threads*. *Acta Neuropathologica*, 1994. **87**(6): p. 554-567.
79. Smith, M.A., et al., *Iron accumulation in Alzheimer disease is a source of redox-generated free radicals*. *Proceedings of the National Academy of Sciences of the United States of America*, 1997. **94**(18): p. 9866-9868.
80. Zheng, H., et al., *[beta]-amyloid precursor protein-deficient mice show reactive gliosis and decreased locomotor activity*. *Cell*, 1995. **81**(4): p. 525-531.
81. Findeis, M.A., *The role of amyloid [beta] peptide 42 in Alzheimer's disease*. *Pharmacology & Therapeutics*, 2007. **116**(2): p. 266-286.
82. Teng, F.Y.H. and B.L. Tang, *Widespread [gamma]-secretase activity in the cell, but do we need it at the mitochondria?* *Biochemical and Biophysical Research Communications*, 2005. **328**(1): p. 1-5.
83. Plant, L.D., et al., *The Production of Amyloid {beta} Peptide Is a Critical Requirement for the Viability of Central Neurons*. *J. Neurosci.*, 2003. **23**(13): p. 5531-5535.
84. Walsh, D.M. and D.J. Selkoe, *A-beta Oligomers - a decade of discovery*. *Journal of Neurochemistry*, 2007. **101**(5): p. 1172-1184.
85. Larson, M.E. and S.E. Lesne, *Soluble A ss oligomer production and toxicity*. *Journal of Neurochemistry*, 2012. **120**: p. 125-139.
86. DaSilva, K.A., J.E. Shaw, and J. McLaurin, *Amyloid- $\beta$  fibrillogenesis: Structural insight and therapeutic intervention*. *Experimental Neurology*, 2010. **223**(2): p. 311-321.
87. Wolfe, K.J. and D.M. Cyr, *Amyloid in neurodegenerative diseases: Friend or foe?* *Seminars in Cell & Developmental Biology*, 2011. **22**(5): p. 476-481.
88. Wang, J., et al., *The Levels of Soluble versus Insoluble Brain A[beta] Distinguish Alzheimer's Disease from Normal and Pathologic Aging*. *Experimental Neurology*, 1999. **158**(2): p. 328-337.

89. Sakono, M. and T. Zako, *Amyloid oligomers: formation and toxicity of A beta oligomers*. FEBS Journal, 2010. **277**(6): p. 1348-1358.
90. Ono, K., M.M. Condron, and D.B. Teplow, *Structure–neurotoxicity relationships of amyloid  $\beta$ -protein oligomers*. Proceedings of the National Academy of Sciences, 2009. **106**(35): p. 14745-14750.
91. Lublin, A.L. and S. Gandy, *Amyloid- $\beta$  Oligomers: Possible Roles as Key Neurotoxins in Alzheimer's Disease*. Mount Sinai Journal of Medicine: A Journal of Translational and Personalized Medicine, 2010. **77**(1): p. 43-49.
92. Glabe, C.G., *Structural Classification of Toxic Amyloid Oligomers*. Journal of Biological Chemistry, 2008. **283**(44): p. 29639-29643.
93. Marcus, F., *Oligomeric Intermediates in Amyloid Formation: Structure Determination and Mechanisms of Toxicity*. Journal of Molecular Biology, (0).
94. Morgado, I. and M. Fändrich, *Assembly of Alzheimer's A $\beta$  peptide into nanostructured amyloid fibrils*. Current Opinion in Colloid & Interface Science, 2011. **16**(6): p. 508-514.
95. Lambert, M.P., et al., *Diffusible, nonfibrillar ligands derived from A $\beta$  1-42 are potent central nervous system neurotoxins*. Proceedings of the National Academy of Sciences of the United States of America, 1998. **95**(11): p. 6448-6453.
96. Lesne, S., et al., *A specific amyloid- $\beta$  protein assembly in the brain impairs memory*. Nature, 2006. **440**(7082): p. 352-357.
97. Huang, T.H.J., et al., *Alternate Aggregation Pathways of the Alzheimer beta -Amyloid Peptide. An In Vito Model of Preamyloid*. J. Biol. Chem., 2000. **275**(46): p. 36436-36440.
98. Nerelius, C., J. Johansson, and A. Sandegren, *Amyloid beta-peptide aggregation. What does it result in and how can it be prevented?* Frontiers in Bioscience, 2009. **14**: p. 1716-U3856.
99. Ghanta, J., et al., *A Strategy for Designing Inhibitors of beta -Amyloid Toxicity*. J. Biol. Chem., 1996. **271**(47): p. 29525-29528.

100. Schladitz, C., et al., *Amyloid-[beta]-Sheet Formation at the Air-Water Interface*. Biophysical Journal, 1999. **77**(6): p. 3305-3310.
101. Coles, M., et al., *Solution Structure of Amyloid Beta Peptide (1-40) in a Water-Micelle Environment. Is the Membrane-Spanning Domain Where We Think It Is?* Biochemistry, 1998. **37**(31): p. 11064-11077.
102. Serpell, L.C., *Alzheimer's amyloid fibrils: structure and assembly*. Biochimica et Biophysica Acta (BBA) - Molecular Basis of Disease, 2000. **1502**(1): p. 16-30.
103. Irie, K., et al., *Structure of beta-amyloid fibrils and its relevance to their neurotoxicity: Implications for the pathogenesis of Alzheimer's disease*. Journal of Bioscience and Bioengineering, 2005. **99**(5): p. 437-447.
104. Tjernberg, L.O., et al., *A Molecular Model of Alzheimer Amyloid beta -Peptide Fibril Formation*. J. Biol. Chem., 1999. **274**(18): p. 12619-12625.
105. Antzutkin, O.N., et al., *Supramolecular Structural Constraints on Alzheimer's beta-Amyloid Fibrils from Electron Microscopy and Solid-State Nuclear Magnetic Resonance*. Biochemistry, 2002. **41**(51): p. 15436-15450.
106. Petkova, A.T., et al., *A structural model for Alzheimer's beta- amyloid fibrils based on experimental constraints from solid state NMR*. Proceedings of the National Academy of Sciences of the United States of America, 2002. **99**(26): p. 16742-16747.
107. Pedersen, J.S. and D.E. Otzen, *Amyloid - a state in many guises: Survival of the fittest fibril fold*. Protein Science, 2008. **17**(1): p. 2-10.
108. Paravastu, A.K., et al., *Seeded growth of beta-amyloid fibrils from Alzheimer's brain-derived fibrils produces a distinct fibril structure*. Proceedings of the National Academy of Sciences of the United States of America, 2009. **106**(18): p. 7443-7448.
109. Van Rooijen, B.D., M.M.A.E. Claessens, and V. Subramaniam, *Membrane Interactions of Oligomeric Alpha-Synuclein: Potential Role in Parkinson's Disease*. Current Protein & Peptide Science, 2010. **11**(5): p. 334-342.
110. Auluck, P.K., G. Caraveo, and S. Lindquist,  *$\alpha$ -Synuclein: Membrane Interactions and Toxicity in Parkinson's Disease*. Annual Review of Cell and Developmental Biology, 2010. **26**(1): p. 211-233.

111. Cara-Lynne, S., *Lipid rafts: Keys to neurodegeneration*. Brain Research Bulletin, 2010. **82**(1–2): p. 7-17.
112. McLaurin, J., et al., *Structural Transitions Associated with the Interaction of Alzheimer beta -Amyloid Peptides with Gangliosides*. J. Biol. Chem., 1998. **273**(8): p. 4506-4515.
113. McLaurin, J. and A. Chakrabartty, *Membrane Disruption by Alzheimer beta -Amyloid Peptides Mediated through Specific Binding to Either Phospholipids or Gangliosides. Implications for Neurotoxicity*. J. Biol. Chem., 1996. **271**(43): p. 26482-26489.
114. Choo-Smith, L.-P.i. and W.K. Surewicz, *The interaction between Alzheimer amyloid [beta](1-40) peptide and ganglioside GM1-containing membranes*. FEBS Letters, 1997. **402**(2-3): p. 95-98.
115. Mandal, P. and J. Pettegrew, *Alzheimer's Disease: NMR Studies of Asialo (GM1) and Trisialo (GT1b) Ganglioside Interactions with Aβ(1-40) Peptide in a Membrane Mimic Environment*. Neurochemical Research, 2004. **29**(2): p. 447-453.
116. Matsuzaki, K. and C. Horikiri, *Interactions of Amyloid-beta Peptide (1-40) with Ganglioside containing Membranes*. Biochemistry, 1999. **38**(13): p. 4137-4142.
117. Chi, E.Y., S.L. Frey, and K.Y.C. Lee, *Ganglioside GM1-Mediated Amyloid-beta Fibrillogenesis and Membrane Disruption*. Biochemistry, 2007. **46**(7): p. 1913-1924.
118. McLaurin, J. and A. Chakrabartty, *Characterization of the interactions of Alzheimer beta-amyloid peptides with phospholipid membranes*. European Journal of Biochemistry, 1997. **245**(2): p. 355-363.
119. Verdier, Y. and B. Penke, *Binding Sites of Amyloid beta-Peptide in Cell Plasma Membrane and Implications for Alzheimer's Disease*. Current Protein & Peptide Science, 2004. **5**(1): p. 19-31.
120. Eckert, G.P., W.G. Wood, and W.E. Müller, *Lipid Membranes and β-Amyloid: A Harmful Connection*. Current Protein & Peptide Science, 2010. **11**(5): p. 319-325.
121. Vetrivel, K.S. and G. Thinakaran, *Membrane rafts in Alzheimer's disease beta-amyloid production*. Biochimica Et Biophysica Acta-Molecular and Cell Biology of Lipids, 2010. **1801**(8): p. 860-867.

122. Waschuk, S.A., et al., *Cellular Membrane Composition Defines Abeta -Lipid Interactions*. J. Biol. Chem., 2001. **276**(36): p. 33561-33568.
123. Terzi, E., G. Holzemann, and J. Seelig, *Alzheimer Beta-Amyloid Peptide 25-35: Electrostatic Interactions with Phospholipid Membranes*. Biochemistry, 1994. **33**(23): p. 7434-7441.
124. Terzi, E., G. Holzemann, and J. Seelig, *Interaction of Alzheimer beta-amyloid peptide(1-40) with lipid membranes*. Biochemistry, 1997. **36**(48): p. 14845-14852.
125. Wang, S.S.S., D.L. Rymer, and T.A. Good, *Reduction in cholesterol and sialic acid content protects cells from the toxic effects of beta-amyloid peptides*. Journal of Biological Chemistry, 2001. **276**(45): p. 42027-42034.
126. Ikeda, K. and K. Matsuzaki, *Driving force of binding of amyloid [beta]-protein to lipid bilayers*. Biochemical and Biophysical Research Communications, 2008. **370**(3): p. 525-529.
127. Jelinek, R. and T. Sheynis, *Amyloid - Membrane Interactions: Experimental Approaches and Techniques*. Current Protein & Peptide Science, 2010. **11**(5): p. 372-384.
128. Schwarz, A. and A.H. Futerman, *The localization of gangliosides in neurons of the central nervous system: the use of anti-ganglioside antibodies*. Biochimica et Biophysica Acta (BBA) - Reviews on Biomembranes, 1996. **1286**(3): p. 247-267.
129. Ariga, T., M.P. McDonald, and R.K. Yu, *Sphingolipids. Role of ganglioside metabolism in the pathogenesis of Alzheimer's disease--a review*. J. Lipid Res., 2008. **49**(6): p. 1157-1175.
130. Lloyd, K.O. and K. Furukawa, *Biosynthesis and functions of gangliosides: recent advances*. Glycoconjugate Journal, 1998. **15**(7): p. 627-636.
131. Matsuzaki, K., *Physicochemical interactions of amyloid [beta]-peptide with lipid bilayers*. Biochimica et Biophysica Acta (BBA) - Biomembranes, 2007. **1768**(8): p. 1935-1942.
132. Crino, P.B., et al., *Brain Gangliosides in Dementia of the Alzheimer Type*. Archives of Neurology, 1989. **46**(4): p. 398-401.

133. Terzi, E., G. Hölzemann, and J. Seelig, *Self-association of [beta]-Amyloid Peptide (1-40) in Solution and Binding to Lipid Membranes*. Journal of Molecular Biology, 1995. **252**(5): p. 633-642.
134. Choo-Smith, L.-P.i., et al., *Acceleration of Amyloid Fibril Formation by Specific Binding of Abeta -(1-40) Peptide to Ganglioside-containing Membrane Vesicles*. J. Biol. Chem., 1997. **272**(37): p. 22987-22990.
135. Ariga, T., et al., *Characterization of high-affinity binding between gangliosides and amyloid beta-protein*. Archives of Biochemistry and Biophysics, 2001. **388**(2): p. 225-230.
136. Simons, K. and E. Ikonen, *Functional rafts in cell membranes*. Nature, 1997. **387**(6633): p. 569-572.
137. Williamson, M.P., et al., *Binding of amyloid beta-peptide to ganglioside micelles is dependent on histidine-13*. Biochem J, 2006. **397**(3): p. 483-490.
138. Ogawa, M., et al., *Ganglioside-mediated aggregation of amyloid beta-proteins (A beta): comparison between A beta-(1-42) and A beta-(1-40)*. Journal of Neurochemistry, 2011. **116**(5): p. 851-857.
139. Klafki, H.-W., et al., *Therapeutic approaches to Alzheimer's disease*. Brain, 2006. **129**(11): p. 2840-2855.
140. Mandavilli, A., *The amyloid code*. Nat Med, 2006. **12**(7): p. 747-751.
141. Lleo, A., *Current therapeutic options for Alzheimer's disease*. Current Genomics, 2007. **8**(8): p. 550-558.
142. Schenk, D., et al., *Immunization with amyloid-[beta] attenuates Alzheimer-disease-like pathology in the PDAPP mouse*. Nature, 1999. **400**(6740): p. 173-177.
143. Bard, F., et al., *Peripherally administered antibodies against amyloid [beta]-peptide enter the central nervous system and reduce pathology in a mouse model of Alzheimer disease*. Nat Med, 2000. **6**(8): p. 916-919.

144. Gilman, S., et al., *Clinical effects of A{beta} immunization (AN1792) in patients with AD in an interrupted trial*. *Neurology*, 2005. **64**(9): p. 1553-1562.
145. Brody, D.L. and D.M. Holtzman, *Active and Passive Immunotherapy for Neurodegenerative Disorders*. *Annual Review of Neuroscience*, 2008. **31**(1): p. 175-193.
146. Scarpini, E., P. Schelterns, and H. Feldman, *Treatment of Alzheimer's disease; current status and new perspectives*. *The Lancet Neurology*, 2003. **2**(9): p. 539-547.
147. Seow, D. and S. Gauthier, *Pharmacotherapy of Alzheimer Disease*. *Canadian Journal of Psychiatry*, 2007. **52**(10): p. 620-629.
148. Barten, D. and C. Albright, *Therapeutic Strategies for Alzheimer's Disease*. *Molecular Neurobiology*, 2008. **37**(2): p. 171-186.
149. Creed, M. and N. Milgram, *Amyloid-modifying therapies for Alzheimer's disease: therapeutic progress and its implications*. *AGE*, 2010. **32**(3): p. 365-384.
150. Hawkes, C.A., V. Ng, and J. McLaurin, *Small Molecule Inhibitors of A beta-Aggregation and Neurotoxicity*. *Drug Development Research*, 2009. **70**(2): p. 111-124.
151. Tjernberg, L.O., et al., *Arrest of beta-amyloid fibril formation by a pentapeptide ligand*. *Journal of Biological Chemistry*, 1996. **271**(15): p. 8545-8548.
152. Soto, C., et al., *beta-sheet breaker peptides inhibit fibrillogenesis in a rat brain model of amyloidosis: Implications for Alzheimer's therapy*. *Nature Medicine*, 1998. **4**(7): p. 822-826.
153. Kenche, V.B. and K.J. Barnham, *Alzheimer's disease & metals: therapeutic opportunities*. *British Journal of Pharmacology*, 2011. **163**(2): p. 211-219.
154. Eckert, G.P., W.E. Muller, and W.G. Wood, *Cholesterol-lowering drugs and Alzheimer's disease*. *Future Lipidology*, 2007. **2**(4): p. 423-432.
155. Makimura, Y., et al., *Chemoenzymatic synthesis and application of a sialoglycopolymer with a chitosan backbone as a potent inhibitor of human influenza virus hemagglutination*. *Carbohydrate Research*, 2006. **341**(11): p. 1803-1808.

156. Cowan, C.B., G.L. Coté, and T.A. Good, *Development of photocrosslinked sialic acid containing polymers for use in amyloid-beta toxicity attenuation*. *Biomaterials*, 2008. **29**(24-25): p. 3408-3414.
157. Umemura, M., et al., *Design of a Sialylglycopolymer with a Chitosan Backbone Having Efficient Inhibitory Activity against Influenza Virus Infection*. *Journal of Medicinal Chemistry*, 2008. **51**(15): p. 4496-4503.
158. Reuter, J.D., et al., *Inhibition of Viral Adhesion and Infection by Sialic-Acid-Conjugated Dendritic Polymers*. *Bioconjugate Chemistry*, 1999. **10**(2): p. 271-278.
159. Landers, J.J., et al. *Prevention of influenza pneumonitis by sialic acid-conjugated dendritic polymers*. 2002.
160. Mishra, V., U. Gupta, and N.K. Jain, *Surface-Engineered Dendrimers: a Solution for Toxicity Issues*. *Journal of Biomaterials Science-Polymer Edition*, 2009. **20**(2): p. 141-166.
161. Patel, D.A., *Understanding the mechanism of preventing beta-amyloid induced neurotoxicity in Alzheimer's Disease*, in *Department of Chemical and Biochemical Engineering*. 2007, University of Maryland. p. 4-24.
162. Cowan, C.B., D.A. Patel, and T.A. Good, *Exploring the mechanism of beta-amyloid toxicity attenuation by multivalent sialic acid polymers through the use of mathematical models*. *Journal of Theoretical Biology*, 2009. **258**(2): p. 189-197.
163. Dash, M., et al., *Chitosan—A versatile semi-synthetic polymer in biomedical applications*. *Progress in Polymer Science*, 2011. **36**(8): p. 981-1014.
164. Marguerite, R., *Chitin and chitosan: Properties and applications*. *Progress in Polymer Science*, 2006. **31**(7): p. 603-632.
165. Pillai, C.K.S., W. Paul, and C.P. Sharma, *Chitin and chitosan polymers: Chemistry, solubility and fiber formation*. *Progress in Polymer Science*, 2009. **34**(7): p. 641-678.
166. Zhang, J.L., et al., *Chitosan Modification and Pharmaceutical/Biomedical Applications*. *Marine Drugs*, 2010. **8**(7): p. 1962-1987.

167. Sarti, F. and A. Bernkop-Schnurch, *Chitosan and Thiolated Chitosan*, in *Chitosan for Biomaterials I*, R. Jayakumar, M. Prabakaran, and R.A.A. Muzzarelli, Editors. 2011, Springer-Verlag Berlin: Berlin. p. 93-110.
168. Kim, I.Y., et al., *Chitosan and its derivatives for tissue engineering applications*. Biotechnology Advances, 2008. **26**(1): p. 1-21.
169. Kumar, M.N.V.R., et al., *Chitosan Chemistry and Pharmaceutical Perspectives*. Chemical Reviews, 2004. **104**(12): p. 6017-6084.
170. Singla, A.K. and M. Chawla, *Chitosan: some pharmaceutical and biological aspects - an update*. Journal of Pharmacy and Pharmacology, 2001. **53**(8): p. 1047-1067.
171. Nagpal, K., S.K. Singh, and D.N. Mishra, *Chitosan Nanoparticles: A Promising System in Novel Drug Delivery*. Chemical & Pharmaceutical Bulletin, 2010. **58**(11): p. 1423-1430.
172. Raafat, D., et al., *Insights into the mode of action of chitosan as an antibacterial compound*. Applied and Environmental Microbiology, 2008. **74**(12): p. 3764-3773.
173. Schipper, N.G.M., K.M. Vårum, and P. Artursson, *Chitosans as Absorption Enhancers for Poorly Absorbable Drugs. 1: Influence of Molecular Weight and Degree of Acetylation on Drug Transport Across Human Intestinal Epithelial (Caco-2) Cells*. Pharmaceutical Research, 1996. **13**(11): p. 1686-1692.
174. Ravi Kumar, M.N.V., *A review of chitin and chitosan applications*. Reactive and Functional Polymers, 2000. **46**(1): p. 1-27.
175. Muzzarelli, R.A.A. and C. Muzzarelli, *Chitosan chemistry: Relevance to the biomedical sciences*, in *Polysaccharides I: Structure, Characterization and Use*. 2005. p. 151-209.
176. Janes, K.A., P. Calvo, and M.J. Alonso, *Polysaccharide colloidal particles as delivery systems for macromolecules*. Advanced Drug Delivery Reviews, 2001. **47**(1): p. 83-97.
177. Eugene, K., *Chitin: a biomaterial in waiting*. Current Opinion in Solid State and Materials Science, 2002. **6**(4): p. 313-317.

178. Janas, T. and T. Janas, *Membrane oligo- and polysialic acids*. *Biochimica et Biophysica Acta (BBA) - Biomembranes*, 2011. **1808**(12): p. 2923-2932.
179. Mattson, G., et al., *A Practical Approach to Cross-Linking*. *Molecular Biology Reports*, 1993. **17**(3): p. 167-183.
180. Hermanson, G.T., *Zero-Length Crosslinkers*, in *Bioconjugate Techniques (Second Edition)*. 2008, Academic Press: New York. p. 213-233.
181. Grabarek, Z. and J. Gergely, *Zero-length crosslinking procedure with the use of active esters*. *Analytical Biochemistry*, 1990. **185**(1): p. 131-135.
182. Zagorski, M.G., et al., *[13] Methodological and chemical factors affecting amyloid  $\beta$  peptide amyloidogenicity*, in *Methods in Enzymology*, W. Ronald, Editor. 1999, Academic Press. p. 189-204.
183. Patel, D. and T. Good, *A rapid method to measure beta-amyloid induced neurotoxicity in vitro*. *Journal of Neuroscience Methods*, 2007. **161**(1): p. 1-10.
184. Murray, M.M., et al., *Amyloid  $\beta$  Protein: A $\beta$ 40 Inhibits A $\beta$ 42 Oligomerization*. *Journal of the American Chemical Society*, 2009. **131**(18): p. 6316-6317.
185. El-Agnaf, O.M.A., et al., *Oligomerization and Toxicity of  $\beta$ -Amyloid-42 Implicated in Alzheimer's Disease*. *Biochemical and Biophysical Research Communications*, 2000. **273**(3): p. 1003-1007.
186. Dahlgren, K.N., et al., *Oligomeric and Fibrillar Species of Amyloid- $\beta$  Peptides Differentially Affect Neuronal Viability*. *Journal of Biological Chemistry*, 2002. **277**(35): p. 32046-32053.
187. Zhang, Y., et al., *Selective cytotoxicity of intracellular amyloid  $\beta$  peptide 1-42 through p53 and Bax in cultured primary human neurons*. *The Journal of Cell Biology*, 2002. **156**(3): p. 519-529.
188. Shanmugam, G. and P.L. Polavarapu, *Structure of Amyloid-b(25-35) Peptide in Different Environments*. *Biophysical Journal*, 2004. **87**(1): p. 622-630.

189. Yamaguchi, Y. and S. Kawashima, *Effects of amyloid- $\beta$ -(25–35) on passive avoidance, radial-arm maze learning and choline acetyltransferase activity in the rat*. *European Journal of Pharmacology*, 2001. **412**(3): p. 265-272.
190. Brining, S.K., *Predicting the In Vitro Toxicity of Synthetic Beta-Amyloid (1-40)*. *Neurobiology of Aging*, 1997. **18**(6): p. 581-589.
191. Jarvis, K., et al., *Beta-amyloid toxicity and reversal in embryonic rat septal neurons*. *Neuroscience Letters*, 2007. **423**(3): p. 184-188.
192. Chonpathompikunlert, P., et al., *TEMPOL protects human neuroblastoma SH-SY5Y cells against  $\beta$ -amyloid-induced cell toxicity*. *European Journal of Pharmacology*, 2011. **650**(2–3): p. 544-549.
193. Lee, K.H., et al., *A hybrid molecule that prohibits amyloid fibrils and alleviates neuronal toxicity induced by  $\beta$ -amyloid (1–42)*. *Biochemical and Biophysical Research Communications*, 2005. **328**(4): p. 816-823.
194. Broersen, K., et al., *A standardized and biocompatible preparation of aggregate-free amyloid beta peptide for biophysical and biological studies of Alzheimer's disease*. *Protein Engineering Design and Selection*, 2011.
195. Milton, N.G.N., *Anandamide and noladin ether prevent neurotoxicity of the human amyloid- $\beta$  peptide*. *Neuroscience Letters*, 2002. **332**(2): p. 127-130.
196. Austen, B.M., et al., *Designing Peptide Inhibitors for Oligomerization and Toxicity of Alzheimer's  $\beta$ -Amyloid Peptide†*. *Biochemistry*, 2008. **47**(7): p. 1984-1992.
197. Garzon-Rodriguez, W., et al., *Soluble Amyloid A $\beta$ -(1–40) Exists as a Stable Dimer at Low Concentrations*. *Journal of Biological Chemistry*, 1997. **272**(34): p. 21037-21044.
198. Mei, Z., et al., *Cryptotanshinione Inhibits  $\beta$ -Amyloid Aggregation and Protects Damage from  $\beta$ -Amyloid in SH-SY5Y Cells*. *Neurochemical Research*, 2012. **37**(3): p. 622-628.
199. Howlett, D.R., et al., *Aggregation State and Neurotoxic Properties of Alzheimer Beta-Amyloid Peptide*. *Neurodegeneration*, 1995. **4**(1): p. 23-32.

200. Lee, S., E.J. Fernandez, and T.A. Good, *Role of aggregation conditions in structure, stability, and toxicity of intermediates in the A $\beta$  fibril formation pathway*. Protein Science, 2007. **16**(4): p. 723-732.
201. Wang, S.S.S., A. Becerra-Arteaga, and T.A. Good, *Development of a novel diffusion-based method to estimate the size of the aggregated A $\beta$  species responsible for neurotoxicity*. Biotechnology and Bioengineering, 2002. **80**(1): p. 50-59.
202. Kanapathipillai, M., et al., *Ectoine and hydroxyectoine inhibit aggregation and neurotoxicity of Alzheimer's  $\beta$ -amyloid*. FEBS Letters, 2005. **579**(21): p. 4775-4780.
203. Green, P.S., et al., *Estradiol attenuation of  $\beta$ -amyloid-induced toxicity: A comparison of MTT and calcein AM assays*. Journal of Neurocytology, 2000. **29**(5): p. 419-423.
204. Lee, S., et al., *Small heat shock proteins differentially affect A $\beta$  aggregation and toxicity*. Biochemical and Biophysical Research Communications, 2006. **347**(2): p. 527-533.
205. Mateos, L., et al., *Estrogen protects against amyloid- $\beta$  toxicity by estrogen receptor  $\alpha$ -mediated inhibition of Daxx translocation*. Neuroscience Letters, 2012. **506**(2): p. 245-250.
206. Li, Q., et al., *Galantamine inhibits calpain-calcineurin signaling activated by beta-amyloid in human neuroblastoma SH-SY5Y cells*. Neuroscience Letters, 2010. **480**(3): p. 173-177.
207. Lee, S., et al., *Hsp20, a novel  $\alpha$ -crystallin, prevents A $\beta$  fibril formation and toxicity*. Protein Science, 2005. **14**(3): p. 593-601.
208. Durairajan, S.S.K., et al., *Salvianolic acid B inhibits A $\beta$  fibril formation and disaggregates preformed fibrils and protects against A $\beta$ -induced cytotoxicity*. Neurochemistry International, 2008. **52**(4-5): p. 741-750.
209. Paradis, E., et al., *Amyloid  $\beta$  Peptide of Alzheimer's Disease Downregulates Bcl-2 and Upregulates Bax Expression in Human Neurons*. The Journal of Neuroscience, 1996. **16**(23): p. 7533-7539.
210. Yong, H.P., et al., *Inhibition of b-amyloid 1-40 Peptide Aggregation and Neurotoxicity by Citrate*. Korean J Physiol Pharmacol, 2009. **13**(4): p. 273-279.

211. Drouet, B., et al., *Laminin 1 Attenuates  $\beta$ -Amyloid Peptide  $A\beta(1-40)$  Neurotoxicity of Cultured Fetal Rat Cortical Neurons*. Journal of Neurochemistry, 1999. **73**(2): p. 742-749.
212. Qu, M., et al., *Mortalin overexpression attenuates beta-amyloid-induced neurotoxicity in SH-SY5Y cells*. Brain Research, 2011. **1368**(0): p. 336-345.
213. Geng, L., et al., *Coenzyme Q10 protects SHSY5Y neuronal cells from beta amyloid toxicity and oxygen-glucose deprivation by inhibiting the opening of the mitochondrial permeability transition pore*. Biofactors, 2005. **25**(1-4): p. 97-107.
214. Iuvone, T., et al., *Neuroprotective effect of cannabidiol, a non-psychoactive component from Cannabis sativa, on  $\beta$ -amyloid-induced toxicity in PC12 cells*. Journal of Neurochemistry, 2004. **89**(1): p. 134-141.
215. Bang, O.Y., et al., *Neuroprotective effect of genistein against beta amyloid-induced neurotoxicity*. Neurobiology of Disease, 2004. **16**(1): p. 21-28.
216. Zhang, L., et al., *Neuroprotective effects of salidroside against beta-amyloid-induced oxidative stress in SH-SY5Y human neuroblastoma cells*. Neurochemistry International, 2010. **57**(5): p. 547-555.
217. Akan, P., et al., *Pregnenolone protects the PC-12 cell line against amyloid beta peptide toxicity but its sulfate ester does not*. Chemo-Biological Interactions, 2009. **177**(1): p. 65-70.
218. Youssef, I., et al., *N-truncated amyloid- $\beta$  oligomers induce learning impairment and neuronal apoptosis*. Neurobiology of Aging, 2008. **29**(9): p. 1319-1333.
219. Granzotto, A., M. Suwalsky, and P. Zatta, *Physiological cholesterol concentration is a neuroprotective factor against  $\beta$ -amyloid and  $\beta$ -amyloid-metal complexes toxicity*. Journal of Inorganic Biochemistry, 2011. **105**(8): p. 1066-1072.
220. Seo, J.-S., et al., *Oriental medicine Jangwonhwan reduces  $A\beta(1-42)$  level and  $\beta$ -amyloid deposition in the brain of Tg-APP<sup>swe</sup>/PS1<sup>dE9</sup> mouse model of Alzheimer disease*. Journal of Ethnopharmacology, 2010. **128**(1): p. 206-212.
221. Yan, Y. and C. Wang,  *$A\beta(42)$  is More Rigid than  $A\beta(40)$  at the C Terminus: Implications for  $A\beta$  Aggregation and Toxicity*. Journal of Molecular Biology, 2006. **364**(5): p. 853-862.

222. Gessel, M.M., et al., *A $\beta$ (39–42) Modulates A $\beta$  Oligomerization but Not Fibril Formation*. *Biochemistry*, 2011. **51**(1): p. 108-117.
223. Fradinger, E.A., et al., *C-terminal peptides coassemble into A $\beta$ 42 oligomers and protect neurons against A $\beta$ 42-induced neurotoxicity*. *Proceedings of the National Academy of Sciences*, 2008. **105**(37): p. 14175-14180.
224. Zhang, J.-J., R.-F. Zhang, and X.-K. Meng, *Protective effect of pyrroloquinoline quinone against A $\beta$ -induced neurotoxicity in human neuroblastoma SH-SY5Y cells*. *Neuroscience Letters*, 2009. **464**(3): p. 165-169.
225. Fabrizi, C., et al., *Role of  $\alpha$ 2-macroglobulin in regulating amyloid  $\beta$ -protein neurotoxicity: protective or detrimental factor?* *Journal of Neurochemistry*, 2001. **78**(2): p. 406-412.
226. Rymer, D.L. and T.A. Good, *The role of G protein activation in the toxicity of amyloidogenic A beta-(1-40), A beta-(25-35), and bovine calcitonin*. *Journal of Biological Chemistry*, 2001. **276**(4): p. 2523-2530.
227. Feng, Z. and J.-t. Zhang, *Protective effect of melatonin on  $\beta$ -amyloid-induced apoptosis in rat astrogloma c6 cells and its mechanism*. *Free Radical Biology and Medicine*, 2004. **37**(11): p. 1790-1801.
228. May, P.C., et al.,  *$\beta$ -amyloid peptide in vitro toxicity: Lot-to-lot variability*. *Neurobiology of Aging*, 1992. **13**(5): p. 605-607.
229. Cowan, C.B., G.L. Coté, and T.A. Good, *Development of photocrosslinked sialic acid containing polymers for use in A[beta] toxicity attenuation*. *Biomaterials*, 2008. **29**(24-25): p. 3408-3414.
230. Luo, Y., et al., *Physiological levels of  $\beta$ -amyloid peptide promote PC12 cell proliferation*. *Neuroscience Letters*, 1996. **217**(2–3): p. 125-128.
231. Selkoe, D.J., *Normal and Abnormal Biology of the beta-Amyloid Precursor Protein*. *Annual Review of Neuroscience*, 1994. **17**(1): p. 489-517.
232. Jan, A., D.M. Hartley, and H.A. Lashuel, *Preparation and characterization of toxic A[beta] aggregates for structural and functional studies in Alzheimer's disease research*. *Nat. Protocols*, 2010. **5**(6): p. 1186-1209.

233. Yu, R.K., et al., *Ganglioside analysis by high-performance thin-layer chromatography*, in *Methods in Enzymology*. 2000, Academic Press. p. 115-134.
234. Ariga, T., et al., *Characterization of High-Affinity Binding between Gangliosides and Amyloid [beta]-Protein*. *Archives of Biochemistry and Biophysics*, 2001. **388**(2): p. 225-230.
235. Kakio, A., et al., *Formation of a membrane-active form of amyloid [beta]-protein in raft-like model membranes*. *Biochemical and Biophysical Research Communications*, 2003. **303**(2): p. 514-518.
236. Matsuzaki, K., K. Kato, and K. Yanagisawa, *A $\beta$  polymerization through interaction with membrane gangliosides*. *Biochimica et Biophysica Acta (BBA) - Molecular and Cell Biology of Lipids*, 2010. **1801**(8): p. 868-877.
237. Cowan, C.B., D.A. Patel, and T.A. Good, *Exploring the mechanism of [beta]amyloid toxicity attenuation by multivalent sialic acid polymers through the use of mathematical models*. *Journal of Theoretical Biology*. **In Press, Accepted Manuscript**.
238. Sashiwa, H. and S.-i. Aiba, *Chemically modified chitin and chitosan as biomaterials*. *Progress in Polymer Science*, 2004. **29**(9): p. 887-908.
239. Warren, L., *The Thiobarbituric Acid Assay of Sialic Acids*. *Journal of Biological Chemistry*, 1959. **234**(8): p. 1971-1975.
240. Okennedy, R., *Some observations on Sialic Acid determination by the Warren Thiobarbituric Acid Method*. *Irish Journal of Medical Science*, 1979. **148**(3): p. 92-96.
241. Warren, L., *The Thiobarbituric Acid Assay of Sialic Acids*. *J. Biol. Chem.*, 1959. **234**(8): p. 1971-1975.
242. Mosmann, T., *Rapid Colorimetric Assay for Cellular Growth and Survival: Application to Proliferation and Cyto-Toxicity Assays*. *Journal of Immunological Methods*, 1983. **65**(1-2): p. 55-63.
243. Liu, Y.B., et al., *Mechanism of cellular 3-(4,5-dimethylthiazol-2-yl)-2,5-diphenyltetrazolium bromide (MTT) reduction*. *Journal of Neurochemistry*, 1997. **69**(2): p. 581-593.

244. Saxton, A.M. *A macro for converting mean separation output to letter groupings in Proc Mixed.* in *In Proc. 23rd SAS Users Group Intl.* 1998. Nashville, TN,: SAS Institute, Cary, NC.
245. Alzheimer's Association, *2011 Alzheimer's disease facts and figures.* Alzheimer's & dementia : the journal of the Alzheimer's Association, 2011. **7**(2): p. 208-244.
246. Hardy, J. and D.J. Selkoe, *The amyloid hypothesis of Alzheimer's disease: progress and problems on the road to therapeutics.* Science, 2002. **297**(5580): p. 353-6.
247. Matsuoka, Y., et al., *Novel Therapeutic Approach for the Treatment of Alzheimer's Disease by Peripheral Administration of Agents with an Affinity to  $\beta$ -Amyloid.* The Journal of Neuroscience, 2003. **23**(1): p. 29-33.
248. Kakio, A., et al., *Cholesterol-dependent formation of GM1 ganglioside-bound amyloid beta-protein, an endogenous seed for Alzheimer amyloid.* J Biol Chem, 2001. **276**(27): p. 24985-90.
249. Dhavale, D. and J. Henry, *Sialic acid-conjugated chitosan for the attenuation of amyloid-beta toxicity in vitro: Degree of labeling study.* Acta biomaterialia, 2012.
250. Wang, S.S., D.L. Rymer, and T.A. Good, *Reduction in cholesterol and sialic acid content protects cells from the toxic effects of beta-amyloid peptides.* J Biol Chem, 2001. **276**(45): p. 42027-34.
251. Aminoff, D., *Methods for Quantitative Estimation of N-Acetylneuraminic acid and their Application to Hydrolysates of Sialomucoids.* Biochemical Journal, 1961. **81**(2): p. 384-392.
252. Mosmann, T., *Rapid colorimetric assay for cellular growth and survival: Application to proliferation and cytotoxicity assays.* Journal of Immunological Methods, 1983. **65**(1-2): p. 55-63.
253. Datki, Z., et al., *Method for measuring neurotoxicity of aggregating polypeptides with the MTT assay on differentiated neuroblastoma cells.* Brain Research Bulletin, 2003. **62**(3): p. 223-229.

254. Wakabayashi, M., et al., *GMI ganglioside-mediated accumulation of amyloid [beta]-protein on cell membranes*. Biochemical and Biophysical Research Communications, 2005. **328**(4): p. 1019-1023.
255. Fischer, D., et al., *In vitro cytotoxicity testing of polycations: influence of polymer structure on cell viability and hemolysis*. Biomaterials, 2003. **24**(7): p. 1121-1131.

## APPENDIX: STATISTICAL OUTPUT DATA BY TUKEY'S TEST

### Stat Analysis for GA Analog Intrinsic Toxicity Ievelenes

The GLM Procedure

Class Level Information		
Class	Levels	Values
concentration	8	0uM 10uM 20uM 30uM 3uM 40uM 48uM 5uM

Number of Observations Read 32

Number of Observations Used 32

### Stat Analysis for GA Analog Intrinsic Toxicity Ievelenes

The GLM Procedure

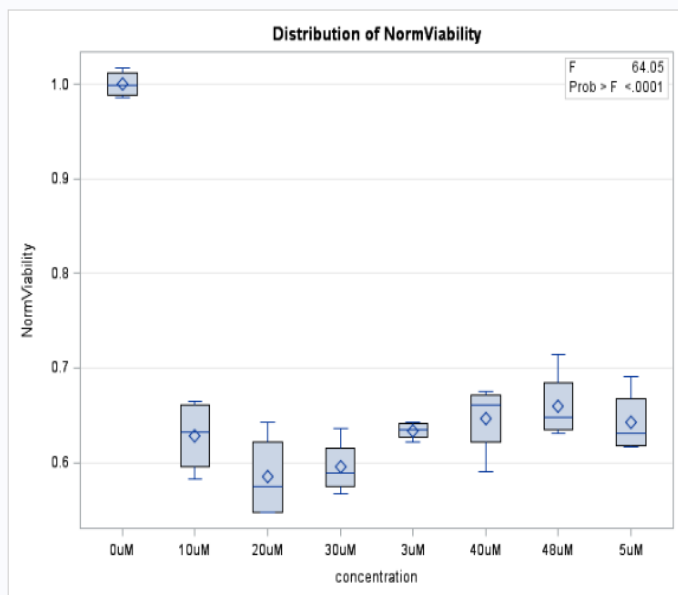
Dependent Variable: NormViability

Source	DF	Sum of Squares	Mean Square	F Value	Pr > F
Model	7	0.50463573	0.07209082	64.05	<.0001
Error	24	0.02701473	0.00112561		
Corrected Total	31	0.53165046			

R-Square	Coeff Var	Root MSE	NormViability Mean
0.949187	4.979551	0.033550	0.673759

Source	DF	Type I SS	Mean Square	F Value	Pr > F
concentration	7	0.50463573	0.07209082	64.05	<.0001

Source	DF	Type III SS	Mean Square	F Value	Pr > F
concentration	7	0.50463573	0.07209082	64.05	<.0001



### Stat Analysis for GA Analog Intrinsic Toxicity Ievelenes

The GLM Procedure

Levene's Test for Homogeneity of NormViability Variance ANOVA of Squared Deviations from Group Means					
Source	DF	Sum of Squares	Mean Square	F Value	Pr > F
concentration	7	7.631E-6	1.09E-6	1.15	0.3676
Error	24	0.000023	9.494E-7		

Level of concentration	N	NormViability	
		Mean	Std Dev
0uM	4	1.00000000	0.01484343
10uM	4	0.62807393	0.03962724
20uM	4	0.58491491	0.04592317
30uM	4	0.59504709	0.02921047
3uM	4	0.63368942	0.00930879
40uM	4	0.64639355	0.03878790
48uM	4	0.65984154	0.03801625
5uM	4	0.64211022	0.03486667





Statistical analysis for complex B 14.1% intrinsic toxicity by Tukey's test								
Differences of Least Squares Means								
concentration	_concentration	Estimate	Standard Error	DF	t Value	Pr >  t	Adjustment	Adj P
0uM	10uM	0.03301	0.02781	21	1.19	0.2485	Tukey	0.8914
0uM	1uM	0.06101	0.02781	21	2.19	0.0397	Tukey	0.3396
0uM	20uM	0.01866	0.02781	21	0.67	0.5095	Tukey	0.9929
0uM	30uM	0.0694	0.02781	21	2.5	0.021	Tukey	0.2106
0uM	3uM	-0.00362	0.02781	21	-0.13	0.8978	Tukey	1
0uM	5uM	0.008982	0.02781	21	0.32	0.7499	Tukey	0.9999
10uM	1uM	0.02799	0.02781	21	1.01	0.3256	Tukey	0.9468
10uM	20uM	-0.01435	0.02781	21	-0.52	0.6113	Tukey	0.9983
10uM	30uM	0.03639	0.02781	21	1.31	0.2048	Tukey	0.8405
10uM	3uM	-0.03663	0.02781	21	-1.32	0.202	Tukey	0.8366
10uM	5uM	-0.02403	0.02781	21	-0.86	0.3973	Tukey	0.9742
1uM	20uM	-0.04234	0.02781	21	-1.52	0.1428	Tukey	0.729
1uM	30uM	0.008398	0.02781	21	0.3	0.7656	Tukey	0.9999
1uM	3uM	-0.06462	0.02781	21	-2.32	0.0303	Tukey	0.2789
1uM	5uM	-0.05202	0.02781	21	-1.87	0.0754	Tukey	0.5193
20uM	30uM	0.05074	0.02781	21	1.82	0.0823	Tukey	0.5472
20uM	3uM	-0.02228	0.02781	21	-0.8	0.432	Tukey	0.9823
20uM	5uM	-0.00968	0.02781	21	-0.35	0.7312	Tukey	0.9998
30uM	3uM	-0.07302	0.02781	21	-2.63	0.0158	Tukey	0.1681
30uM	5uM	-0.06042	0.02781	21	-2.17	0.0414	Tukey	0.3501
3uM	5uM	0.0126	0.02781	21	0.45	0.6552	Tukey	0.9992
Effect=concentration Method=Tukey(P<.05) Set=1								
Obs	concentration	Estimate	Standard Error	Letter				
				Group				
1	3uM	1.0036	0.01966	A				
2	0uM	1	0.01966	A				
3	5uM	0.991	0.01966	A				
4	20uM	0.9813	0.01966	A				
5	10uM	0.967	0.01966	A				
6	1uM	0.939	0.01966	A				
7	30uM	0.9306	0.01966	A				











Statistical analysis of SA-Chi complex and chitosan at 1uM concentration by Tukey's test								
Differences of Least Squares Means								
complex	_complex	Estimate	Standard Error	DF	t Value	Pr >  t	adjustmen	Adj P
A7.8	B14.1	0.03359	0.04147	24	0.81	0.4258	Tukey	0.9908
A7.8	C17.6	-0.1103	0.04147	24	-2.66	0.0137	Tukey	0.1833
A7.8	Chi0	-0.01155	0.04147	24	-0.28	0.783	Tukey	1
A7.8	D24.5	-0.01924	0.04147	24	-0.46	0.6469	Tukey	0.9997
A7.8	E37.3	0.1452	0.04147	24	3.5	0.0018	Tukey	0.033
A7.8	F40.7	0.242	0.04147	24	5.84	<.0001	Tukey	0.0001
A7.8	G48	0.4557	0.04147	24	10.99	<.0001	Tukey	<.0001
B14.1	C17.6	-0.1439	0.04147	24	-3.47	0.002	Tukey	0.0353
B14.1	Chi0	-0.04514	0.04147	24	-1.09	0.2871	Tukey	0.9532
B14.1	D24.5	-0.05283	0.04147	24	-1.27	0.2148	Tukey	0.8996
B14.1	E37.3	0.1116	0.04147	24	2.69	0.0128	Tukey	0.1734
B14.1	F40.7	0.2084	0.04147	24	5.03	<.0001	Tukey	0.0009
B14.1	G48	0.4222	0.04147	24	10.18	<.0001	Tukey	<.0001
C17.6	Chi0	0.09878	0.04147	24	2.38	0.0255	Tukey	0.2938
C17.6	D24.5	0.09109	0.04147	24	2.2	0.0379	Tukey	0.3879
C17.6	E37.3	0.2555	0.04147	24	6.16	<.0001	Tukey	<.0001
C17.6	F40.7	0.3523	0.04147	24	8.5	<.0001	Tukey	<.0001
C17.6	G48	0.5661	0.04147	24	13.65	<.0001	Tukey	<.0001
Chi0	D24.5	-0.00769	0.04147	24	-0.19	0.8544	Tukey	1
Chi0	E37.3	0.1567	0.04147	24	3.78	0.0009	Tukey	0.0175
Chi0	F40.7	0.2536	0.04147	24	6.11	<.0001	Tukey	<.0001
Chi0	G48	0.4673	0.04147	24	11.27	<.0001	Tukey	<.0001
D24.5	E37.3	0.1644	0.04147	24	3.97	0.0006	Tukey	0.0114
D24.5	F40.7	0.2612	0.04147	24	6.3	<.0001	Tukey	<.0001
D24.5	G48	0.475	0.04147	24	11.45	<.0001	Tukey	<.0001
E37.3	F40.7	0.09681	0.04147	24	2.33	0.0283	Tukey	0.3164
E37.3	G48	0.3105	0.04147	24	7.49	<.0001	Tukey	<.0001
F40.7	G48	0.2137	0.04147	24	5.15	<.0001	Tukey	0.0006
Effect=complex Method=Tukey(P<.05) Set=1								
Obs	complex	Estimate	Standard Error	Letter				
				Group				
1	C17.6	1.0829	0.02932	A				
2	D24.5	0.9918	0.02932	AB				
3	Chi0	0.9841	0.02932	AB				
4	A7.8	0.9726	0.02932	AB				
5	B14.1	0.939	0.02932	BC				
6	E37.3	0.8274	0.02932	CD				
7	F40.7	0.7306	0.02932	D				
8	G48	0.5168	0.02932	E				



Statistical analysis of SA-Chi complex and chitosan at 5uM concentration by Tukey's test								
Differences of Least Squares Means								
complex	_complex	Estimate	Standard Error	DF	t Value	Pr >  t	Adjustment	Adj P
A7.8	B14.1	-0.04907	0.03983	24	-1.23	0.2299	Tukey	0.9141
A7.8	C17.6	-0.04232	0.03983	24	-1.06	0.2986	Tukey	0.9587
A7.8	Chi0	0.01423	0.03983	24	0.36	0.724	Tukey	1
A7.8	D24.5	-0.1207	0.03983	24	-3.03	0.0058	Tukey	0.09
A7.8	E37.3	-0.09742	0.03983	24	-2.45	0.0221	Tukey	0.2651
A7.8	F40.7	0.07191	0.03983	24	1.81	0.0835	Tukey	0.6225
A7.8	G48	0.3326	0.03983	24	8.35	<.0001	Tukey	<.0001
B14.1	C17.6	0.006752	0.03983	24	0.17	0.8668	Tukey	1
B14.1	Chi0	0.0633	0.03983	24	1.59	0.1251	Tukey	0.7518
B14.1	D24.5	-0.07167	0.03983	24	-1.8	0.0845	Tukey	0.6262
B14.1	E37.3	-0.04835	0.03983	24	-1.21	0.2365	Tukey	0.9198
B14.1	F40.7	0.121	0.03983	24	3.04	0.0057	Tukey	0.0889
B14.1	G48	0.3817	0.03983	24	9.58	<.0001	Tukey	<.0001
C17.6	Chi0	0.05655	0.03983	24	1.42	0.1685	Tukey	0.8394
C17.6	D24.5	-0.07843	0.03983	24	-1.97	0.0606	Tukey	0.521
C17.6	E37.3	-0.05511	0.03983	24	-1.38	0.1792	Tukey	0.8558
C17.6	F40.7	0.1142	0.03983	24	2.87	0.0085	Tukey	0.1244
C17.6	G48	0.3749	0.03983	24	9.41	<.0001	Tukey	<.0001
Chi0	D24.5	-0.135	0.03983	24	-3.39	0.0024	Tukey	0.0423
Chi0	E37.3	-0.1117	0.03983	24	-2.8	0.0099	Tukey	0.1408
Chi0	F40.7	0.05768	0.03983	24	1.45	0.1605	Tukey	0.8259
Chi0	G48	0.3184	0.03983	24	7.99	<.0001	Tukey	<.0001
D24.5	E37.3	0.02332	0.03983	24	0.59	0.5637	Tukey	0.9988
D24.5	F40.7	0.1927	0.03983	24	4.84	<.0001	Tukey	0.0014
D24.5	G48	0.4533	0.03983	24	11.38	<.0001	Tukey	<.0001
E37.3	F40.7	0.1693	0.03983	24	4.25	0.0003	Tukey	0.0058
E37.3	G48	0.43	0.03983	24	10.8	<.0001	Tukey	<.0001
F40.7	G48	0.2607	0.03983	24	6.55	<.0001	Tukey	<.0001
Effect=complex Method=Tukey(P<.05) Set=1								
Obs	complex	Estimate	Standard Error	Letter Group				
1	D24.5	1.0627	0.02816	A				
2	E37.3	1.0394	0.02816	AB				
3	B14.1	0.991	0.02816	ABC				
4	C17.6	0.9843	0.02816	ABC				
5	A7.8	0.9419	0.02816	ABC				
6	Chi0	0.9277	0.02816	BC				
7	F40.7	0.87	0.02816	C				
8	G48	0.6094	0.02816	D				

Statistical analysis of SA-Chi complex and chitosan at 10uM concentration by Tukey's test								
Differences of Least Squares Means								
complex	_complex	Estimate	Standard Error	DF	t Value	Pr >  t	Adjustment	Adj P
A7.8	B14.1	-0.01236	0.03426	24	-0.36	0.7213	Tukey	0.9999
A7.8	C17.6	-0.00809	0.03426	24	-0.24	0.8152	Tukey	1
A7.8	Chi0	0.03678	0.03426	24	1.07	0.2937	Tukey	0.9564
A7.8	D24.5	-0.01489	0.03426	24	-0.43	0.6677	Tukey	0.9998
A7.8	E37.3	-0.04801	0.03426	24	-1.4	0.1739	Tukey	0.8479
A7.8	F40.7	0.1314	0.03426	24	3.84	0.0008	Tukey	0.0154
A7.8	G48	0.3132	0.03426	24	9.14	<.0001	Tukey	<.0001
B14.1	C17.6	0.00427	0.03426	24	0.12	0.9018	Tukey	1
B14.1	Chi0	0.04915	0.03426	24	1.43	0.1643	Tukey	0.8325
B14.1	D24.5	-0.00253	0.03426	24	-0.07	0.9418	Tukey	1
B14.1	E37.3	-0.03565	0.03426	24	-1.04	0.3085	Tukey	0.9629
B14.1	F40.7	0.1438	0.03426	24	4.2	0.0003	Tukey	0.0066
B14.1	G48	0.3256	0.03426	24	9.5	<.0001	Tukey	<.0001
C17.6	Chi0	0.04488	0.03426	24	1.31	0.2026	Tukey	0.8863
C17.6	D24.5	-0.0068	0.03426	24	-0.2	0.8444	Tukey	1
C17.6	E37.3	-0.03992	0.03426	24	-1.17	0.2554	Tukey	0.9342
C17.6	F40.7	0.1395	0.03426	24	4.07	0.0004	Tukey	0.0088
C17.6	G48	0.3213	0.03426	24	9.38	<.0001	Tukey	<.0001
Chi0	D24.5	-0.05168	0.03426	24	-1.51	0.1445	Tukey	0.7957
Chi0	E37.3	-0.0848	0.03426	24	-2.48	0.0208	Tukey	0.2527
Chi0	F40.7	0.09462	0.03426	24	2.76	0.0108	Tukey	0.1522
Chi0	G48	0.2765	0.03426	24	8.07	<.0001	Tukey	<.0001
D24.5	E37.3	-0.03312	0.03426	24	-0.97	0.3433	Tukey	0.975
D24.5	F40.7	0.1463	0.03426	24	4.27	0.0003	Tukey	0.0055
D24.5	G48	0.3281	0.03426	24	9.58	<.0001	Tukey	<.0001
E37.3	F40.7	0.1794	0.03426	24	5.24	<.0001	Tukey	0.0005
E37.3	G48	0.3613	0.03426	24	10.54	<.0001	Tukey	<.0001
F40.7	G48	0.1818	0.03426	24	5.31	<.0001	Tukey	0.0004
Effect=complex Method=Tukey(P<.05) Set=1								
Obs	complex	Estimate	Standard Error	Letter				
				Group				
1	E37.3	1.0026	0.02423	A				
2	D24.5	0.9695	0.02423	A				
3	B14.1	0.967	0.02423	A				
4	C17.6	0.9627	0.02423	A				
5	A7.8	0.9546	0.02423	A				
6	Chi0	0.9178	0.02423	AB				
7	F40.7	0.8232	0.02423	B				
8	G48	0.6414	0.02423	C				



Statistical analysis of SA-Chi complex and chitosan at 30uM concentration by Tukey's test								
Differences of Least Squares Means								
complex	_complex	Estimate	Standard Error	DF	t Value	Pr >  t	adjustmen	Adj P
A7.8	B14.1	0.05366	0.03776	24	1.42	0.1682	Tukey	0.8389
A7.8	C17.6	0.00959	0.03776	24	0.25	0.8017	Tukey	1
A7.8	Chi0	0.005949	0.03776	24	0.16	0.8761	Tukey	1
A7.8	D24.5	0.00539	0.03776	24	0.14	0.8877	Tukey	1
A7.8	E37.3	0.02596	0.03776	24	0.69	0.4984	Tukey	0.9966
A7.8	F40.7	0.1995	0.03776	24	5.28	<.0001	Tukey	0.0005
A7.8	G48	0.2663	0.03776	24	7.05	<.0001	Tukey	<.0001
B14.1	C17.6	-0.04407	0.03776	24	-1.17	0.2547	Tukey	0.9337
B14.1	Chi0	-0.04771	0.03776	24	-1.26	0.2186	Tukey	0.9034
B14.1	D24.5	-0.04827	0.03776	24	-1.28	0.2134	Tukey	0.8982
B14.1	E37.3	-0.0277	0.03776	24	-0.73	0.4704	Tukey	0.9949
B14.1	F40.7	0.1458	0.03776	24	3.86	0.0007	Tukey	0.0145
B14.1	G48	0.2126	0.03776	24	5.63	<.0001	Tukey	0.0002
C17.6	Chi0	-0.00364	0.03776	24	-0.1	0.924	Tukey	1
C17.6	D24.5	-0.0042	0.03776	24	-0.11	0.9124	Tukey	1
C17.6	E37.3	0.01637	0.03776	24	0.43	0.6686	Tukey	0.9998
C17.6	F40.7	0.1899	0.03776	24	5.03	<.0001	Tukey	0.0009
C17.6	G48	0.2567	0.03776	24	6.8	<.0001	Tukey	<.0001
Chi0	D24.5	-0.00056	0.03776	24	-0.01	0.9883	Tukey	1
Chi0	E37.3	0.02001	0.03776	24	0.53	0.6011	Tukey	0.9993
Chi0	F40.7	0.1935	0.03776	24	5.13	<.0001	Tukey	0.0007
Chi0	G48	0.2603	0.03776	24	6.89	<.0001	Tukey	<.0001
D24.5	E37.3	0.02057	0.03776	24	0.54	0.591	Tukey	0.9992
D24.5	F40.7	0.1941	0.03776	24	5.14	<.0001	Tukey	0.0007
D24.5	G48	0.2609	0.03776	24	6.91	<.0001	Tukey	<.0001
E37.3	F40.7	0.1735	0.03776	24	4.6	0.0001	Tukey	0.0025
E37.3	G48	0.2403	0.03776	24	6.36	<.0001	Tukey	<.0001
F40.7	G48	0.06678	0.03776	24	1.77	0.0897	Tukey	0.6455
Effect=complex Method=Tukey(P<.05) Set=1								
Obs	complex	Estimate	Standard Error	Letter				
				Group				
1	A7.8	0.9843	0.0267	A				
2	D24.5	0.9789	0.0267	A				
3	Chi0	0.9783	0.0267	A				
4	C17.6	0.9747	0.0267	A				
5	E37.3	0.9583	0.0267	A				
6	B14.1	0.9306	0.0267	A				
7	F40.7	0.7848	0.0267	B				
8	G48	0.718	0.0267	B				

## Statistical Output for Sialic Acid-Labeled Chitosan: A $\beta$ Toxicity Attenuation Studies

Statistical analysis of unlabeled chitosan by Tukey's test: Abeta studies								
Differences of Least Squares Means								
concentration	_concentration	Estimate	Standard Error	DF	t Value	Pr >  t	Adjustment	Adj P
0uM	10uM	-0.5544	0.02772	21	-20	<.0001	Tukey	<.0001
0uM	1uM	-0.4382	0.02772	21	-15.81	<.0001	Tukey	<.0001
0uM	20uM	-0.5596	0.02772	21	-20.19	<.0001	Tukey	<.0001
0uM	30uM	-0.5205	0.02772	21	-18.78	<.0001	Tukey	<.0001
0uM	3uM	-0.4198	0.02772	21	-15.15	<.0001	Tukey	<.0001
0uM	5uM	-0.4632	0.02772	21	-16.71	<.0001	Tukey	<.0001
10uM	1uM	0.1162	0.02772	21	4.19	0.0004	Tukey	0.0064
10uM	20uM	-0.00522	0.02772	21	-0.19	0.8525	Tukey	1
10uM	30uM	0.03385	0.02772	21	1.22	0.2355	Tukey	0.8781
10uM	3uM	0.1345	0.02772	21	4.85	<.0001	Tukey	0.0014
10uM	5uM	0.09117	0.02772	21	3.29	0.0035	Tukey	0.0462
1uM	20uM	-0.1214	0.02772	21	-4.38	0.0003	Tukey	0.0041
1uM	30uM	-0.08237	0.02772	21	-2.97	0.0073	Tukey	0.0879
1uM	3uM	0.01831	0.02772	21	0.66	0.5161	Tukey	0.9935
1uM	5uM	-0.02506	0.02772	21	-0.9	0.3763	Tukey	0.9679
20uM	30uM	0.03907	0.02772	21	1.41	0.1733	Tukey	0.7909
20uM	3uM	0.1398	0.02772	21	5.04	<.0001	Tukey	0.0009
20uM	5uM	0.09639	0.02772	21	3.48	0.0023	Tukey	0.031
30uM	3uM	0.1007	0.02772	21	3.63	0.0016	Tukey	0.0222
30uM	5uM	0.05732	0.02772	21	2.07	0.0512	Tukey	0.4054
3uM	5uM	-0.04337	0.02772	21	-1.56	0.1327	Tukey	0.7048
Effect=concentration Method=Tukey(P<.05) Set=1								
Obs	concentration	Estimate	Standard Error	Letter Group				
1	20uM	0.7599	0.0196	A				
2	10uM	0.7547	0.0196	A				
3	30uM	0.7208	0.0196	AB				
4	5uM	0.6635	0.0196	BC				
5	1uM	0.6384	0.0196	BC				
6	3uM	0.6201	0.0196	C				
7	0uM	0.2003	0.0196	D				

Statistical analysis of complex A 7.8% by Tukey's test: Abeta studies

Differences of Least Squares Means								
concentration	concentration	Estimate	Standard Error	DF	t Value	Pr >  t	adjustment	Adj P
0uM	10uM	-0.3304	0.02255	21	-14.65	<.0001	Tukey	<.0001
0uM	1uM	-0.3062	0.02255	21	-13.58	<.0001	Tukey	<.0001
0uM	20uM	-0.3001	0.02255	21	-13.31	<.0001	Tukey	<.0001
0uM	30uM	-0.3056	0.02255	21	-13.55	<.0001	Tukey	<.0001
0uM	3uM	-0.2752	0.02255	21	-12.2	<.0001	Tukey	<.0001
0uM	5uM	-0.2856	0.02255	21	-12.67	<.0001	Tukey	<.0001
10uM	1uM	0.02427	0.02255	21	1.08	0.294	Tukey	0.9283
10uM	20uM	0.03029	0.02255	21	1.34	0.1935	Tukey	0.8242
10uM	30uM	0.02488	0.02255	21	1.1	0.2823	Tukey	0.9201
10uM	3uM	0.05527	0.02255	21	2.45	0.0231	Tukey	0.227
10uM	5uM	0.04478	0.02255	21	1.99	0.0602	Tukey	0.4513
1uM	20uM	0.006019	0.02255	21	0.27	0.7921	Tukey	1
1uM	30uM	0.000611	0.02255	21	0.03	0.9786	Tukey	1
1uM	3uM	0.031	0.02255	21	1.37	0.1837	Tukey	0.8086
1uM	5uM	0.02051	0.02255	21	0.91	0.3733	Tukey	0.9669
20uM	30uM	-0.00541	0.02255	21	-0.24	0.8128	Tukey	1
20uM	3uM	0.02498	0.02255	21	1.11	0.2804	Tukey	0.9187
20uM	5uM	0.0145	0.02255	21	0.64	0.5273	Tukey	0.9944
30uM	3uM	0.03039	0.02255	21	1.35	0.1921	Tukey	0.822
30uM	5uM	0.0199	0.02255	21	0.88	0.3874	Tukey	0.9714
3uM	5uM	-0.01049	0.02255	21	-0.47	0.6466	Tukey	0.9991
Effect=concentration Method=Tukey(P<.05) Set=1								
Obs	concentration	Estimate	Standard Error	Letter				
				Group				
1	10uM	0.5307	0.01594	A				
2	1uM	0.5064	0.01594	A				
3	30uM	0.5058	0.01594	A				
4	20uM	0.5004	0.01594	A				
5	5uM	0.4859	0.01594	A				
6	3uM	0.4754	0.01594	A				
7	0uM	0.2003	0.01594	B				





Statistical analysis of complex D 24.5% by Tukey's test: Abeta studies								
Differences of Least Squares Means								
concentration	concentration	Estimate	Standard Error	DF	t Value	Pr >  t	adjustment	Adj P
0uM	10uM	-0.592	0.01989	21	-29.76	<.0001	Tukey	<.0001
0uM	1uM	-0.5943	0.01989	21	-29.88	<.0001	Tukey	<.0001
0uM	20uM	-0.5962	0.01989	21	-29.97	<.0001	Tukey	<.0001
0uM	30uM	-0.5763	0.01989	21	-28.97	<.0001	Tukey	<.0001
0uM	3uM	-0.5719	0.01989	21	-28.75	<.0001	Tukey	<.0001
0uM	5uM	-0.5937	0.01989	21	-29.85	<.0001	Tukey	<.0001
10uM	1uM	-0.00223	0.01989	21	-0.11	0.9119	Tukey	1
10uM	20uM	-0.00415	0.01989	21	-0.21	0.8368	Tukey	1
10uM	30uM	0.01579	0.01989	21	0.79	0.4363	Tukey	0.9831
10uM	3uM	0.0201	0.01989	21	1.01	0.3238	Tukey	0.9459
10uM	5uM	-0.00162	0.01989	21	-0.08	0.9358	Tukey	1
1uM	20uM	-0.00192	0.01989	21	-0.1	0.924	Tukey	1
1uM	30uM	0.01801	0.01989	21	0.91	0.3755	Tukey	0.9676
1uM	3uM	0.02233	0.01989	21	1.12	0.2743	Tukey	0.914
1uM	5uM	0.000604	0.01989	21	0.03	0.9761	Tukey	1
20uM	30uM	0.01993	0.01989	21	1	0.3277	Tukey	0.9479
20uM	3uM	0.02425	0.01989	21	1.22	0.2363	Tukey	0.879
20uM	5uM	0.002525	0.01989	21	0.13	0.9002	Tukey	1
30uM	3uM	0.004314	0.01989	21	0.22	0.8304	Tukey	1
30uM	5uM	-0.01741	0.01989	21	-0.88	0.3914	Tukey	0.9725
3uM	5uM	-0.02172	0.01989	21	-1.09	0.2872	Tukey	0.9236
Effect=concentration Method=Tukey(P<.05) Set=1								
Obs	concentration	Estimate	Standard Error	Letter Group				
1	20uM	0.7965	0.01407	A				
2	1uM	0.7945	0.01407	A				
3	5uM	0.7939	0.01407	A				
4	10uM	0.7923	0.01407	A				
5	30uM	0.7765	0.01407	A				
6	3uM	0.7722	0.01407	A				
7	0uM	0.2003	0.01407	B				





Statistical analysis of complex G 48% by Tukey's test: Abeta studies								
Differences of Least Squares Means								
concentration	_concentration	Estimate	Standard Error	DF	t Value	Pr >  t	Adjustment	Adj P
0uM	10uM	-0.4314	0.02247	21	-19.2	<.0001	Tukey	<.0001
0uM	1uM	-0.4162	0.02247	21	-18.52	<.0001	Tukey	<.0001
0uM	20uM	-0.4036	0.02247	21	-17.96	<.0001	Tukey	<.0001
0uM	30uM	-0.42	0.02247	21	-18.69	<.0001	Tukey	<.0001
0uM	3uM	-0.4211	0.02247	21	-18.74	<.0001	Tukey	<.0001
0uM	5uM	-0.3937	0.02247	21	-17.52	<.0001	Tukey	<.0001
10uM	1uM	0.01519	0.02247	21	0.68	0.5065	Tukey	0.9926
10uM	20uM	0.02783	0.02247	21	1.24	0.2293	Tukey	0.8712
10uM	30uM	0.01144	0.02247	21	0.51	0.6159	Tukey	0.9984
10uM	3uM	0.01032	0.02247	21	0.46	0.6508	Tukey	0.9991
10uM	5uM	0.03768	0.02247	21	1.68	0.1084	Tukey	0.6376
1uM	20uM	0.01264	0.02247	21	0.56	0.5798	Tukey	0.9973
1uM	30uM	-0.00375	0.02247	21	-0.17	0.8692	Tukey	1
1uM	3uM	-0.00487	0.02247	21	-0.22	0.8305	Tukey	1
1uM	5uM	0.02249	0.02247	21	1	0.3284	Tukey	0.9482
20uM	30uM	-0.01639	0.02247	21	-0.73	0.474	Tukey	0.989
20uM	3uM	-0.01751	0.02247	21	-0.78	0.4446	Tukey	0.9846
20uM	5uM	0.00985	0.02247	21	0.44	0.6657	Tukey	0.9993
30uM	3uM	-0.00112	0.02247	21	-0.05	0.9606	Tukey	1
30uM	5uM	0.02624	0.02247	21	1.17	0.2561	Tukey	0.8986
3uM	5uM	0.02736	0.02247	21	1.22	0.2369	Tukey	0.8796
Effect=concentration Method=Tukey(P<.05) Set=1								
Obs	concentration	Estimate	Standard Error	Letter Group				
1	10uM	0.6317	0.01589	A				
2	3uM	0.6214	0.01589	A				
3	30uM	0.6202	0.01589	A				
4	1uM	0.6165	0.01589	A				
5	20uM	0.6038	0.01589	A				
6	5uM	0.594	0.01589	A				
7	0uM	0.2003	0.01589	B				





















Statistical analysis of sugar analogs intrinsic toxicity at 3uM concentration by Tukey's test										
Differences of Least Squares Means										
concentration	complex	_concentration	_complex	Estimate	Standard Error	DF	t Value	Pr >  t	adjustment	Adj P
3uM	CHC-A	3uM	GA-A	0.4147	0.02646	12	15.68	<.0001	Tukey	<.0001
3uM	CHC-A	3uM	KDN-A	0.09992	0.02646	12	3.78	0.0026	Tukey	0.0122
3uM	CHC-A	3uM	Pyran-A	0.3729	0.02646	12	14.1	<.0001	Tukey	<.0001
3uM	GA-A	3uM	KDN-A	-0.3148	0.02646	12	-11.9	<.0001	Tukey	<.0001
3uM	GA-A	3uM	Pyran-A	-0.0418	0.02646	12	-1.58	0.1401	Tukey	0.4248
3uM	KDN-A	3uM	Pyran-A	0.273	0.02646	12	10.32	<.0001	Tukey	<.0001
Complex Method=Tukey(P<.05) Set=1										
Obs	concentration	complex	Estimate	Standard Error	Letter Group					
1	3uM	CHC-A	1.0484	0.01871	A					
2	3uM	KDN-A	0.9485	0.01871	B					
3	3uM	Pyran-A	0.6755	0.01871	C					
4	3uM	GA-A	0.6337	0.01871	C					

Statistical analysis of sugar analogs intrinsic toxicity at 5uM concentration by Tukey's test										
Differences of Least Squares Means										
concentration	complex	_concentration	_complex	Estimate	Standard Error	DF	t Value	Pr >  t	Adjustment	Adj P
5uM	CHC-A	5uM	GA-A	0.3778	0.02668	12	14.16	<.0001	Tukey	<.0001
5uM	CHC-A	5uM	KDN-A	0.04757	0.02668	12	1.78	0.0999	Tukey	0.3273
5uM	CHC-A	5uM	Pyran-A	0.2557	0.02668	12	9.59	<.0001	Tukey	<.0001
5uM	GA-A	5uM	KDN-A	-0.3303	0.02668	12	-12.38	<.0001	Tukey	<.0001
5uM	GA-A	5uM	Pyran-A	-0.1221	0.02668	12	-4.58	0.0006	Tukey	0.0031
5uM	KDN-A	5uM	Pyran-A	0.2082	0.02668	12	7.8	<.0001	Tukey	<.0001
Effect=concentration*complex Method=Tukey(P<.05) Set=1										
Obs	concentration	complex	Estimate	Standard Error	Letter Group					
1	5uM	CHC-A	1.02	0.01887	A					
2	5uM	KDN-A	0.9724	0.01887	A					
3	5uM	Pyran-A	0.7642	0.01887	B					
4	5uM	GA-A	0.6421	0.01887	C					

Statistical analysis of sugar analogs intrinsic toxicity at 10uM concentration by Tukey's test										
Differences of Least Squares Means										
concentration	complex	concentration	complex	Estimate	Standard Error	DF	t Value	Pr >  t	adjustment	Adj P
10uM	CHC-A	10uM	GA-A	0.3526	0.02714	12	12.99	<.0001	Tukey	<.0001
10uM	CHC-A	10uM	KDN-A	0.01547	0.02714	12	0.57	0.5794	Tukey	0.9392
10uM	CHC-A	10uM	Pyran-A	0.2625	0.02714	12	9.67	<.0001	Tukey	<.0001
10uM	GA-A	10uM	KDN-A	-0.3371	0.02714	12	-12.42	<.0001	Tukey	<.0001
10uM	GA-A	10uM	Pyran-A	-0.09007	0.02714	12	-3.32	0.0061	Tukey	0.0272
10uM	KDN-A	10uM	Pyran-A	0.247	0.02714	12	9.1	<.0001	Tukey	<.0001
Effect=concentration*complex Method=Tukey(P<.05) Set=1										
Obs	concentration	complex	Estimate	Standard Error	Letter Group					
1	10uM	CHC-A	0.9806	0.01919	A					
2	10uM	KDN-A	0.9652	0.01919	A					
3	10uM	Pyran-A	0.7181	0.01919	B					
4	10uM	GA-A	0.6281	0.01919	C					

Statistical analysis of sugar analogs intrinsic toxicity at 20uM concentration by Tukey's test										
Differences of Least Squares Means										
concentration	complex	concentration	complex	Estimate	Standard Error	DF	t Value	Pr >  t	adjustment	Adj P
20uM	CHC-A	20uM	GA-A	0.3684	0.02836	12	12.99	<.0001	Tukey	<.0001
20uM	CHC-A	20uM	KDN-A	0.06939	0.02836	12	2.45	0.0308	Tukey	0.1205
20uM	CHC-A	20uM	Pyran-A	0.09888	0.02836	12	3.49	0.0045	Tukey	0.0203
20uM	GA-A	20uM	KDN-A	-0.299	0.02836	12	-10.54	<.0001	Tukey	<.0001
20uM	GA-A	20uM	Pyran-A	-0.2695	0.02836	12	-9.5	<.0001	Tukey	<.0001
20uM	KDN-A	20uM	Pyran-A	0.02948	0.02836	12	1.04	0.3191	Tukey	0.7305
Effect=concentration*complex Method=Tukey(P<.05) Set=1										
Obs	concentration	complex	Estimate	Standard Error	Letter Group					
1	20uM	CHC-A	0.9533	0.02006	A					
2	20uM	KDN-A	0.8839	0.02006	AB					
3	20uM	Pyran-A	0.8544	0.02006	B					
4	20uM	GA-A	0.5849	0.02006	C					

Statistical analysis of sugar analogs intrinsic toxicity at 30uM concentration by Tukey's test										
Differences of Least Squares Means										
concentration	complex	concentration	_complex	Estimate	Standard Error	DF	t Value	Pr >  t	Adjustment	Adj P
30uM	CHC-A	30uM	GA-A	0.3839	0.02413	12	15.91	<.0001	Tukey	<.0001
30uM	CHC-A	30uM	KDN-A	0.09025	0.02413	12	3.74	0.0028	Tukey	0.013
30uM	CHC-A	30uM	Pyran-A	0.1681	0.02413	12	6.97	<.0001	Tukey	<.0001
30uM	GA-A	30uM	KDN-A	-0.2936	0.02413	12	-12.17	<.0001	Tukey	<.0001
30uM	GA-A	30uM	Pyran-A	-0.2158	0.02413	12	-8.94	<.0001	Tukey	<.0001
30uM	KDN-A	30uM	Pyran-A	0.07781	0.02413	12	3.23	0.0073	Tukey	0.032
Effect=concentration*complex Method=Tukey(P<.05) Set=1										
Obs	concentration	complex	Estimate	Standard Error	Letter Group					
1	30uM	CHC-A	0.9789	0.01706	A					
2	30uM	KDN-A	0.8887	0.01706	B					
3	30uM	Pyran-A	0.8109	0.01706	C					
4	30uM	GA-A	0.595	0.01706	D					

Statistical analysis of sugar analogs intrinsic toxicity at 40uM concentration by Tukey's test										
Differences of Least Squares Means										
concentration	complex	_concentration	_complex	Estimate	Standard Error	DF	t Value	Pr >  t	Adjustment	Adj P
40uM	CHC-A	40uM	GA-A	0.3872	0.02901	12	13.35	<.0001	Tukey	<.0001
40uM	CHC-A	40uM	KDN-A	0.1342	0.02901	12	4.63	0.0006	Tukey	0.0028
40uM	CHC-A	40uM	Pyran-A	0.2293	0.02901	12	7.91	<.0001	Tukey	<.0001
40uM	GA-A	40uM	KDN-A	-0.253	0.02901	12	-8.72	<.0001	Tukey	<.0001
40uM	GA-A	40uM	Pyran-A	-0.1579	0.02901	12	-5.44	0.0001	Tukey	0.0007
40uM	KDN-A	40uM	Pyran-A	0.09509	0.02901	12	3.28	0.0066	Tukey	0.0292
Effect=concentration*complex Method=Tukey(P<.05) Set=1										
Obs	concentration	complex	Estimate	Standard Error	Letter Group					
1	40uM	CHC-A	1.0336	0.02051	A					
2	40uM	KDN-A	0.8994	0.02051	B					
3	40uM	Pyran-A	0.8043	0.02051	C					
4	40uM	GA-A	0.6464	0.02051	D					

Statistical analysis of sugar analogs intrinsic toxicity at 48uM concentration by Tukey's test											
Differences of Least Squares Means											
concentration	complex	_concentration	_complex	Estimate	Standard Error	DF	t Value	Pr >  t	Adjustment	Adj P	
48uM	CHC-A	48uM	GA-A	0.355	0.03174	12	11.19	<.0001	Tukey	<.0001	
48uM	CHC-A	48uM	KDN-A	0.1016	0.03174	12	3.2	0.0076	Tukey	0.0334	
48uM	CHC-A	48uM	Pyran-A	0.202	0.03174	12	6.37	<.0001	Tukey	0.0002	
48uM	GA-A	48uM	KDN-A	-0.2534	0.03174	12	-7.98	<.0001	Tukey	<.0001	
48uM	GA-A	48uM	Pyran-A	-0.153	0.03174	12	-4.82	0.0004	Tukey	0.002	
48uM	KDN-A	48uM	Pyran-A	0.1004	0.03174	12	3.16	0.0082	Tukey	0.0357	
Effect=concentratio*complex Method=Tukey(P<.05) Set=1											
Obs	concentration	complex	Estimate	Standard Error	Letter						
					Group						
1	48uM	CHC-A	1.0148	0.02244	A						
2	48uM	KDN-A	0.9132	0.02244	B						
3	48uM	Pyran-A	0.8128	0.02244	C						
4	48uM	GA-A	0.6598	0.02244	D						

## Statistical Output for Sugar-Chitosan Complexes: Intrinsic Toxicity Studies

Statistical Analysis of KDN-Complex Intrinsic Toxicity by Tukey's test								
Differences of Least Squares Means								
concentration	concentration	Estimate	Standard Error	DF	t Value	Pr >  t	Adjustment	Adj P
0uM	10uM	0.0585	0.02363	24	2.48	0.0207	Tukey	0.2525
0uM	20uM	0.1317	0.02363	24	5.57	<.0001	Tukey	0.0002
0uM	30uM	0.1503	0.02363	24	6.36	<.0001	Tukey	<.0001
0uM	3uM	0.09444	0.02363	24	4	0.0005	Tukey	0.0106
0uM	40uM	0.2011	0.02363	24	8.51	<.0001	Tukey	<.0001
0uM	48uM	0.2026	0.02363	24	8.57	<.0001	Tukey	<.0001
0uM	5uM	0.11	0.02363	24	4.65	<.0001	Tukey	0.0022
10uM	20uM	0.0732	0.02363	24	3.1	0.0049	Tukey	0.0786
10uM	30uM	0.09177	0.02363	24	3.88	0.0007	Tukey	0.0138
10uM	3uM	0.03594	0.02363	24	1.52	0.1414	Tukey	0.7892
10uM	40uM	0.1426	0.02363	24	6.03	<.0001	Tukey	<.0001
10uM	48uM	0.1441	0.02363	24	6.1	<.0001	Tukey	<.0001
10uM	5uM	0.05149	0.02363	24	2.18	0.0394	Tukey	0.3976
20uM	30uM	0.01857	0.02363	24	0.79	0.4396	Tukey	0.9923
20uM	3uM	-0.03726	0.02363	24	-1.58	0.1279	Tukey	0.7587
20uM	40uM	0.06936	0.02363	24	2.94	0.0072	Tukey	0.1091
20uM	48uM	0.0709	0.02363	24	3	0.0062	Tukey	0.0958
20uM	5uM	-0.02171	0.02363	24	-0.92	0.3673	Tukey	0.9811
30uM	3uM	-0.05583	0.02363	24	-2.36	0.0266	Tukey	0.3028
30uM	40uM	0.05079	0.02363	24	2.15	0.0419	Tukey	0.4141
30uM	48uM	0.05233	0.02363	24	2.21	0.0365	Tukey	0.378
30uM	5uM	-0.04028	0.02363	24	-1.7	0.1011	Tukey	0.6843
3uM	40uM	0.1066	0.02363	24	4.51	0.0001	Tukey	0.0031
3uM	48uM	0.1082	0.02363	24	4.58	0.0001	Tukey	0.0026
3uM	5uM	0.01555	0.02363	24	0.66	0.5167	Tukey	0.9974
40uM	48uM	0.001541	0.02363	24	0.07	0.9485	Tukey	1
40uM	5uM	-0.09108	0.02363	24	-3.85	0.0008	Tukey	0.0147
48uM	5uM	-0.09262	0.02363	24	-3.92	0.0006	Tukey	0.0127
Effect=concentration Method=Tukey(P<.05) Set=1								
Obs	concentration	Estimate	Standard Error	Letter Group				
1	0uM	1	0.01671	A				
2	10uM	0.9415	0.01671	AB				
3	3uM	0.9056	0.01671	BC				
4	5uM	0.89	0.01671	BC				
5	20uM	0.8683	0.01671	BCD				
6	30uM	0.8497	0.01671	CD				
7	40uM	0.7989	0.01671	D				
8	48uM	0.7974	0.01671	D				

Statistical Analysis of GA-Complex Intrinsic Toxicity by Tukey's test								
Differences of Least Squares Means								
concentration	_concentration	Estimate	Standard Error	DF	t Value	Pr >  t	adjustmen	Adj P
0uM	10uM	0.2485	0.0202	24	12.3	<.0001	Tukey	<.0001
0uM	20uM	0.3378	0.0202	24	16.72	<.0001	Tukey	<.0001
0uM	30uM	0.3658	0.0202	24	18.11	<.0001	Tukey	<.0001
0uM	3uM	0.2978	0.0202	24	14.74	<.0001	Tukey	<.0001
0uM	40uM	0.3853	0.0202	24	19.07	<.0001	Tukey	<.0001
0uM	48uM	0.3916	0.0202	24	19.38	<.0001	Tukey	<.0001
0uM	5uM	0.295	0.0202	24	14.6	<.0001	Tukey	<.0001
10uM	20uM	0.08925	0.0202	24	4.42	0.0002	Tukey	0.0039
10uM	30uM	0.1173	0.0202	24	5.81	<.0001	Tukey	0.0001
10uM	3uM	0.04924	0.0202	24	2.44	0.0226	Tukey	0.269
10uM	40uM	0.1368	0.0202	24	6.77	<.0001	Tukey	<.0001
10uM	48uM	0.143	0.0202	24	7.08	<.0001	Tukey	<.0001
10uM	5uM	0.04644	0.0202	24	2.3	0.0305	Tukey	0.3343
20uM	30uM	0.02806	0.0202	24	1.39	0.1776	Tukey	0.8535
20uM	3uM	-0.04001	0.0202	24	-1.98	0.0593	Tukey	0.5142
20uM	40uM	0.04753	0.0202	24	2.35	0.0272	Tukey	0.3077
20uM	48uM	0.05379	0.0202	24	2.66	0.0136	Tukey	0.1828
20uM	5uM	-0.04281	0.0202	24	-2.12	0.0447	Tukey	0.4317
30uM	3uM	-0.06807	0.0202	24	-3.37	0.0025	Tukey	0.0442
30uM	40uM	0.01947	0.0202	24	0.96	0.3448	Tukey	0.9754
30uM	48uM	0.02573	0.0202	24	1.27	0.2151	Tukey	0.8999
30uM	5uM	-0.07087	0.0202	24	-3.51	0.0018	Tukey	0.0325
3uM	40uM	0.08754	0.0202	24	4.33	0.0002	Tukey	0.0047
3uM	48uM	0.0938	0.0202	24	4.64	0.0001	Tukey	0.0022
3uM	5uM	-0.0028	0.0202	24	-0.14	0.8909	Tukey	1
40uM	48uM	0.006257	0.0202	24	0.31	0.7595	Tukey	1
40uM	5uM	-0.09034	0.0202	24	-4.47	0.0002	Tukey	0.0034
48uM	5uM	-0.0966	0.0202	24	-4.78	<.0001	Tukey	0.0016
Effect=concentration Method=Tukey(P<.05) Set=1								
Obs	concentration	Estimate	Standard Error	Letter Group				
1	0uM	1	0.01429	A				
2	10uM	0.7515	0.01429	B				
3	5uM	0.705	0.01429	BC				
4	3uM	0.7022	0.01429	BC				
5	20uM	0.6622	0.01429	CD				
6	30uM	0.6342	0.01429	D				
7	40uM	0.6147	0.01429	D				
8	48uM	0.6084	0.01429	D				

Statistical Analysis of Pyran-Complex Intrinsic Toxicity by Tukey's test								
Differences of Least Squares Means								
concentration	_concentration	Estimate	Standard Error	DF	t Value	Pr >  t	Adjustment	Adj P
0uM	10uM	0.08056	0.02795	24	2.88	0.0082	Tukey	0.121
0uM	20uM	0.04285	0.02795	24	1.53	0.1383	Tukey	0.7826
0uM	30uM	0.01396	0.02795	24	0.5	0.6219	Tukey	0.9996
0uM	3uM	0.03921	0.02795	24	1.4	0.1734	Tukey	0.8471
0uM	40uM	0.01886	0.02795	24	0.67	0.5062	Tukey	0.997
0uM	48uM	0.02842	0.02795	24	1.02	0.3193	Tukey	0.9671
0uM	5uM	0.06601	0.02795	24	2.36	0.0266	Tukey	0.3032
10uM	20uM	-0.03771	0.02795	24	-1.35	0.1898	Tukey	0.8705
10uM	30uM	-0.06659	0.02795	24	-2.38	0.0254	Tukey	0.2934
10uM	3uM	-0.04135	0.02795	24	-1.48	0.152	Tukey	0.8105
10uM	40uM	-0.0617	0.02795	24	-2.21	0.0371	Tukey	0.3818
10uM	48uM	-0.05213	0.02795	24	-1.87	0.0744	Tukey	0.5853
10uM	5uM	-0.01454	0.02795	24	-0.52	0.6075	Tukey	0.9994
20uM	30uM	-0.02889	0.02795	24	-1.03	0.3116	Tukey	0.9642
20uM	3uM	-0.00364	0.02795	24	-0.13	0.8975	Tukey	1
20uM	40uM	-0.02399	0.02795	24	-0.86	0.3992	Tukey	0.9872
20uM	48uM	-0.01442	0.02795	24	-0.52	0.6105	Tukey	0.9994
20uM	5uM	0.02316	0.02795	24	0.83	0.4154	Tukey	0.9895
30uM	3uM	0.02525	0.02795	24	0.9	0.3753	Tukey	0.9828
30uM	40uM	0.004897	0.02795	24	0.18	0.8624	Tukey	1
30uM	48uM	0.01446	0.02795	24	0.52	0.6095	Tukey	0.9994
30uM	5uM	0.05205	0.02795	24	1.86	0.0748	Tukey	0.5871
3uM	40uM	-0.02035	0.02795	24	-0.73	0.4736	Tukey	0.9952
3uM	48uM	-0.01078	0.02795	24	-0.39	0.703	Tukey	0.9999
3uM	5uM	0.0268	0.02795	24	0.96	0.3471	Tukey	0.9761
40uM	48uM	0.009565	0.02795	24	0.34	0.7351	Tukey	1
40uM	5uM	0.04715	0.02795	24	1.69	0.1045	Tukey	0.6949
48uM	5uM	0.03759	0.02795	24	1.34	0.1912	Tukey	0.8723
Effect=concentration Method=Tukey(P<.05) Set=1								
Obs	concentration	Estimate	Standard Error	Letter Group				
1	0uM	1	0.01976	A				
2	30uM	0.986	0.01976	A				
3	40uM	0.9811	0.01976	A				
4	48uM	0.9716	0.01976	A				
5	3uM	0.9608	0.01976	A				
6	20uM	0.9572	0.01976	A				
7	5uM	0.934	0.01976	A				
8	10uM	0.9194	0.01976	A				

Statistical Analysis of CHC-Complex Intrinsic Toxicity by Tukey's test								
Differences of Least Squares Means								
concentration	_concentration	Estimate	Standard Error	DF	t Value	Pr >  t	adjustmen	Adj P
0uM	10uM	-0.01907	0.02728	24	-0.7	0.4911	Tukey	0.9962
0uM	20uM	0.03016	0.02728	24	1.11	0.2799	Tukey	0.9493
0uM	30uM	0.01208	0.02728	24	0.44	0.6617	Tukey	0.9998
0uM	3uM	-0.03866	0.02728	24	-1.42	0.1692	Tukey	0.8405
0uM	40uM	0.1325	0.02728	24	4.86	<.0001	Tukey	0.0013
0uM	48uM	0.1776	0.02728	24	6.51	<.0001	Tukey	<.0001
0uM	5uM	-0.02486	0.02728	24	-0.91	0.3712	Tukey	0.982
10uM	20uM	0.04923	0.02728	24	1.8	0.0837	Tukey	0.623
10uM	30uM	0.03116	0.02728	24	1.14	0.2646	Tukey	0.9403
10uM	3uM	-0.01959	0.02728	24	-0.72	0.4796	Tukey	0.9955
10uM	40uM	0.1515	0.02728	24	5.56	<.0001	Tukey	0.0002
10uM	48uM	0.1967	0.02728	24	7.21	<.0001	Tukey	<.0001
10uM	5uM	-0.00579	0.02728	24	-0.21	0.8338	Tukey	1
20uM	30uM	-0.01807	0.02728	24	-0.66	0.514	Tukey	0.9973
20uM	3uM	-0.06882	0.02728	24	-2.52	0.0187	Tukey	0.2332
20uM	40uM	0.1023	0.02728	24	3.75	0.001	Tukey	0.0188
20uM	48uM	0.1475	0.02728	24	5.41	<.0001	Tukey	0.0003
20uM	5uM	-0.05501	0.02728	24	-2.02	0.055	Tukey	0.4919
30uM	3uM	-0.05075	0.02728	24	-1.86	0.0751	Tukey	0.5884
30uM	40uM	0.1204	0.02728	24	4.41	0.0002	Tukey	0.0039
30uM	48uM	0.1655	0.02728	24	6.07	<.0001	Tukey	<.0001
30uM	5uM	-0.03694	0.02728	24	-1.35	0.1882	Tukey	0.8684
3uM	40uM	0.1711	0.02728	24	6.27	<.0001	Tukey	<.0001
3uM	48uM	0.2163	0.02728	24	7.93	<.0001	Tukey	<.0001
3uM	5uM	0.0138	0.02728	24	0.51	0.6175	Tukey	0.9995
40uM	48uM	0.04518	0.02728	24	1.66	0.1107	Tukey	0.7132
40uM	5uM	-0.1573	0.02728	24	-5.77	<.0001	Tukey	0.0001
48uM	5uM	-0.2025	0.02728	24	-7.42	<.0001	Tukey	<.0001
Effect=concentration Method=Tukey(P<.05) Set=1								
Obs	concentration	Estimate	Standard Error	Letter				
				Group				
1	3uM	1.0387	0.01929	A				
2	5uM	1.0249	0.01929	A				
3	10uM	1.0191	0.01929	A				
4	0uM	1	0.01929	A				
5	30uM	0.9879	0.01929	A				
6	20uM	0.9698	0.01929	A				
7	40uM	0.8675	0.01929	B				
8	48uM	0.8224	0.01929	B				

Statistical Analysis for Sugar-Complexes Intrinsic Toxicity at 3uM Concentration by Tukey's test								
Differences of Least Squares Means								
complex	_complex	Estimate	Standard Error	DF	t Value	Pr >  t	adjustmen	Adj P
CHC-Cmpl	GA-Cmplx	0.3364	0.02769	12	12.15	<.0001	Tukey	<.0001
CHC-Cmpl	KDN-Cmpl	0.1331	0.02769	12	4.81	0.0004	Tukey	0.0021
CHC-Cmpl	Pyran-Cm	0.07787	0.02769	12	2.81	0.0157	Tukey	0.0655
GA-Cmplx	KDN-Cmpl	-0.2033	0.02769	12	-7.34	<.0001	Tukey	<.0001
GA-Cmplx	Pyran-Cm	-0.2586	0.02769	12	-9.34	<.0001	Tukey	<.0001
KDN-Cmpl	Pyran-Cm	-0.05523	0.02769	12	-1.99	0.0694	Tukey	0.2432
Effect=complex Method=Tukey(P<.05) Set=1								
Obs	complex	Estimate	Standard Error	Letter				
				Group				
1	CHC-Cmpl	1.0387	0.01958	A				
2	Pyran-Cm	0.9608	0.01958	AB				
3	KDN-Cmpl	0.9056	0.01958	B				
4	GA-Cmplx	0.7022	0.01958	C				

Statistical Analysis for Sugar-Complexes Intrinsic Toxicity at 5uM Concentration by Tukey's test								
Differences of Least Squares Means								
complex	_complex	Estimate	Standard Error	DF	t Value	Pr >  t	Adjustment	Adj P
CHC-Cmpl	GA-Cmplx	0.3198	0.01513	12	21.13	<.0001	Tukey	<.0001
CHC-Cmpl	KDN-Cmpl	0.1348	0.01513	12	8.91	<.0001	Tukey	<.0001
CHC-Cmpl	Pyran-Cm	0.09087	0.01513	12	6	<.0001	Tukey	0.0003
GA-Cmplx	KDN-Cmpl	-0.185	0.01513	12	-12.22	<.0001	Tukey	<.0001
GA-Cmplx	Pyran-Cm	-0.229	0.01513	12	-15.13	<.0001	Tukey	<.0001
KDN-Cmpl	Pyran-Cm	-0.04398	0.01513	12	-2.91	0.0132	Tukey	0.0557
Effect=complex Method=Tukey(P<.05) Set=1								
Obs	complex	Estimate	Standard Error	Letter				
				Group				
1	CHC-Cmpl	1.0249	0.0107	A				
2	Pyran-Cm	0.934	0.0107	B				
3	KDN-Cmpl	0.89	0.0107	B				
4	GA-Cmplx	0.705	0.0107	C				

Statistical Analysis for Sugar-Complexes Intrinsic Toxicity at 10uM Concentration by Tukey's test								
Differences of Least Squares Means								
complex	_complex	Estimate	Standard Error	DF	t Value	Pr >  t	Adjustment	Adj P
CHC-Cmpl	GA-Cmplx	0.2676	0.02609	12	10.26	<.0001	Tukey	<.0001
CHC-Cmpl	KDN-Cmpl	0.07757	0.02609	12	2.97	0.0116	Tukey	0.0496
CHC-Cmpl	Pyran-Cm	0.09963	0.02609	12	3.82	0.0024	Tukey	0.0113
GA-Cmplx	KDN-Cmpl	-0.19	0.02609	12	-7.28	<.0001	Tukey	<.0001
GA-Cmplx	Pyran-Cm	-0.168	0.02609	12	-6.44	<.0001	Tukey	0.0002
KDN-Cmpl	Pyran-Cm	0.02206	0.02609	12	0.85	0.4143	Tukey	0.8319
Effect=complex Method=Tukey(P<.05) Set=1								
Obs	complex	Estimate	Standard Error	Letter Group				
1	CHC-Cmpl	1.0191	0.01845	A				
2	KDN-Cmpl	0.9415	0.01845	B				
3	Pyran-Cm	0.9194	0.01845	B				
4	GA-Cmplx	0.7515	0.01845	C				

Statistical Analysis for Sugar-Complexes Intrinsic Toxicity at 20uM Concentration by Tukey's test								
Differences of Least Squares Means								
complex	_complex	Estimate	Standard Error	DF	t Value	Pr >  t	Adjustment	Adj P
CHC-Cmpl	GA-Cmplx	0.3076	0.01408	12	21.84	<.0001	Tukey	<.0001
CHC-Cmpl	KDN-Cmpl	0.1015	0.01408	12	7.21	<.0001	Tukey	<.0001
CHC-Cmpl	Pyran-Cm	0.01269	0.01408	12	0.9	0.3852	Tukey	0.8044
GA-Cmplx	KDN-Cmpl	-0.2061	0.01408	12	-14.63	<.0001	Tukey	<.0001
GA-Cmplx	Pyran-Cm	-0.2949	0.01408	12	-20.94	<.0001	Tukey	<.0001
KDN-Cmpl	Pyran-Cm	-0.08885	0.01408	12	-6.31	<.0001	Tukey	0.0002
Effect=complex Method=Tukey(P<.05) Set=1								
Obs	complex	Estimate	Standard Error	Letter Group				
1	CHC-Cmpl	0.9698	0.009958	A				
2	Pyran-Cm	0.9572	0.009958	A				
3	KDN-Cmpl	0.8683	0.009958	B				
4	GA-Cmplx	0.6622	0.009958	C				

Statistical Analysis for Sugar-Complexes Intrinsic Toxicity at 30uM Concentration by Tukey's test								
Differences of Least Squares Means								
complex	_complex	Estimate	Standard Error	DF	t Value	Pr >  t	adjustmen	Adj P
CHC-Cmpl	GA-Cmplx	0.3538	0.02379	12	14.87	<.0001	Tukey	<.0001
CHC-Cmpl	KDN-Cmpl	0.1382	0.02379	12	5.81	<.0001	Tukey	0.0004
CHC-Cmpl	Pyran-Cm	0.001878	0.02379	12	0.08	0.9384	Tukey	0.9998
GA-Cmplx	KDN-Cmpl	-0.2156	0.02379	12	-9.06	<.0001	Tukey	<.0001
GA-Cmplx	Pyran-Cm	-0.3519	0.02379	12	-14.79	<.0001	Tukey	<.0001
KDN-Cmpl	Pyran-Cm	-0.1363	0.02379	12	-5.73	<.0001	Tukey	0.0005
Effect=complex Method=Tukey(P<.05) Set=1								
Obs	complex	Estimate	Standard Error	Letter Group				
1	CHC-Cmpl	0.9879	0.01683	A				
2	Pyran-Cm	0.986	0.01683	A				
3	KDN-Cmpl	0.8497	0.01683	B				
4	GA-Cmplx	0.6342	0.01683	C				

Statistical Analysis for Sugar-Complexes Intrinsic Toxicity at 40uM Concentration by Tukey's test								
Differences of Least Squares Means								
complex	_complex	Estimate	Standard Error	DF	t Value	Pr >  t	Adjustme	Adj P
CHC-Cmpl	GA-Cmplx	0.2529	0.03405	12	7.43	<.0001	Tukey	<.0001
CHC-Cmpl	KDN-Cmpl	0.06861	0.03405	12	2.01	0.0669	Tukey	0.236
CHC-Cmpl	Pyran-Cm	-0.1136	0.03405	12	-3.34	0.0059	Tukey	0.0264
GA-Cmplx	KDN-Cmpl	-0.1843	0.03405	12	-5.41	0.0002	Tukey	0.0008
GA-Cmplx	Pyran-Cm	-0.3665	0.03405	12	-10.76	<.0001	Tukey	<.0001
KDN-Cmpl	Pyran-Cm	-0.1822	0.03405	12	-5.35	0.0002	Tukey	0.0009
Effect=complex Method=Tukey(P<.05) Set=1								
Obs	complex	Estimate	Standard Error	Letter Group				
1	Pyran-Cm	0.9811	0.02408	A				
2	CHC-Cmpl	0.8675	0.02408	B				
3	KDN-Cmpl	0.7989	0.02408	B				
4	GA-Cmplx	0.6147	0.02408	C				

Statistical Analysis for Sugar-Complexes Intrinsic Toxicity at 48uM Concentration by Tukey's test								
Differences of Least Squares Means								
complex	_complex	Estimate	Standard Error	DF	t Value	Pr >  t	Adjustment	Adj P
CHC-Cmpl	GA-Cmplx	0.2139	0.0351	12	6.1	<.0001	Tukey	0.0003
CHC-Cmpl	KDN-Cmpl	0.02497	0.0351	12	0.71	0.4904	Tukey	0.8907
CHC-Cmpl	Pyran-Cm	-0.1492	0.0351	12	-4.25	0.0011	Tukey	0.0054
GA-Cmplx	KDN-Cmpl	-0.189	0.0351	12	-5.38	0.0002	Tukey	0.0008
GA-Cmplx	Pyran-Cm	-0.3631	0.0351	12	-10.35	<.0001	Tukey	<.0001
KDN-Cmpl	Pyran-Cm	-0.1742	0.0351	12	-4.96	0.0003	Tukey	0.0016
Effect=complex Method=Tukey(P<.05) Set=1								
Obs	complex	Estimate	Standard Error	Letter Group				
1	Pyran-Cm	0.9716	0.02482	A				
2	CHC-Cmpl	0.8224	0.02482	B				
3	KDN-Cmpl	0.7974	0.02482	B				
4	GA-Cmplx	0.6084	0.02482	C				

## Statistical Output for Sugar-Analogs: A $\beta$ Toxicity Attenuation Studies

Statistical Analysis of KDN Analog Ab Attenuation Studies by Tukey's test										
Differences of Least Squares Means										
complex	concentration	_complex	_concentration	Estimate	Standard Error	DF	t Value	Pr >  t	adjustmen	Adj P
KDN-A	0uM	KDN-A	10uM	-0.02577	0.01885	24	-1.37	0.1842	Tukey	0.8629
KDN-A	0uM	KDN-A	20uM	0.008042	0.01885	24	0.43	0.6734	Tukey	0.9998
KDN-A	0uM	KDN-A	30uM	-0.05024	0.01885	24	-2.67	0.0135	Tukey	0.1817
KDN-A	0uM	KDN-A	3uM	0.02806	0.01885	24	1.49	0.1495	Tukey	0.8057
KDN-A	0uM	KDN-A	40uM	-0.0184	0.01885	24	-0.98	0.3388	Tukey	0.9737
KDN-A	0uM	KDN-A	48uM	0.006658	0.01885	24	0.35	0.727	Tukey	1
KDN-A	0uM	KDN-A	5uM	-0.05192	0.01885	24	-2.75	0.011	Tukey	0.1544
KDN-A	10uM	KDN-A	20uM	0.03381	0.01885	24	1.79	0.0854	Tukey	0.6297
KDN-A	10uM	KDN-A	30uM	-0.02447	0.01885	24	-1.3	0.2065	Tukey	0.8907
KDN-A	10uM	KDN-A	3uM	0.05384	0.01885	24	2.86	0.0087	Tukey	0.1273
KDN-A	10uM	KDN-A	40uM	0.007377	0.01885	24	0.39	0.699	Tukey	0.9999
KDN-A	10uM	KDN-A	48uM	0.03243	0.01885	24	1.72	0.0982	Tukey	0.6748
KDN-A	10uM	KDN-A	5uM	-0.02614	0.01885	24	-1.39	0.1782	Tukey	0.8543
KDN-A	20uM	KDN-A	30uM	-0.05829	0.01885	24	-3.09	0.005	Tukey	0.0795
KDN-A	20uM	KDN-A	3uM	0.02002	0.01885	24	1.06	0.2987	Tukey	0.9587
KDN-A	20uM	KDN-A	40uM	-0.02644	0.01885	24	-1.4	0.1735	Tukey	0.8473
KDN-A	20uM	KDN-A	48uM	-0.00138	0.01885	24	-0.07	0.9421	Tukey	1
KDN-A	20uM	KDN-A	5uM	-0.05996	0.01885	24	-3.18	0.004	Tukey	0.0661
KDN-A	30uM	KDN-A	3uM	0.07831	0.01885	24	4.15	0.0004	Tukey	0.0073
KDN-A	30uM	KDN-A	40uM	0.03185	0.01885	24	1.69	0.104	Tukey	0.6934
KDN-A	30uM	KDN-A	48uM	0.0569	0.01885	24	3.02	0.0059	Tukey	0.0923
KDN-A	30uM	KDN-A	5uM	-0.00167	0.01885	24	-0.09	0.93	Tukey	1
KDN-A	3uM	KDN-A	40uM	-0.04646	0.01885	24	-2.46	0.0212	Tukey	0.257
KDN-A	3uM	KDN-A	48uM	-0.02141	0.01885	24	-1.14	0.2673	Tukey	0.942
KDN-A	3uM	KDN-A	5uM	-0.07998	0.01885	24	-4.24	0.0003	Tukey	0.0059
KDN-A	40uM	KDN-A	48uM	0.02505	0.01885	24	1.33	0.1963	Tukey	0.8787
KDN-A	40uM	KDN-A	5uM	-0.03352	0.01885	24	-1.78	0.088	Tukey	0.6393
KDN-A	48uM	KDN-A	5uM	-0.05857	0.01885	24	-3.11	0.0048	Tukey	0.077
Effect=complex*concentratio Method=Tukey(P<.05) Set=1										
Obs	complex	concentration	Estimate	Standard Error	Letter Group					
1	KDN-A	5uM	0.764	0.01333	A					
2	KDN-A	30uM	0.7623	0.01333	A					
3	KDN-A	10uM	0.7378	0.01333	AB					
4	KDN-A	40uM	0.7305	0.01333	AB					
5	KDN-A	0uM	0.7121	0.01333	AB					
6	KDN-A	48uM	0.7054	0.01333	AB					
7	KDN-A	20uM	0.704	0.01333	AB					
8	KDN-A	3uM	0.684	0.01333	B					

Statistical Analysis of GA Analog Ab Attenuation Studies by Tukey's test										
Differences of Least Squares Means										
complex	concentration	_complex	_concentration	Estimate	Standard Error	DF	t Value	Pr >  t	adjustmen	Adj P
GA-A	0uM	GA-A	10uM	0.06787	0.01863	24	3.64	0.0013	Tukey	0.0239
GA-A	0uM	GA-A	20uM	0.08862	0.01863	24	4.76	<.0001	Tukey	0.0017
GA-A	0uM	GA-A	30uM	0.06867	0.01863	24	3.69	0.0012	Tukey	0.0217
GA-A	0uM	GA-A	3uM	0.002304	0.01863	24	0.12	0.9026	Tukey	1
GA-A	0uM	GA-A	40uM	0.0437	0.01863	24	2.35	0.0275	Tukey	0.3107
GA-A	0uM	GA-A	48uM	-0.01028	0.01863	24	-0.55	0.5862	Tukey	0.9992
GA-A	0uM	GA-A	5uM	0.03799	0.01863	24	2.04	0.0526	Tukey	0.4783
GA-A	10uM	GA-A	20uM	0.02075	0.01863	24	1.11	0.2763	Tukey	0.9473
GA-A	10uM	GA-A	30uM	0.000801	0.01863	24	0.04	0.9661	Tukey	1
GA-A	10uM	GA-A	3uM	-0.06556	0.01863	24	-3.52	0.0018	Tukey	0.0316
GA-A	10uM	GA-A	40uM	-0.02416	0.01863	24	-1.3	0.2068	Tukey	0.8911
GA-A	10uM	GA-A	48uM	-0.07815	0.01863	24	-4.2	0.0003	Tukey	0.0066
GA-A	10uM	GA-A	5uM	-0.02988	0.01863	24	-1.6	0.1217	Tukey	0.7434
GA-A	20uM	GA-A	30uM	-0.01995	0.01863	24	-1.07	0.2948	Tukey	0.9569
GA-A	20uM	GA-A	3uM	-0.08632	0.01863	24	-4.63	0.0001	Tukey	0.0023
GA-A	20uM	GA-A	40uM	-0.04492	0.01863	24	-2.41	0.0239	Tukey	0.2804
GA-A	20uM	GA-A	48uM	-0.0989	0.01863	24	-5.31	<.0001	Tukey	0.0004
GA-A	20uM	GA-A	5uM	-0.05063	0.01863	24	-2.72	0.012	Tukey	0.165
GA-A	30uM	GA-A	3uM	-0.06637	0.01863	24	-3.56	0.0016	Tukey	0.0287
GA-A	30uM	GA-A	40uM	-0.02496	0.01863	24	-1.34	0.1927	Tukey	0.8742
GA-A	30uM	GA-A	48uM	-0.07895	0.01863	24	-4.24	0.0003	Tukey	0.0059
GA-A	30uM	GA-A	5uM	-0.03068	0.01863	24	-1.65	0.1125	Tukey	0.7185
GA-A	3uM	GA-A	40uM	0.0414	0.01863	24	2.22	0.0359	Tukey	0.3737
GA-A	3uM	GA-A	48uM	-0.01258	0.01863	24	-0.68	0.5058	Tukey	0.9969
GA-A	3uM	GA-A	5uM	0.03568	0.01863	24	1.92	0.0674	Tukey	0.5539
GA-A	40uM	GA-A	48uM	-0.05398	0.01863	24	-2.9	0.0079	Tukey	0.1173
GA-A	40uM	GA-A	5uM	-0.00572	0.01863	24	-0.31	0.7615	Tukey	1
GA-A	48uM	GA-A	5uM	0.04827	0.01863	24	2.59	0.016	Tukey	0.2073
Effect=complex*concentratio Method=Tukey(P<.05) Set=1										
Obs	complex	concentration	Estimate	Standard Err	Letter	Group				
1	GA-A	48uM	0.7223	0.01317	A					
2	GA-A	0uM	0.7121	0.01317	A					
3	GA-A	3uM	0.7098	0.01317	A					
4	GA-A	5uM	0.6741	0.01317	AB					
5	GA-A	40uM	0.6684	0.01317	AB					
6	GA-A	10uM	0.6442	0.01317	B					
7	GA-A	30uM	0.6434	0.01317	B					
8	GA-A	20uM	0.6234	0.01317	B					





Statistical Analysis for Sugar Analogs at 3uM Concentration by Tukey's test										
Differences of Least Squares Means										
Concentration	Complex	Concentration	Complex	Estimate	Standard Error	DF	t Value	Pr >  t	Adjustment	Adj P
3uM	CHC-A	3uM	GA-A	-0.06607	0.01475	12	-4.48	0.0008	Tukey	0.0036
3uM	CHC-A	3uM	KDN-A	-0.04031	0.01475	12	-2.73	0.0182	Tukey	0.0749
3uM	CHC-A	3uM	Pyran-A	0.06424	0.01475	12	4.36	0.0009	Tukey	0.0045
3uM	GA-A	3uM	KDN-A	0.02576	0.01475	12	1.75	0.1063	Tukey	0.3437
3uM	GA-A	3uM	Pyran-A	0.1303	0.01475	12	8.83	<.0001	Tukey	<.0001
3uM	KDN-A	3uM	Pyran-A	0.1046	0.01475	12	7.09	<.0001	Tukey	<.0001
Effect=concentration*complex Method=Tukey(P<.05) Set=1										
Obs	Concentration	Complex	Estimate	Standard Error	Letter Group					
1	3uM	GA-A	0.7098	0.01043	A					
2	3uM	KDN-A	0.684	0.01043	AB					
3	3uM	CHC-A	0.6437	0.01043	B					
4	3uM	Pyran-A	0.5794	0.01043	C					

Statistical Analysis for Sugar Analogs at 5uM Concentration by Tukey's test										
Differences of Least Squares Means										
Concentration	Complex	Concentration	Complex	Estimate	Standard Error	DF	t Value	Pr >  t	Adjustment	Adj P
5uM	CHC-A	5uM	GA-A	-0.0287	0.01624	12	-1.77	0.1026	Tukey	0.3344
5uM	CHC-A	5uM	KDN-A	-0.1186	0.01624	12	-7.3	<.0001	Tukey	<.0001
5uM	CHC-A	5uM	Pyran-A	0.05486	0.01624	12	3.38	0.0055	Tukey	0.0245
5uM	GA-A	5uM	KDN-A	-0.0899	0.01624	12	-5.54	0.0001	Tukey	0.0006
5uM	GA-A	5uM	Pyran-A	0.08356	0.01624	12	5.14	0.0002	Tukey	0.0012
5uM	KDN-A	5uM	Pyran-A	0.1735	0.01624	12	10.68	<.0001	Tukey	<.0001
Effect=concentration*complex Method=Tukey(P<.05) Set=1										
Obs	Concentration	Complex	Estimate	Standard Error	Letter Group					
1	5uM	KDN-A	0.764	0.01149	A					
2	5uM	GA-A	0.6741	0.01149	B					
3	5uM	CHC-A	0.6454	0.01149	B					
4	5uM	Pyran-A	0.5905	0.01149	C					

Statistical Analysis for Sugar Analogs at 10uM Concentration by Tukey's test										
Differences of Least Squares Means										
Concentration	Complex	Concentration	Complex	Estimate	Standard Error	DF	t Value	Pr >  t	Adjustment	Adj P
10uM	CHC-A	10uM	GA-A	0.03552	0.02533	12	1.4	0.1861	Tukey	0.5212
10uM	CHC-A	10uM	KDN-A	-0.05812	0.02533	12	-2.29	0.0406	Tukey	0.1538
10uM	CHC-A	10uM	Pyran-A	0.06601	0.02533	12	2.61	0.023	Tukey	0.0926
10uM	GA-A	10uM	KDN-A	-0.09364	0.02533	12	-3.7	0.0031	Tukey	0.014
10uM	GA-A	10uM	Pyran-A	0.03049	0.02533	12	1.2	0.2519	Tukey	0.6362
10uM	KDN-A	10uM	Pyran-A	0.1241	0.02533	12	4.9	0.0004	Tukey	0.0018
Effect=concentration*complex Method=Tukey(P<.05) Set=1										
Obs	Concentration	Complex	Estimate	Standard Error	Letter Group					
1	10uM	KDN-A	0.7378	0.01791	A					
2	10uM	CHC-A	0.6797	0.01791	AB					
3	10uM	GA-A	0.6442	0.01791	B					
4	10uM	Pyran-A	0.6137	0.01791	B					

Statistical analysis for sugar analogs at 20uM concentration by Tukey's test										
Differences of Least Squares Means										
Concentration	Complex	Concentration	Complex	Estimate	Standard Error	DF	t Value	Pr >  t	Adjustment	Adj P
20uM	CHC-A	20uM	GA-A	0.05743	0.01872	12	3.07	0.0098	Tukey	0.0422
20uM	CHC-A	20uM	KDN-A	-0.02315	0.01872	12	-1.24	0.24	Tukey	0.6171
20uM	CHC-A	20uM	Pyran-A	0.06193	0.01872	12	3.31	0.0063	Tukey	0.0277
20uM	GA-A	20uM	KDN-A	-0.08058	0.01872	12	-4.3	0.001	Tukey	0.0049
20uM	GA-A	20uM	Pyran-A	0.004503	0.01872	12	0.24	0.814	Tukey	0.9948
20uM	KDN-A	20uM	Pyran-A	0.08508	0.01872	12	4.54	0.0007	Tukey	0.0033
Effect=concentration*complex Method=Tukey(P<.05) Set=1										
Obs	Concentration	Complex	Estimate	Standard Error	Letter Group					
1	20uM	KDN-A	0.704	0.01324	A					
2	20uM	CHC-A	0.6809	0.01324	A					
3	20uM	GA-A	0.6234	0.01324	B					
4	20uM	Pyran-A	0.6189	0.01324	B					

Statistical analysis for sugar analogs at 30uM concentration by Tukey's test										
Differences of Least Squares Means										
Concentration	Complex	Concentration	Complex	Estimate	Standard Error	DF	t Value	Pr >  t	Adjustment	Adj P
30uM	CHC-A	30uM	GA-A	0.06033	0.02173	12	2.78	0.0168	Tukey	0.0696
30uM	CHC-A	30uM	KDN-A	-0.05859	0.02173	12	-2.7	0.0195	Tukey	0.0797
30uM	CHC-A	30uM	Pyran-A	0.109	0.02173	12	5.02	0.0003	Tukey	0.0015
30uM	GA-A	30uM	KDN-A	-0.1189	0.02173	12	-5.47	0.0001	Tukey	0.0007
30uM	GA-A	30uM	Pyran-A	0.04866	0.02173	12	2.24	0.0449	Tukey	0.1679
30uM	KDN-A	30uM	Pyran-A	0.1676	0.02173	12	7.71	<.0001	Tukey	<.0001
Effect=concentration*complex Method=Tukey(P<.05) Set=1										
Obs	Concentration	Complex	Estimate	Standard Error	Letter Group					
1	30uM	KDN-A	0.7623	0.01537	A					
2	30uM	CHC-A	0.7037	0.01537	AB					
3	30uM	GA-A	0.6434	0.01537	BC					
4	30uM	Pyran-A	0.5947	0.01537	C					

Statistical analysis for sugar analogs at 40uM concentration by Tukey's test										
Differences of Least Squares Means										
Concentration	Complex	Concentration	Complex	Estimate	Standard Error	DF	t Value	Pr >  t	Adjustment	Adj P
40uM	CHC-A	40uM	GA-A	0.04234	0.02412	12	1.76	0.1046	Tukey	0.3395
40uM	CHC-A	40uM	KDN-A	-0.01976	0.02412	12	-0.82	0.4285	Tukey	0.8442
40uM	CHC-A	40uM	Pyran-A	0.1142	0.02412	12	4.74	0.0005	Tukey	0.0024
40uM	GA-A	40uM	KDN-A	-0.0621	0.02412	12	-2.58	0.0243	Tukey	0.0976
40uM	GA-A	40uM	Pyran-A	0.07189	0.02412	12	2.98	0.0115	Tukey	0.049
40uM	KDN-A	40uM	Pyran-A	0.134	0.02412	12	5.56	0.0001	Tukey	0.0006
Effect=concentration*complex Method=Tukey(P<.05) Set=1										
Obs	Concentration	Complex	Estimate	Standard Error	Letter Group					
1	40uM	KDN-A	0.7305	0.01705	A					
2	40uM	CHC-A	0.7107	0.01705	A					
3	40uM	GA-A	0.6684	0.01705	A					
4	40uM	Pyran-A	0.5965	0.01705	B					

Statistical analysis for sugar analogs at 48uM concentration by Tukey's test										
Differences of Least Squares Means										
concentratic	complex	concentratic	complex	Estimate	andard Err	DF	t Value	Pr >  t	adjustmen	Adj P
48uM	CHC-A	48uM	GA-A	-0.00983	0.02367	12	-0.42	0.6853	Tukey	0.9748
48uM	CHC-A	48uM	KDN-A	0.007108	0.02367	12	0.3	0.7691	Tukey	0.9901
48uM	CHC-A	48uM	Pyran-A	0.08402	0.02367	12	3.55	0.004	Tukey	0.0182
48uM	GA-A	48uM	KDN-A	0.01694	0.02367	12	0.72	0.488	Tukey	0.8891
48uM	GA-A	48uM	Pyran-A	0.09384	0.02367	12	3.96	0.0019	Tukey	0.0088
48uM	KDN-A	48uM	Pyran-A	0.07691	0.02367	12	3.25	0.007	Tukey	0.0307
Effect=concentratio*complex Method=Tukey(P<.05) Set=1										
Obs	concentratic	complex	Estimate	andard Err	Letter Group					
1	48uM	GA-A	0.7223	0.01674	A					
2	48uM	CHC-A	0.7125	0.01674	A					
3	48uM	KDN-A	0.7054	0.01674	A					
4	48uM	Pyran-A	0.6285	0.01674	B					

## Statistical Output for Sugar-Chitosan Complexes: A $\beta$ Toxicity Attenuation Studies

Statistical Analysis for KDN-Complex Ab Attenuation Studies by Tukey's test										
Differences of Least Squares Means										
complex	concentration	_complex	_concentration	Estimate	Standard Error	DF	t Value	Pr >  t	Adjustment	Adj P
KDN-Cmpl	0uM	KDN-Cmpl	10uM	-0.1434	0.01944	24	-7.38	<.0001	Tukey	<.0001
KDN-Cmpl	0uM	KDN-Cmpl	20uM	-0.08166	0.01944	24	-4.2	0.0003	Tukey	0.0065
KDN-Cmpl	0uM	KDN-Cmpl	30uM	-0.04994	0.01944	24	-2.57	0.0168	Tukey	0.2155
KDN-Cmpl	0uM	KDN-Cmpl	3uM	-0.06473	0.01944	24	-3.33	0.0028	Tukey	0.0481
KDN-Cmpl	0uM	KDN-Cmpl	40uM	-0.05165	0.01944	24	-2.66	0.0138	Tukey	0.1846
KDN-Cmpl	0uM	KDN-Cmpl	48uM	0.02479	0.01944	24	1.28	0.2145	Tukey	0.8992
KDN-Cmpl	0uM	KDN-Cmpl	5uM	-0.124	0.01944	24	-6.38	<.0001	Tukey	<.0001
KDN-Cmpl	10uM	KDN-Cmpl	20uM	0.06178	0.01944	24	3.18	0.004	Tukey	0.0665
KDN-Cmpl	10uM	KDN-Cmpl	30uM	0.0935	0.01944	24	4.81	<.0001	Tukey	0.0015
KDN-Cmpl	10uM	KDN-Cmpl	3uM	0.07871	0.01944	24	4.05	0.0005	Tukey	0.0093
KDN-Cmpl	10uM	KDN-Cmpl	40uM	0.09179	0.01944	24	4.72	<.0001	Tukey	0.0018
KDN-Cmpl	10uM	KDN-Cmpl	48uM	0.1682	0.01944	24	8.65	<.0001	Tukey	<.0001
KDN-Cmpl	10uM	KDN-Cmpl	5uM	0.01943	0.01944	24	1	0.3274	Tukey	0.97
KDN-Cmpl	20uM	KDN-Cmpl	30uM	0.03171	0.01944	24	1.63	0.1159	Tukey	0.7278
KDN-Cmpl	20uM	KDN-Cmpl	3uM	0.01693	0.01944	24	0.87	0.3925	Tukey	0.9861
KDN-Cmpl	20uM	KDN-Cmpl	40uM	0.03001	0.01944	24	1.54	0.1358	Tukey	0.7771
KDN-Cmpl	20uM	KDN-Cmpl	48uM	0.1064	0.01944	24	5.48	<.0001	Tukey	0.0003
KDN-Cmpl	20uM	KDN-Cmpl	5uM	-0.04235	0.01944	24	-2.18	0.0394	Tukey	0.3979
KDN-Cmpl	30uM	KDN-Cmpl	3uM	-0.01478	0.01944	24	-0.76	0.4543	Tukey	0.9937
KDN-Cmpl	30uM	KDN-Cmpl	40uM	-0.00171	0.01944	24	-0.09	0.9307	Tukey	1
KDN-Cmpl	30uM	KDN-Cmpl	48uM	0.07473	0.01944	24	3.84	0.0008	Tukey	0.0151
KDN-Cmpl	30uM	KDN-Cmpl	5uM	-0.07406	0.01944	24	-3.81	0.0009	Tukey	0.0164
KDN-Cmpl	3uM	KDN-Cmpl	40uM	0.01308	0.01944	24	0.67	0.5076	Tukey	0.997
KDN-Cmpl	3uM	KDN-Cmpl	48uM	0.08952	0.01944	24	4.6	0.0001	Tukey	0.0025
KDN-Cmpl	3uM	KDN-Cmpl	5uM	-0.05928	0.01944	24	-3.05	0.0055	Tukey	0.0868
KDN-Cmpl	40uM	KDN-Cmpl	48uM	0.07644	0.01944	24	3.93	0.0006	Tukey	0.0123
KDN-Cmpl	40uM	KDN-Cmpl	5uM	-0.07235	0.01944	24	-3.72	0.0011	Tukey	0.02
KDN-Cmpl	48uM	KDN-Cmpl	5uM	-0.1488	0.01944	24	-7.65	<.0001	Tukey	<.0001
Effect=complex*concentratio Method=Tukey(P<.05) Set=1										
Obs	complex	concentration	Estimate	Standard Error	Letter Group					
1	KDN-Cmpl	10uM	0.8555	0.01375	A					
2	KDN-Cmpl	5uM	0.8361	0.01375	AB					
3	KDN-Cmpl	20uM	0.7937	0.01375	ABC					
4	KDN-Cmpl	3uM	0.7768	0.01375	BC					
5	KDN-Cmpl	40uM	0.7637	0.01375	CD					
6	KDN-Cmpl	30uM	0.762	0.01375	CD					
7	KDN-Cmpl	0uM	0.7121	0.01375	DE					
8	KDN-Cmpl	48uM	0.6873	0.01375	E					

Statistical Analysis for GA-Complex Ab Attenuation Studies by Tukey's test											
Differences of Least Squares Means											
complex	concentra	_complex	_concentr	Estimate	Standard Error	DF	t Value	Pr >  t	Adjustme	Adj P	
GA-Cmplx	0uM	GA-Cmplx	10uM	0.000569	0.03103	24	0.02	0.9855	Tukey		1
GA-Cmplx	0uM	GA-Cmplx	20uM	0.08763	0.03103	24	2.82	0.0094	Tukey		0.1353
GA-Cmplx	0uM	GA-Cmplx	30uM	0.09198	0.03103	24	2.96	0.0068	Tukey		0.103
GA-Cmplx	0uM	GA-Cmplx	3uM	-0.00085	0.03103	24	-0.03	0.9785	Tukey		1
GA-Cmplx	0uM	GA-Cmplx	40uM	0.1055	0.03103	24	3.4	0.0024	Tukey		0.0412
GA-Cmplx	0uM	GA-Cmplx	48uM	0.0769	0.03103	24	2.48	0.0206	Tukey		0.2514
GA-Cmplx	0uM	GA-Cmplx	5uM	-0.02335	0.03103	24	-0.75	0.459	Tukey		0.9941
GA-Cmplx	10uM	GA-Cmplx	20uM	0.08706	0.03103	24	2.81	0.0098	Tukey		0.1402
GA-Cmplx	10uM	GA-Cmplx	30uM	0.09142	0.03103	24	2.95	0.0071	Tukey		0.1068
GA-Cmplx	10uM	GA-Cmplx	3uM	-0.00141	0.03103	24	-0.05	0.964	Tukey		1
GA-Cmplx	10uM	GA-Cmplx	40uM	0.105	0.03103	24	3.38	0.0025	Tukey		0.0429
GA-Cmplx	10uM	GA-Cmplx	48uM	0.07633	0.03103	24	2.46	0.0215	Tukey		0.2591
GA-Cmplx	10uM	GA-Cmplx	5uM	-0.02392	0.03103	24	-0.77	0.4482	Tukey		0.9932
GA-Cmplx	20uM	GA-Cmplx	30uM	0.004351	0.03103	24	0.14	0.8896	Tukey		1
GA-Cmplx	20uM	GA-Cmplx	3uM	-0.08848	0.03103	24	-2.85	0.0088	Tukey		0.1285
GA-Cmplx	20uM	GA-Cmplx	40uM	0.0179	0.03103	24	0.58	0.5694	Tukey		0.9989
GA-Cmplx	20uM	GA-Cmplx	48uM	-0.01073	0.03103	24	-0.35	0.7325	Tukey		1
GA-Cmplx	20uM	GA-Cmplx	5uM	-0.111	0.03103	24	-3.58	0.0015	Tukey		0.0279
GA-Cmplx	30uM	GA-Cmplx	3uM	-0.09283	0.03103	24	-2.99	0.0063	Tukey		0.0975
GA-Cmplx	30uM	GA-Cmplx	40uM	0.01355	0.03103	24	0.44	0.6663	Tukey		0.9998
GA-Cmplx	30uM	GA-Cmplx	48uM	-0.01508	0.03103	24	-0.49	0.6313	Tukey		0.9996
GA-Cmplx	30uM	GA-Cmplx	5uM	-0.1153	0.03103	24	-3.72	0.0011	Tukey		0.0203
GA-Cmplx	3uM	GA-Cmplx	40uM	0.1064	0.03103	24	3.43	0.0022	Tukey		0.0388
GA-Cmplx	3uM	GA-Cmplx	48uM	0.07775	0.03103	24	2.51	0.0194	Tukey		0.2402
GA-Cmplx	3uM	GA-Cmplx	5uM	-0.02251	0.03103	24	-0.73	0.4752	Tukey		0.9953
GA-Cmplx	40uM	GA-Cmplx	48uM	-0.02863	0.03103	24	-0.92	0.3653	Tukey		0.9807
GA-Cmplx	40uM	GA-Cmplx	5uM	-0.1289	0.03103	24	-4.15	0.0004	Tukey		0.0073
GA-Cmplx	48uM	GA-Cmplx	5uM	-0.1003	0.03103	24	-3.23	0.0036	Tukey		0.0595
Effect=complex*concentratio Method=Tukey(P<.05) Set=1											
Obs	complex	concentration	Estimate	Standard	Letter Group						
1	GA-Cmplx	5uM	0.7354	0.02194	A						
2	GA-Cmplx	3uM	0.7129	0.02194	AB						
3	GA-Cmplx	0uM	0.7121	0.02194	AB						
4	GA-Cmplx	10uM	0.7115	0.02194	AB						
5	GA-Cmplx	48uM	0.6352	0.02194	ABC						
6	GA-Cmplx	20uM	0.6244	0.02194	BC						
7	GA-Cmplx	30uM	0.6201	0.02194	BC						
8	GA-Cmplx	40uM	0.6065	0.02194	C						

Statistical Analysis for Pyran-Complex Ab Attenuation Studies by Tukey's test										
Differences of Least Squares Means										
complex	concentration	_complex	_concen	Estimate	Standard Error	DF	t Value	Pr >  t	Adjustme	Adj P
Pyran-Cm	0uM	Pyran-Cm	10uM	-0.08309	0.0211	24	-3.94	0.0006	Tukey	0.0121
Pyran-Cm	0uM	Pyran-Cm	20uM	-0.00706	0.0211	24	-0.33	0.7409	Tukey	1
Pyran-Cm	0uM	Pyran-Cm	30uM	-0.03276	0.0211	24	-1.55	0.1336	Tukey	0.7722
Pyran-Cm	0uM	Pyran-Cm	3uM	-0.03322	0.0211	24	-1.57	0.1285	Tukey	0.7601
Pyran-Cm	0uM	Pyran-Cm	40uM	-0.00499	0.0211	24	-0.24	0.8149	Tukey	1
Pyran-Cm	0uM	Pyran-Cm	48uM	-0.01063	0.0211	24	-0.5	0.6188	Tukey	0.9995
Pyran-Cm	0uM	Pyran-Cm	5uM	-0.107	0.0211	24	-5.07	<.0001	Tukey	0.0008
Pyran-Cm	10uM	Pyran-Cm	20uM	0.07603	0.0211	24	3.6	0.0014	Tukey	0.0262
Pyran-Cm	10uM	Pyran-Cm	30uM	0.05033	0.0211	24	2.39	0.0253	Tukey	0.2922
Pyran-Cm	10uM	Pyran-Cm	3uM	0.04987	0.0211	24	2.36	0.0265	Tukey	0.3025
Pyran-Cm	10uM	Pyran-Cm	40uM	0.07809	0.0211	24	3.7	0.0011	Tukey	0.021
Pyran-Cm	10uM	Pyran-Cm	48uM	0.07245	0.0211	24	3.43	0.0022	Tukey	0.0383
Pyran-Cm	10uM	Pyran-Cm	5uM	-0.0239	0.0211	24	-1.13	0.2685	Tukey	0.9427
Pyran-Cm	20uM	Pyran-Cm	30uM	-0.0257	0.0211	24	-1.22	0.235	Tukey	0.9185
Pyran-Cm	20uM	Pyran-Cm	3uM	-0.02616	0.0211	24	-1.24	0.227	Tukey	0.9114
Pyran-Cm	20uM	Pyran-Cm	40uM	0.002064	0.0211	24	0.1	0.9229	Tukey	1
Pyran-Cm	20uM	Pyran-Cm	48uM	-0.00358	0.0211	24	-0.17	0.8668	Tukey	1
Pyran-Cm	20uM	Pyran-Cm	5uM	-0.09993	0.0211	24	-4.74	<.0001	Tukey	0.0018
Pyran-Cm	30uM	Pyran-Cm	3uM	-0.00046	0.0211	24	-0.02	0.9827	Tukey	1
Pyran-Cm	30uM	Pyran-Cm	40uM	0.02776	0.0211	24	1.32	0.2006	Tukey	0.8839
Pyran-Cm	30uM	Pyran-Cm	48uM	0.02212	0.0211	24	1.05	0.3048	Tukey	0.9614
Pyran-Cm	30uM	Pyran-Cm	5uM	-0.07423	0.0211	24	-3.52	0.0018	Tukey	0.0318
Pyran-Cm	3uM	Pyran-Cm	40uM	0.02823	0.0211	24	1.34	0.1935	Tukey	0.8752
Pyran-Cm	3uM	Pyran-Cm	48uM	0.02258	0.0211	24	1.07	0.2951	Tukey	0.957
Pyran-Cm	3uM	Pyran-Cm	5uM	-0.07377	0.0211	24	-3.5	0.0019	Tukey	0.0334
Pyran-Cm	40uM	Pyran-Cm	48uM	-0.00564	0.0211	24	-0.27	0.7914	Tukey	1
Pyran-Cm	40uM	Pyran-Cm	5uM	-0.102	0.0211	24	-4.83	<.0001	Tukey	0.0014
Pyran-Cm	48uM	Pyran-Cm	5uM	-0.09635	0.0211	24	-4.57	0.0001	Tukey	0.002
Effect=complex*concentration Method=Tukey(P<.05) Set=1										
Obs	complex	conc	Estimate	Standard Error	Letter Group					
1	Pyran-Cm	5uM	0.819	0.01492	A					
2	Pyran-Cm	10uM	0.7951	0.01492	AB					
3	Pyran-Cm	3uM	0.7453	0.01492	BC					
4	Pyran-Cm	30uM	0.7448	0.01492	BC					
5	Pyran-Cm	48uM	0.7227	0.01492	C					
6	Pyran-Cm	20uM	0.7191	0.01492	C					
7	Pyran-Cm	40uM	0.7171	0.01492	C					
8	Pyran-Cm	0uM	0.7121	0.01492	C					

Statistical Analysis for CHC-Complex Ab Attenuation Studies by Tukey's test										
Differences of Least Squares Means										
complex	concentration	_complex	_concentration	Estimate	andard Errr	DF	t Value	Pr >  t	adjustmen	Adj P
CHC-Cmpl	0uM	CHC-Cmpl	10uM	0.03447	0.02069	24	1.67	0.1087	Tukey	0.7075
CHC-Cmpl	0uM	CHC-Cmpl	20uM	0.03417	0.02069	24	1.65	0.1117	Tukey	0.7161
CHC-Cmpl	0uM	CHC-Cmpl	30uM	0.09055	0.02069	24	4.38	0.0002	Tukey	0.0043
CHC-Cmpl	0uM	CHC-Cmpl	3uM	-0.00933	0.02069	24	-0.45	0.6562	Tukey	0.9998
CHC-Cmpl	0uM	CHC-Cmpl	40uM	0.1135	0.02069	24	5.48	<.0001	Tukey	0.0003
CHC-Cmpl	0uM	CHC-Cmpl	48uM	0.1557	0.02069	24	7.53	<.0001	Tukey	<.0001
CHC-Cmpl	0uM	CHC-Cmpl	5uM	-0.01147	0.02069	24	-0.55	0.5845	Tukey	0.9991
CHC-Cmpl	10uM	CHC-Cmpl	20uM	-0.0003	0.02069	24	-0.01	0.9885	Tukey	1
CHC-Cmpl	10uM	CHC-Cmpl	30uM	0.05608	0.02069	24	2.71	0.0122	Tukey	0.1674
CHC-Cmpl	10uM	CHC-Cmpl	3uM	-0.04379	0.02069	24	-2.12	0.0448	Tukey	0.4328
CHC-Cmpl	10uM	CHC-Cmpl	40uM	0.079	0.02069	24	3.82	0.0008	Tukey	0.016
CHC-Cmpl	10uM	CHC-Cmpl	48uM	0.1212	0.02069	24	5.86	<.0001	Tukey	0.0001
CHC-Cmpl	10uM	CHC-Cmpl	5uM	-0.04593	0.02069	24	-2.22	0.0361	Tukey	0.375
CHC-Cmpl	20uM	CHC-Cmpl	30uM	0.05638	0.02069	24	2.73	0.0118	Tukey	0.163
CHC-Cmpl	20uM	CHC-Cmpl	3uM	-0.04349	0.02069	24	-2.1	0.0462	Tukey	0.4412
CHC-Cmpl	20uM	CHC-Cmpl	40uM	0.0793	0.02069	24	3.83	0.0008	Tukey	0.0155
CHC-Cmpl	20uM	CHC-Cmpl	48uM	0.1215	0.02069	24	5.88	<.0001	Tukey	0.0001
CHC-Cmpl	20uM	CHC-Cmpl	5uM	-0.04563	0.02069	24	-2.21	0.0372	Tukey	0.383
CHC-Cmpl	30uM	CHC-Cmpl	3uM	-0.09987	0.02069	24	-4.83	<.0001	Tukey	0.0014
CHC-Cmpl	30uM	CHC-Cmpl	40uM	0.02292	0.02069	24	1.11	0.2788	Tukey	0.9488
CHC-Cmpl	30uM	CHC-Cmpl	48uM	0.06517	0.02069	24	3.15	0.0043	Tukey	0.0705
CHC-Cmpl	30uM	CHC-Cmpl	5uM	-0.102	0.02069	24	-4.93	<.0001	Tukey	0.0011
CHC-Cmpl	3uM	CHC-Cmpl	40uM	0.1228	0.02069	24	5.94	<.0001	Tukey	<.0001
CHC-Cmpl	3uM	CHC-Cmpl	48uM	0.165	0.02069	24	7.98	<.0001	Tukey	<.0001
CHC-Cmpl	3uM	CHC-Cmpl	5uM	-0.00214	0.02069	24	-0.1	0.9185	Tukey	1
CHC-Cmpl	40uM	CHC-Cmpl	48uM	0.04225	0.02069	24	2.04	0.0523	Tukey	0.4768
CHC-Cmpl	40uM	CHC-Cmpl	5uM	-0.1249	0.02069	24	-6.04	<.0001	Tukey	<.0001
CHC-Cmpl	48uM	CHC-Cmpl	5uM	-0.1672	0.02069	24	-8.08	<.0001	Tukey	<.0001
Effect=complex*concentratio Method=Tukey(P<.05) Set=1										
Obs	complex	concentration	Estimate	andard Errr	Letter Group					
1	CHC-Cmpl	5uM	0.7235	0.01463	A					
2	CHC-Cmpl	3uM	0.7214	0.01463	A					
3	CHC-Cmpl	0uM	0.7121	0.01463	A					
4	CHC-Cmpl	20uM	0.6779	0.01463	AB					
5	CHC-Cmpl	10uM	0.6776	0.01463	AB					
6	CHC-Cmpl	30uM	0.6215	0.01463	BC					
7	CHC-Cmpl	40uM	0.5986	0.01463	C					
8	CHC-Cmpl	48uM	0.5563	0.01463	C					

Statistical Analysis for Sugar Complex Ab Attenuation Studies at 3uM by Tukey's test										
Differences of Least Squares Means										
Concentration	Complex	Concentration	Complex	Estimate	Standard Error	DF	t Value	Pr >  t	Adjustment	Adj P
3uM	CHC-Cmpl	3uM	GA-Cmplx	0.00848	0.02646	12	0.32	0.7541	Tukey	0.988
3uM	CHC-Cmpl	3uM	KDN-Cmpl	-0.0554	0.02646	12	-2.09	0.0582	Tukey	0.2097
3uM	CHC-Cmpl	3uM	Pyran-Cm	-0.02389	0.02646	12	-0.9	0.3842	Tukey	0.8035
3uM	GA-Cmplx	3uM	KDN-Cmpl	-0.06388	0.02646	12	-2.41	0.0326	Tukey	0.127
3uM	GA-Cmplx	3uM	Pyran-Cm	-0.03237	0.02646	12	-1.22	0.2446	Tukey	0.6245
3uM	KDN-Cmpl	3uM	Pyran-Cm	0.03151	0.02646	12	1.19	0.2567	Tukey	0.6436
Effect=concentration*complex Method=Tukey(P<.05) Set=1										
Obs	Concentration	Complex	Estimate	Standard Error	Letter Group					
1	3uM	KDN-Cmpl	0.7768	0.01871	A					
2	3uM	Pyran-Cm	0.7453	0.01871	A					
3	3uM	CHC-Cmpl	0.7214	0.01871	A					
4	3uM	GA-Cmplx	0.7129	0.01871	A					

Statistical Analysis for Sugar Complex Ab Attenuation Studies at 5uM by Tukey's test										
Differences of Least Squares Means										
Concentration	Complex	Concentration	Complex	Estimate	Standard Error	DF	t Value	Pr >  t	Adjustment	Adj P
5uM	CHC-Cmpl	5uM	GA-Cmplx	-0.01189	0.02468	12	-0.48	0.6386	Tukey	0.9617
5uM	CHC-Cmpl	5uM	KDN-Cmpl	-0.1125	0.02468	12	-4.56	0.0007	Tukey	0.0032
5uM	CHC-Cmpl	5uM	Pyran-Cm	-0.09552	0.02468	12	-3.87	0.0022	Tukey	0.0103
5uM	GA-Cmplx	5uM	KDN-Cmpl	-0.1006	0.02468	12	-4.08	0.0015	Tukey	0.0072
5uM	GA-Cmplx	5uM	Pyran-Cm	-0.08363	0.02468	12	-3.39	0.0054	Tukey	0.024
5uM	KDN-Cmpl	5uM	Pyran-Cm	0.01702	0.02468	12	0.69	0.5036	Tukey	0.8991
Effect=concentration*complex Method=Tukey(P<.05) Set=1										
Obs	Concentration	Complex	Estimate	Standard Error	Letter Group					
1	5uM	KDN-Cmpl	0.8361	0.01745	A					
2	5uM	Pyran-Cm	0.819	0.01745	A					
3	5uM	GA-Cmplx	0.7354	0.01745	B					
4	5uM	CHC-Cmpl	0.7235	0.01745	B					

Statistical Analysis for Sugar Complex Ab Attenuation Studies at 10uM by Tukey's test										
Differences of Least Squares Means										
concentratio	complex	concentratio	_complex	Estimate	andard Err	DF	t Value	Pr >  t	adjustmen	Adj P
10uM	CHC-Cmpl	10uM	GA-Cmplx	-0.0339	0.01784	12	-1.9	0.0817	Tukey	0.2783
10uM	CHC-Cmpl	10uM	KDN-Cmpl	-0.1779	0.01784	12	-9.97	<.0001	Tukey	<.0001
10uM	CHC-Cmpl	10uM	Pyran-Cm	-0.1176	0.01784	12	-6.59	<.0001	Tukey	0.0001
10uM	GA-Cmplx	10uM	KDN-Cmpl	-0.144	0.01784	12	-8.07	<.0001	Tukey	<.0001
10uM	GA-Cmplx	10uM	Pyran-Cm	-0.08366	0.01784	12	-4.69	0.0005	Tukey	0.0025
10uM	KDN-Cmpl	10uM	Pyran-Cm	0.06035	0.01784	12	3.38	0.0054	Tukey	0.0243
Effect=concentratio*complex Method=Tukey(P<.05) Set=1										
Obs	concentratio	complex	Estimate	andard Err	Letter Group					
1	10uM	KDN-Cmpl	0.8555	0.01261	A					
2	10uM	Pyran-Cm	0.7951	0.01261	B					
3	10uM	GA-Cmplx	0.7115	0.01261	C					
4	10uM	CHC-Cmpl	0.6776	0.01261	C					

Statistical Analysis for Sugar Complex Ab Attenuation Studies at 20uM by Tukey's test										
Differences of Least Squares Means										
concentratio	complex	concentratio	_complex	Estimate	andard Err	DF	t Value	Pr >  t	adjustmen	Adj P
20uM	CHC-Cmpl	20uM	GA-Cmplx	0.05347	0.02558	12	2.09	0.0586	Tukey	0.211
20uM	CHC-Cmpl	20uM	KDN-Cmpl	-0.1158	0.02558	12	-4.53	0.0007	Tukey	0.0033
20uM	CHC-Cmpl	20uM	Pyran-Cm	-0.04122	0.02558	12	-1.61	0.1331	Tukey	0.4087
20uM	GA-Cmplx	20uM	KDN-Cmpl	-0.1693	0.02558	12	-6.62	<.0001	Tukey	0.0001
20uM	GA-Cmplx	20uM	Pyran-Cm	-0.09469	0.02558	12	-3.7	0.003	Tukey	0.0139
20uM	KDN-Cmpl	20uM	Pyran-Cm	0.0746	0.02558	12	2.92	0.0129	Tukey	0.0548
Effect=concentratio*complex Method=Tukey(P<.05) Set=1										
Obs	concentratio	complex	Estimate	andard Err	Letter Group					
1	20uM	KDN-Cmpl	0.7937	0.01809	A					
2	20uM	Pyran-Cm	0.7191	0.01809	AB					
3	20uM	CHC-Cmpl	0.6779	0.01809	BC					
4	20uM	GA-Cmplx	0.6244	0.01809	C					

Statistical Analysis for Sugar Complex Ab Attenuation Studies at 30uM by Tukey's test										
Differences of Least Squares Means										
concentratio	complex	concentratio	_complex	Estimate	andard Err	DF	t Value	Pr >  t	adjustmen	Adj P
30uM	CHC-Cmpl	30uM	GA-Cmplx	0.001437	0.03142	12	0.05	0.9643	Tukey	1
30uM	CHC-Cmpl	30uM	KDN-Cmpl	-0.1405	0.03142	12	-4.47	0.0008	Tukey	0.0037
30uM	CHC-Cmpl	30uM	Pyran-Cm	-0.1233	0.03142	12	-3.92	0.002	Tukey	0.0094
30uM	GA-Cmplx	30uM	KDN-Cmpl	-0.1419	0.03142	12	-4.52	0.0007	Tukey	0.0034
30uM	GA-Cmplx	30uM	Pyran-Cm	-0.1247	0.03142	12	-3.97	0.0019	Tukey	0.0087
30uM	KDN-Cmpl	30uM	Pyran-Cm	0.01719	0.03142	12	0.55	0.5944	Tukey	0.9456
Effect=concentratio*complex Method=Tukey(P<.05) Set=1										
Obs	concentratio	complex	Estimate	andard Err	Letter Group					
1	30uM	KDN-Cmpl	0.762	0.02222	A					
2	30uM	Pyran-Cm	0.7448	0.02222	A					
3	30uM	CHC-Cmpl	0.6215	0.02222	B					
4	30uM	GA-Cmplx	0.6201	0.02222	B					

Statistical Analysis for Sugar Complex Ab Attenuation Studies at 40uM by Tukey's test										
Differences of Least Squares Means										
concentratio	complex	concentratio	_complex	Estimate	andard Err	DF	t Value	Pr >  t	adjustmen	Adj P
40uM	CHC-Cmpl	40uM	GA-Cmplx	-0.00794	0.02058	12	-0.39	0.7064	Tukey	0.9796
40uM	CHC-Cmpl	40uM	KDN-Cmpl	-0.1651	0.02058	12	-8.02	<.0001	Tukey	<.0001
40uM	CHC-Cmpl	40uM	Pyran-Cm	-0.1185	0.02058	12	-5.76	<.0001	Tukey	0.0005
40uM	GA-Cmplx	40uM	KDN-Cmpl	-0.1572	0.02058	12	-7.64	<.0001	Tukey	<.0001
40uM	GA-Cmplx	40uM	Pyran-Cm	-0.1105	0.02058	12	-5.37	0.0002	Tukey	0.0008
40uM	KDN-Cmpl	40uM	Pyran-Cm	0.04666	0.02058	12	2.27	0.0426	Tukey	0.1606
Effect=concentratio*complex Method=Tukey(P<.05) Set=1										
Obs	concentratio	complex	Estimate	andard Err	Letter Group					
1	40uM	KDN-Cmpl	0.7637	0.01455	A					
2	40uM	Pyran-Cm	0.7171	0.01455	A					
3	40uM	GA-Cmplx	0.6065	0.01455	B					
4	40uM	CHC-Cmpl	0.5986	0.01455	B					

Statistical Analysis for Sugar Complex Ab Attenuation Studies at 48uM by Tukey's test										
Differences of Least Squares Means										
concentration	complex	_concentration	_complex	Estimate	andard Err	DF	t Value	Pr >  t	adjustmen	Adj P
48uM	CHC-Cmpl	48uM	GA-Cmplx	-0.07881	0.02636	12	-2.99	0.0113	Tukey	0.0483
48uM	CHC-Cmpl	48uM	KDN-Cmpl	-0.1309	0.02636	12	-4.97	0.0003	Tukey	0.0016
48uM	CHC-Cmpl	48uM	Pyran-Cm	-0.1663	0.02636	12	-6.31	<.0001	Tukey	0.0002
48uM	GA-Cmplx	48uM	KDN-Cmpl	-0.05211	0.02636	12	-1.98	0.0715	Tukey	0.2495
48uM	GA-Cmplx	48uM	Pyran-Cm	-0.08754	0.02636	12	-3.32	0.0061	Tukey	0.0271
48uM	KDN-Cmpl	48uM	Pyran-Cm	-0.03542	0.02636	12	-1.34	0.2039	Tukey	0.5548
Effect=concentratio*complex Method=Tukey(P<.05) Set=1										
Obs	concentration	complex	Estimate	andard Err	Letter Group					
1	48uM	Pyran-Cm	0.7227	0.01864	A					
2	48uM	KDN-Cmpl	0.6873	0.01864	AB					
3	48uM	GA-Cmplx	0.6352	0.01864	B					
4	48uM	CHC-Cmpl	0.5563	0.01864	C					

## VITA

Dhruva Dilip Dhavale was born in Pune, India, in December 1984. After completing his high school and secondary college, he graduated from University of Pune, India, with a Bachelor of Engineering degree in Chemical Engineering discipline in August 2006. After working at National Chemical Laboratory, Pune, as a project assistant for one year, Dhruva was admitted in August 2007 into the Graduate program of the Department of Chemical Engineering at Louisiana State University at Baton Rouge. There he worked on the development of sialic acid labeled chitosan for the attenuation of amyloid-beta toxicity under the guidance of Dr. James Henry, and received his Master of Science in Chemical Engineering degree at the Fall 2009 commencement. He is continuing the work on developing novel conjugated compounds for the prevention of amyloid-beta toxicity under Dr. James Henry and Dr. Michael Benton at Louisiana State University for the Doctor of Philosophy degree in chemical engineering. He plans to graduate with a doctorate at the spring 2012 commencement.